

**DEVELOPMENT OF METHODS FOR DOSIMETRY
QUALITY ASSURANCE IN INTENSITY MODULATED
RADIATION THERAPY/ IMAGE GUIDED RADIATION
THERAPY (IMRT/IGRT)**

By

**Rajesh Kumar
(PHYS01200804017)
Bhabha Atomic Research Centre, Mumbai**

A thesis submitted to the

Board of Studies in Physical Sciences

In partial fulfilment of requirements for the Degree of

DOCTOR OF PHILOSOPHY

of

HOMI BHABHA NATIONAL INSTITUTE



December 2014

Homi Bhabha National Institute

Recommendations of the Viva Voce Committee

As members of the Viva Voce Committee, we certify that we have read the dissertation prepared by Rajesh Kumar entitled ‘Development of Methods for Dosimetry Quality Assurance in Intensity Modulated Radiation Therapy/ Image Guided Radiation Therapy (IMRT/IGRT)’ and recommend that it may be accepted as fulfilling the thesis requirement for the award of Degree of Doctor of Philosophy.

Chairman – Dr. S. C. Gupta

Date:

Guide / Convener – Dr. Y.S.Mayya

Date:

Member 1 – Dr. A. Sinha

Date:

Member 2- Dr. D.D.Deshpande

Date:

Technology Advisor – Dr. S.D.Sharma

Date:

CERTIFICATE

I hereby certify that I have read this thesis prepared under my direction and recommend that it may be accepted as fulfilling the thesis requirement.

Date:

Place: Mumbai

(Prof. Y. S. Mayya)

Guide

STATEMENT BY AUTHOR

This dissertation has been submitted in partial fulfilment of requirements for an advanced degree at Homi Bhabha National Institute (HBNI) and is deposited in the Library to be made available to borrowers under rules of the HBNI.

Brief quotations from this dissertation are allowable without special permission, provided that accurate acknowledgement of source is made. Requests for permission for extended quotation from or reproduction of this manuscript in whole or in part may be granted by the Competent Authority of HBNI when in his or her judgment the proposed use of the material is in the interests of scholarship. In all other instances, however, permission must be obtained from the author.

(Rajesh Kumar)

DECLARATION

I, hereby declare that the investigation presented in the thesis has been carried out by me. The work is original and has not been submitted earlier as a whole or in part for a degree / diploma at this or any other Institution / University.

(Rajesh Kumar)

List of Publications arising from the thesis

Journal

Rajesh Kumar, S.D. Sharma, Sudesh Deshpande, Yogesh Ghadi, V.S. Shaiju , H.I. Amols and Y. S. Mayya. “*Acrylonitrile Butadiene Styrene (ABS) plastic-based low cost tissue equivalent phantom for verification dosimetry in IMRT*”. J Appl Clin Med Phys., 17;11(1):3030. (2009)

Kumar R, Sharma S.D, Amols H.I., Mayya Y.S. and Kushwaha H. S. “*A Survey on the Quality Assurance Procedures Used in Intensity Modulated Radiation Therapy (IMRT) at Indian Hospitals*”. J Cancer Sci Ther, 2: 166-170(2010)

Deshpande S, **Kumar R**, Ghadi, Y., Neharu, R.M., Kannan, V. “*Dosimetry Investigation of MOSFET for Clinical IMRT Dose Verification*” Technol Cancer Res Treat 12, 193-198 (2013)

Rajesh Kumar, S. D. Sharma, S. Deshpande, M.Sreshty, B.C.Bhatt, Howard I. Amols, G Chourasiya and Y.S. Mayya. “*Analysis of Patient Specific dosimetry quality assurance measurements in Intensity Modulated Radiotherapy: A Multi Centre Study*”. J Can Res Ther 2014 Ahead of print

Communicated

Rajesh Kumar, C.P.Bhatt, S.D.Sharma, G.Chourasiya, D.A.R.Babu, J.Singh, A.Apte, H.I.Amols and Y.S. Mayya. “*Three Dimensional Gamma Analysis in Volumetric Dose Verification in Intensity Modulated Radiation Therapy*” Medical Dosimetry

Conferences

Rajesh Kumar, S. D. Sharma, S. Deshpande, K. Thakur, S. Patkar, G Chourasiya and D.A.R. Babu. “*A Portable IMRT Dosimetry Quality Audit phantom*” Souvenir and Abstract Book,

National Conference of Association of Medical Physicists of India. Kolkata, November 13-16,2013 Pp 144-145

Rajesh Kumar, S.D. Sharma, Suresh Choudhari, Yogesh Ghadi , D.D. Deshpande, G. Chourasiya . “*Dosimetry Studies using different type of IMRT Phantoms*”. J. Med. Phys. Book of Abstract AMPICON-2010 Special Issue-JMP(2010), pp 68

Sudesh Deshpande, **Rajesh Kumar**, S.D. Sharma, Parimal Patwe, Ritesh Mahatre “*IMRT dosimetric studies as per AAPM TG119 Suits*”, J. Med. Phys. Book of Abstract, AMPICON-2010 Special Issue-JMP (2010), Pp 30

Rajesh Kumar, S D Sharma, S. Deshpande, Y. Ghadi and Y S Mayya. “*Patient specific dosimetric verification in IMRT using indigenously developed low cost tissue equivalent phantom*”. Souvenir and Abstract Book, International Conference on Medical Physics, Mumbai, November 26-29, 2008.

Rajesh Kumar, C.P.Bhatt, S.D.Sharma, G.Chourasiya, D.A.R.Babu, J.Singh, A.Apte, H.I.Amols and Y.S. Mayya. “*Gamma Analysis in Volumetric Dose Verification in Intensity Modulated Radiation Therapy*”. Indian Association for Radiation Protection National Conference (IARPNC-2014), Mumbai. March 19-21, 2014

(Rajesh Kumar)

*Dedicated to
My Parents and
to my wife Neelam, sons Shubham and Mehul*

ACKNOWLEDGEMENTS

I would like to express my deepest gratitude my guide Dr. Y S. Mayya, Adjunct Professor, IIT Mumbai and Former Head, Radiological Physics & Advisory Division. His valuable guidance, spontaneous support and constant encouragement were the driving force for the successful completion of this work.

I owe a heavy debt of gratitude to Dr H. I. Amols as remote supervisor and Dr. S. D. Sharma as local supervisor for their unrelenting inspiration, vigorous support, valuable advice, critical review, guidance and helpful suggestions through this work.

It is my pleasure to sincerely acknowledge IAEA and Dr Ahemad Meghzifene for awarding me Doctoral Co-ordinated Research Project to carry this research work. I sincerely thank Dr. M. Lovelock and Dr T. Lossaso of Department of Medical Physics, Memorial Sloan Kettering Cancer Centre New York for their support during work carried out at his centre.

The following professors kindly served on my doctoral committee: S.C. Gupta, A. Sinha and D. D. Deshpande. I thank them for their valuable time and help. I deeply express my gratitude to Shri D. A. R. Babu, Head, RPAD and Dr. D. N. Sharma, Director, HS & EG for their support and encouragement.

I record my grateful acknowledgement to all my colleagues of Medical Physics Group particularly Mrs. Philomina A for all types of help during entire course of the work.

My special thanks and acknowledgement goes to Shri Sudesh Deshpande for his wholehearted help in carrying out most of the experimental work and Dr. D. C. Kar for thesis

preparation. I also wish to thank all those who have directly or indirectly helped me during the course of this work.

I owe my loving thanks to my wife Neelam, my sons Shubham and Mehul. They had sacrificed many moments during this research. Without their continuous encouragement and kind understanding it would have been impossible for me to carry and complete this work.

Rajesh Kumar

CONTENTS

Synopsis	xvi
List of Figures	xxxix
List of Tables	xxxviii
Chapter 1: Introduction: Cancer, Radiotherapy, Dosimetry Quality Assurance and Quality Audit	1
1.1 Cancer	1
1.2 Radiotherapy	4
1.3 Intensity-Modulated Radiation Therapy	5
1.3.1 Static (Step and Shoot) IMRT	7
1.3.2 Dynamic IMRT	7
1.4 Radiotherapy Treatment Planning	7
1.4.1 Forward Treatment Planning System	8
1.4.2 Inverse Treatment Planning System	8
1.4.3 Gross Tumor Volume	9
1.4.4 Clinical Target Volume	9
1.4.5 Internal Target Volume	10
1.4.6 Planning Target Volume	10
1.4.7 Organs at risk	11
1.4.8 Planning Organ at Risk Volume	11
1.5 Quality Assurance in Radiotherapy	11

1.6	Quality Audit in Radiotherapy	13
1.7	Dose Measurement	14
1.8	Literature Survey	16
1.9	Objectives of the work undertaken for the thesis	48
Chapter 2:	Studies on Patient Specific IMRT QA in India	51
2.1	Introduction	51
2.2	Materials and Methods	53
2.2.1	Part-A: A Survey on the Quality Assurance Procedures Used in Intensity Modulated Radiation Therapy (IMRT) at Indian Hospitals	53
2.2.2	Part-B: Multi-Centre Patient Specific IMRT dosimetric Inter-Comparison in India	55
2.2.2.1	The Phantoms and the dosimetry system	55
2.2.2.2	Treatment Planning and Beam Delivery Systems	57
2.2.2.3	Dose Verification Method	58
2.2.3	Part-C: Analysis of Patient Specific Dosimetry Quality Assurance Measurements in Intensity Modulated Radiotherapy: A Multi Centre Study	60
2.3	Results and Discussions	61
2.3.1	Part-A: A Survey on the Quality Assurance Procedures Used in Intensity Modulated Radiation Therapy (IMRT) at Indian Hospitals	61
2.3.2	Part-B: Multi-Centre Patient Specific IMRT dosimetric Inter-	67

Comparison in India	
2.3.3 Part-C: Analysis of Patient Specific Dosimetry Quality Assurance	74
Measurements in Intensity Modulated Radiotherapy: A Multi Centre Study	
2.4 Conclusions	83
Chapter 3: Development of Low Cost Tissue Equivalent Phantom for Dosimetry QA in IMRT	85
3.1 Introduction	85
3.2 Materials and Methods	86
3.3 Results and Discussion:	92
3.4 Conclusions	97
Chapter 4: Development of Phantom and Methodology for IMRT Dosimetric Quality Audit for Thorax Region	99
4.1 Introduction	99
4.2 Materials and Methods	101
4.2.1 Design of Phantoms	101
4.2.2 Gafchromic film and Epson Expression 10000XL flatbed scanner	103
4.2.3 TLDs and TLD Reader	107
4.2.4 QAu method for IMRT	109
4.3 Results and Discussions	112
4.4 Conclusions	119
Chapter 5: Development of Quick, Efficient and Effective Patient Specific IMRT QA using Log File and EPID	121

5.1	Introduction	121
5.2	Materials and Methods	123
5.2.1	Multileaf Collimator System	123
5.2.2	Electronic Portal Imaging Device (EPID)	123
5.2.3	Trajectory Log	124
5.2.4	Experiment	124
5.2.4.1	Calibration and Determining the Centre of EPID detector system	126
5.2.4.2	Effect of Leaf Velocity	126
5.2.4.3	IMRT cases	127
5.2.5	Software Developments	128
5.3	Results and Discussion	128
5.3.1	C-Series Machine	128
5.3.2	Truebeam Machine	133
5.4	Conclusions	140
Chapter 6:	Three Dimensional Gamma Analysis in Volumetric Dose Verification in Intensity Modulated Radiation Therapy	142
6.1	Introduction	142
6.2	Materials and Methods	144
6.2.2	CERR	146
6.2.3	3D Gamma calculation	147
6.3	Results and Discussions	150
6.4	Conclusions	164

Chapter 7: Development of a Dynamic Phantom for QA in 4D Radiotherapy	166
7.1 Introduction	166
7.2 Materials and Methods	167
7.2.1 Dynamic Phantom System	167
7.2.2 Motion Control System	168
7.2.3 Experimental Method	172
7.3 Results and Discussions	177
7.4 Conclusions	179
Chapter 8: Summary And Conclusions	181
8.1 Summary And Conclusions	181
8.2 Future Work	189
Bibliography	190

SYNOPSIS

Cancer is a disease which is characterized by unregulated cell growth. It arises from a loss of normal growth control. Cancer is an important cause of adult death in India. As per a study report [Dikshit et al 2012], in 2010, more than 556000 cancer deaths were estimated in India for people of all ages and 71.1% occurred in people aged 30–69 years which is considered as most productive age group. Cancer deaths accounted for 8.0% of the 2.5 million total male deaths and 12.3% of the 1.6 million total female deaths at age 30–69 years. Overall including all age group the cancer is cause of 6% death to the total death tally. Cancer burden is further rising in India due to combined effect of increased lifespan and high risk lifestyle factors such as use of tobacco and dietary habits. Increasing burden calls for greater availability of cost effective treatment modalities and health care for larger populations in India.

The basic modalities of cancer treatment are surgery, radiation therapy and chemotherapy. Often, modalities are combined to create a program that is most appropriate for the patient. Radiotherapy is the use of ionizing radiation for the treatment of cancer. The goal of radiotherapy is to kill the cancer cells by delivering a prescribed dose to a tumor, while at the same time sparing the normal surrounding organs and tissues. In conventional radiotherapy, radiation was delivered using either square or rectangular treatment portals; and in some situations, it was not possible to deliver tumoricidal doses without irradiating normal tissues significantly. However, with the advent of sophisticated multileaf collimators (MLC), computer controlled electron medical linear accelerators and modern imaging systems, it became possible to shape the treatment portal conforming to the tumor geometry in three dimensions. This mode of the treatment was given the name “three dimensional conformal radiotherapy (3-D CRT)” where the uniform intensity radiation beam at a plane is used for the treatment. Intensity

modulated radiation therapy (IMRT), which is a further advancement in 3-D CRT. In IMRT, patients are treated with optimised beams from different direction having non-uniform fluences to deliver highly conformal dose to the tumor and low dose to the surrounding healthy organs. Pre-defined dose distribution criteria for required optimised treatment plan are specified by the treatment planner and the optimal fluence profiles for a given set of beam directions are determined by dividing each beam into a large number of beamlets and setting the weight for each of the beamlets through the process called inverse planning [Brahme 1988, Web 1989, Convery and Rosenbloom 1992, Holmes et al 1994, Mageras et al 1993]. The fluence files thus generated are electronically transmitted to the medical linear accelerator, equipped with the required software and hardware to deliver the intensity-modulated beams (IMBs) as calculated.

In recent years, a number of significant radiation therapy errors have been identified and reported to the public [Bogdanich 2010]. It has been suggested that the increasing dependence on advanced technology could be one of the sources of error. The QA in radiotherapy reduces uncertainties and errors in dosimetry, treatment planning, equipment performance and treatment delivery, thereby improving dosimetric and geometric accuracy and the precision of dose delivery. It not only reduces the likelihood of accidents and errors occurring, it also increases the probability that they will be recognized and rectified sooner if they do occur, thereby reducing their consequences for patient treatment. It also allows a reliable comparison of results among different radiotherapy centers, ensuring a more uniform and accurate dosimetry and treatment delivery. Improved technology and more complex treatments in modern radiotherapy can only be fully exploited if a high level of accuracy and consistency is achieved [IAEA, 2005]. The proper QA program can avoid patient death, severe complication, minor and major treatment deviations, litigation and lost of revenue due to radiotherapy error. Therefore safe and effective

implementation of IMRT requires the development and implementation of the requisite dedicated QA methodology.

Because of the complexity in beam intensity modulation methods, each IMRT field often includes many small, irregular, steep dose gradient regions, off-axis fields. In the case of IMRT, penumbral and peripheral field doses play significant role in generating the composite dose distribution. Fluence shape and intensity vary during treatment which further complicates the dosimetry of IMRT [Low et al 2011]. IMRT techniques are capable of generating high dose gradients. The high dose gradients with IMRT demands accurately localized dose distributions. Small errors in positioning of the patient can mean that a target volume is missed or that a sensitive normal structure is irradiated to a higher dose than intended and perhaps higher than that can be tolerated [Molineu et al 2005]. These features impose newer requirements for QA in IMRT delivery than the conventional treatment techniques. Regular patient related quality assurance procedures are uncommon for IMRT in contrast to conventional treatment techniques. To do this type of QA, there is a need to develop simple and effective methods, phantoms and tools. Pre-treatment verification of IMRT fields requires dedicated tissue-equivalent IMRT phantom with the provision of holding different types of detectors. A number of IMRT phantoms with the facility for holding different types of detectors are available commercially for this purpose [Civaco website, CIRS website, IBA website, Standard Imaging website]. The majority of these phantoms are made up of solid/plastic water material. Though these phantoms are suitable for pre-treatment dose verification in IMRT, they are very costly and some have limited measurement options. Therefore there is a need to design and fabricate an IMRT phantom which is made up of tissue-equivalent material, with options to verify the dose at a point and obtain dose distribution in 2D and 3D. In addition, the phantom should be made available at a

reasonable price. Planning and delivery of the IMRT is inherently 3-D in nature. Input constraints for IMRT planning are provided in term of dose-volume to planning target volume or organ at risk [Ezzell et al 2003]. However, mostly 2-D or at a single point dose verification methods are used till date at hospitals. The 2D dose verification methods are capable of detecting the systematic procedural errors. However, it is very difficult to understand the impact of the errors quantified in a 2D dose verification system at a single depth in a water phantom on the cumulative errors in the three-dimensional dose distribution in the patient from all beams in the IMRT plan. This makes it difficult to access the clinically significant dosimetric error [Steciw et al 2005]. Gel dosimetry system has been reported as 3D dosimetry system and used for 3D dose verification in IMRT [Gustavsson et al 2003, Xu and Wu 2006]. However, it has not been accepted as routine clinical 3D dosimetry system because of labour intensive procedure. Thus, there is a need to develop methodology for 3-D pre-treatment dose verification method for IMRT which can be used routinely in clinical practice. Measurement based patient specific IMRT QA is performed only for limited number of times and it demands considerable time of the delivery system as well as that of medical physicist. However catastrophic type of errors can occurs at any time during the course of treatment. If the treatment planning system has been commissioned suitably for the IMRT and adequate periodic machine QA for IMRT are in place, measurement based patient specific IMRT QA can be replaced with software based IMRT QA. Trajectory log file which is 'free information' generated by some delivery system for each IMRT treatment field can be harvested for the purposes of documenting individual patient treatments. There is a need to develop methodology to assure the accuracy of leaf positions data of log file for use as tools for quick, efficient and effective patient specific IMRT QA. Further, IMRT is a precision radiotherapy technique which demands higher degree of conformity of the dose to the tumor

while sparing the surrounding healthy tissue. However, respiration-induced internal tumor motion can introduce significant errors in the treatment especially in the thorax or abdominal region particularly. A method to correct for respiratory motion is incorporated in four-dimensional radiation therapy (4D RT), which is defined as the explicit inclusion of the temporal changes of anatomy during the imaging, planning and delivery of radiotherapy. QA of 4D radiotherapy system requires a dedicated phantom with option of moving object simulating the organ motion with breathing pattern. Few commercial systems are available [CIRS website, Standard Imaging website, Modus Medical website] but they are costly. The indigenous development of such dedicated phantom will support in the safe implementing 4D radiotherapy for clinical practice in the country. Lastly, institutional dosimetry QA is basically a self-evaluation which is prone to miss systematic errors that may be involved in the planning, treatment, and dose analysis procedures. To improve the overall quality of IMRT in the country, third party remote quality audit program will play major role. The current quality audit program of the country is aimed for conventional radiotherapy procedure which is not suitable for IMRT. There is a need to develop suitable methodology and phantom for postal audit program for IMRT.

Given the limitations in IMRT QA mentioned above, there is considerable scope to develop techniques and instruments to facilitate the safe use of radiation in radiotherapy, in India. The aim of this thesis is to presents these developments by identifying the following objectives:

Objectives of the work undertaken for the thesis

1. To Study the role of different type of solid phantom for patient specific IMRT QA and collect data of IMRT QA procedure in the country,

2. Develop a low cost tissue equivalent phantom for pre-treatment dosimetry QA using different type dosimetry system and compare its suitability in comparison with equivalent commercial phantom.
3. To develop phantom and methodology for IMRT Dosimetric Quality Audit.
4. To develop method for Volumetric Dose Verification in IMRT using 3D gamma.
5. Development of a Quick, Efficient and Effective Patient Specific IMRT QA using log file and EPID.
6. Development of a Dynamic Phantom for QA in 4D Radiotherapy

The thesis comprises eight chapters containing details about radiotherapy techniques, delivery devices, dosimetry parameters and formalisms, studies and outcomes on pre-treatment dosimetry QA using indigenously developed low cost IMRT phantom, Survey of IMRT QA procedure, role of different type of phantom solid phantom on patient specific IMRT QA, postal dosimetry quality audit method for IMRT, Volumetric Dose Verification in IMRT using 3D gamma, Patient Specific IMRT QA using log file and EPID and Dynamic Phantom for QA in 4D Radiotherapy and the conclusions arrived as a result of the work presented in the thesis.

Chapter 1(Introduction) describes introductory aspect of radiotherapy as cancer treatment. A brief description has been provided for different form of radiotherapy and equipment used. Role of Quality Assurance, Quality Audit for improving the overall performance of radiotherapy briefly discussed. The parameter and equipment used in general for dosimetry QA in IMRT has been described in this chapter. This chapter also contains literature review of the techniques/methods and phantoms available for the dosimetry QA in IMRT and their limitation. Based on this, the chapter formulates the scope and objectives of the work undertaken for this thesis.

Chapter 2 (Studies on Patient Specific IMRT QA in India) presents results of a national survey to obtain information about QA procedures and methods being followed at Indian radiotherapy centers for IMRT. A questionnaire containing parameters relevant to IMRT QA was evolved to collect the information pertaining to the QA of IMRT delivery system, QA of IMRT treatment planning system, and patient specific IMRT QA. The questionnaire was circulated to 40 hospitals in the country and responses of 31 centers were received. Survey results showed that 71% centers are having adequate machine specific IMRT QA programme, 19% centers have inadequate machine specific IMRT QA programme and 9% centres have irrelevant machine specific IMRT QA programme. No specific answer for question of QA tests of TPS specific to IMRT were received from the user. Almost all the centers have programme of setup verification of the patient by means of EPID/DRR/OBI. However, 91% of centers could not provide any information about the QA methodology of the devices used for setup verification. For patient specific dosimetric QA, almost all the hospitals have the program of pre-treatment dose verification using calibrated ionization chambers of sensitive volumes in the range of 0.01 to 0.65 cc. Dosimetric verification is performed by combining dose from all gantry angles to a single gantry angle. 2D dosimetry systems such as radiographic and radiochromic films, 2D array of ionization chambers/ semiconductor diodes and EPID are also used in patient specific dosimetry verifications. Majority of the centers (about 48%) accept the plan with 3% dose difference and 3 mm distance to agreement criteria with gamma index less than unity. However, a number of other acceptance criteria specific to institution and tumor site are being also followed. This survey reveals that a variety of IMRT QA program is being followed at the Indian hospitals. This study has brought into focus the need to evolve a national protocol for IMRT QA so that treatment outcomes of all the IMRT centers of country can be compared. This

chapter also deals with Analysis of Patient Specific dosimetry quality assurance measurements in IMRT carried out at ten radiotherapy centre having different make and model of treatment planning and delivery system. About 1800 pre-treatment dose verification data were collected and analysed for mean, median, standard deviation (SD), range, minimum and maximum % deviation. The percentage of cases having positive and negative dose differences as well dose differences within $\pm 3\%$ were also determined. The mean values of percentage variation in difference between D_{TPS} and D_{Meas} are found to be from -1.79 to 1.48 and median from -1.79 to 1.51. The standard deviations are found to be from 0.76 to 3.70. The range of variation at these centres varies from 3.99 to 16.45 while minimum and maximum values of percentage variation in difference between D_{TPS} and D_{Meas} ranges from -10.33 to 13.38. The percentage of cases having positive dose difference ranges from 8 to 94 and cases having negative dose difference ranges from 6 to 92. The percentage of cases having dose difference within $\pm 3\%$ varies from 57 to 100. IMRT centres are having random and biased (skewed towards over or under dose) distribution of the percentage variation in difference between measured and planned doses. The analysis of results of the IMRT pre-treatment dose verification reveals that there are systematic errors in the chain of IMRT treatment process at a few centres. The dosimetry quality audit prior to commissioning of IMRT may play an important role in avoiding such discrepancies. This chapter also include details of multi-centre patient specific IMRT dosimetric inter-comparison in India which have been carried out using slab, homogeneous and inhomogeneous IMRT phantom and miniature ionisation chamber having volume 0.13 cc by on site visit. The dosimetric measurements were carried out at 25 IMRT centres in the country. These centres use a variety of treatment planning and beam delivery systems. Considering the complexity of head and neck (H&N) IMRT treatment, ten H&N cases treated by IMRT techniques were randomly selected

from each hospital. CT dataset of homogeneous and inhomogeneous phantoms along with the contour of the body and chamber sensitive volume were sent to each centre in DICOM-CT and DICOM-RT-Structure format, respectively. Dosimetry QA plans of H&N IMRT treatment plans of the patients without changing gantry and couch angles were transferred on the homogeneous and inhomogeneous phantoms assuming the centre of ionization chamber as the centre of the tumour with the same fluence. For slab phantoms gantry and couch angles were set to zero degree for the entire fields while other parameter kept unchanged. The total dose from all the fields at a point of measurement were recorded and the dose difference (DD) between measured dose (D_{meas}) values and TPS calculated dose (D_{cal}) values were obtained using the relation: $DD_{P/M} = (D_{meas} - D_{cal, P/M}) * 100 / D_{cal, P/M}$ where, DD_P is the dose difference for point dose, DD_M is the dose difference for mean dose, $D_{cal,P}$ is the TPS calculated dose at the chamber centre and $D_{cal,M}$ is the TPS calculated dose averaged over the outlined volume of the ionization chamber. The variation of percentage dose differences between the measured and calculated point doses ranged from -10.27 to 13.57 with mean and standard deviation of -0.12 and 3; -10.34 to 8.5 with mean and standard deviation of 0.33 and 2.93; -10.33 to 7.64 with mean and standard deviation of 0.036 and 2.97 for point dose in slab, homogeneous and inhomogeneous phantom respectively. However, the variation of percentage dose differences between the measured and calculated mean doses ranged from -9.27 to 12.26 with mean and standard deviation of -0.32 and 2.86; -10.28 to 8.5 with mean and standard deviation of 0.12 and 2.64; -11.23 to 6.44 with mean and standard deviation of 0.039 and 2.89 for slab, homogeneous and inhomogeneous phantom respectively. The variations in planned and measured dose are within the tolerance limit. However, certain hospitals data are biased in one direction. IMRT audit may play important role in minimizing the error in dose delivery in IMRT.

Chapter 3 (Development of low cost tissue equivalent phantom for dosimetry QA in IMRT)

deals with design and features of a novel IMRT dosimetry QA phantom fabricated using Acrylonitrile Butadiene Styrene (ABS) plastic. Physical properties of ABS plastic related to radiation interaction and dosimetry were compared with commonly available phantom materials for dose measurements in radiotherapy. The ABS IMRT phantom has provisions to hold various types of detectors such as ion chambers, radiographic/radiochromic films, TLDs, MOSFETs, and gel dosimeters. The measurements related to pre-treatment dose verification in IMRT of carcinoma prostate were carried out using ABS and Scanditronix-Wellhofer RW3 IMRT phantoms for five different cases. Point dose data were acquired using ionization chamber and TLD discs, while Gafchromic EBT and radiographic EDR2 films were used for generating 2D dose distributions. Treatment planning system (TPS) calculated and measured doses in ABS plastic and commercial IMRT phantom were in agreement within $\pm 2\%$. The dose values at a point in a given patient acquired using ABS and commercial phantoms were found comparable within 1%. Fluence maps and dose distributions of these patients generated by TPS and measured in ABS IMRT phantom were also found comparable both numerically and spatially. This study indicates that ABS plastic IMRT phantom is a tissue-equivalent phantom and, dosimetrically, it is similar to solid/plastic water IMRT phantoms. Although this material is demonstrated for IMRT dose verification, it can also be used as a tissue-equivalent phantom material for other dosimetry purposes in radiotherapy.

Chapter 4 (Development of phantom and methodology for IMRT Dosimetric Quality Audit for Thorax Region) contains development of phantom and methodology for postal IMRT dosimetric quality audit. Anatomy specific IMRT dosimetry audit phantom representing the thorax region was design, developed and fabricated for postal dosimetry audit. The phantom is

made up of elliptical shape perspex of dimension 30 cm x 17 cm x 15 cm with lung equivalent, bone equivalent, tissue equivalent inserts. In phantom, planning target volume (PTV) is a C shape that surrounds a central avoidance structure referred as core. The CT data of phantom along with contoured structured were supplied to the participating hospitals. The goal for hospitals were set as (1) 95% of PTV to receive at least 5000 cGy and 10% of PTV volume to receive not more than 5500 cGy (2) 5% of critical structure (core) volume to receive not more than 3000 cGy with 6 MV and 9 field beam arrangement. The phantom was irradiated by above mentioned plan with radiochromic film and a number of TLD-100 dosimeters in place. Point dose variations between planned and measured doses were ranges from -5.91% to 3.95%, however for most of the points of measurement, percentage deviation were found to be less than 3%.The large variation at some location may be due to the high dose gradient region at the detector location. The results of planar dose distribution were found to be in the range of 91.3% to 98.51%. The results of initial studies conducted using this phantom were found encouraging indicating that the in-house developed dosimetry audit phantom is able to serve the intended purpose.

Chapter 5 (Development of Quick, Efficient and Effective Patient Specific IMRT QA using log file and EPID) describes the development of quick, efficient and effective patient specific IMRT QA method using log file and EPID. Control system of varian's LINAC generates a trajectory log file which records the actual axis position and delivered MUs at periodic intervals of 20 ms along with their expected values. Trajectory log file which is 'free information' can harvested for purposes of QA for individual patient treatments. Log file data, however, is not independent as miscalibration of leaf positions or failures in MLC positioning pots can result in the erroneous command from MLC controller as signal for both positioning and monitoring of

leaf position is coming from the same erroneous source. Such a system, however, is not completely 'foolproof' as the leaf position data in the Log/Trajectory files is produced by the MLC controller itself. There is thus no independent verification of these data as the same MLC controller that moves the leaves also monitors leaf positions and writes the Log/Trajectory files. EPID images, on the other hand, can monitor MLC leaf position completely independently of the MLC controller and MLC position pots. Confirmation of MLC leaf positions independently with the EPID can therefore be used for routine verification of every patients IMRT treatment plan and treatment delivery without extra dose to patient, or physics QA time on the Linac. Matlab based software was developed to compare leaf positions as measured from EPID images for IMRT treatment to the data in the Log/Trajectory files and used them as tools for quick, efficient and effective patient specific IMRT QA. The EPID images were acquired in cine mode along with trajectory log. Header information available with images was used to synchronise the log file data and images. The leaf positions were determined from the EPID images were compared with leaf positions recorded in trajectory log. For stationary field the difference in leaf position determined from EPID images are within 0.5 mm. However in case of moving leaf, errors are within 2 mm. This methodology was demonstrated for IMRT QA. The method presented in this chapter is a quick, efficient and effective patient specific IMRT QA tool using log file and EPID images which can routinely be used for the QA of IMRT delivery.

Chapter 6 (Three Dimensional Gamma Analysis in Volumetric Dose Verification in Intensity Modulated Radiation Therapy): IMRT treatments are planned and finalised with predetermined volumetric dose distribution to PTV and OAR. However dose verification using planar detector and point dose are not sufficient to verify the volumetric dose criteria set during the planning of IMRT. 3D dosimetry systems allow volumetric comparisons of planned and

delivered dose using the dose volume histogram for organ of interest. To be more practical 3D gamma analysis methods make it possible to analyze planned and delivered dose verification by taking into account for small setup errors of the dosimeter phantom and/or detector. This chapter describes the results of volumetric dose verification using dose at 98%, 95%, 2% to volume of interest and 3D gamma analysis methods in IMRT using computational environment for radiotherapy research software platform by incorporating quantitative 3D gamma analysis tools. The COMPASS 3D dosimetry system consists of two major components: dose computational software and a Matrixx/ transmission detector system with a gantry attachable inclinometer. The system used was having Matrixx evolution as detector system. The measured fluences at different gantry angles were used to calculate dose distribution on the patient CT data. This dose distribution is called as indirectly measured dose distribution and used to compare the planned dose distribution imported from the treatment planning system three dimensionally. The DICOM files (RT plan, RT dose, RT structures, and CT images) of all the ten patients from the TPS were imported into COMPASS system. The dosimetric comparisons were done with TPS planned and COMPASS reconstructed dose distribution. The 3D gamma evaluations for the indirectly measured and planned dose distribution were calculated by modifying the software known as CERR. Using gamma 3D calculation tools, the % fail and pass volume of interest were determined. Percentage of passing voxel for which gamma values are one or less than one for body contour, PTV and organ at risk having dose more than 5% for set acceptance criteria of 3% and 3 mm were evaluated. For contoured body structure, percentage of passing voxel is more than 90%. The average value of percentage of passing voxel is about 95%. The body contours have maximum volume and can be considered as representative of overall accuracy of treatment delivery. For PTV, percentage of passing voxel is more than 94%. The average value of

percentage of passing voxel is more than 97%. For OAR, percentage of passing voxel ranges from 64.59 to 100%. The average value of percentage of passing voxel is about 95%. It is very important to know what percentage of a volume is outside the set criteria in finalising an effective treatment. This method may be considered as most appropriate method for three dimensional dose verification in complex radiotherapy process.

Chapter 7 (Development of a Dynamic Phantom for QA in 4D Radiotherapy) contains development of a dynamic phantom for QA in 4D radiotherapy. The dynamic phantom system consists of a tissue equivalent body; lung equivalent cylinder, motion control system and software. The phantom body which represents average human thorax in shape, proportion and composition, a lung equivalent cylinder containing a target with provision to hold different type of detector was inserted in the lung equivalent lobe of the phantom. The lung equivalent cylinder is connected to an actuator that induces three dimensional motions to the target through linear translation and rotation of the lung equivalent rod. The target and surrogate motion is independently controlled with motion control software. A GUI was also developed to control the patient specific respiratory motion. It also describe the results of QA of imaging and delivery system used for 4D radiotherapy

Chapter 8 (Summary and future work) highlights the major contributions and achievements made in the research works. These may be listed as follows:

- Status of QA procedure and of multi-centre patient specific IMRT dosimetric inter-comparison in India
- Development low cost tissue equivalent phantom for dosimetry QA in IMRT
- Development of phantom and methodology for IMRT Dosimetric Quality Audit for Thorax Region

- Development of Quick, Efficient and Effective Patient Specific IMRT QA using log file and EPID
- Three Dimensional Gamma Analysis in Volumetric Dose Verification in Intensity Modulated Radiation Therapy
- Development of a Dynamic Phantom for QA in 4D Radiotherapy

The chapter concludes by noting how the above developments constitute definite progress towards design and development of phantom and methodology for dosimetry QA and Quality Audit program for safe and effective implementation of advance radiotherapy such as IMRT.

List of Figures

2.1	Surface plot of the scanned CT images of the phantom showing the location of ionisation chamber (a) slab (solid water) phantom, (b) homogeneous (abdomen) phantom, and (c) inhomogeneous (thorax) phantom.	56
2.2	Pie chart of the machine specific QA for IMRT	63
2.3	Bar diagram of the acceptance criteria of IMRT plans followed by the hospitals for pre-treatment dose verification;	64
2.4	Bar diagram of IMRT treatment sites practiced at Indian hospitals	65
2.5	Distribution of differences in measured and planned dose calculated for a point and mean dose to chamber volume	70
2.6	Differences in measured and planned dose calculated for point and mean dose to chamber volume in Inhomogeneous Phantom (Vendor wise)	71
2.7a	Differences in measured and planned dose calculated for point and mean dose to chamber volume in Slab Phantom (Hospital wise)	72
2.7b	Differences in measured and planned dose calculated for point and mean dose to chamber volume in Homogeneous Phantom (Hospital wise)	72
2.7c	Differences in measured and planned dose calculated for point and mean dose to chamber volume in In-homogeneous Phantom (Hospital wise)	73
2.8	Histogram of the measured and planned dose difference of Group A hospitals (H1 and H2) using medical electron linear accelerator of vendor 1 for intensity-modulated radiotherapy delivery	76
2.9	Histogram of the measured and planned dose difference of Group B hospitals (H3 and H4) using medical electron linear accelerator of vendor 1 for	76

	intensity-modulated radiotherapy delivery	
2.10:	Histogram of the measured and planned dose difference of Group C hospitals (H5 and H6) using medical electron linear accelerator of vendor 1 for intensity-modulated radiotherapy delivery.	77
2.11	Histogram of the measured and planned dose difference of hospitals H7 and H8 using medical electron linear accelerator of vendor 2 for intensity-modulated radiotherapy delivery	78
2.12	Histogram of the measured and planned dose difference of hospitals H9 and H10 using medical electron linear accelerator of vendor 3 for intensity-modulated radiotherapy delivery	78
3.1	Schematic line diagram of ABS plastic IMRT phantom	88
3.2(a)	Holder for Gel dosimeter container.	89
3.2(b)	Schematic line diagram of radiochromic film holder.	90
3.2(c)	Photograph of radiochromic film holder.	90
3.3	Final assembly of the locally fabricated IMRT phantom.	95
3.4	(a) Fluence map in coronal plane recorded on Gafchromic EBT film of an IMRT plan in ABS plastic phantom, (b) TPS generated fluence map in coronal plane of an IMRT plan, (c) Comparison of isodose lines recorded on Gafchromic EBT film in ABS plastic phantom and TPS generated isodose line of an IMRT plan in coronal plane, and (d) Gamma analysis of an IMRT plan.	96

3.5	(a) Fluence map in transverse plane recorded on EDR2 film of an IMRT plan in ABS plastic phantom, (b) TPS generated fluence map in coronal plane of an IMRT plan, (c) Comparison of isodose lines recorded on EDR2 film in ABS plastic phantom and TPS generated isodose line of an IMRT plan in transverse plane, and (d) Gamma analysis of an IMRT plan.	97
4.1	Photograph showing IMRT Audit Phantom	102
4.2	Photograph showing removal of Part B containing PTV OAR and Detectors	102
4.3	Photograph showing locations of TLDs and Gafchromic Film for point and planar dose verification.	103
4.4	Photographs showing EBT3 Film (a) unexposed and (b) exposed for IMRT irradiation.	103
4.5	Schematic diagram of EBT3 Gafchromic film	104
4.6	Absorption spectra of pre and post exposed EBT3 film.	105
4.7	Photograph of flatbed scanner used in this work	106
4.8	Screenshot showing scanner setting used during scanning of Gafchromic film	107
4.9	Photograph of computerised TLD reader system used in this work	108
4.10	Screen shot showing volumetric CT images of phantom	109
4.11	Screen shot showing contour for Body, PTV and OAR	110
4.12	Photograph showing setup of IMRT audit phantom	111
4.13	Screenshot showing 95% volume of PTV receiving 5000 cGy	113
4.14	Screenshot showing 10% volume of PTV not receiving more 5500 cGy	113
4.15	Screenshot showing 5% volume of OAR not receiving more 2500 cGy	114

4.16	Screenshot showing planned dose distribution on different plane of IMRT Audit Phantom	114
4.17	Screenshot showing measured fluence (A), computed fluence (B), comparison of computed and measured dose distribution (C) and calculated gamma (D) of IMRT audit plan.	117
4.18	Screenshot showing statistics for calculated gamma of IMRT audit plan.	117
5.1	Schematic diagram for synchronisation of Trajectory log records and EPID images	127
5.2	Plot of Beam hold OFF flag during A-bank and B-bank moving condition for dose of 50 MU and dose rate of 600 MU/min.	130
5.3a	Plot of leaf position information derived from log file record (50 MU and 600 MU/Min)	130
5.3b	Plot of leaf position information derived from EPID images (50 MU and 600 MU/Min)	131
5.4a	Plot of leaf position information derived from log file record (1000 MU and 600 MU/Min)	131
5.4b	Plot of leaf position information derived from EPID images (1000 MU and 600 MU/Min)	132
5.5	Matrix and error histogram showing difference in leaf positions determined from log file record and EPID images for A and B bank for an IMRT treatment field(C-Series Machine).	134
5.6	Error histograms of differences in leaf positions determined from trajectory log record and EPID images for A and B bank respectively for stationary field	135

	(1by1 cm ²)	
5.7	Error histograms of differences in leaf positions determined from trajectory log record and EPID images for A and B bank while leaves of A-bank are moving and leaves of B-bank were stationary.	136
5.8	Error histograms of differences in leaf positions determined from trajectory log record and EPID images for A and B bank while leaves of B-bank are moving and leaves of A-bank were stationary.	137
5.9	Error histograms of differences in leaf positions determined from trajectory log record and EPID images for A and B bank for one field of a five fields IMRT case (TrueBeam LINAC).	138
5.10	Error histograms of differences in leaf positions determined from trajectory log record and EPID images for A and B bank for other fields of a IMRT case.	139
6.1	Schematic of 3D gamma calculation in CERR	148
6.2	Screenshot showing input field for 3D gamma calculation	149
6.3	Screenshot showing result for 3D gamma calculation	149
6.4	Screenshot showing comparison in term of dose difference of planned and indirectly measured dose distribution on patient CT data and dose volume histogram (a) Planned dose distribution (b) Indirectly measured dose distribution (c) Dose Volume histogram comparison for planned and indirectly measured dose distribution (d) Map of dose difference between planned and indirectly measured dose distribution.	150
6.5	Screenshot showing comparison in term of dose difference of planned and indirectly measured dose distribution on patient CT data in (a) Transverse (b)	151

	Coronal and (c) Sagittal Plane	
6.6	Dose difference of planned and indirectly measured dose distribution on patient CT data for 98 %, 50 %, 2 % volume of PTV in ten IMRT cases	161
6.7	Dose difference of planned and indirectly measured dose distributions on patients CT data for 98 %, 50 %, 2 % volume of different organ at risk in ten IMRT cases	161
6.8	Screenshot showing 3D gamma distribution in different plans of patient CT. Colour shows the value of calculated gamma.	162
6.9	Bar diagram showing % of passing voxel in contoured body structure of patient CT data having dose more than 5% with 3% and 3mm set criteria of gamma evaluation	162
6.10	Bar diagram showing % of passing voxel in PTV with 3% and 3mm set criteria of gamma evaluation	163
6.11	Bar diagram showing % of passing voxel in contoured OAR having dose more than 5% with 3% and 3mm set criteria of gamma evaluation	163
7.1	Photograph of indigenously developed dynamic phantom with control system	170
7.2	Photograph of some of inserts available with dynamic phantom	170
7.3	Screenshot of control system of dynamic phantom.	171
7.4	3D graph showing the trajectory of target during motion.	171
7.5	Screen shot showing the motion pattern played during the 4D CT data acquisition.	172
7.6	Photograph showing experimental set up during 4D imaging of Dynamic Phantom.	173

7.7	Screenshot showing Graphical User Interface of Real Time Position Management system	175
7.8	Screenshot showing sorted images of the phantom at 30% phase and associated motion pattern.	176
7.9	Screenshot showing reconstructed image of the phantom: (a) Three dimensional view (b) Transversal Section (c) Coronal Section (d) Sagittal Section. Target placed in lung equivalent lobe is visible in the three sections.	176
7.10	Screenshot captured during motion of target and showing displacement of copper marker placed inside the target in different section.	177
7.11	Screenshot showing dose distribution in different plane along with resulted dose volume histogram for gated radiotherapy planned on Dynamic Phantom.	179

List of Tables

2.1	Format of IMRT QA survey questionnaire which was circulated to radiotherapy centres in India.	54
2.2	List of treatment planning and beam delivery systems used for IMRT at the hospitals where dosimetric measurements were conducted.	59
2.3	Dose difference observed in slab, homogeneous and inhomogeneous phantoms.	68
2.4	Results of statistical analysis of difference between measured and planned doses of different hospitals having medical electron linear accelerator of vendor 1	75
2.5	Results of statistical analysis of difference between measured and planned doses of different hospitals having medical electron linear accelerator of vendor 2	79
2.6	Results of statistical analysis of difference between measured and planned doses of different hospitals having medical electron linear accelerator of vendor 3	79
3.1	Physical properties of common phantom materials and ABS plastic. The data for ABS plastic was numerically calculated from its elemental composition.	87
3.2	TPS calculated and ionization chamber measured dose values in Scanditronix-Wellhofer RW3 and ABS plastic IMRT phantoms.	93
3.3	TPS calculated and ionization chamber measured dose values at 5 cm depth in Scanditronix-Wellhofer RW3 and ABS plastic IMRT phantoms.	94
4.1	Percentage dose variation between measured and planned dose.	115

4.2	Consolidated result of trail IMRT dosimetry Audit conducted at different hospitals using TLD and Gafchromic film (H1: Hospital1, H2: Hospital2, H3: Hospital3, H4: Hospital4, H5: Hospital5)	118
5.1	Number of record/frame generated in log file/EPID images on C-series machine	129
6.1.1	Volumetric dose analysis of TPS calculated and measured dose for patient 1	153
6.1.2	Volumetric dose analysis of TPS calculated and measured dose for patient 2	154
6.1.3	Volumetric dose analysis of TPS calculated and measured dose for patient 3	155
6.1.4	Volumetric dose analysis of TPS calculated and measured dose for patient 4	156
6.1.5	Volumetric dose analysis of TPS calculated and measured dose for patient 5	157
6.1.6	Volumetric dose analysis of TPS calculated and measured dose for patient 6	157
6.1.7	Volumetric dose analysis of TPS calculated and measured dose for patient 7	158
6.1.8	Volumetric dose analysis of TPS calculated and measured dose for patient 8	159
6.1.9	Volumetric dose analysis of TPS calculated and measured dose for patient 9	160
6.1.10	Volumetric dose analysis of TPS calculated and measured dose for patient 10	160
7.1	Comparison of positional accuracy of copper marker during motion	178
7.2	Volume of aluminium cube determined from reconstructed software for different phase of image acquisition	179

CHAPTER 1

INTRODUCTION: CANCER, RADIOTHERAPY, DOSIMETRY QUALITY ASSURANCE AND QUALITY AUDIT

1.1 CANCER

Cancer is a disease which is characterized by unregulated cell growth. It arises from loss of normal growth control. In normal tissues, the rates of new cell growth and old cell death are kept in balance while in cancerous tissue, this balance is disrupted. This disruption can result into uncontrolled cell growth or loss of a cell's ability to undergo cell suicide by a process called "apoptosis". There are more than 100 different types of cancer. Most cancers are named for the organ or type of cell in which they start. Cancer types can be grouped into broader categories. The main categories of cancer include:

- Carcinoma - cancer that begins in the skin or in tissues that line or cover internal organs.
- Sarcoma - cancer that begins in bone, cartilage, fat, muscle, blood vessels, or other connective or supportive tissue.
- Leukemia - cancer that starts in blood-forming tissue such as the bone marrow and causes large numbers of abnormal blood cells to be produced and enter the blood.
- Lymphoma and myeloma - cancers that begin in the cells of the immune system.
- Central nervous system cancers - cancers that begin in the tissues of the brain and spinal cord.

Not all tumors are cancerous; tumors can be benign or malignant.

- Benign tumors aren't cancerous. They can often be removed, and in most cases, they do not come back again. Cells in benign tumors do not spread to other parts of the body.
- Malignant tumors are cancerous. Cells in these tumors can invade nearby tissues and spread to other parts of the body. The spread of cancer from one part of the body to another is called metastasis.

Cancer can cause death to the individuals due to its ability to compress/invade the vital organ to an extent from where vital organ no longer can work; cancer cells can replace the functional normal cells; cancer cells can compete so strongly for space and nutrients that they will crowded out normal cells. When cancer cells take over, the normal cells are unable to carry out the function of the organ cells and vital organ will be unable to function.

Cancer is an important cause of adult deaths in India. As per a study report [Dikshit et al 2012] more than 556 000 cancer deaths were estimated in India for people of all ages and 71.1% occurred in people aged 30–69 years which is considered as most productive age group. At 30–69 years, the three most common fatal cancers were oral (including lip and pharynx, 45 800 [22.9%]), stomach (25 200 [12.6%]), and lung (including trachea and larynx, 22 900 [11.4%]) in men, and cervical (33 400 [17.1%]), stomach (27 500 [14.1%]), and breast (19 900 [10.2%]) in women. Cancer deaths accounted for 8.0% of the 2.5 million total male deaths and 12.3% of the 1.6 million total female deaths at age 30–69 years. Overall including all age group the cancer is cause of 6% death to the total death tally. Rates of cancer deaths in India are about 40% lower in adult men and 30% lower in women than in men and women in the USA or UK. However, Cancer burden is further rising in India due to combined effect of increased lifespan and high risk lifestyle factors such as use of tobacco and dietary habits.

The basic modalities of cancer treatment are:

- Surgery
- Radiation therapy
- Chemotherapy

Often, modalities are combined to create a program that is appropriate for the patient. Surgery is the oldest form of effective cancer therapy. It may be used alone or in combination with other modalities. In case of chemotherapy, the ideal chemotherapeutic drug would target and destroy only cancer cells. Radiotherapy uses ionising radiation to destroy the cancer cells by damaging or completely breaking DNA strands, and hence stopping the cancer cells from reproducing.

Curative treatment for cancer involves surgery, radiation, chemotherapy, hormone therapy or some other combination of these modalities. However, radiation therapy remains an important component of cancer treatment with approximately 50% of all cancer patients receiving radiation therapy during their course of illness; it contributes towards 40% of curative treatment for cancer [Baskar et al 2012].

Radiotherapy is most often used as a treatment by itself, or in combination with surgical removal of the cancer or with chemotherapy; it provides advantages in organ preservation, quality of life, palliation of symptoms, and survival rates. Many curable cancers that consist of solid tumours, are still treated surgically; however unlike in the past the tendency is not to attempt to remove the entire tumour and surrounding tissue, but to remove a large portion in less radical surgery (for example, by performing a lumpectomy as opposed to removing the entire breast in a mastectomy) and use radiotherapy or chemotherapy to treat or ‘clean up’ surrounding areas. If the probability of

cure from either surgery or radiotherapy is equal, the choice of treatment depends on the preference and knowledge of the prescribing doctor, the availability of either treatment, and the relative risk of morbidity or adverse effects.

1.2 RADIOTHERAPY

Radiotherapy is based on the principle that ionising radiation can impair the cell proliferation capability. Cancerous cells are more sensitive but have poor repair capability than normal cells. This property of cells facilitates use of ionising radiation as means of cancer treatment. There are two principal modes for the administration of radiotherapy, namely, beam therapy (also called external beam therapy or teletherapy) and brachytherapy. Beam therapy is the most common form of radiotherapy where radiation source is kept at a certain distance from the patient body. It is generally performed with gamma rays and x-rays, however, electrons, protons and other charged and neutral particle beams are also used. Brachytherapy is a treatment where sealed radioactive sources are placed within or in the vicinity of the tumour volume to deliver a localized dose to the tumour.

The main aim of radiotherapy is to deliver the highest possible dose to cancerous cells and the least dose to surrounding normal organs and tissues. However, till date it is not possible to irradiate only tumour cells. Local tumor control rate can be increased with escalating dose to the tumor but dose escalation to tumor is limited due complication arise in the surrounding normal/ healthy structure. To achieve higher dose to tumor and lesser dose to the surrounding normal tissue structure, high precision radiotherapy is needed. On the basis of definition of treatment field size and its conformation to the tumour geometry in the given plane or volume, beam therapy is classified as conventional and conformal beam therapy. In conventional beam therapy, either square or rectangular treatment fields are used to treat the tumour. In conformal beam therapy (CBT) or

conformal radiotherapy (CRT), regular or irregular treatment field geometry is created to conform to the tumour geometry. The 3-D conformal radiotherapy (3-D CRT) is the term used to describe the design and delivery of radiotherapy treatment plans based on 3-D image data with treatment fields individually shaped to treat only the target tissue [IAEA-TECDOC-1588, 2008]. Conformal radiotherapy permits the delivery of a radical dose to targets while limiting the dose to normal tissue structures, thus minimizing the adverse effects of treatment. The beam modifying devices which include wedge, compensator, bolus and blocks play vital role in conformal radiotherapy to modify the beam intensity within the field to attempt to achieve dose distributions with improved dose homogeneity. The invention of multileaf collimators (MLCs), which consists a number of thin leaves to generate regular as well as irregular shaped radiation beam, is increasingly used in modern modalities of treatment. The MLC has replaced other beam modifying devices to make the beam shape conform to the tumour shape. MLCs have revolutionized the implementation of 3-D CRT with cost effectiveness and significant time saving [Boyer et al 2001, Ezzell et al 2003] and given birth to a new radiotherapy treatment technique known as intensity-modulated radiation therapy (IMRT).

1.3 Intensity-Modulated Radiation Therapy (IMRT)

IMRT is an advanced form of 3D CRT that can be called as better form of conformal radiotherapy. In case of 3DCRT, a number of beams of uniform intensity (or modified with wedge or compensator), which are shaped to fit the target from multiple beams from different directions are used. In addition, IMRT provides varying intensity across the field in order to account for the tumour shape in the third dimension [Kuban and Dong 2004]. This allows, higher dose delivery to the tumour and sparing critical sensitive structures. It utilises sophisticated computer controlled radiation beam delivery system to improve the conformity of the dose distribution in the shape of

the tumour. This is achieved by splitting the beam portal into a number of beamlets and delivering different beam intensity from each of them to get varying intensity pattern. Although IMRT is actually just one of the techniques that allow complex dose planning and delivery, it utilises preset dose objective for planning and calculation to conform the dose to three dimensional volumes. This method is often referred to as inverse treatment planning. IMRT incorporates computerised inverse treatment plan optimisation in contrast to the manual optimisation techniques of conventional 3DCRT. In the inverse treatment planning system, number, energy and direction of beam are decided by planner in the conventional manner but once beam have been specified, computer take control over all other beam properties and design a customised intensity pattern to best meet the specified dose volume constraint for planning target volume and normal tissues which have been specified in advance [Brahme 1988, Källman 1988, Web 1989, Convery 1992].

Commonly MLC or compensator based IMRT are in practice. In compensator based IMRT, a compensator made up of solid metal, usually brass or aluminium, are milled to the patients' tumor size and shape as required for desired dose distribution using computer controlled milling machine. Each field will require a compensator and it will be unique for that particular field and patient. The compensators are attached individually to the linear accelerator. As the radiation beam passes through the compensator, it is shaped in a way that it provides the planned dose distribution to achieve maximum dose to the tumor and minimum dose to the surrounding healthy areas. Major disadvantage of this technique is staff need to go into the treatment room and replace customized compensators between treatment fields for a particular patient. Preparation of compensators is very labour-intensive also.

There are two modes of IMRT, delivered with MLCs, viz., the static (step and shoot) mode and the dynamic mode.

1.3.1 Static (Step and Shoot) IMRT: In this mode of IMRT, patient is treated by a number of fields and each field is subdivided into a set of subfields. These subfields irradiate tumors with uniform beam intensity levels. The subfields are created one by one by the MLC automatically. The radiation beam is turned OFF while the leaves move to create the next subfield and beam is ON once leaves form a subfield. The addition of dose delivered by each subfield forms the intensity-modulated beam as planned by the treatment-planning system.

1.3.2 Dynamic IMRT: In this form of IMRT, the leaves involved (opposing leaves) in generating the required dose distribution move simultaneously in one direction with different velocity as a function of time and so create a gap of different sizes between opposing leaves. The duration and the width of the gap between leaves depend upon their speed. The radiation beam is on while leaves are in motion. This arrangement makes the delivery of variable intensity possible at different points in the field. The main advantage of dynamic IMRT is that the continuous leaf motion enables to achieve higher resolution intensity profile. The Static (Step and Shoot) IMRT, is similar to treatment with multiple static fields, final position of leaves play important role in dose delivery while in dynamic IMRT real time leaf position has to be monitored to avoid the dosimetric error. So for static IMRT QA is somewhat easier than dynamic IMRT. The static method with large number of leaves can be made almost equivalent to the dynamic method in term of intensity resolution but requires many segments of short beam-on-time, which may present monitor unit linearity problems for some linear accelerators.

1.4 Radiotherapy Treatment Planning

Radiotherapy treatment planning is the process through which therapeutic strategy of the radiation oncologist is realised as a set of treatment instructions together with a physical description of dose

to the patient. The main aim of radiotherapy treatment planning is to maximise the dose to the tumour volume while minimising dose to the normal tissue and organ at risk. In short, radiotherapy treatment planning is the task to make sure radiation treatment beams have been placed in practice in best possible way. Computerised radiotherapy treatment planning system plays major role in over all treatment planning process. For IMRT, commonly inverse planning algorithms are used; however, forward planning algorithms (conventional 3D CRT) also can be used.

1.4.1 Forward Treatment Planning System: In forward treatment planning process, first 3D dose distribution is calculated on the patient CT data by choosing the treatment parameters such as beam energies, beam angles, beam modifier, type of radiation. Thereafter quality of the plan is evaluated using dose volume histograms (DVH). If the plan is found unacceptable, the parameters are modified and the dose distribution is re-calculated and re-evaluated. In this process, unknown dose distributions are calculated from known treatment parameters. Forward treatment planning is a trial and error process where quality of treatment plan highly depends on the skill of the person designing the plan.

1.4.2 Inverse Treatment Planning System: In inverse treatment planning process, unknown treatment parameters are derived for a known dose distribution. Inverse treatment planning requires dose constraints to the entire volume of interest. In simple words, inverse planning system maximise the dose to contoured tumor volume and minimise dose to the only contoured sensitive volume. If the structure of a organ is not contoured, organ will not be considered for dose optimisation process, which lead to unacceptable dose to that particular organ. Unlike forward treatment planning, Inverse IMRT planning is a trial-error process in searching for a proper dose

constraint specification. If dose constraints specification is not proper it may lead to an inferior plan.

For radiotherapy treatment, parameters such as volume and dose have to be specified for prescription, recording, and reporting purposes. To ensure the accuracy and consistency in overall process among different radiotherapy centres, the ICRU (ICRU-50 1993, ICRU-60 1999, ICRU-83 2010) has recommended a convention for dose reporting. The ICRU has defined number of volumes which need to be delineated during the treatment planning process. Delineation of these volumes is a mandatory requirement since absorbed dose cannot be prescribed, recorded, and reported without delineating the target volumes and volumes of normal tissue at risk.

1.4.3 Gross Tumor Volume (GTV): It is the gross demonstrable extent and location of the tumor which can be clearly observed by the physician's on imaging data available of the patient. GTV may consist of a primary tumor, metastatic regional node(s) or distant metastasis. Mostly, different GTVs are defined for the primary tumor and the regional node(s). But in some cases, metastatic node cannot be distinguished from the primary tumor, in such situations, a single GTV encompassing both the primary tumor and the node(s) is delineated. GTV is not defined for post-operative irradiation. GTV is described and reported for staging the tumor, delivering the adequate dose to the whole GTV to obtain local tumor control, evaluation of the regression of the GTV for redefining the volume, changes of the GTV during treatment might be predictive of treatment outcome.

1.4.4 Clinical Target Volume (CTV): The CTV is a volume of tissue that includes GTV and subclinical malignant tumor which are not visible in images. Delineation of CTV around the GTV

by selecting the tissues containing microscopic disease outside of the GTV is a clinical judgment where the type of malignancy, the consequence of failure, and the expected feasibility of salvage treatment are considered. There is no CTV associated with a benign tumour GTV since there is no risk of microscopic or metastatic tumour infiltration into the regional nodes or any other nearby structure.

1.4.5 Internal Target Volume (ITV): The ITV was defined as the CTV plus a margin taking into account uncertainties in size, shape, and position of the CTV within the patient (ICRU 60, 1999). Such a margin was called the internal margin as opposed to the set-up margin. The ITV useful only in clinical case where uncertainty related to the CTV location dominates setup uncertainties and/or when they are independent. Knowledge of ITV helps in delineating PTV.

1.4.6 Planning Target Volume (PTV): The Planning Target Volume is a geometrical concept introduced for treatment planning and evaluation. The PTV is drawn surrounding the CTV with suitable margin such that the planned dose is delivered to the CTV. This margin takes into account both the internal and the setup uncertainties. The delineation of the PTV requires knowledge of the presence and impact of uncertainties and variations in both the tumor location and machine parameters. The concept of PTV was first introduced in ICRU Report 50 (ICRU-50 1993) and restated in ICRU Reports 62, 71, and 78 (ICRU-62 1999, ICRU-71 2004, ICRU-78 2007). It is the recommended tool to shape dose distributions to ensure that the prescribed dose will actually be delivered to all parts of the CTV with a clinically acceptable probability, despite geometrical uncertainties such as organ motion and setup variations. In earlier ICRU documents, the possibility of compromising the margins of the PTV if they encroached on organs at risk was suggested (ICRU-62 1999, ICRU-71 2004, ICRU-78 2007), but is no longer recommended.

As per the ICRU 83, to ensure accurate reporting of dose to the PTV in cases where the PTV encroaches or overlaps another PTV, Organ at Risk (OAR) or Planning Organ at Risk Volume (PRV), it is now recommended that the delineation of the primary PTV margins should not be compromised. The ITV is considered an optional tool in helping to delineate the PTV.

1.4.7 Organs at risk (OAR):

The organs at risk (OAR) or critical normal structures are tissues, which if irradiated could suffer significant morbidity, and thus might influence the treatment planning and/or the dose prescription. In principle, all non-target tissues could be organs at risk. However, normal tissues considered as OARs typically depend on the location of the CTV and/or the prescribed dose.

1.4.8 Planning Organ at Risk Volume (PRV):

Uncertainties and variations in the position of the Organs at Risk during treatment similar to PTV is also considered to avoid serious complications. A margin is added to the OARs to compensate for these uncertainties and variations as for the PTV. This leads, in analogy with the PTV, to the concept of PRV.

1.5 Quality Assurance (QA) in Radiotherapy

Quality Assurance in radiotherapy is well defined by the World Health Organisation (WHO 1988). It is a term used to describe the set of procedures that ensure consistency of the medical prescription and the safe fulfilment of that prescription as regards dose to the target volume together with minimal dose to normal tissue, minimal exposure of personnel and adequate patient monitoring aimed at determining the end result of the treatment.

Radiotherapy treatment involves a series of steps starting from basic dosimetry, tumor localization, treatment planning, dose calculation, patient immobilization and then multiple irradiations. Each of these steps may contribute to the total uncertainty in the absorbed dose delivered to the patients. Besides these inherent uncertainties, there are systematic or random errors, which can occur due to the necessity of the transfer of large amounts of information between the many steps in the radiotherapy treatment process. These errors and uncertainties can be the direct cause of complications or treatment failures. The success of radiation treatment is therefore essentially related to a high degree of accuracy in dose delivery. An appropriate quality assurance program plays important role in assuring and improving the overall accuracy in dose delivery.

The QA in radiotherapy reduces uncertainties and errors in dosimetry, treatment planning, equipment performance and treatment delivery, thereby improving dosimetric and geometric accuracy and the precision of dose delivery. It not only reduces the likelihood of accidents and errors occurring, it also increases the probability that they will be recognized and rectified sooner if they do occur, thereby reducing their consequences for patient treatment. It also allows a reliable comparison of results among different radiotherapy centers, ensuring a more uniform and accurate dosimetry and treatment delivery. Improved technology and more complex treatments in modern radiotherapy can only be fully exploited if a high level of accuracy and consistency is achieved [Thwaites et al 2005]. The proper QA program can avoid patient death, severe complication, major treatment deviation, minor treatment deviation, litigation and loss of revenue due to radiotherapy error.

1.6 Quality Audit in Radiotherapy

Institutional QA is basically a self-evaluation which is prone to miss systematic errors that may be involved in the planning, treatment, and dose analysis procedures. External quality audit is a systematic and independent review (examination and evaluation) of the QA system, to determine whether the system is implemented effectively and whether the activities produce the required final results complying with the pre-determined standards. Quality audits are performed by personnel not directly responsible for the areas being audited, preferably in co-operation with the incumbent staff. It is a general thinking that some, or even many, facility not involved in external quality audit programs may deliver inferior radiotherapy treatment due to inadequate dosimetry practices. It is important to highlight here that during institutional QA program, institutions are free to take action related to their QA result but in case of a dosimetric audit there is a well-recognized authority which compares the local dose to its golden standard (for example, the audit by Radiological Physics Center, USA; International Atomic Energy Agency (IAEA) or The ESTRO-QUALity assurance network (EQUAL)). Sometimes the centre is obliged to undertake some actions if an unacceptable deviation is detected or otherwise hospitals will have to bear the consequences. The quality audit is carried out either by on-site visit to the hospitals or by postal audit program comprising suitable dosimetry and phantom system. The quality audit through on-site visits is considered as more comprehensive and provides a thorough review of hospital QA programs. The drawback of on-site quality audit program is its high cost; so it can be organized at a limited scale mostly on national level. Postal audit systems provide a more cost-effective check of the accuracy of treatments by the participating department and can control radiotherapy centres on a broader scale even on international level. Regular audits aim to establish high precision of radiotherapy dosimetry in a given country or region. There are international programs which make

available dosimetric audits, based on mailed thermoluminescence dosimeters (TLDs)/ film that they remit to any local radiotherapy centre on a regular basis. If a deviation has been detected, the audit organisation will, if necessary, assist the centre in tracing and correcting the origin.

1.7 Dose Measurement

Absorbed dose to water at point is estimated using an ionisation chamber and compatible electrometer. Charge collected in the ion chamber during irradiation is converted to dose using the IAEA's TRS-398 formalism

$$D_{w,Q} = M_Q \cdot N_{D,w,Q_0} \cdot K_{Q,Q_0} \cdot K_s \cdot K_{tp} \cdot K_{pol}$$

Where

M_Q : meter reading,

N_{D,w,Q_0} : Calibration factor in terms of absorbed dose to water for a dosimeter at a reference beam quality Q_0 .

K_{Q,Q_0} -Factor to correct for the difference between the response of an ionization chamber in the reference beam quality Q_0 used for calibrating the chamber and in the actual user beam quality, Q . The subscript Q_0 is omitted when the reference quality is ^{60}Co gamma radiation (i.e., the reduced notation k_Q always corresponds to the reference quality ^{60}Co).

K_s - factor to correct the response of an ionization chamber for the lack of complete charge collection (due to ion recombination).

K_{tp} - factor to correct the response of an ionization chamber for the effect of the difference that may exist between the standard reference temperature and pressure specified by the standards

laboratory and the temperature and pressure of the chamber in the user facility under different environmental conditions.

K_{pol} -factor to correct the response of an ionization chamber for the effect of a change in polarity of the polarizing voltage applied to the chamber.

Most commonly in case of IMRT dose verification small volume ionisation chamber is used to avoid the error which can arise due to higher dose gradient, volume averaging effect and leakage current. Planar doses are measured using silver halide based film / radiochromic film, Electronic Portal Imaging Device (EPID) or using 2-D detector array. In case of silver halide based film, mostly EDR2 film (Kodak, Rochester, NY) the ready-pack films in the paper envelopes are used for planar dose verification in IMRT. EDR2 film is a slow speed, fine grain film. EDR2 film is designed specifically for oncology applications. EDR 2 film has a responsive range of 25-400 cGy and an approximate saturation exposure of 700 cGy. Exact dose responses depend on a number of factors including processing conditions, the density sampling, and exposure monitoring equipment.

Radiochromic film has high spatial resolution and offer the benefit of being self-developing. GAFCHROMIC EBT film, released in 2004 by International Specialty Products (ISP, Wayne, NJ), was the first type of radiochromic film suitable for use with doses as low as the typical doses occurring in radiation therapy. In 2009, the GAFCHROMIC EBT film was replaced by the GAFCHROMIC EBT2 film that incorporates a yellow marker dye in the active layer and a synthetic polymer as the binder component. In 2011, ISP released a new film generation, the GAFCHROMIC EBT3 film. EBT3 is the latest film made by laminating an active layer between two identical polyester layers, which makes the film more robust and allows water immersion.

While the active layer composition and response is unchanged, the real EBT3 improvements are: symmetric structure that will avoid the potential errors in optical density measurements due to scanning side as was in case of EBT2, matte polyester substrate that prevents Newton's Rings formation, and presence of fiducial marks that allows for the film automatic alignment for isocentre localisation.

1.8 Review of Literature on Accidents and QA in IMRT

International Atomic Energy Agency (2004) have reported accidental overexposure of radiotherapy patients in Bialystok., according to this report, In February 2001, an accident related to radiotherapy in Poland occurred, in which five patients were delivered significantly higher doses than intended and caused radiation induced injuries. The accident resulted due to transitory loss of electrical power that caused an automatic shutdown of the linear accelerator. The power cut occurred during the radiation treatment of a patient. Following the restoration of electrical power, the machine was restarted after its controls had been checked. The treatments were resumed for the patient receiving radiotherapy at the time of the power cut and four additional patients were treated. Two patients experienced itching and burning sensations during their irradiation. This prompted the staff to halt the treatment. Subsequent dosimetry measurements revealed that the machine's output was significantly higher than expected. Further checks revealed that the dose monitoring system of the accelerator was not functioning properly, and that one of the electronic components of the safety interlock system was damaged. Subsequently, all five patients developed local radiation injuries of varying severity. In order to help prevent other possible overexposures from occurring in similar circumstances, QA programmes appropriate for accelerators that are used in the medical field need to include dosimetry checks of beam output prior to the resumption

of patient therapy following power failures or any other unusual occurrence, such as an anomalous reading in the dose rate display.

New York State Department of Health (2005) have reported, in March 2005, a patient receiving treatment for cancer located at the base of the tongue was fatally overexposed. Instead of receiving the prescribed absorbed dose of 2 Gy per fraction, he had received 13-14 Gy per fraction during three fractions to a volume between the larynx and the base of the skull. Total dose received was approximately 39-42 Gy. The patient's treatment was started with an inadequate 5-field sliding-window IMRT plan. After reviewing the case, the physician asked to re-plan the case to reduce the absorbed dose to the teeth. A new treatment plan was created and approved. As per the standard practice dosimetrist initiated storage of the plan to the database. The storage step involves the storage of three information objects in the following order: actual fluence, a digitally reconstructed radiograph (DRR), and the MLC control points. A fundamental feature of database design is that if not all elements of a data object are successfully transferred, an automatic roll-back to a previous consistent state of the database is initiated. Although the actual fluence was stored to the database, the DRR storage could not be completed owing to a "volume cache access" error. Therefore, the entire storage process was halted; an error message notified the user and asked whether the data should be saved before the application was aborted. By selecting the 'Yes' option, a second save process was initiated; however, it was unable to complete because the previous DRR transaction was still open and the software appeared to be frozen. Manual termination of the software (likely by 'ctrl-alt-del') caused a roll-back to the last consistent database state, which included the actual fluence, but lacked the DRR and the MLC control point data. The plan was opened on another computer, and the final dose distribution was calculated (which does not require the control point data). The missing MLC information was not detected, and the plan was approved

for treatment. Because of the rush to start the patient on the new plan, no pre-treatment EPID dosimetry was performed until three fractions which had been delivered with the MLC fully retracted. After the three fractions, fatal error about the MLC positions was revealed. Patient died several weeks later in 2007. New York Times reported, almost at the same time, at the State University of New York Downstate Medical Center in Brooklyn, a female cancer patient while being treated for breast cancer received radiation overdoses of about 3 times the correctly prescribed amount in 27 days of treatment. The radiation burned a gaping wound in her chest, so painful that she considered committing suicide. It is true that radiation therapy can save lives and serious accidents are rare. The New York Times (NYT) had analyzed the records from New York State hospitals. Overall, the NYT found 621 mistakes between 2001 and 2008 associated with radiotherapy. Furthermore, they also found that on 133 occasions, "devices used to shape or modulate radiation beams were left out, wrongly positioned, or otherwise misused." (<http://lansing.legalexaminer.com/medical-malpractice/radiation-therapy-offers-cure-but-greater-risk-for-harm-without-proper-safety-procedures/>). New York State Department of Health (2010) have reported about 230 misadministration cases between 2001 and 2009 in New York.

Scottish ministers for the ionising radiation (medical exposures) regulations (2006) have reported, in January 2006, a 15-year-old patient received a 58% higher absorbed dose than intended during treatment of the central nervous system (CNS) in Glasgow. The accident was mainly related to procedural errors. Department was upgraded for computerised treatment management system where all the manual transfer of treatment information were replaced with electronic transfer. However at beginning, for some complex treatment site, the manual transfer of the data was retained. The patient for which accident occurred, several mistakes were made by the treatment planners involved in the planning process. For these plans, the treatment parameters,

including the number of MUs per fraction normalised to 1 Gy, were transferred to the radiotherapy technologist via a paper form. The MUs were calculated for a fractionation schedule of 1.67×21 Gy, rather than for the prescribed absorbed dose of 1.75×20 Gy. However, the serious overexposure was not caused by the miscalculation, but by the failure to enter the MUs normalised to 1 Gy into the form. The radiographer calculated the MUs for input to the linear accelerator by multiplying the fraction absorbed dose of 1.75 Gy with the planned number of MUs, resulting in an actual fraction dose of 2.92 Gy. The mistake was not discovered until after 19 fractions had been delivered. At that point, another treatment planner observed the same planner making the same mistake again. The head fields were delivered with 58% more MUs than intended. The patient died of recurrent pineoblastoma eight months after the accident.

Nuclear Safety Authority (ASN) France (2007) have reported that use of a measuring device not suitable for calibrating the smallest microbeams generated by microMLC was detected in worldwide intercomparison study by vendor. Treatment based on the incorrect data went on for a year. All patients treated with microMLC were affected (145 of 172 stereotactic patients). The dosimetric impact was evaluated as small in most cases, with 6 patients identified for whom over 5% of the volume of healthy organs may have been affected by dose exceeding limits.

Ash and Bates (1994) have reported, between 1982 to 1991, about 1045 patients received lower doses of radiation than were prescribed for the treatment of their cancers because of a miscalculation of radiation doses. This occurred as a result of the introduction of a new technique of treatment planning. An error in the application of the planning system led to an under dosage of radiation between 5 and 35 %. In patients who received radiation alone for radical treatment a dose reduction of 20 % or more resulted in a lower than expected local control rate. Most of the errors in radiotherapy are related to the human error.

Dutreix et al (1994) have reported the result of European Quality Assurance Network for external radiotherapy. The results concerning 125 beams from 66 centres were analysed. Twenty-two beams presented minor deviations (3-6%) and 15 beams from 11 centres presented major deviations ($\geq 6\%$).

Sawyer et al. (1996) have mentioned in their publication 'Do It by Design' encourage manufacturers to improve the safety of medical devices and equipment by reducing the likelihood of user error. This can be accomplished by the systematic and careful design of the user interface, i.e., the hardware and software features that define the interaction between users and equipment. In the past whatever accident had been reported, mostly could have been eliminated with help of proper QA program.

Xing and Li (2000) have discussed computerised methods to verify the fluence map for IMRT. The dosimetric accuracy of the dynamic delivery of IMRT depends on the functionality of the software module called leaf sequencer and it is important to verify independently the correctness of the leaf sequences for each field of a patient treatment. This verification is unique to the IMRT treatment and has been done using radiographic film, electronic portal imaging device (EPID) or electronic imaging system (BIS). In this paper, they have proposed a quality assurance (QA) of the leaf sequencer using a simple computer algorithm for the verification of the leaf sequences. The software reads in the leaf sequences and simulates the motion of the MLC leaves. The generated fluence map is then compared quantitatively with the reference map from the treatment planning system. A set of pre-defined QA indices was introduced to measure the "closeness" between the computed and the reference maps.

Izewska and Andreo (2000) have reported the finding of IAEA/WHO TLD postal programme for radiotherapy hospitals. They have reported that only 65% of those hospitals who receive TLDs for the first time have results within the acceptance limits (i.e. 5%); while more than 80% of the users that have benefited from a previous TLD audit are successful. They have concluded that the unsatisfactory status of the dosimetry for radiotherapy, as noted in the past, is gradually improving; however, the dosimetry practices in many hospitals in developing countries need to be revised in order to reach adequate conformity to hospitals that perform modern radiotherapy in Europe, USA and Australia.

Zhen *et al.* (2001) reported in their paper about QA on equipment performance, equipment safety, and patient setup reproducibility through absolute dose measurements using ion chambers and relative dose measurements using film dosimetry.

Watanabe (2001) discussed a method to verify the monitor units for IMRT treatment plans (both step-and-shoot and sliding-window techniques). The results of applications to actual treatment plans showed that the calculated total isocentre doses were accurate within $\pm 2\%$ of planned doses for six-field prostate plans when calculation points are in a uniform dose region. Head and neck cases showed a slightly larger difference than prostate cases. They reported that the difference could be greater than 5% when calculation points are located in a region of high dose gradient.

De Brabandere (2002) has reported a feasibility study about the quality assurance in intensity modulated radiotherapy by identifying standards and patterns in treatment preparation. They have concluded that it is possible to identify parameters quantifying the characteristic patterns found in fluence distributions of intensity modulated fields of a specific treatment, allowing the development of a platform for automatic pre-treatment quality control.

Litzenberg *et al.* (2002) have developed a software program to evaluate the delivered fluence of step-and-shoot segmental and sliding window dynamic multileaf collimator (MLC) fields on the basis of leaves position data available in linac generated log file.

Low *et al.* (2002) evaluated a document scanner as densitometer for routine IMRT QA using film. They have concluded While the document scanners are not as flexible as dedicated film densitometers but using the intensity and scatter corrections, the document scanners provides accurate and precise measurements up to an optical density of 2.0 which is sufficient for routine IMRT film QA.

Ju *et al.* (2002) used X-ray film for the dosimetry of intensity modulated radiation therapy. They reported the over-response of the film to low-energy photons which is a significant problem in photon beam dosimetry, especially in regions outside penumbra. In this study they demonstrated that film dosimetry for IMRT involves sources of error due to its over-response to low-energy photons, with the error most transparent in the low-dose region. They have provided methodology using lead filters to enhance the accuracy in film dosimetry for IMRT.

Childress *et al* (2002) developed a rapid radiographic film calibration method measuring a film sensitometric curve using a single sheet of film exposed with a two field step-and-shoot MLC treatment and tested with Kodak XV2 and EDR2 films. They have concluded this single film method proved to be superior to the traditional calibration method and allows fast daily calibrations of films for highly accurate IMRT delivery verifications.

Chuang *et al* (2002) evaluated MOSFET for IMRT dose verification. For each IMRT phantom verification, an ionization chamber and 3 to 5 MOSFETs were used to measure multiple point doses at different locations. They found that the agreement between dose measured by MOSFET

and that calculated by treatment planning system was within 5% error, while the agreement between ionization chamber measurement and the calculation is within 3% error. They concluded that MOSFET detectors are suitable for routine IMRT dose verification.

Izewska et al (2002) have presented results of IAEA/WHO TLD postal dose audit service and high precision measurements for radiotherapy level dosimetry. They have reported that the IAEA TLD audit programme has checked approximately 4000 clinical beams in over 1100 hospitals and in many instances significant errors have been detected in the beam calibration. Subsequent follow-up actions help to resolve the discrepancies, thus preventing further mistreatment of patients. The audits for Secondary Standard Dosimetry Laboratories (SSDLs) check the implementation of the dosimetry protocol in order to assure proper dissemination of dosimetry standards to the end-users. The TLD audit results for SSDLs show good consistency in the basic dosimetry worldwide.

Yang and Xing (2003) have reported a method for routine QA for MLC leaf positioning using volumetric effect of a finite-sized detector. The technique is based on the fact that, when a finite-sized detector is placed under a leaf, the relative output of the detector will depend on the relative fractional volume irradiated. A small error in leaf positioning would change the fractional volume irradiated and lead to a deviation of the relative output from the normal reading. According to their study, an error of 0.1 mm in MLC leaf position can be detected by this method.

Li et al (2003) used two dimensional diode array to validate the dynamic MLC-controller log files. Large discrepancies between the intended and delivered segment MUs were found. The discrepancies were larger for small MU segments at higher dose rate, with some small MU segments completely undelivered. The recorded fractional MUs in the log files were found to

agree with what was delivered within the limits of experimental uncertainty. They concluded that it is important to verify the delivery accuracy of small MU segments that could potentially occur in a patient treatment and that the log files are useful in checking the integrity of the linac delivery once validated. Thus validated log files can be used as a QA tool for general IMRT delivery and patient-specific plan verification.

Leybovich *et al.* (2003) used 0.6, 0.125 and 0.009 cm³ ion chambers for the absolute dose verification for tomographic and step-and-shoot IMRT plans. They found that with the largest, 0.6 cm³ chamber, the measured dose was equal to calculated dose within 0.5%, when no leakage corrections were made. Without leakage corrections, the error of measurement with a 0.125 cm³ chamber was 2.6% (tomographic IMRT) and 1.5% (step-and-shoot IMRT). When doses measured by a 0.125 cm³ chamber were corrected for leakage, the difference between the calculated and measured doses reduced to 0.5%. Leakage corrected doses obtained with the 0.009 cm³ chamber were within 1.5%–1.7% of calculated doses. Without leakage corrections, the measurement error was 16% (tomographic IMRT) and 7% (step-and-shoot IMRT).

Low *et al* (2003) discussed the gamma tool to quantitatively compare measured and calculated dose distributions. Before computing gamma, the dose and distance scales of the two distributions, one is referred to as evaluated and second one is referred as reference, are renormalized by dose and distance criteria, respectively. The renormalization allows the dose distribution comparison to be conducted simultaneously along dose and distance axes. The gamma quantity calculated independently for each reference point and it is the minimum distance in the renormalized multidimensional space between the evaluated distribution and the reference point. The gamma quantity defaults to the dose-difference and distance-to-agreement tests in shallow and very steep dose gradient regions, respectively.

Jones et al (2003) discussed about an IMRT quality assurance program using film and MOSFET detectors in a polystyrene phantom.

Jursinic et al (2003) used a two-dimensional array of diodes for measuring dose generated in a plane by a radiation beam. They performed a time analysis for typical IMRT quality assurance measurements and reported it takes significantly less time than required to do similar analysis with radiographic film.

Higgins et al (2003) in their study used diodes for IMRT patients. They found that about 90% of the diode measurements agreed to within + 10% of the planned doses and 63% fields achieved + 5% agreement.

Izewska et al (2003) have reported the finding of IAEA/WHO TLD postal dose quality audits for radiotherapy hospitals of developing country. They have reported that TLD results are within the 5% acceptance limit for 84% of the participants. They have reported that most hospitals have Farmer type ionization chambers calibrated in terms of air kerma by a standards laboratory. Less than 10% of the hospitals use new codes of practice based on standards of absorbed dose to water. Correct implementation of any of the dosimetry protocols should ensure that significant errors in dosimetry are avoided.

Le'tourneau et al (2003) used 2D diode array (MapCheck) for IMRT quality assurance and reported the fundamental properties of it such as reproducibility, linearity and temperature dependence for high-energy photon beams. They also assessed accuracy of the correction for difference of diode sensitivity. The diode array was benchmarked against film and ion chambers for conventional and IMRT treatments. They have concluded that the MapCheck offers the

dosimetric characteristics required for performing both relative and absolute dose measurements. Its use in the clinic can simplify and reduce the IMRT QA workload.

Yeo et al (2004) have investigated the dosimetric performance of EDR2 film for the verification of IMRT fields at more clinically relevant conditions by comparing the film doses with the doses measured with an ion chamber and XV films. The effects of using a low energy scattered photon filter on EDR2 film dosimetry was also studied. In contrast to previous reports their results show that EDR2 film still exhibits considerable energy dependence (a maximum discrepancy of 9%, compared with an ion chamber) at clinically relevant conditions (10 cm depth for IMRT fields). However, by using the low-energy filters the discrepancy is reduced to within 3%. Therefore, EDR2 film, in combination with the filters, is found to be a promising two-dimensional dosimeter for verification of IMRT treatment fields.

Létourneau et al (2004) evaluated the dosimetric characteristics of a new 2D diode array MapCheck and assessed the role it can play in routine IMRT QA. Clinical performance of the for relative and absolute dosimetry was demonstrated with seven beam (6 MV) head and neck IMRT plans, and compared well with film and ion chamber measurements. The MapCheck offers the dosimetric characteristics required for performing both relative and absolute dose measurements.

Yang and Ling (2004) have suggested a method for quantitative measurement of MLC leaves displacement using electronic portal imaging device. They have found that the technique can detect a leaf positional error as small as 0.1 mm at an arbitrary point within the field in the absence of EPID set-up error and 0.3 mm when the uncertainty is considered. Given its simplicity, efficiency and accuracy they believe that the technique is ideally suitable for routine MLC leaf positioning QA.

Bouchard et al (2004) addressed reference dose measurements using thimble ionization chambers for quality assurance in IMRT fields. They therefore proposed that for accurate reference dosimetry of complete IMRT deliveries, an ionization chamber fluence perturbation correction factors must be taken into account.

Chang et al (2004) have discussed an alternative method for routine leaf position accuracy QA of dynamic multi-leaf collimator (DMLC) using an EPID. They conclude that since EPID images can be acquired, analyzed and stored much more conveniently than film, EPID is a good alternative to film for routine DMLC QA.

Izewska et al (2004) have reported the results of IAEA/WHO postal dose audits for radiotherapy hospitals in Eastern and South-Eastern Europe. They have reported finding of 5200 high-energy photon beams in over 1300 radiotherapy hospitals in 115 countries worldwide was checked. Of these, 18% of the audits were performed in Eastern and South-Eastern Europe. There are large contrasts in the region; while the results are very good for most countries, a few countries struggle with basic problems in dosimetry. Only about 2/3 of TLD audit participants in Eastern Europe have the appropriate dosimetry equipment.

Moran et al (2005) have discussed a new gradient compensation method for the evaluation of local dosimetric differences as a function of the dose gradient at each point in the dose distribution. They propose this method as dose gradient analysis tool for IMRT QA.

Winkler et al (2005) presented a system for dosimetric verification of IMRT treatment plans using absolute calibrated radiographic films for IMRT treatment plans prior to patient irradiation. Based on their results, they specified 5% dose difference and 3 mm distance-to-agreement as their tolerance levels for patient-specific quality assurance for IMRT treatments.

Woo et al (2005) have reported that during QA for IMRT involving an ion chamber measurement in a phantom, degree of agreement between the measurement and the calculation vary from plan to plan, from linac to linac, as well as over time, with a discrepancy up to 8%. They have examined the role leaf end position accuracy for such poor reproducibility. They performed a series of measurements to irradiate an ion chamber using small beam segments where one multileaf collimator edge covers half of the chamber. It was shown that the reproducibility varied up to 13%, which provides a possible explanation for the observed discrepancies above.

Wiezorek et al (2005) have tested and compared various 2-D real-time detectors for dosimetric QA of IMRT with the vision to replace radiographic films for 2-D dosimetry. They have used three different 2-D detectors, each based on a different physical (interaction) principle, were tested for the field-related IMRT verification: (1) the MapCheck diode system (2) the IMRT QA scintillation detector, and the ionization chamber array. The results obtained with all three 2-D detector systems were in good agreement with calculations performed with the treatment-planning system and with the standard dosimetric tools, i.e., films or various point dose detectors. They concluded that the commercial 2-D detectors have the potential to replace films as an "area detector" for field-related verification of IMRT.

Dineshkumar et al (2005) have demonstrated the utility of Dynalog file information for planar dose verification in IMRT QA. They developed a program to convert the dyanlog file to DMLC field file. These file were used for further dose calculation (called as delivered dose distribution). Planned, Measured and Delivered dose distributions are compared using gamma evaluation in Scanditronix, Omni Pro IMRT software. The Planned and Delivered planar dose distributions agree within 2% dose difference and 2 mm DTA. Measured dose distributions agree within 4%

dose difference and 4 mm DTA with Planned dose distribution. They concluded that Dynalog file as a promising tool for dynamic IMRT QA.

Vieira et al (2006) have reported a fast method for daily linac verification for segmented IMRT using electronic portal imaging. They have studied the low MU performance of medical linear accelerator for IMRT from Varian Siemens and Elekta using electronic portal imaging device in comparison with ionisation chamber measurements. They have also studied the daily MLC leaves motion. They concluded that long-term leaf gap reproducibility (1 standard deviation) was 0.1 mm for the Varian, and 0.2 mm for the Siemens and the Elekta accelerators. Down to the lowest MU, beam output measurements performed with the EPID agreed within 1+/-1% (1SD) with ionisation chamber measurements.

van Zijtveld et al (2006) have reported their three clinical experience about dosimetric pre-treatment verification of IMRT based portal dose image using an EPID. They have analysed predicted and measured portal dose images using the gamma index with 3% local dose difference and 3mm distance to agreement as reference values. They have found four clinically relevant errors out of 270 patients pre-treatment checks. They have also reported that the patient-averaged mean gamma value inside the field was 0.43 +/- 0.13 (1SD) and only 6.1 +/- 6.8% of pixels had a gamma value larger than one.

Soares et al (2006) discussed about a new radiochromic emulsion which has been developed for IMRT dosimetry. Measurements of the sensitivity and uniformity of samples of this new film were reported, using a spectrophotometer and two scanning laser densitometers. However, there is a strong polarization effect in the samples examined, requiring care in film orientation during readout.

Dobler et al (2006) have compared different combinations of IMRT system components with regard to quality assurance (QA), especially robustness against malfunctions and dosimetry. They have concluded that not only single components but the whole chain from planning to delivery has to be evaluated in commissioning and checked regularly for QA.

Zeidan et al (2006) presented an evaluation of a new and improved radiochromic film, type EBT, for its implementation to IMRT dose verification. They show that EBT film has several favorable features that allow for its use in routine IMRT patient-specific QA.

Yoon et al (2007) have examined the degree of calculated-to-measured dose difference for nasopharyngeal target volume in intensity-modulated radiotherapy (IMRT) based on the observed/expected ratio using patient anatomy with humanoid head-and-neck phantom. The plans were designed with a clinical treatment planning system that uses a measurement-based pencil beam dose-calculation algorithm. Their experimental results show that when the beams pass through the oral cavity in anthropomorphic head-and-neck phantom, the average dose difference becomes significant, revealing about 10% dose difference to prescribed dose at isocenter.

Nelms and Simon (2007) have carried out survey on planar IMRT QA carried out by electronic two-dimensional diode array device. Their survey results showed that a significant proportion of responding institutions (32.8%) use the single-gantry-angle composite method for IMRT QA analysis instead of field-by-field analysis. Most institutions perform absolute dose comparisons rather than relative dose comparisons, with the 3% criterion being used most often for the percentage difference analysis, and the 3 mm criterion for distance-to-agreement analysis. The most prevalent standard for acceptance testing is the combined 3% and 3 mm criteria. A significant percentage of responding institutions report not yet having standard benchmarks for acceptance

testing-specifically, 26.6%, 35.3%, and 67.6% had not yet established standard acceptance criteria for prostate, head and neck, and breast IMRT respectively.

De Martin et al (2007) have analysed their pre-treatment QA data in order to establish uniquely defined agreement criteria between planned and delivered dose distribution for clinical QA practice in IMRT of head and neck patients. Analysis is performed by comparing planned and measured dose distributions in terms of absolute point dose measurements, planar dose verification and gamma function analysis using 4%/3mm values as acceptance criteria. They have concluded that statistical analyses of gamma evaluation of QA pre-treatment dosimetry are useful to properly define confidence limits of the agreement between expected and measured fluences based on our institutional experience.

Poppe et al (2007) discussed about the spatial resolution of 2D detector arrays equipped with ionization chambers or diodes. They noticed that the array is limited by the size of the single detector and the centre-to-centre distance between the detectors. They studied 2D-ARRAY Type 10024 (PTW-Freiburg, Germany). Consequently, the dose verification, e.g., by means of the gamma index, is performed by comparing the measured values of the 2D array with the values of the convolution product of the treatment planning system (TPS) calculated dose distribution. Overall it was shown that the spatial resolution of the 2D-ARRAY Type 10024 was appropriate for the dose verification of IMRT plans.

Palta et al. (2008) have discussed about need of more elaborate QA for IMRT planning delivery system in addition to patient specific QA considering complex beam intensity modulation, each IMRT field often includes many small irregular off-axis fields, resulting in

isodose distributions for each IMRT plan that are more conformal than those from conventional treatment plans.

Basran and Woo (2008) have discussed the relationships between two different types of IMRT QA processes in order to define, or refine, appropriate tolerance values. They have examined discrepancies between (a) the treatment planning system (TPS) and results from a commercial independent monitor unit (MU) calculation program; (b) TPS and results from a commercial diode-array measurement system; and (c) the independent MU calculation and the diode-array measurements for 115 IMRT plans. They have reported that there is no evidence that the average total dose discrepancy in the monitor unit calculation depends on the disease site. Second, the discrepancies in the two IMRT QA methods are independent. Third, there is marginal benefit in repeating the independent MU calculation with a more suitable dose point, if the initial IMRT QA failed a certain tolerance. They proposed acceptable tolerances based on disease site and IMRT QA method.

Pawlicki et al (2008) have investigated IMRT QA using Statistical Process Control. Control charts a method to describe the performance of a process were used to analyze the IMRT QA processes from several institutions in the academic and community setting. They concluded that there is room to improve the processes of IMRT QA measurements and independent computer calculations.

Amin et al (2008) investigated the feasibility of using a set of multiple MOSFETs in conjunction with the mobile MOSFET wireless dosimetry system, to perform a comprehensive and efficient quality assurance (QA) of IMRT plans. The results indicate that multiple MOSFET detectors

arranged in an anatomy specific configuration, in conjunction with image guidance, can be utilized to perform a comprehensive and efficient quality assurance of IMRT plans.

Howell et al (2008) have carried out study to establish the action level for EPID based QA for IMRT. They have evaluated maximum gamma (gamma max), average gamma (gamma avg), and percentage of the field area with a gamma value greater than 1.0 (gamma % > 1) for 152 treatment plans (1152 treatment fields). These data were then used to set clinical action levels based on the institutional mean and standard deviations and concluded that action levels are a useful tool for standardizing the evaluation of EPID-based IMRT QA.

Oldham et al (2008) discussed about a highly modulated 11 field IMRT plan delivered to a cylindrical PRESAGE™ dosimeter and the dose distribution was readout using a commercial scanning laser optical-CT scanner. They have compared result of PRESAGE, GAFCHROMIC EBT film measurements, and the calculated dose distribution from a commissioned treatment planning system ECLIPSE. They concluded that for the complex IMRT plan studied, and in the absence of in-homogeneities, the ECLIPSE dose calculation was found to agree with both independent measurements, to within 3%, 3 mm gamma criteria.

Han et al (2008) have discussed about an anthropomorphic phantom designed and constructed to conduct a remote-audit program for IMRT treatments. The phantom has option to incorporate thermoluminescent dosimeter (TLD) holders inside the target and the OARs for the measurements of absolute dose. In addition, the phantom allowed measurements with ionization chambers placed at the TLD locations and also has option to measure dose distribution using film. They concluded that the TLD measurements in the developed phantom agreed with IC and MC results with less than 3% of an average difference.

Koh et al (2009) have discussed about internal audit of a comprehensive IMRT program. On the basis of this audit they have concluded that they are able to generate the IMRT plan with acceptable toxicities.

Collomb et al (2009) have evaluated a high-resolution plastic scintillator based 2-D tissue equivalent dosimeter (DOSIMAP) for linac QA and IMRT verification. For IMRT QA they have made comparison between DOSIMAP and the film and their result shows DOSIMAP is capable to verify the complex IMRT irradiation fields with almost the same spatial resolution of the dosimetric films.

Sadagopan et al (2009) have characterized, commissioned, and evaluated the QA capabilities of a novel commercial IMRT device Delta4. They found this device is suitable for IMRT QA.

Fraser et al (2009) et al have studied the performance of three cylindrical chambers of varying volumes in terms of measurement reproducibility, dose measurement linearity for patient specific IMRT QA. Fifty IMRT patient specific quality assurance dose measurements were performed with each chamber. They have concluded that measurements of absorbed dose to water in IMRT fields are highly chamber and IMRT plan dependent

Ferreira et al (2009) attempted in their study to fully assess the performance of the scanner Epson Expression 10000XL in order to quantify all parameters and needed corrections to minimize dose uncertainties. A protocol to read EBT films using the Epson Expression 10000XL scanner was established for IMRT verification. The contribution for the overall uncertainty in film dosimetry coming from the scanning process was estimated to be around 0.5% for doses higher than 0.5 Gy when reading parameters are optimized. Total scan uncertainty achieved is about 2% when using a perpendicular calibration. It can further be reduced if a parallel calibration is used.

Anjum et al (2009) discussed about the different gamma histogram criteria for the comparison of planned dose with irradiated dose distribution and find that what percent of pixels passing a certain criteria imitate a good quality plan.

Saminathan et al (2010) in their study have analyzed the dosimetric characteristics of 2D ion chamber array matrix for verification of radiotherapy treatments. On the basis of this study they have concluded that ImatriXX can be used for quantifying absolute dose and planar dose distribution. Time-consuming procedure of making ionometric measurement for absolute dose estimation and film for dose distribution verification can be avoided.

Anjum et al (2010) have used a second treatment planning system (TPS) for independent verification of the dose calculated by primary TPS for patient-specific IMRT QA.. They have concluded that the use of the second TPS as an independent, accurate, robust, and time-efficient method for patient-specific IMRT QA.

Bailey et al (2010) have discussed the implementation of an electronic method to perform and analyze intensity-modulated radiation therapy quality assurance (IMRT QA) using an aSi megavoltage electronic portal imaging device in a network comprised of independent treatment planning, record and verify (R&V), and delivery systems.

Kruse et al (2010) have reported the insensitivity of single field planar dosimetry to IMRT inaccuracies. They have concluded that deconstruction of an IMRT plan for field-by-field QA requires complex analysis methods such as the gamma function. Distance to agreement, a component of the gamma function, has clinical relevance in a composite plan but when applied to individual, highly modulated fields, it can mask important dosimetric errors. While single field

planar dosimetry may comprise one part of an effective QA protocol, gamma analysis of single field measurements is insensitive to important dosimetric inaccuracies of the overall plan.

Nelms et al (2011) have pointed out that per-beam, planar IMRT QA passing rates do not predict clinically relevant patient dose errors. They have studied ninety six unique data sets by inducing four types of dose errors in 24 clinical head and neck IMRT plans. The error-free beams/plans were used as "simulated measurements" to compare to the corresponding data calculated by the error-induced plans. The results also show numerous instances of false positives or cases where low IMRT QA passing rates do not imply large errors in anatomy dose metrics. They concluded that there is a lack of correlation between conventional IMRT QA performance metrics (Gamma passing rates) and dose errors in anatomic regions-of-interest. The most common acceptance criteria and published actions levels therefore have insufficient, or at least unproven, predictive power for per-patient IMRT QA.

Low et al (2011) have reported a comprehensive overview of how dosimeters, phantoms, and dose distribution analysis techniques should be used to support the commissioning and quality assurance requirements of an IMRT program.

Korevaar et al (2011) have discussed about LINAC head-mounted 2D detector array (COMPASS) based quality assurance system in head and neck IMRT. They have tested whether COMPASS QA results correctly identified treatment plans that did or did not fulfil QA requirements in IMRT. They found good agreement between COMPASS reconstructed dose and film measured dose in a phantom.

Olch (2012) has evaluated mapcheck2 and 3DVH software for patient-specific IMRT QA. They have compared the point dose and dose distribution evaluated from mapcheck 2 and 3DVH with

ionisation chamber and film measured dose value along with TPS predicted dose data. They found that no statistically significant differences were found for any of the planar dosimetric comparisons.

Wu et al (2012) have investigated 3D γ analysis for IMRT and VMAT QA. They have calculated 3D gamma from TPS computed and EPID back-projection reconstructed doses in patient's CT images and then compared the outcome with 2D γ measured with map check. They have found that when 3% (global)/3 mm criteria was used, all IMRT and 90% of VMAT plans passed QA with a γ pass rate $\geq 90\%$. A significant statistical correlation was observed between 3D and 2D γ -analysis results for IMRT QA if 3D γ (voxel getting dose more than 10% of global maxima) and γ (MC) are concerned, but no significant relation is found between γ (PTV-3D) and γ (MC-2D).

Sun et al (2012) have compared the efficiency and effectiveness of independent dose calculation followed by machine log file analysis to conventional measurement-based methods includes ion chamber and 2D diode array measurements in detecting errors in IMRT delivery. They have studied sixteen IMRT treatment cases of different sites. They concluded that independent dose calculation followed by machine log file analysis is fast and can be a reliable tool to verify IMRT treatments.

Stasi et al (2012) have investigated the correlation between % gamma passing rate obtained during standard per-beam pre-treatment QA tests, based on real retrospective data with a common 2D array of actual clinical plans, with different acceptance dose discrepancy, between planned dose-volume-histogram (DVH) and patients' predicted DVH, calculated by 3DVH software. They have concluded that there is a lack of correlation between conventional IMRT QA performance metrics gamma passing rates and dose errors in DVHs values and the low sensitivity of 3%/3 mm

global gamma method show that the most common published acceptance criteria have disputable pre-dictive power for per-patient IMRT QA.

Chung et al (2013) have evaluated the transit dose based patient specific quality assurance (QA) of IMRT for verification of the accuracy of dose delivered to the patient. They concluded that transit dose based IMRT QA may be superior to the traditional QA method since the former can show whether the in-homogeneity correction algorithm from TPS is accurate. In addition, transit dose based IMRT QA can be used to verify the accuracy of the dose delivered to the patient during treatment by revealing significant increases in the failure rate of the gamma index resulting from errors in patient positioning during treatment.

Carlone et al (2013) have investigated the use of receiver operating characteristic methods in patient specific IMRT QA in order to determine unbiased methods to set threshold criteria for γ -distance to agreement measurements. They concluded that the use of patient specific QA as a safety tool can effectively prevent large errors (e.g., $\sigma > 3$ mm) as opposed to a tool to improve the quality of IMRT delivery.

Siochi et al (2013) Point/Counterpoint review they have argued Patient-specific QA for IMRT should be performed using software rather than hardware methods to reduce the machine as well as physicist time.

Qin et al (2013) have discussed about a systematic approach to statistical analysis in dosimetry and patient-specific IMRT plan verification measurements. They concluded that the result from a single QA measurement without the appropriate statistical analysis can be misleading. When the required number of measurements is comparable to the planned number of fractions and the

variance is unacceptably high, action must be taken to either modify the plan or adjust the beam delivery system.

Hussein et al (2013) have investigated the variability of the global gamma index (γ) analysis in various commercial IMRT/VMAT QA systems and to assess the impact of measurement with low resolution detector arrays on γ . They have investigated five commercial QA systems. They have reported that the detector array configuration and resolution have greater impact on the experimental calculation of γ due to under-sampling of the dose distribution, blurring effects, noise, or a combination.

Caivano et al (2014) have explored a novel patient-dose DVH-based method for pre-treatment dose quality assurance tests. They have concluded QA-methods based on DVH-metrics have potential to predict the impact of delivered dose.

Bakhtiari et al (2014) have presented accuracy and consistency of dosimetry QA system based on comparison of direct dose-volume histogram (DVH) analysis vs. treatment planning system (TPS) DVH. They have concluded 3D dose distribution predicted by the planned dose perturbation (PDP) algorithm is both QA system are accurate and consistent.

Pulliam et al (2014) have presented the result of Survey of IMRT QA Practices in USA using a questionnaire, They have reported that most common planar gamma criteria was 3%/3 mm with a 95% of pixels passing criteria. The most common QA device was diode arrays. The most common first response to a plan failing QA was to re-measure at the same point the point dose (89%), second was to re-measure at a new point (13%), and third was to analyze the plan in relative instead of absolute mode (10%). Some institutions, however, claimed that they had never observed a plan failure.

The literature survey [Bogdanich (2010), International Atomic Energy Agency (2004) , New York State Department of Health (2005) , Scottish ministers for the ionizing radiation (medical exposures) regulations (2006) , Nuclear Safety Authority(ASN) France (2007) , Ash and Bates (1994) , Sawyer *et al.* (1996)] highlights the consequences of absence of adequate QA program in radiotherapy institutions. It may also be noted that while a number of serious and fatal radiotherapy accident have been reported, there is a fair chance that many more such accidents might have occurred but not been reported. Further there is continuous technological development for improving the outcome of radiotherapy application. Therefore accident prevention mechanisms where QA and QAu are considered as major components, need continuous research to keep the pace with requirement of technological development.

Further, IMRT is a complex radiotherapy technique which allows the delivery of radiation doses to targets in conformity with their complex shaped volumes and at the same time efficiently sparing the surrounding normal/healthy structures. Thus it is the treatment of choice for curative radiotherapy. The IMRT involves a high risk of mistreatment due to its nature of sharp dose gradient at the boundary, complicated treatment planning and delivery procedure. Any small geometrical miss in patient setup as well as in mechanical accuracy of beam delivery can lead to a large deviation of delivered dose from the planned one. Since high geometric and dosimetric accuracy is required for this advanced technique, verification of the delivery of IMRT [IMRT Collaborative Working Group, 2001] dose distributions is a prerequisite for its safe and efficient application [Saarilahtia et al 2005]. In general, IMRT QA has three component namely, QA of delivery system, QA of treatment planning system and patient specific QA. The QA of planning system focuses on the capability of treatment planning system to handle the dosimetric challenges occurs during IMRT beam delivery. The QA of delivery system deals with the ability of delivery

system, to act consistently as per the requirement of IMRT beam designed by treatment planning system. Patient specific QA, which is performed specially in IMRT process, ensure the accurate and safe treatment of the patient. For patient specific QA, IMRT plan is first generated with the volumetric patient CT scan of patient and then optimized fluences are superimposed to a volumetric CT scan of a water equivalent phantom. The treatment planning system recalculates doses for the phantom geometry. The generated plan is executed on delivery system with dose measuring device placed in the phantom. The calculated and measured doses are compared. It is assumed that if measured dose and calculated dose for a phantom agrees within a few percent, then delivered dose and calculated dose in a patient should also agree within a few percent.

Moreover, the successful use of IMRT technique lies in the implementation of comprehensive QA programme before and during the IMRT in routine clinical practice. Since the beginning of its deployment in clinical practice, a number of reports and chapters in books have been published [IMRT Collaborative Working Group 2001, Ezzell et al 2003, Galvin et al 2004, Bortfeld et al 2006, AAPM Medical Physics Monograph No. 29 2003]. All these reports emphasize the importance of performing comprehensive acceptance testing, commissioning and QA programme of IMRT equipment. The need for these types of verification programmes has been demonstrated during an independent dose evaluation performed by the Radiological Physics Centre (RPC) in institutions wishing to participate in a Radiation Therapy Oncology Group (RTOG) IMRT protocol (Molineu et al 2005, Ibbott 2006). In this study, about one third of surveyed hospitals failed to meet the acceptance criteria set by RPC. These results clearly demonstrate that institutions vary significantly in their ability to deliver dose distributions that agree with their own treatment plans, and that QA tests play a critical role in IMRT planning and delivery. IMRT requires verification of a number of parameters related to planning and delivery

system which is still an ad hoc process at majority of the centres. This is because new systems are continuously becoming available and no clear guidelines and criteria exist for the accuracy required. Many centres have developed their own QA procedures for IMRT and recently highly specific suggestions for tolerance limits and action levels for planning and delivery of IMRT have been provided [Stock et al 2005, McDermott 2007, Sanchez-Doblado et al 2007, Palta et al 2003].

From the literature survey, it can be understood that IMRT patient specific QA poses a challenging and difficult task. Minimum incongruity between measured and calculated dose distributions is essential for expected result. Galvin et al (2004), Ezzell et al (2003), Gillis et al (2005), Van et al (2002), Arnfield et al (2001) described approaches used to verify patient IMRT treatment fields prior to delivery. Phantom based measurements are routinely used for absolute and relative dose evaluations for patient specific IMRT QA. To ensure that IMRT plans are accurately delivered to the patients, phantoms containing film and ion chambers have traditionally been employed to verify that the measured and calculated doses are in agreement. Pre-treatment patient specific IMRT QA has become an essential part of IMRT in making sure that the delivered dose distributions agree with the planned dose. Patient-specific IMRT QA, as a total system check, provides a unique opportunity to identify these potential sources of errors and plays an essential role in ensuring the safe and accurate delivery of IMRT [Palta et al 2008].

In addition, as mentioned in the literature survey, different types of methods [Leybovich et al (2003), Bouchard et al (2004), Doblado et al (2005), Chuang et al (2002), Low *et al.* (2002), Ju *et al.* (2002), Low *et al.* (2003), Jursinic *et al.* (2003), Le'tourneau *et al.* (2003), Chang *et al.* (2004), Moran *et al.* (2005), Wiezorek *et al.* (2005), Vieira *et al.* (2006), van Zijtveld *et al.* (2006), Soares *et al.* (2006), Zeidan *et al.* (2006), Both *et al.* (2007), Collomb *et al.* (2009), Ferreira *et al.* (2009),

Carlone *et al.* (2013), Gustavsson *et al.* 2003, Xu and Wu 2006, Oldham *et al.* (2008), Godart *et al.* (2011), Godart *et al.* (2011), Zhen *et al.* (2011), Olch (2012), Wu *et al.* (2012), Stasi *et al.* (2012), Visser *et al.* (2013)], acceptance criteria [Watanabe (2001) , Winkler *et al.* (2005) , van Zijtveld *et al.* (2006) Nelms and Simon (2007), De Martin *et al.* (2007), Howell *et al.* (2008) , Wu *et al.* (2012), Stasi *et al.* (2012)] and equipments [Leybovich *et al.* (2003) , Chuang *et al.* (2002) , Higgins *et al.* (2003), Le´tourneau *et al.* (2003), Chang *et al.* (2004), Collomb *et al.* (2009), Sadagopan *et al.* (2009) , Godart *et al.* (2011)] are being used for IMRT dosimetry QA. Since there is no common QA protocol for IMRT, hospitals use their own QA methods. Such diversity in QA program complicates the intercomparison between the institutions [Mijnheer *et al.* 2002, Gillis *et al.* 2005, Pulliam *et al.* 2014].

Furthermore, as stated above, patient specific QA is additional QA for IMRT, which needs to be carried out for safe and effective IMRT treatment. A number of methods such as point dose method [*Saw et al.* (2001) , De Brabandere (2002), Chuang *et al.* (2002) , Higgins *et al.* (2003), Yang and Xing (2003) Leybovich *et al.* (2003), Bouchard *et al.* (2004), Doblado *et al.* (2005), Budgell *et al.* 2011, Deshpande *et al.* 2013] where measured dose at point in a phantom is verified with dose calculated at that point by treatment planning system, planar dose verification method [*Low et al.* (2002), Ju *et al.* (2002) Low *et al.* (2003b), Paul *et al.* (2003), Le´tourneau *et al.* (2003), Chang *et al.* (2004), Moran *et al.* (2005), Wiezorek *et al.* (2005), Vieira *et al.* (2006), van Zijtveld *et al.* (2006), Soares *et al.* (2006), Zeidan *et al.* (2006), Both *et al.* (2007) , Collomb *et al.* (2009), Ferreira *et al.* (2009), Carlone *et al.* (2013)] where planar detectors are used and three dimensional dose verification method where either three dimensional dosimeter [Gustavsson *et al.* 2003, Wu and Xu 2006, Oldham *et al.* (2008)] or software reconstructed 3D data [Godart *et al.* (2011), Korevaar *et al.* (2011), Zhen *et al.* (2011), Olch (2012), Wu *et al.* (2012), Stasi *et al.* (2012), Visser

et al. (2013)] are used to compare the planned and delivered dose distribution. The core requirement for patient specific QA is a suitable versatile phantom which can incorporate different types of detectors and at the same time it should be available at low price.

The biological effect of radiation on tumors and normal tissues follow sigmoid shaped dose response relationship. Clinical dose response curves are very steep and typically 5% change in dose results in 10% to 30% change in biological response when steepest portion of such curves are considered. Based on the sigmoid shaped dose response relationship, many national and international recommendations [ICRU-24 1976] have specified the need of $\pm 5\%$ accuracy in dose delivery to the target volume of the patient. Comprehensive QA programmes should be established to cover all steps from dose prescription to dose delivery to achieve such level of accuracy. These programmes should include detailed internal checks performed by the radiotherapy centres and external audits made by independent bodies [Kutcher et al 1994, IAEA TECDOC-1040 2000, Dixon and O'Sullivan 2003]. The dosimetry audit performed by an independent external body, a national or international organization, or a peer review by qualified medical radiation physicists is considered as a fundamental step of a dosimetry QA programme. Literature survey [Dutreix et al. 1994, Izewska and Andreo 2000, Izevaska, et al 2002, 2003 and 2004] reveals that dosimetric intercomparison or suitable external audit program are found to be very effective in highlighting the problem area and the overall quality of treatment. Therefore, QA programs of a country should not only rely on the QA test performed by the local hospital physicists, but also requires external audit programmes conducted by an independent external body, a national or international organisation, or a peer review by qualified medical physicists. There are evidences reported in the literature that IMRT treatments may not always be as accurate as users believe. In 2008, the Radiological Physics Center (RPC) of USA reported that out of the 250 irradiations of a head and

neck phantom as part of an IMRT credentialing process, 71 (28%) had failed to meet accuracy criteria of 7% for dose in a low gradient region and/or 4 mm distance to agreement in a high gradient region [Ibbott et al 2008]. This was an alarming result, especially considering that this was conducted in those institutions that felt confident enough in their IMRT planning and delivery process to apply for credentialing and presumably expected to pass. Further, role of intercomparison and external audit becomes very important where treatment technologies are complex, advanced and keep on updated frequently [Molineu et al. 2005, Ibbott et al. 2006, Ibbott et al. 2008]. ESTRO QUASIMODO used a horseshoe-shaped PTV surrounded by a cylindrical OAR along with ionization chamber measurement and radiographic film in a pelvic phantom to assess the quality of IMRT treatment delivery in a few hospitals [Gillis et al 2005]. The irradiated films, the results of the ionization chamber measurements and the computed dose distributions were collected and analyzed at a nodal center that compared the measured and computed dose distributions with the gamma method and composite dose-area histograms. American Association of Physicists in Medicine Task Group 119 [Ezzell et al, 2009] developed nine test cases to assess the goodness of IMRT commissioning conducted trial in nine hospitals. These nine hospitals included in the study had passed the RPC credentialing tests for IMRT. The degree of agreement has been quantified using the concept of “confidence limit” which is defined as $\frac{\text{mean deviation}}{\sigma} + 1.96 \sigma$. The agreement between the planned and measured doses was determined using ionization chamber and films [Ezzell et al 2009]. The current quality audit program of the country which is similar to IAEA TLD postal audit program is aimed for conventional radiotherapy procedure and not suitable for IMRT. Therefore, there is a need to develop suitable methodology and phantom for postal audit program for IMRT.

It can be noted that planning and delivery of the IMRT is inherently 3D in nature. Input constraints required to produce requisite dose distribution for IMRT planning are provided in terms of dose-volume to planning target volume or organ at risk to the treatment planning system. Accordingly, treatment planning system optimized the beam parameters to generate the acceptable treatment plan. However, as pointed out from the literature survey, mostly 2D or single point dose based patient specific QA are used till date at hospitals. The 2D dose verification methods are considered as better than point dose based method and capable of detecting the systematic procedural errors. However, it is very difficult to understand the impact of the errors quantified in a 2D dose verification system at a single depth in a water phantom on the cumulative errors in the three-dimensional dose distribution in the patient from all beams in the IMRT plan. This makes it difficult to access the clinically significant dosimetric error. Gel dosimetry system has been reported as 3D dosimetry system and used for 3D dose verification in IMRT [35, 36]. However, it has not been accepted as routine clinical 3D dosimetry system because of labour intensive procedure. Apart from gel dosimeter system, in recent past few software based 3D dosimetry system have been reported [Godart et al. 2011, Korevaar et al. 2011, Zhen et al.2011, Olch 2012, Wu et al. 2012, Stasi et al.2012, Visser et al. 2013] for dosimetry QA in IMRT. However, their appropriateness to be used as 3D pre-treatment dose verification system for routine clinical practice has to be studied in detail.

Most of the above discussed patient specific dosimetry QA methods are based on the measurements. Measurement based patient specific IMRT QA is performed only for limited number of times and it demands considerable time of the delivery system as well as that of medical physicist. Apart from this, it cannot guarantee error free treatment for entire course of the IMRT treatment as such kind of QA cannot be performed for every treatment fraction. Literature survey

divulges that trajectory log file get generated automatically by some delivery system for each IMRT treatment field. The log file gets generated automatically by the delivery system at the end of delivery of each IMRT field, with suitable methodology it can be reaped for the purposes of patient specific QA without consuming time of delivery system and medical physicists. The file generated for each patient can be analyzed for each fraction. Xing and Li 2000, Litzenberg *et al.* 2002, Li et al. 2003, Dineshkumar et al. 2005, Sun et al. 2012 and Ramsey et al 2001, have utilized data of log file directly or indirectly for the QA in IMRT without providing enough proof about genuineness of these data as these are generated by the same controller which have responsibility to place MLC leaves position at correct positions during IMRT.

In addition, IMRT is a precision radiotherapy technique which demands higher degree of conformity of the dose to the tumor while sparing the surrounding healthy tissue. However, respiration-induced internal tumor motion can introduce significant errors in the treatment especially in the thorax or abdominal region particularly. A method to resolve the issues which arise due to respiratory motion is incorporated in four-dimensional radiation therapy (4D RT), which is defined as the explicit inclusion of the temporal changes of anatomy during the imaging, planning and delivery of radiotherapy. Safe and effective fulfillment of such advance techniques require suitable quality assurance program. The QA of 4D RT system needs a dedicated phantom with option of moving object simulating the organ motion with breathing pattern. Few commercial systems are available [CIRS website, Standard Imaging website, Modus Medical website] for this purpose but they are costly. The indigenous development of such dedicated phantom will support safe implementation of 4D RT for clinical practice in the country.

Thus Dosimetry QA related issues of IMRT are complex and need continuous research starting from development of phantom, study merits and demerits of patient specific QA procedures, development of methodology for quick and efficient dosimetry QA, exploring the possibility with 3D dosimetry QA, development of suitable phantom taking into account of tumor motion and ultimately establishing suitable quality audit program to improve overall IMRT treatment in the country. The proper QA program can avoid patient death, severe complication, major treatment deviation, minor treatment deviation, litigation and loss of revenue due to radiotherapy error.

Given the limitations and necessities in IMRT QA mentioned above, there is considerable scope to develop techniques and instruments to facilitate the safe and effective use of ionizing radiation in advanced radiotherapy, in India. The aim of this thesis is to presents these developments by identifying the following objectives:

1.9 Objectives of the work undertaken for the thesis:

- Develop a low cost tissue equivalent phantom for pre-treatment dosimetry QA using different type dosimetry system and evaluate its suitability in comparison with equivalent commercial phantom.
- To Study Patient Specific IMRT QA in India.
- To Develop Phantom and Methodology for IMRT Dosimetric Quality Audit.
- To Develop Method for Volumetric Dose Verification in IMRT using 3D gamma.
- Development of a Quick, Efficient and Effective Patient Specific IMRT QA using log file and EPID.
- Development of a Dynamic Phantom for QA in 4D Radiotherapy

The thesis comprises of eight chapters dealing with the above objectives. The chapters contain details about radiotherapy techniques, delivery devices, dosimetry parameters and formalisms, studies and outcomes on pre-treatment dosimetry QA using indigenously developed low cost IMRT phantom, survey of IMRT QA procedure, role of different type of solid phantoms on patient specific IMRT QA, postal dosimetry quality audit method for IMRT, volumetric dose verification in IMRT using 3D gamma, patient specific IMRT QA using log file and EPID and Dynamic Phantom for QA in 4D Radiotherapy. The conclusions arrived as a result of the work presented in the thesis are given the last chapter.

In the present work, efforts have been made in the direction of dosimetry QA in IMRT such as survey of present IMRT QA procedure in the country, on-site dosimetric intercomparison, statistical analysis of pre-treatment dose verification data of different hospitals, development of IMRT QA phantom, development of QAu phantom and methodology, 3D dose verification methodology, log file and EPID based IMRT QA methods and development of 4D RT QA phantom, which would contribute towards improvement of accuracy in IMRT dose delivery in the country.

CHAPTER 2
STUDIES ON PATIENT SPECIFIC IMRT QA IN INDIA

2.1 Introduction

The success of implementation of QA programs in a country largely depends upon the dedication and compliance of the concerned hospitals to established procedures and guidelines. One of the best ways to obtain a broad picture about this aspect is to carry out survey based studies and analysis of the data of hospitals. We have followed three-pronged approach namely survey based approach, on site pre-treatment dose verification and analysis of hospital's patient specific pre-treatment dose verification data for this purpose. This study gives direction in improving the patient specific IMRT QA methodology in the country. This chapter presents such a study conducted in various hospitals in India. It consists of three parts namely, (Part-A) A Survey on the Quality Assurance Procedures used in IMRT at Indian Hospitals, (Part-B) Multi-Centre Patient Specific IMRT dosimetric Inter-Comparison in India, and (Part-C) Analysis of Patient Specific Dosimetry Quality Assurance Measurements in Intensity Modulated Radiotherapy: A Multi Centre Study.

As discussed in chapter 1, there is no universal protocol for dosimetry QA worldwide including India. Further, quicker and precise QA methods are preferred considering large patient loads in country. Hence there is a need to evolve a national protocol in IMRT so that treatment outcomes of all the IMRT centres of country can be compared. Before evolving such a protocol it is equally important to know the existing procedure of QA in IMRT used at these centres. Keeping this in mind, a national survey on QA procedure/ methods was conducted. This section describes the results of IMRT QA survey which aim to understand the current QA methodologies, refining them

to be as intuitive, efficient, and meaningful as possible; provide input to evolve a unified IMRT QA protocol, based on socio-economic status, experience and relevant clinical end points for Indian scenario.

As it is evident from literature survey section 1.8, verification of the delivery of IMRT dose distributions is a prerequisite for its safe and efficient application and it is conducted world wide using various methodologies. In the survey mentioned in Part-A of this chapter, almost all the hospitals have the program of pre-treatment dose verification using ionization chambers of different volumes. Survey also reveals that dosimetric verification was performed by combining dose from all gantry angles to a single gantry angle using a slab phantom. However, patients are treated from different gantry angles. Further, patients are neither flat in geometry nor homogenous. In view of the multi phantom dosimetry study using slab, homogeneous and inhomogeneous phantoms were conducted to investigate the accuracy of pre-treatment dose verification in IMRT at Indian hospitals.

Further, considering wide variability in delivery, planning, QA and pre-treatment dose verification methods; dose verification data acquired by the hospitals as part of their institutional pre-treatment dose verification program in IMRT were collected from 10 different hospitals in the country. The statistical analysis of these data was conducted to assess the quality of the IMRT practice at these institutions. User specific and equipment specific approach was adopted.

2.2 Materials and Methods

2.2.1 Part A: A Survey on the Quality Assurance Procedures Used in Intensity Modulated Radiation Therapy (IMRT) at Indian Hospitals

A questionnaire containing parameters relevant to IMRT QA was evolved to collect the information about the exact practice of IMRT QA being followed at the hospitals. As the aim of this survey was to understand and extract the information about the QA methods being used by the hospitals, emphasis was given on descriptive answer over multiple choice type answers. Table 2.1 shows the IMRT QA questionnaire which was evolved for conducting the survey. The questionnaire contains three major part of IMRT QA namely, (i) QA for IMRT delivery system, (ii) QA for IMRT treatment planning system (IMRT-TPS), and (iii) patient specific IMRT QA. Under QA for delivery system, information about detailed machine specific QA which includes details of the machine parameters that are evaluated in the IMRT equipped medical LINAC and methods and tools for testing these parameters have been included. In the QA for IMRT-TPS, description about the procedure adopted for QA of dosimetric and non-dosimetric parameters used for IMRT planning and their test methods were enquired. Though the section on patient specific QA was further divided: (a) QA for setup verification, and (b) QA specific to the dosimetric methods. But, importance was given to extracting information related to methodologies followed for the dosimetric verification. Information about the make and model of multi leaf collimator (MLC) which is used for delivering the IMRT was asked to understand suitable QA methodology related to MLC. Considering the importance of imaging in IMRT, imaging modalities used for IMRT planning in the hospitals were also explored. Question related to acceptance criteria of an IMRT plan for treatment after the pre-treatment dose verification was also included. Information regarding site as well as centre specific IMRT planning such as margin for PTV and acceptance

Table 2.1: Format of IMRT QA survey questionnaire which was circulated to radiotherapy centres in India.

Name and address of the hospital:		Phone:	Fax:
Name of the Medical Physicist:		Phone:	Email:
1.	Make and model of Medical linear accelerator		
2.	Photon energy used for IMRT	6MV/15MV/18MV	
3.	Make and model of MLC used for IMRT		
4.	Procedure adopted for QA of delivery system (machine specific QA). Describe the parameter, test methods and tools used.) (please write in details , add separate page if needed)		
5.	Make and model of the treatment planning system		
6.	Procedure adopted for QA of treatment planning system used for IMRT/IGRT (TPS specific QA). Describe the parameter such dosimetric and non dosimetric parameters, test methods and tools used.(please write in details , add separate page if needed)		
7.	Make and model of the imaging systems used for IMRT (e.g. CT-Sim, Sim-CT, PET-CT etc)		
8.	Procedure adopted for Patient specific QA about: QA for setup verification 1. QA for set-up verification 2. Dosimetric QA Describe the parameter, test methods and tools used.(please write in details , add separate page if needed)		
9.	Is there any QA related to IMRT/IGRT carried out daily? if yes please describe it.		
10.	Available QA tools, Make and models of dosimetry systems used in QA. (Such as map checks, Imatrix, diode, MOSFET etc)		
11.	Frequency of QA 1.TPS specific QA: 2.Machine specific QA: 3.Patient specific QA:	Daily/ weekly/ monthly/ others Daily/ weekly/Monthly/Others Daily/ weekly/Monthly/Others	
12.	Sites and number of IMRT cases treated at your centre.		
13.	Margins for PTV in various cases such as for H&N, Prostate, etc		
14.	Criteria for accepting IMRT plan (e.g. spatial agreement, dose agreement etc)		
15.	Have you ever detected deviation larger than acceptable limit during the QA measurement? (if yes provide details)		
16.	Are you satisfied with IMRT QA procedure?		
17.	Major hurdle in performing IMRT QA		
18.	Any suggestion for improving the IMRT QA procedure in Indian condition		
19.	Any other suggestion/information		

criteria were enquired. It was also enquired whether user has detected any deviation larger than acceptable tolerance during their QA so far. At the time of this survey, there were about 280 radiotherapy centre in India, out of which about 60 centres practise IMRT.

The implementation of IMRT in Indian Hospitals is increasing at the rapid rate and in the future more number of centres will be practicing this technique. The questionire was sent to 40 IMRT practicing hospitals. The hospitals were chosen from different part of the country, government and private hospitals and hospitals from metro and small town with aim to cover a whole spectrum of the IMRT QA in the country.

Analysis of the machine specific QA were done by scrutiny of the data received from different hospitals. This scrutiny was done by dividing the hospitals in three categories: (a) Centres with Adequate Machine specific IMRT QA program - those hospitals which have programme of machine specific QA relevant to IMRT following standard recommendations/ protocols (b) Centres with Inadequate Machine specific IMRT QA program- If the information provided by the hospitals were not sufficient, and (c) Centres with Irrelevant Machine specific IMRT QA program.

2.2.2 Part-B: Multi-Centre Patient Specific IMRT dosimetric Inter-Comparison in India

2.2.2.1 The Phantoms and the dosimetry system

Slab (solid water/ PMMA), homogeneous (abdomen phantom, CIRS Inc., USA) and inhomogeneous (thorax phantom, CIRS Inc., USA) phantoms were used in this study. Fig. 2.2b shows the surface plot of the slab, homogeneous and inhomogeneous phantoms. The CT scans of all the phantoms along with the respective ionization chambers were taken for computing the dose to the chamber centre by the TPS. The solid water slab phantom of dimension 30 cm x 30 cm x 20 cm was used for point dose measurements at most of the centres. A hole was milled in the central

slab (2 cm thick) to position the ionization chamber. The chamber's sensitive volume was thus located at the centre of the phantom (10 cm depth). At one of the hospital the point dose was measured using a dedicated IMRT phantom (Universal IMRT verification phantom, type 40020, PTW Freiburg, Germany) available with the hospital. This phantom consists of two PMMA blocks, one of dimension 30 cm x 30 cm x 5cm and the other of dimension 30 cm x 30 cm x 2 cm making overall dimension of the phantom as 30 cm x 30 cm x 7 cm. The phantom has the provision to accommodate a film sample of size 25 cm x 30 cm at 5 cm depth and it can also accommodate five 0.125 cc ion chambers (Ion chambers type 31002/31010, PTW Freiburg, Germany) at 6 cm depth.

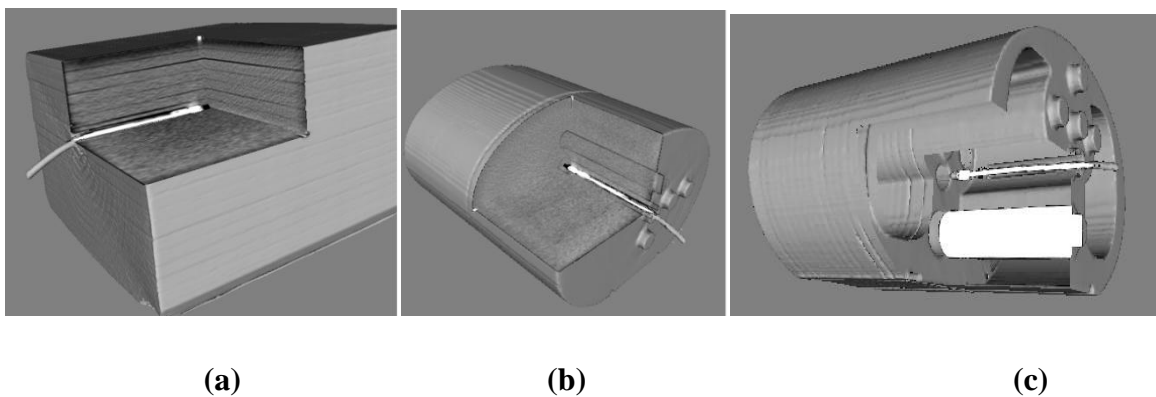


Figure 2.1: Surface plot of the scanned CT images of the phantom showing the location of ionisation chamber (a) slab (solid water) phantom, (b) homogeneous (abdomen) phantom, and (c) inhomogeneous (thorax) phantom.

The homogeneous phantom represents human anatomy in size and proportion while inhomogeneous phantom represents an average human torso in proportion, density and three-dimensional structure. The homogeneous and inhomogeneous phantoms are elliptical in shape of dimension 30 cm (long) x 30 cm (wide) x 20 cm (thick). The homogeneous phantom is made up of two elliptical slices each of length 15 cm. One slice can accommodate different ionization chambers using appropriate inserts allowing the usage of different ionization chamber

types in predefined positions. The inhomogeneous phantom has two sections. The first section consists of a 15 cm long slice and the second section consists of 15 standard slices each of length 1 cm. The inhomogeneous phantom is made of water equivalent material with in-homogeneities mimicking lungs of density 0.21 g/cc and a bony vertebra of density 1.6 g/cc, with invariant geometry and density distribution in the longitudinal direction. The first section of this phantom can accommodate different ionization chambers whereas the second section can accommodate radiographic/ radiochromic films to verify the dose distribution in transverse sections. These phantoms have three pins to prick the film for isocentre localisation. During the dosimetric measurements, the ionization chamber was positioned at the 10 cm depth in these phantoms.

The point dose measurements in homogeneous and in homogeneous phantoms were carried out using 0.13 cc ionisation chamber (CC013, IBA dosimetry, Sweden) along with DOSE1 electrometer (IBA dosimetry, Sweden). In case of slab phantom either 0.13 or 0.125 cc ionisation chambers, depending on the insert available with hospital, along with compatible electrometers was used for the point dose measurements. The meter readings of the ionometric dosimeters (in the unit of coulomb) were converted to absorbed dose using respective absorbed dose to water calibration factor ($N_{D,w}$) following the methodology of IAEA TRS 398 [IAEA Technical Report Series 398, 2006].

2.2.2.2 Treatment Planning and Beam Delivery Systems

The dosimetric measurements were carried out at 25 IMRT centres in the country. These centres use a variety of treatment planning and beam delivery systems. Table 2.2 lists out the make and models of treatment planning and beam delivery systems which were used in this study. The Varian beam delivery systems delivers the IMRT treatment by dynamic method whereas Elekta and Siemens beam delivery systems deliver IMRT treatment by step and shoot method.

2.2.2.3 Dose Verification Method

Patient specific IMRT dosimetric inter-comparison for about 250 patients from 25 different radiotherapy hospitals treating the cancer patient with IMRT techniques were carried out. Considering the complexity of head and neck (H&N) IMRT treatment, ten H&N cases treated by IMRT techniques were randomly selected from each hospital. The homogeneous and inhomogeneous phantoms along with ionisation chamber and electrometer were circulated to all the hospitals. Volumetric CT scan with slice thickness 1.25 mm of these phantoms along with the ionization chamber were acquired. CT slices of 1.25 mm width were taken to facilitate the proper contouring of the small sensitive volume of the ionization chamber. CT dataset of these phantoms along with the contour of the body and chamber sensitive volume were provided to each centre in DICOM-CT and DICOM-RT-Structure format, respectively.

Slab phantom along with the ionisation chamber and electrometer of the respective hospital were used. These systems were already in use at these hospitals for IMRT dosimetric verification. The CT scan data of each of these phantoms were transferred into the treatment planning system of the hospitals. H&N IMRT treatment plans of the patients without changing gantry and couch angles were transferred on the homogeneous and inhomogeneous phantoms assuming the centre of ionization chamber as the centre of the tumour with the same fluence. For slab phantoms, gantry and couch angle were set to zero degree for the entire fields while other parameters were kept unchanged. The isocentre was fixed at the centre of ionisation chamber. Dose at chamber centre and mean dose in the contoured chamber volume, called here as point dose and mean dose respectively, were calculated using the treatment planning system of the hospitals for each of the patients. The plans were transferred on treatment delivery system through hospital network and executed on each phantom one by one. The reading of the electrometer was converted into absorbed

dose to water using methodology of IAEA TRS 398. The total dose from all the fields at a point of measurement was recorded and the dose difference (DD) between measured dose (D_{meas}) and TPS calculated dose (D_{cal}) was obtained using the following relation:

$$DD_{P/M} = (D_{meas} - D_{cal, P/M}) * 100 / D_{cal, P/M}$$

Where, DD_P is the dose difference for point dose, DD_M is the dose difference for mean dose, $D_{cal,P}$ is the TPS calculated dose at the chamber centre and $D_{cal,M}$ is the TPS calculated dose averaged over the outlined volume of the ionization chamber. To maintain the uniformity in the study, all the dosimetric works were supervised at each hospital.

Table 2.2: List of treatment planning and beam delivery systems used for IMRT at the hospitals where dosimetric measurements were conducted.

Treatment Planning Systems	Beam Delivery Systems
Eclipse (Varian)	Clinac iX with 120 millennium MLC (Varian)
Oncentra Master Plan (Nucletron)	Clinac 2300 C/D (Varian)
Precise Plan (Elekta)	Trilogy (Varian)
Monnaco (Elekta)	Unique Performance (Varian)
Iplan RT dose (BrainLab)	Clinac DHX (Varian)
CMS Xio (Elekta)	Clinac 2100 C/D (Varian)
	Elekta Precise (Elekta)
	Elekta Synergy (Elekta)
	ARTISTE (Siemens)
	PRIMUS (Siemens)
	ONCOR (Siemens)

2.2.3 Part-C: Analysis of Patient Specific Dosimetry Quality Assurance Measurements in Intensity Modulated Radiotherapy: A Multi Centre Study

The dose verification data acquired by the institutional physicist of 10 different hospitals for various types of patients were included in the statistical analysis. The sites treated using IMRT at these centers include head and neck, breast, cervix, prostate, lung, etc. Randomly selected dose verification data of these centers which includes different types of cases were collected for the analysis. The beam delivery devices used at these centers were Varian Clinac 2300 CD, 6EX and Trilogy equipped with Varian 120 leaves millennium MLC (Varian Oncology System, USA); Elekta Synergy equipped with Elekta 80 leaves MLC (Elekta, UK) and Siemens Oncor equipped with Siemens 80 leaves MLC (Siemens Healthcare, Germany). The radiotherapy treatment planning systems used by the hospitals were Varian Eclipse v6.0, CMS Xio v2.33.02, Elekta Precise Plan 2.6.9 v11 and Siemens KonRad v2.2. The hospitals have been identified here as H1 to H10 and the vendors of the beam delivery systems have been identified as vendor 1 to vendor 3 so that their exact identity could not be disclosed.

Pre-treatment dose verifications at these centers were performed by measuring the point dose using ionization chamber in a slab phantom. The 0.125/0.6 cc (PTW Freiburg, Germany) and 0.13/0.65 cc (IBA Sweden) ionization chambers were used by these hospitals for dose verification measurements. The computed tomography (CT) images of the $30\text{ cm}^3 \times 30\text{ cm}^3 \times 20\text{ cm}^3$ slab phantom containing ionization chamber at 5 cm depth from the anterior surface of the phantom was acquired. Surface plot of the CT data with chamber in the place is shown in Figure 2.1c. The active volume of the ion-chamber was contoured as a region of interest on CT images so that mean dose to the chamber volume can be calculated by the treatment planning system. A verification plan with the same fluence maps as in the treatment plan was generated on CT images of the

phantom in the TPS by resetting the planned gantry, collimator and couch angle to 0° angles. The dose to the ionization chamber location was determined and referred here as difference between treatment planning systems calculated dose (D_{TPS}). The generated plans were transferred through the record and verify system of the hospitals to the linear accelerator for execution on the phantom. The cumulative reading of IMRT delivery of each patient at the point of measurement was recorded. The reading of the ionization chamber was converted into absorbed dose to water, which is referred here as measured dose (D_{Meas}) using methodologies described in the International Atomic Energy Agency TRS 398 [IAEA Technical Series Report 398, 2006]. The difference between D_{Meas} and D_{TPS} was calculated using the following formula [Chung et al, 2011]:

$$\text{Dose difference (\%)} = (D_{Meas} - D_{TPS}) * 100/D_{TPS} \quad (1)$$

In this study, difference between individual field doses was not considered. Collected data were analyzed for mean, median, standard deviation (SD), range, minimum and maximum % deviation using Statistica 6.0 (StatSoft Inc., OK, USA). The percentage of cases having positive and negative dose differences as well dose differences within $\pm 3\%$ were also determined.

2.3 Results and Discussion

2.3.1 Part-A: A Survey on the Quality Assurance Procedures Used in Intensity Modulated Radiation Therapy (IMRT) at Indian Hospitals

Out of 40 radiotherapy centres in India practicing IMRT, 31 centres responded to this survey. Figure 2.2 shows the pie chart of the information provided by the hospitals related to machine specific QA for IMRT. It can be observed from this chart that 71% centres have adequate machine specific IMRT QA programme, 19% centres do not have an adequate machine specific IMRT QA

programme and 10% centres have irrelevant machine specific IMRT QA programme. The 10% centres have described QA program relevant to a conventional medical electron linear accelerator with some arbitrary test methods. Regarding the question of QA tests of TPS specific to IMRT, a variety of answer were received from the hospitals. Almost all the hospitals have a different answer for this question. Some of the users have described a few QA tests for TPS listed in IAEA TRS 430 [IAEA Technical Series Report 430, 2004] and some of them refer AAPM Report 62 [Benedick et al 1998]. As is known to all, neither TRS 430 nor AAPM Report 62 describes comprehensive test procedures for TPS relevant to IMRT and hence it can be concluded from the response of the hospitals that none of them are having adequate QA test program for TPS specific to IMRT. This kind of response from the users may probably be due to an inadequate availability of a comprehensive QA protocol for treatment planning system specific to IMRT. Therefore the hospital practising IMRT are in need of a suitable QA protocol for treatment planning system specific to IMRT. Almost all the centres have reported that they have specific programme of setup verification of the patient by means of Electronin Portal imaging device (EPID) / Digitaly Reconstructed radiograph (DRR) /On board imaging (OBI). However, 91% of centres could not provide any information about the QA methodology of the devices used for setup verification. This observation indicates that 91% of the centres may not have understood the question properly because the periodic performance evaluations of these devices are also recommended by the manufacturer. In this case the measurement of absorbed dose is carried out at a point which is selected in a region of low dose gradient. Two dimensional (2D) dosimetry systems such as radiographic and radiochromic films, 2D array of ionization chambers/ semiconductor diodes and EPID are also used in patient specific dosimetry verifications. However, it is not clear from the survey data whether both of these methods are used simultaneously for a patient or either of the

devices is used. For patient specific dosimetric QA, almost all the hospitals have the program of pre-treatment dose verification using calibrated ionization chambers of sensitive volumes in the range of 0.01-0.65cc. As per the information submitted by the user, dosimetric verification is performed by combining doses from all angles to a single gantry angle.

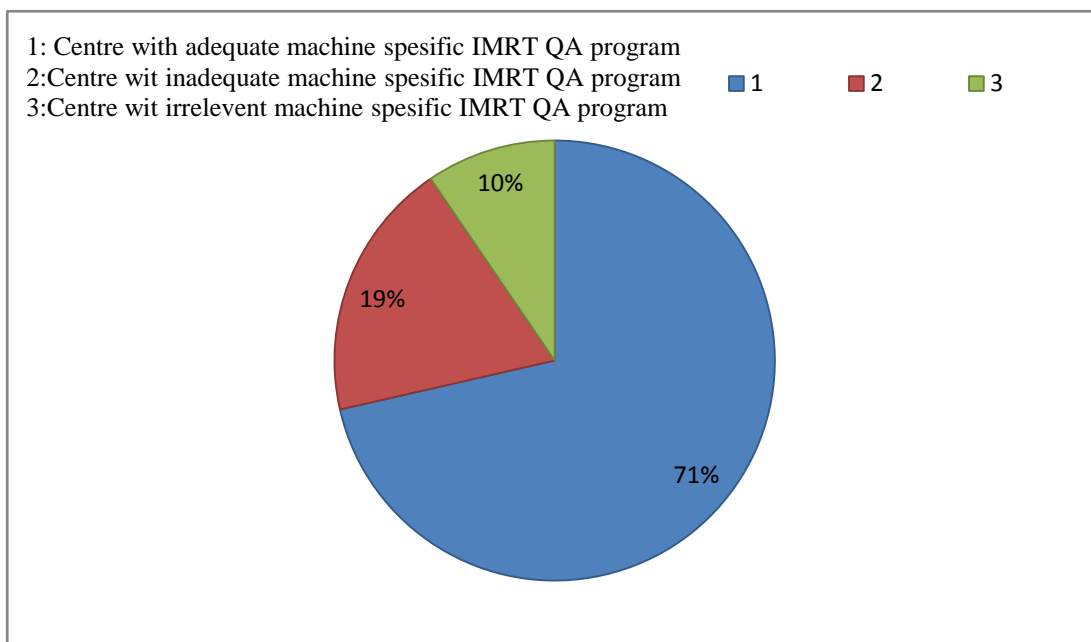


Figure 2.2: Pie chart of the machine specific QA for IMRT (% of Participated Hospitals).
 1: Centres with Adequate Machine specific IMRT QA program
 2: Centres with Inadequate Machine specific IMRT QA program
 3: Centres with Irrelevant Machine specific IMRT QA program

However, it is not well known whether this type of verification reflects the dose delivered to the patient by all gantry angles. Hence, a thorough study needs to be carried out to demonstrate the similarities/ differences in the dose if the verification is carried out at a single gantry angle composite plan in place of multiple angle treatment plans.

Figure 2.3 Shows the bar diagram of the acceptance criteria of IMRT plans followed by the hospitals for pre-treatment dose verification. It can be observed here that institution specific

treatment plan acceptance criteria after pre-treatment dose verification are followed at the hospitals practicing IMRT. Majority of the centres (about 48%) accept the plan with 3% dose difference and 3 mm dose to distance agreement (DTA) criteria with gamma index less than unity. About 10% centres accept the IMRT treatment plan with 2% dose difference and 2 mm DTA.

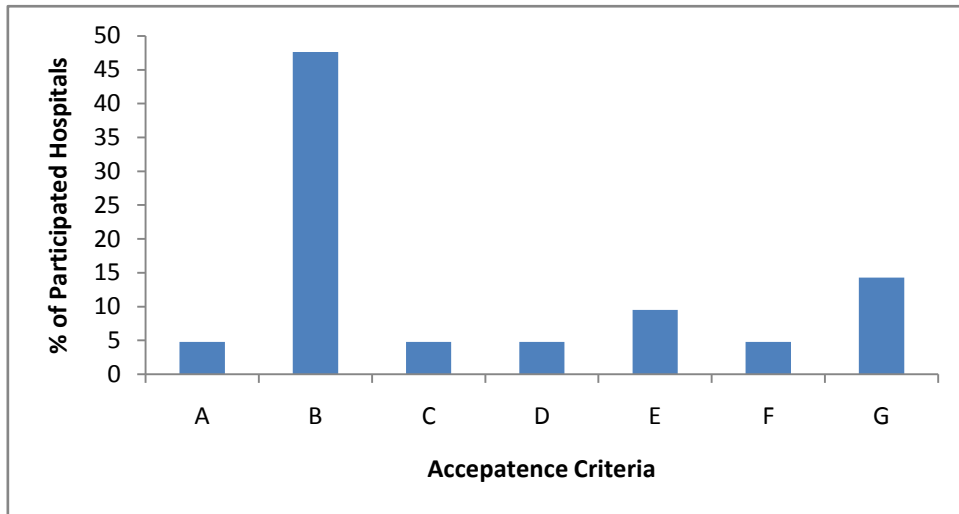


Figure 2.3: Bar diagram of the acceptance criteria of IMRT plans followed by the hospitals for pre-treatment dose verification; A: 5% dose difference and 3 mm DTA; B: 3% dose difference and 3mm DTA ; C: 3% dose difference and 3mm DTA (Large field); 2% dose difference and 2mm DTA (Small field); D: 4% dose difference and 3mm DTA (Low dose low gradient) , 3% dose difference and 3mm (High dose low gradient) 5-7% dose difference and 4mm DTA (Low dose high gradient) 3- 5% dose difference and 4mm DTA (High dose high gradient); E: 2% dose difference and 2 mm DTA ; F: 3% dose difference and 3 mm DTA/ 5% dose difference and 5 mm DTA (in some specific cases); G: inadequate information

The varying acceptance criteria, namely (i) 5% dose difference and 3 mm DTA, (ii) 3% dose difference and 3 mm DTA (large field)/ 2% dose difference and 2 mm DTA (small field), (iii) 4% dose difference and 3 mm DTA (low dose low gradient)/ 3% dose difference and 3 mm DTA (high dose low gradient)/ 5-7% dose difference and 4 mm DTA (low dose high gradient)/ 3- 5% dose difference and 4 mm DTA (high dose high gradient), (iv) 3% dose difference and 3 mm

DTA/ 5% dose difference and 5 mm DTA (in some specific cases) are followed at 20% (each of the criteria followed at 5% of the centres) of the centres while 14% of the centres provided inadequate data to understand their acceptance criteria for pre-treatment verification.

Figure 2.4 presents the bar diagram of different types of cases treated by IMRT techniques at Indian hospitals. This diagram reveals head and neck and pelvic region (abdomen, cervix, prostate) cases are treated at all the centres participated in the survey. Tumours of thorax region are treated by IMRT at about 53% of the centres.

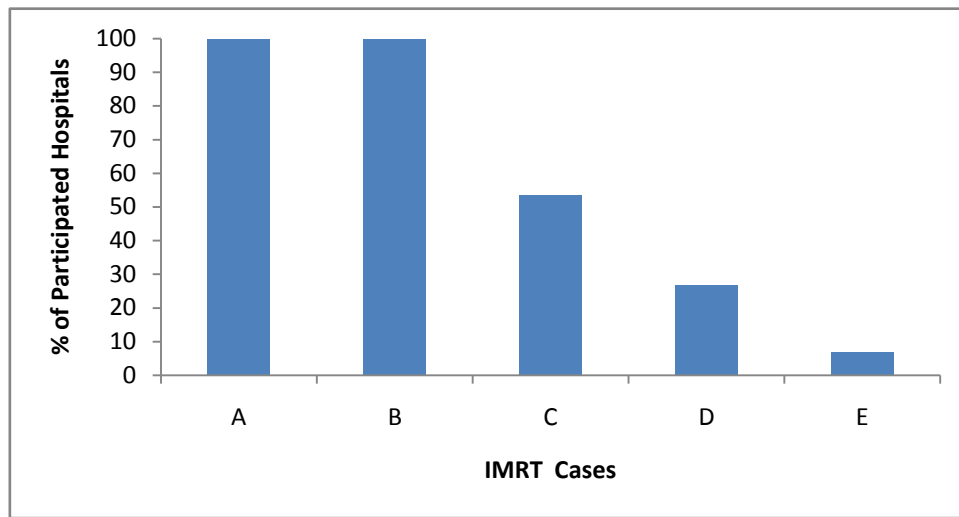


Figure 2.4: Bar diagram of IMRT treatment sites practiced at Indian hospitals (% centre of hospitals responded to the survey); A: Head and Neck, B: Pelvic Region (Abdomen, Cervix, Prostate), C: Thorax, D: Breast and, E: Lung

About 27% centres use IMRT for the breast while 7% centres use IMRT for lung cases. It can be observed from this survey that head and neck and pelvic region cases are most preferred site for IMRT in India. However, breast as well as lung cases, which are considered most complex site for the IMRT, are also treated at Indian hospitals. Considering the wide variety of cancer cases treated by IMRT in India, it is highly recommended that IMRT centres of the country should have a proper IMRT QA programme in place and external QA audit should also be initiated to ensure safety and

efficacy of this treatment technique. Evolving a unified but simple to execute QA programme to deal with all types of treatment sites will be a very important development in this direction.

In response to the question about margins for Planning Target Volume (PTV) in various cancer cases, majority of centres responded quoting margins in head and neck and Pelvic region cases only. A few centres also provided the information for PTV margins in some other cancer cases also. Most of the centres use 0.5 cm PTV margin in head and neck cases and 0.5 - 1.0 cm PTV margin in the pelvic region during IMRT planning. Very few centres reported PTV margin of 0.6 cm in head and neck and up to 1.5 cm in pelvic region of IMRT planning.

About 67% user reported that they have not detected any deviation more than acceptable limit during their dosimetric QA so far. However, about 33% users reported that they have observed deviations more than acceptable limits. These centres have indicated that erroneous measurement techniques are the reasons of this deviation from the acceptable limits. One of the hospital also informed that the deviation was due to some problem with the TPS which was later rectified. Users have reported that they perform IMRT machine specific QA periodically (monthly and quarterly) as well as after major repair on treatment delivery devices and after upgradation of software on TPS. The patient specific IMRT QA is carried out before starting the treatment of a patient. Against our query on hurdles in implementing the adequate IMRT QA programme, majority of the users have quoted their busy clinical schedule and limited availability of the equipment for QA as major hurdles in these aspects. Accordingly, they need a QA programme and test procedures which should be simple and quick to perform. Users have also suggested for a unified QA protocol in the country so that treatment outcome of different centres can be compared. Maximum preference of patient specific dosimetric QA and least preference of the TPS QA are the important observations of this survey.

In this survey a number of centres have reported QA program for delivery system and planning system similar to a conventional treatment modality which uses conventional static fields for dose delivery. Quality assurance procedures for a linear accelerator and multileaf collimator designed for conventional static fields will not be sufficient to address issues pertinent to the accuracy and precision of dose delivery by IMRT. IMRT fields are composed of many irregular, small, off-centre, and abutting field segments throughout the target volume, each delivering only a few MU. Therefore, emphasis should be placed on beam stability for small MU, leaf position accuracy with gantry rotation, Leaf speed, leaf transmission etc. IMRT delivery system is complex enough, there is requirement that tolerance limit of QA test parameter need to be stringent than a conventional medical linear accelerator. IMRT and other advance techniques need stricter performance tolerance of linear accelerator for precise dose delivery. The types of treatments delivered with the machine should have a role in determining the QA program that is appropriate for that treatment machine [Eric E. Klein *et al.*, 2009]. It is worth mentioning here that separate tolerance limit has been assigned for different QA parameters for a treatment machine capable of delivering IMRT or other advanced treatment modalities in AAPM Task Group 142 report along with conventional treatment machines.

2.3.2 Part-B: Multi-Centre Patient Specific IMRT dosimetric Inter-Comparison in India

The percentage dose differences between the measured and calculated doses are shown in table 2.3. It can be observed that variation of percentage dose differences between the measured and calculated point dose ranges from -10.27 to 13.57 with mean and standard deviation of -0.12 and 3; -10.34 to 8.5 with mean and standard deviation of 0.33 and 2.93; -10.33 to 7.64 with mean and

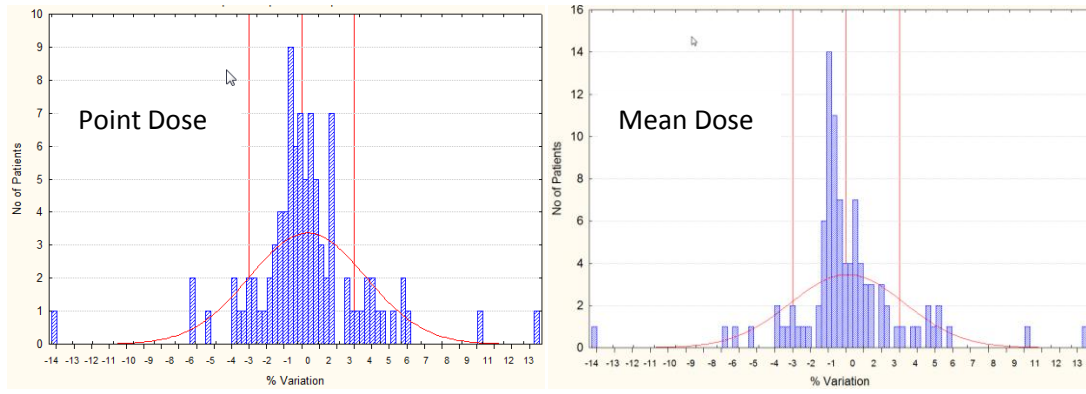
standard deviation of 0.036 and 2.97 for point dose in slab, homogeneous and inhomogeneous phantom respectively. However, the variation of percentage dose differences between the measured and calculated mean dose ranges from -9.27 to 12.26 with mean and standard deviation of -0.32 and 2.86; -10.28 to 8.5 with mean and standard deviation of 0.12 and 2.64; -11.23 to 6.44 with mean and standard deviation of 0.039 and 2.89 for slab, homogeneous and inhomogeneous phantom respectively.

Table 2.3: Dose difference observed in slab, homogeneous and inhomogeneous phantoms.

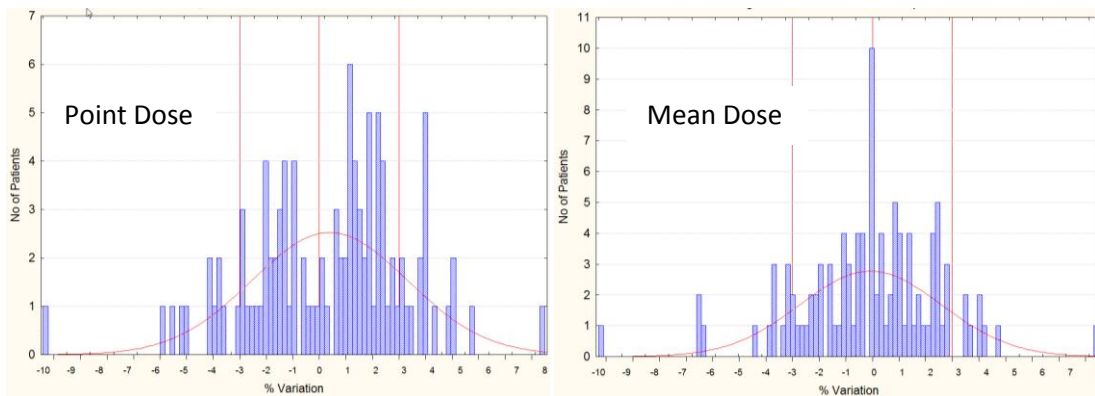
Phantom	Dose differences (%)							
	Mean		Standard deviation (s)		Maximum		Minimum	
	Point Dose	Mean dose	Point Dose	Mean dose	Point Dose	Mean dose	Point Dose	Mean dose
Slab	-0.12	-0.32	3.0	2.86	13.57	12.26	-10.27	-9.27
Homogeneous	0.33	-0.12	2.93	2.64	8.5	8.5	-10.34	-10.28
Inhomogeneous	0.036	-0.039	2.97	2.89	7.64	6.44	-10.33	-11.23

Figure 2.5 shows the distribution of differences in measured and planned dose calculated for a point and mean dose to chamber volume of individual patient. It can be inferred from the figure that the data are well distributed on both sides of zero percent of dose difference for all the phantoms. However, in slab phantom about 80% patients were within $\pm 3\%$ when measured doses are compared with mean doses of chamber volume and 76.8% when measured doses are compared

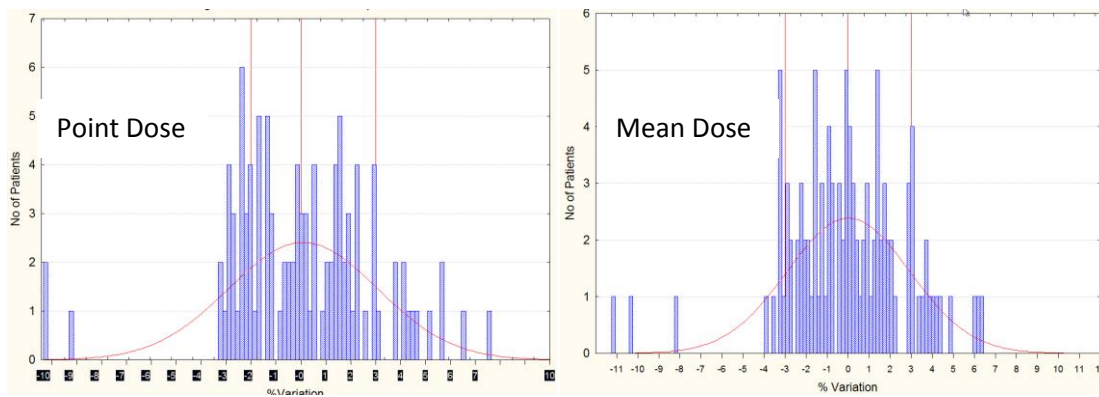
with the point dose. In case of homogeneous phantom, about 80% patients were found within $\pm 3\%$ when measured doses are compared with mean dose of chamber volume and 74% when measured doses are compared with the point dose. For inhomogeneous phantom, about 78% patients were found within $\pm 3\%$ when measured doses are compared with mean dose of chamber volume and 82.8 % when measured doses are compared with the point dose. Figure 2.6 shows the differences in measured and planned dose calculated for point and mean dose to chamber volume, specific to vendor of delivery system. Analysis of the results shown in figures reveal that differences in measured and planned doses for the vendor1 is more than 3% for a large number of the patients than vendor2 and vendor3. Centres using delivery system from the vendor1 have implemented dynamic mode of IMRT where positional accuracy of the MLC with time plays very important role while step and shoot mode of IMRT was in practice at centres using delivery system of other two vendors. From the figure 2.6 a, it can be inferred that data are almost distributed on both sides of zero percent of dose difference for vendor1 and vendor2 while data are biased towards negative dose difference for centre using delivery system of vendor3. However, such finding was not seen in figure 2.6b and 2.6c where data are generated using homogenous and in-homogenous phantoms. It may be noted that the number of the centres selected in this study using the machine of vendor1 is more so patients' data available for the vendor1 is also large. It is thus difficult to conclude that the source of error is vendor specific. Figure 2.7b shows the differences in measured and planned dose calculated hospital wise for point and mean dose to chamber volume in slab, homogeneous and Inhomogeneous phantoms. Analysis of the result shown in figure indicates that for most of the patients, variations between measured and planned doses are within 3%.



(a): Slab Phantom

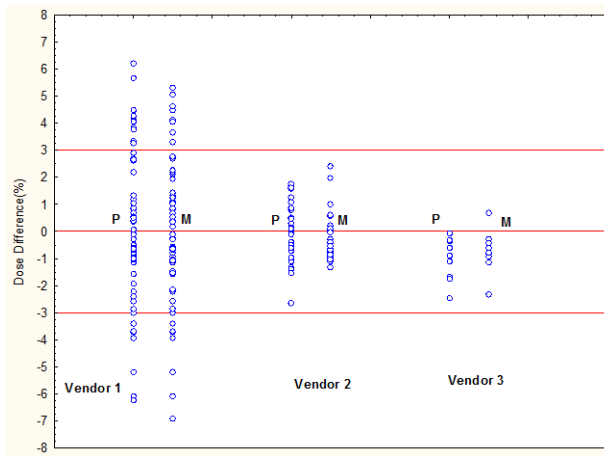


(b): Homogeneous Phantom

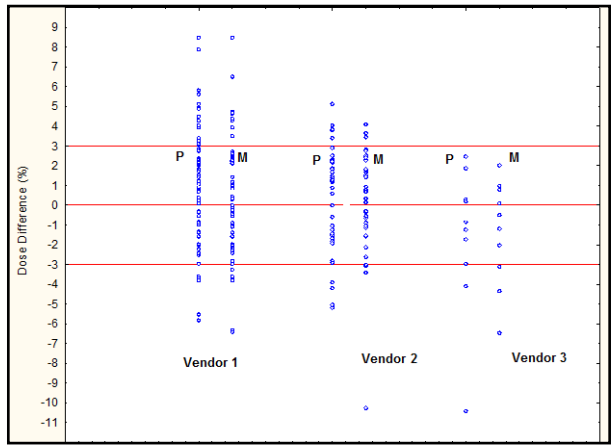


(c): Inhomogeneous Phantom

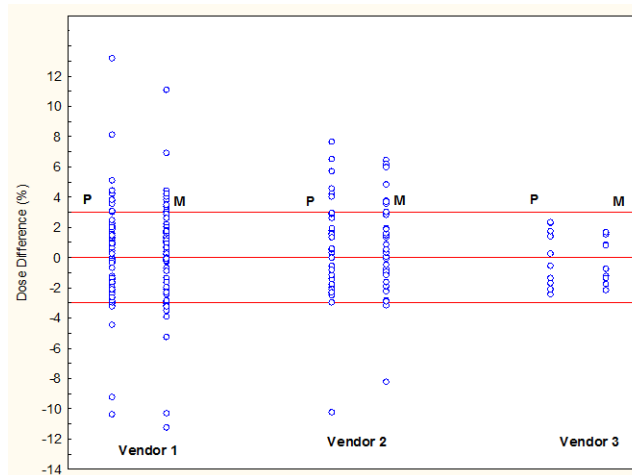
Figure 2.5: Distribution of differences in measured and planned dose calculated for a point and mean dose to chamber volume



(a): Slab Phantom



(b): Homogeneous Phantom



(c): Homogeneous Phantom

Figure 2.6: Differences in measured and planned dose calculated for point and mean dose to chamber volume in Inhomogeneous Phantom (Vendor wise)

However, for some hospitals these data are biased, they are either positive or negative. Such observations indicate some kind of systematic error in the overall commissioning process. It can

also be observed that for some hospitals, some patient's data are out of tolerance limit of 3% which are attributed to the higher dose gradient in the chamber volume.

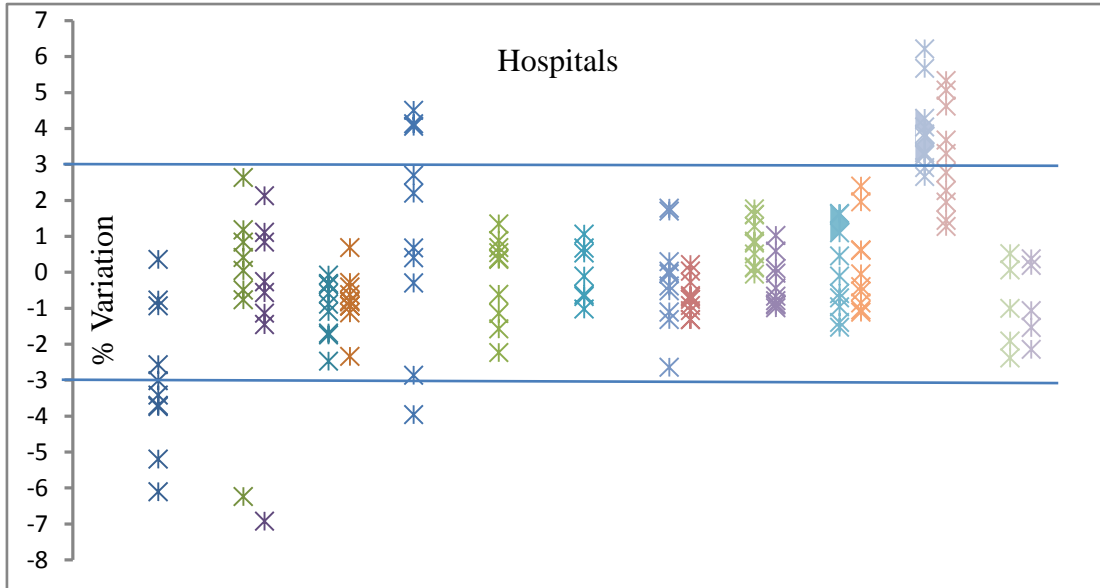


Figure 2.7a: Differences in measured and planned dose calculated for point and mean dose to chamber volume in Slab Phantom (Hospital wise)

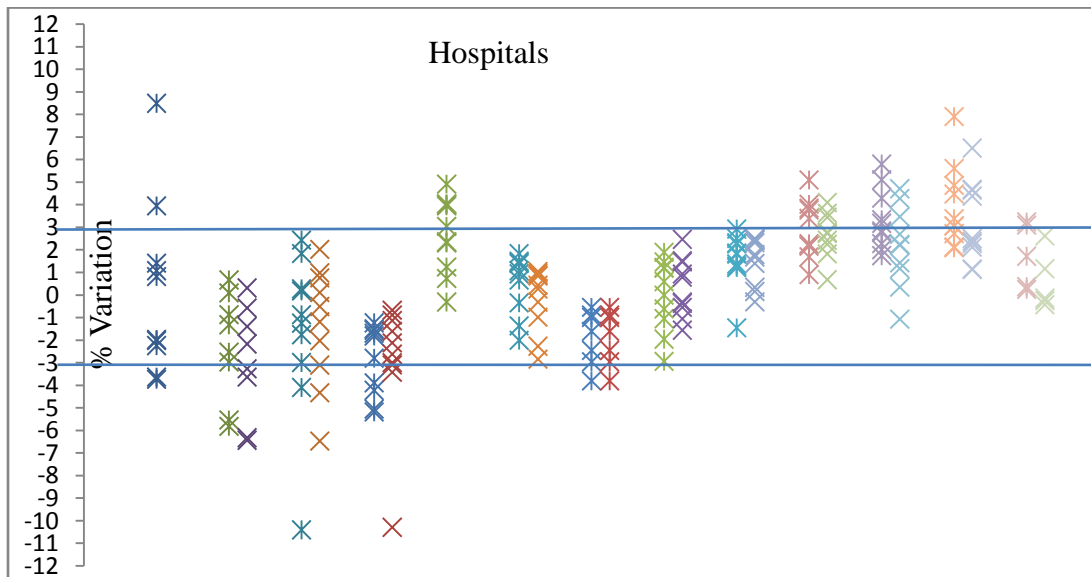


Figure 2.7b: Differences in measured and planned dose calculated for point and mean dose to chamber volume in Homogeneous Phantom (Hospital wise)

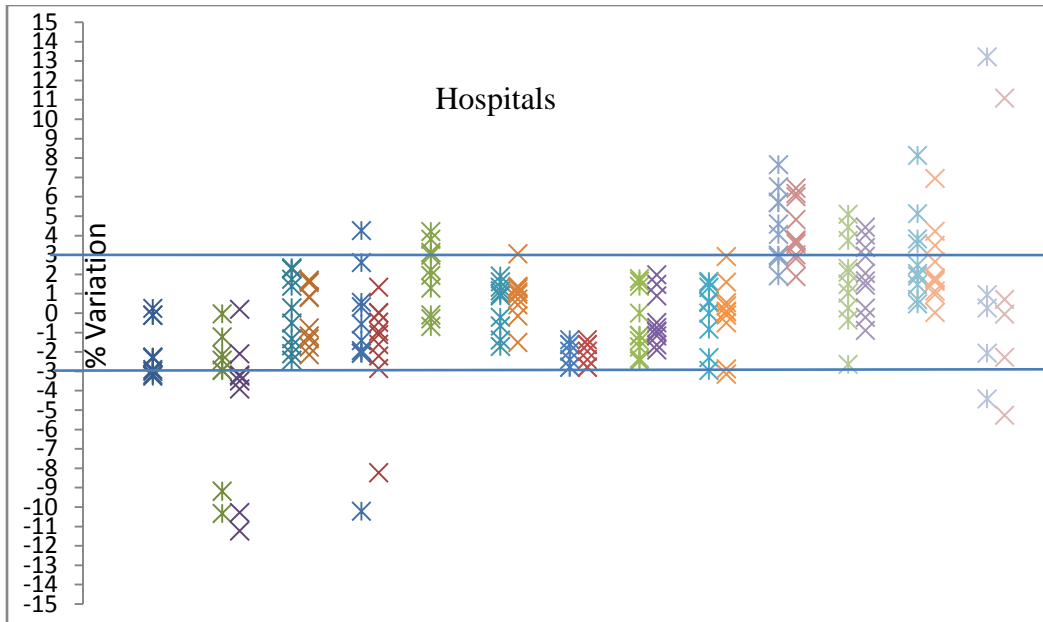


Figure 2.7c: Differences in measured and planned dose calculated for point and mean dose to chamber volume in In-homogeneous Phantom (Hospital wise)

Results of comprehensive study on IMRT dosimetry QA by point dose measurement method shows that for most of the patients' differences in measured and planned doses are within 3%, however for certain numbers of patients, differences in measured and planned doses are more than 3%. It is also observed that agreement between TPS calculated mean dose in sensitive volume of ionisation chamber with measured dose are better than agreement between TPS calculated point dose with measured dose. This observation is irrespective of the type of the phantom. The roles of different type of phantoms on overall dosimetry QA results are not very significant. However, option of locating the chamber in less dose gradient region is needed. It can be achieved by moving the couch and redefining the QA in the TPS. Slab phantom is sufficient for IMRT dosimetry QA without compromising the significant information. However, if the hospitals are using the slab phantom as IMRT QA phantom, a stringent periodic QA program for MLC and delivery system should be in place to assure that system performance is as per the expectation at different gantry angles.

2.3.3 Part-C: Analysis of Patient Specific Dosimetry Quality Assurance Measurements in Intensity Modulated Radiotherapy: A Multi Centre Study

The results of statistical analysis of difference between measured and planned doses of different hospitals having medical electron linear accelerator of vendor 1 are shown in Table 2.1c. Table contains mean, median, SD, range, minimum and maximum of percentage variation in difference between D_{TPS} and D_{Meas} . In addition, the table also presents percentage of cases with positive (+ve) and negative (-ve) dose difference along with percentage of cases having dose difference within $\pm 3\%$. The mean values of percentage variation in difference between D_{TPS} and D_{Meas} of the six hospitals are found to be from -1.79 to 1.48 and median from -1.79 to 1.48 . The SDs of these hospitals are found to be from 0.076 to 2.91 . The range of variation at these centers varies from 3.99 to 15.4 while minimum and maximum values of percentage variation in difference between D_{TPS} and D_{Meas} ranges from -9.41 to 7.9 . The percentage of cases having positive dose difference ranges from 8 to 94 while the percentage of cases having negative dose difference ranges from 6 to 92 . The percentage of cases having dose difference within $\pm 3\%$ varies from 74 to 100 . The data of hospital 1 (H1) and hospital 2 (H2); hospital 3 (H3) and hospital 4 (H4); and hospital 5 (H5) and hospital 6 (H6) show the similar trend and hence they were grouped as Group A (H1 and H2), Group B (H3 and H4) and Group C (H5 and H6) hospitals, respectively. Figure 2.1c presents the histogram of the dose difference between measured and planned dose values of Group A hospitals. It can be observed from this figure that the dose differences of these hospitals are skewed toward negative side. Figure 2.2c presents the histogram of dose difference between measured and planned dose values of Group C hospitals.

Table 2.4: Results of statistical analysis of difference between measured and planned doses of different hospitals having medical electron linear accelerator of vendor 1

Parameters	H1	H2	H3	H4	H5	H6
No. of patients	227	105	146	160	151	145
Mean	-1.79	-0.66	-0.14	0.38	1.48	1.31
Median	-1.85	-0.87	0.32	0.27	1.7	1.38
Standard deviation	1.53	1.07	2.91	1.89	2.09	0.76
Range	13.8	7.77	14.9	15.4	13.7	3.99
Minimum	-8.5	-2.42	-9.4	-7.5	-5.57	-1.00
Maximum	5.3	5.35	5.5	7.9	7.13	2.99
Percentage of measured dose with +ve deviation	8	17	57	56	81	94
Percentage of measured dose with -ve deviation	92	83	43	44	19	6
Percentage of data within $\pm 3\%$ variation	83	99	74	94	78.80	100
H1, H2, H3, H4, H5 and H6 are the identification number of the hospitals						

It can be seen from this figure that the dose difference data are skewed towards positive side. Figure 2.3c presents the histogram of dose difference between measured and planned dose values of Group B hospitals. It can be seen from this figure that the dose difference data of these hospitals are randomly distributed. The results of statistical analysis of dose difference data of hospital 7 (H7) and hospital 8 (H8) equipped with medical electron linear accelerator of vendor 2 are given in Table 2.5. It can be observed from the data in this table that the mean values of percentage variation in difference between D_{TPS} and D_{Meas} of these hospitals are found to be -0.30 and 1.51 ; median values are -0.12 and 1.57 . The SDs of these data is found to be 0.94 and 3.7 .

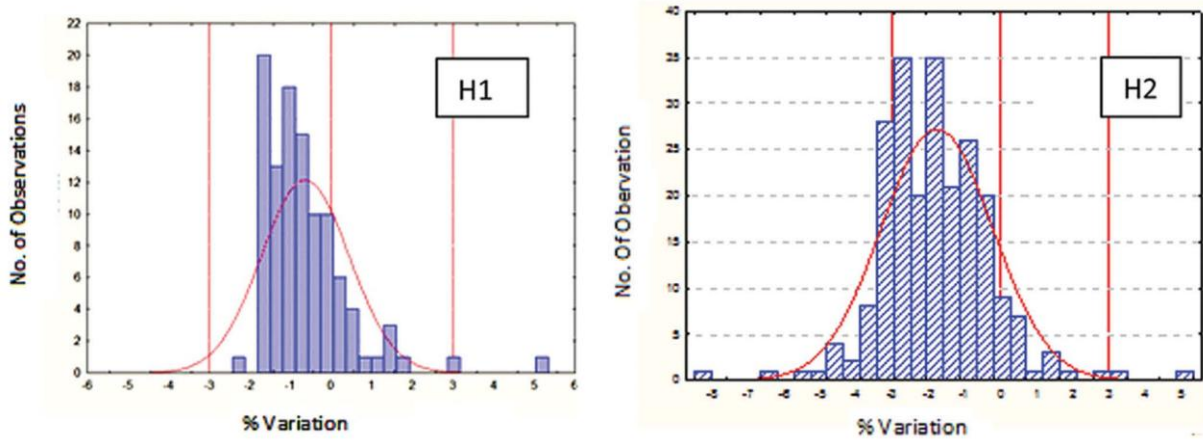


Figure 2.8: Histogram of the measured and planned dose difference of Group A hospitals (H1 and H2) using medical electron linear accelerator of vendor 1 for intensity-modulated radiotherapy delivery

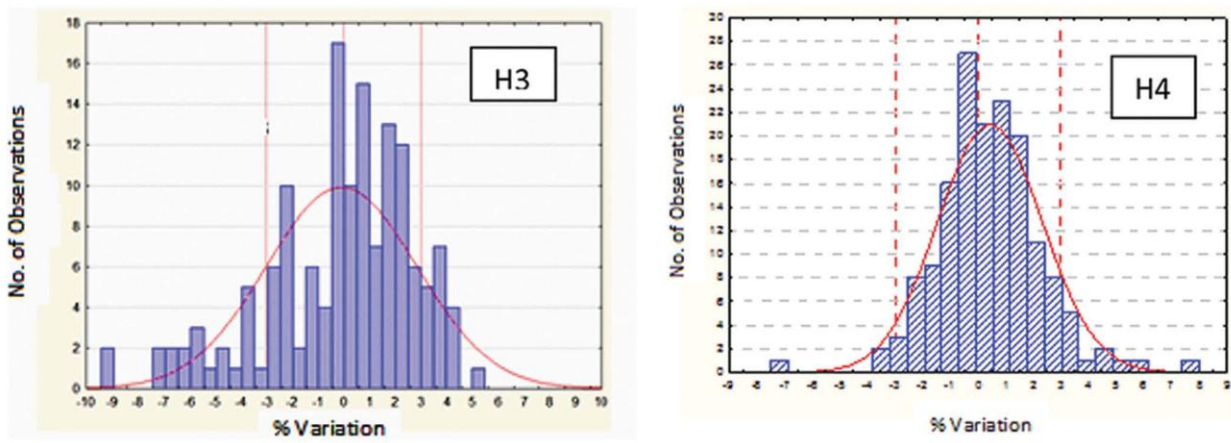


Figure 2.9: Histogram of the measured and planned dose difference of Group B hospitals (H3 and H4) using medical electron linear accelerator of vendor 1 for intensity-modulated radiotherapy delivery

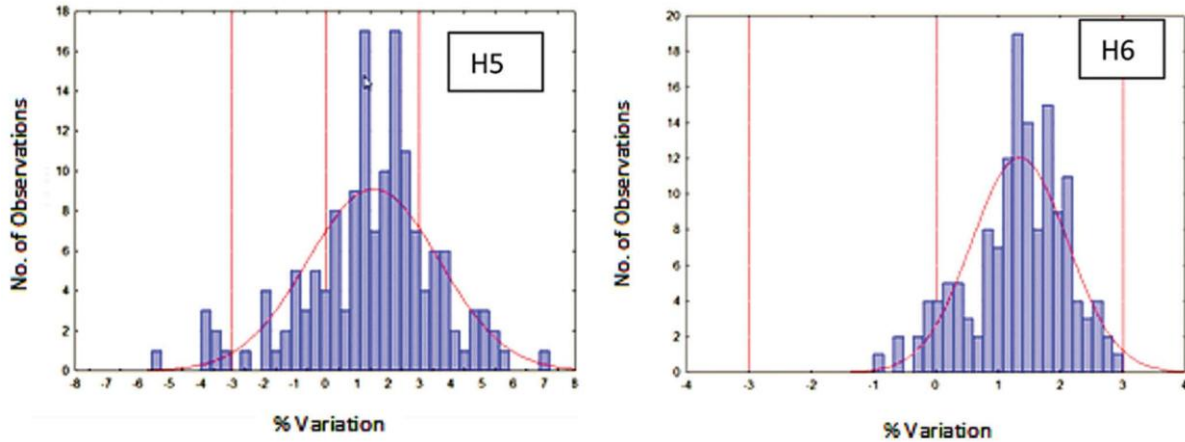


Figure 2.10: Histogram of the measured and planned dose difference of Group C hospitals (H5 and H6) using medical electron linear accelerator of vendor 1 for intensity-modulated radiotherapy delivery.

The range of variation in dose difference of these centers is 5.73 and 9 while minimum and maximum values of percentage variation in difference between D_{TPS} and D_{Meas} ranges from -10.33 to 13.38 . The percentage of cases having positive dose differences of these hospitals are 31 and 43. The percentage of cases having negative dose difference are 57 and 69. The percentage of cases having dose difference within $\pm 3\%$ varies from 57 to 100. Figure 2.11 presents the histogram of the dose difference between measured and planned dose values of H7 and H8. It can be seen from this figure that the dose difference data of these hospitals are almost randomly distributed. Table 2.6 shows the results of statistical analysis of dose difference data of hospital 9 (H9) and hospital 10 (H10) equipped with medical electron linear accelerator of vendor 3. The mean, median and SD of percentage variation in difference between D_{TPS} and D_{Meas} of these hospitals are found to be from -0.43 to 1.15 , from -0.43 to -1.01 and from 1.76 to 2.52 , respectively. The range in dose difference of these centers varies from 10.82 to 16.45 while minimum and maximum values of

percentage variation in difference between D_{TPS} and D_{Meas} ranges from -6.89 to -8.97 and 3.93 to 7.48 , respectively.

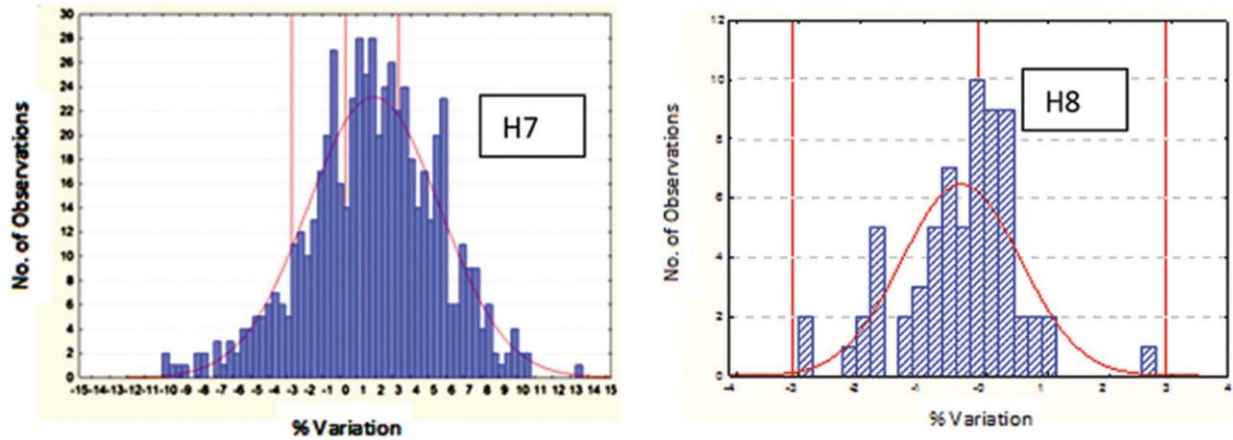


Figure 2.11: Histogram of the measured and planned dose difference of hospitals H7 and H8 using medical electron linear accelerator of vendor 2 for intensity-modulated radiotherapy delivery

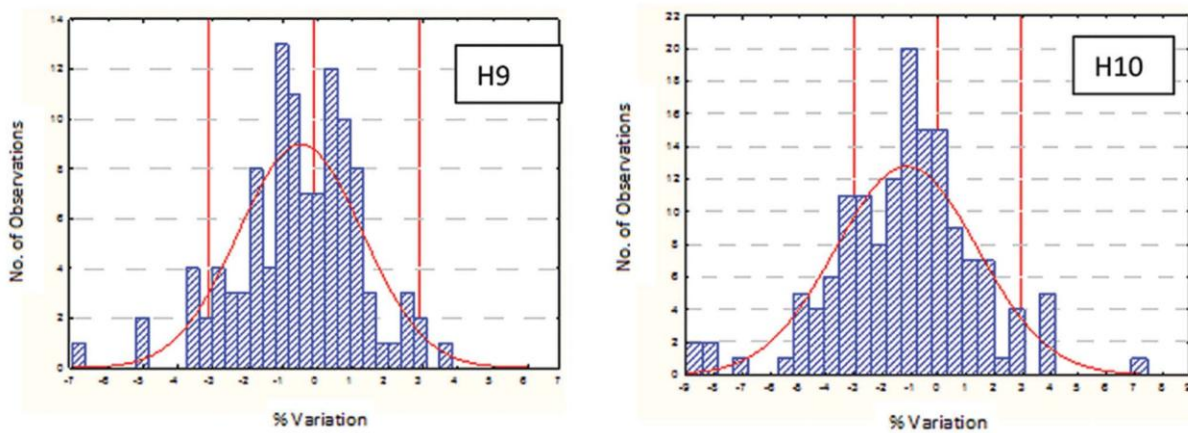


Figure 2.12: Histogram of the measured and planned dose difference of hospitals H9 and H10 using medical electron linear accelerator of vendor 3 for intensity-modulated radiotherapy delivery

Table 2.5: Results of statistical analysis of difference between measured and planned doses of different hospitals having medical electron linear accelerator of vendor 2

Parameters	H7	H8
No. of patients	590	67
Mean	1.51	-0.30
Median	1.57	-0.12
Standard deviation	3.70	0.94
Range	9.00	5.73
Minimum	-10.33	-2.89
Maximum	13.38	2.84
Percentage of measured dose with +ve deviation	31	43
Percentage of measured dose with -ve deviation	69	57
Percentage of data within $\pm 3\%$ variation	57	100
H7 and H8 are the identification number of the hospitals		

Table 2.6: Results of statistical analysis of difference between measured and planned doses of different hospitals having medical electron linear accelerator of vendor 3

Parameters	H9	H10
No. of patients	110	147
Mean	-0.43	-1.15
Median	-0.43	-1.01
Standard deviation	1.76	2.52
Range	10.82	16.45
Minimum	-6.89	-8.97
Maximum	3.93	7.48
Percentage of measured dose with +ve deviation	62	31
Percentage of measured dose with -ve deviation	58	69
Percentage of data within $\pm 3\%$ variation	93	78
H9 and H10 are the identification number of the hospitals		

The percentage of cases having positive and negative dose difference ranges from 31 to 62 and from 58 to 69, respectively. The percentage of cases having dose difference within $\pm 3\%$ varies from 78 to 93. Figure 2.12 presents the histogram of the dose difference between measured and planned dose values of H9 and H10. It can be seen from this figure that the dose difference data of these hospitals are almost randomly distributed.

Results of intercomparison of IMRT dose verification studies have been reported by a number of investigators [Gillis et al 2005, Clark et al 2009a, Van Esch et al 2002, Clark et al 2009b, Budgell et al 2011, Ibbott et al 2006, 2008, Schiefer et al 2010]. ESTRO QUASIMODO study revealed maximum local deviation of less than 3.5% in the mean planned and measured dose values for the PTV and mean local deviation of 1.4%. However, local deviations in planned and measured dose values for the OAR were up to 5.8% [Gillis et al 2005]. In case of IMRT dose verification by ionization chamber, AAPM TG 119 reported 4.5% difference between measured and planned doses in the target region for 95% of the test cases [Ezzell et al 2009]. PARSPORT Trial Management Group have reported for two-dimensional dose comparison, 94% passing rate in gamma criteria of 3%/3 mm for individual fields and 75% in gamma criteria of 4%/3 mm for combined fields were proposed in multi-center head and neck IMRT trials [Clark et al 2009a, Low et al 2003].

The acceptance criteria of pre-treatment patient specific IMRT QA for point dose at the most of the radiotherapy centers is $\pm 3\%$ and for gamma index it is 3%/3 mm [Kumar et al 2010]. It can be inferred from the results presented in of Tables 2.1c - 2.3c that percentage variation in difference between D_{TPS} and D_{Meas} is more than the acceptable limit except H6. In case the dose difference is more than the acceptance limit, the doubt goes to the limitation of point dose measurement method and if the point of measurement is within the high dose gradient zone, the measured dose may

differ by more than $\pm 3\%$. In such cases ideally a point of low dose gradient should be identified and dosimetry measurements should be repeated. However, this is not a common practice for all the radiotherapy centers in India. Because, some of the individuals assume that the error may be due to the high dose gradient at the point of measurement and they do not repeat the dosimetry measurements by identifying a suitable measurement point of relatively low dose gradient.

The sources of error between measured and planned doses are broadly attributed to positioning errors of MLC, insufficient dosimetric data of MLC in TPS, inaccurate handling of small field dosimetry, human errors and inaccurate measurement devices for IMRT QA procedures [Jang et al 2008, Das et al 2008, Papatheodorou et al 2000, Xing et al 1999, Capote et al 2004]. The other reported source of error in TPS can be the tongue and-groove effect that often results in the systematic under-dosage [Deng et al 2001, Li 2010]. It is also reported that, highly-modulated treatment plans are more sensitive to accuracies of the above sources of errors than a mildly-modulated plans [Kruse 2010].

Chung *et al.* 2011 in their study have reported that in case of dynamic IMRT, the tongue and grove effect could be a reason for systematic under-dosage where treatment planning has been done using the older version of the Eclipse treatment planning system. They have also reported that with upgraded version of the TPS there were no noticeable systematic biases.

Sarkar *et al.* 2010 have reported a biased variation in difference between D_{TPS} and D_{Meas} where they have used the Elekta precise as treatment delivery machine and Nucletron Plato sunrise as the treatment planning system and they have address, variation is biased even for the open field dosimetry and pointed out systematic error in the TPS commissioning as one of the reasons.

We have observed that there are IMRT centers having random and biased (skewed towards over or under dose) distribution of the percentage variation in difference between D_{TPS} and D_{Meas} , while they are having the TPS and beam delivery systems of the same vendor [Figures 2.1c-2.3c]. Similarly, the dose difference data of H8 [Figure 2.4c] and H10 [Figure 2.5c] are more biased while the dose difference data of hospitals H7 [Figure 2.4c] and H9 [Figure 2.5c] are random in nature.

Budgell *et al.* 2011 have carried out dosimetric audit of IMRT implementation in over 90% of radiotherapy centers in UK. Their audit result shows that IMRT TPS modeling and delivery is accurate, suggesting that the implementation of IMRT has been carried out safely. They have also reported a histogram of percentage variation in difference between the ion chamber measurements relative to predicted doses which is random in nature. In addition, they have reported that percentage error is ranging from -14% to 20% with the mean difference of 0.02% and SD of 3.1% . However, we observed that dose difference is having biased distribution for the hospitals included in this study.

This study also reveals that there are systematic errors involved in dosimetry and planning and delivery at these radiotherapy centers. The sources of error are not common in nature. This analysis suggests that in implementations of IMRT, some parameters in the chain have not been properly tuned. Though the magnitude of discrepancy is not alarming but certainly need correction. This work suggests a strong justification for a third party verification of the commissioning of treatment delivery and planning system before commissioning of IMRT treatments. If there would have been a third party mechanism for verification in place such unpredicted variation would not have been observed. It is important to identify the actual cause of discrepancy at these radiotherapy centers through a systematic dosimetry approach.

2.4 Conclusions

A national survey on IMRT QA by means of a properly designed questionnaire was carried out at 40 radiotherapy centres in India. The survey reveals that majority of Indian hospitals have adequate machine specific IMRT QA programme but highly inadequate QA programme for the treatment planning systems. Pre-treatment dose verification is carried out at almost all the centres but measurement techniques and plan acceptance criteria are institution specific. Thus, a variety of IMRT QA program in totality is being followed at the Indian hospitals. There is a need to evolve a national protocol for IMRT QA so that treatment outcomes of all the IMRT centres of country can be compared. Onsite IMRT dosimetry QA in India was carried out using different types of phantoms. The type of the phantom does not play significant role in overall results of point dose based dosimetry QA. Mostly, the variations in planned and measured doses are within the tolerance limit. However, certain hospitals data are biased in one direction. Dose verification data acquired by the hospitals as part of their institutional pre-treatment dose verification program in IMRT were collected, and the statistical analysis of these data was conducted to assess the quality of the IMRT practice. This study reveals that IMRT centers are having random and biased (skewed towards over or under dose) distribution of the percentage variation in difference between measured and planned doses, while they are using the TPS and beam delivery systems of the same vendor. The analysis of results of the IMRT pre-treatment dose verification also reveals that there are systematic errors in the chain of IMRT treatment process at a few centers included in this study. The dosimetry quality audit prior to commissioning of IMRT may play an important role in avoiding such discrepancies.

CHAPTER 3

DEVELOPMENT OF LOW COST TISSUE EQUIVALENT PHANTOM FOR DOSIMETRY QA IN IMRT

3.1 Introduction

As an outcome of our IMRT QA survey, it was observed that the radiotherapy centres in the country are having some kind of pre-treatment patient specific dose verification programme. However, it is highly disorganised in nature making impossible to intercompare the results of institutions. One of the limitations in having the harmonised pre-treatment patient specific dose verification programme is the non-availability of a low cost versatile tissue equivalent IMRT phantom which can be universally used for such purposes. It is important to highlight here that a number of IMRT phantom with facility for holding different types of detectors are available commercially for this purpose [CIRS USA, IBA dosimetry Sweden, Standard Imaging USA, Civco USA]. Majority of these phantoms are made up of Solid / Plastic water material. Though these phantoms are suitable for pre-treatment dose verification in IMRT but they are very costly and some of these have limited measurement options. Therefore there is a need to design and fabricate IMRT phantom which is made up of tissue equivalent material with options to verify the dose at a point and obtain dose distribution in 2-D & 3-D. In addition, the phantom should be made available to Indian users at affordable costs. In the light of these requirements, a versatile IMRT phantom was designed and fabricated from a low cost tissue equivalent material. The tissue equivalency of a material for the dosimetry purpose depends on type and energy of the radiation. In the case of photon beam, total attenuation coefficient and in case of electron beam, stopping power of the material should be comparable with that of the tissue at the given energy of radiation [ICRU Report-44, 1989]. Acrylonitrile Butadiene Styrene (ABS) plastic was used as tissue equivalent material for fabrication of IMRT phantom. This ABS plastic phantom was used for the

pre-treatment dose verification measurement in IMRT using ionization chamber, TLDs, radiochromic and radiographic film to demonstrate its suitability. A few measurements were also carried out with a commercially available Scanditronix-Wellhofer IMRT RW3 phantom (IBA dosimetry, Uppsala, Sweden) to compare the results obtained using ABS IMRT phantom. This paper describes the design features of ABS plastic IMRT phantom and measurement results of pre-treatment dose verification.

3.2 Materials and Methods

An IMRT phantom was designed and fabricated using tissue equivalent material commercially known as Acrylonitrile Butadiene Styrene (ABS) plastic. Cost of a sheet of 1.2x2.4 m² of thickness 5 mm is about \$ 200. ABS [(C₈H₈·C₄H₆·C₃H₃N)_n] is a copolymer made by polymerizing acrylonitrile and styrene in the presence of polybutadiene. The composition of ABS is: acrylonitrile -15 to 35%; butadiene - 5 to 30% and styrene- 40 to 60%. Electron density of the phantom material relative to water was estimated by importing its CT scanned images to a recently calibrated treatment planning system for electron density as well as by numerical evaluation using chemical composition of ABS. The total attenuation coefficient for the phantom material was also calculated using attenuation coefficient of its constituent elements. Table 3.1 presents dosimetry related physical parameters of commonly used phantom materials along with ABS for ⁶⁰Co gamma rays and 6 and 15 MV X-rays. These data indicate that physical parameters of the ABS are comparable to other standard phantom materials. The ABS phantom is in elliptical in shape with dimensions sufficient to provide full scatter conditions similar to the irradiation of a patient. Fig. 3.1 shows the schematic line diagram of ABS plastic IMRT phantom.

Table 3.1: Physical properties of common phantom materials and ABS plastic. The data for ABS plastic was numerically calculated from its elemental composition.

Energy	Material	Effective Z	Electron Density relative to water	Physical Density Relative to water	Attenuation coefficient (μ/ρ) ($\times 10^{-2} \text{ cm}^2/\text{g}$)
Co-60	Water	7.42	1.000	1.00	6.32
	PMMA	6.47	1.03	1.19	6.14
	Polystyrene	5.69	0.97	1.06	6.12
	Solid water (WT1)	7.54	0.97	1.02	6.23
	RW-3	-	0.97	1.04	6.11
	ABS	5.76	0.98	1.04	6.14
	6MV	Water	7.42	1.00	1.00
PMMA		6.47	1.03	1.19	4.80
Polystyrene		5.69	0.97	1.06	4.78
Solid water (WT1)		7.54	0.97	1.02	4.80
RW-3		-	0.97	1.04	4.77
ABS		5.76	0.98	1.04	4.80
15MV		Water	7.42	1.00	1.00
	PMMA	6.47	1.04	1.19	2.30
	Polystyrene	5.69	0.97	1.06	2.90
	Solid water (WT1)	7.54	0.97	1.02	2.92
	RW-3	-	0.97	1.04	2.89
	ABS	5.76	0.98	1.04	2.90

This phantom has two parts, namely the first part which has provisions to incorporate ionization chambers, TLD discs, radiochromic films and gel dosimeter while the second part has the provision to hold radiographic film only. First part is design in such a way that cylindrical ionization chamber can be positioned within a $1 \times 1 \times 1 \text{ cm}^3$ spaced grid in the central region of the phantom. The positioning of the chamber within $1 \times 1 \times 1 \text{ cm}^3$ spaced grid is possible by moving suitable compensating inserts. Three fiducial marks are also available in the first part of the phantom for its reproducible positioning. The second part of the phantom consists of elliptical slice of thickness 1 cm and each of these slices contains three fiducial marks to identify the film orientation.

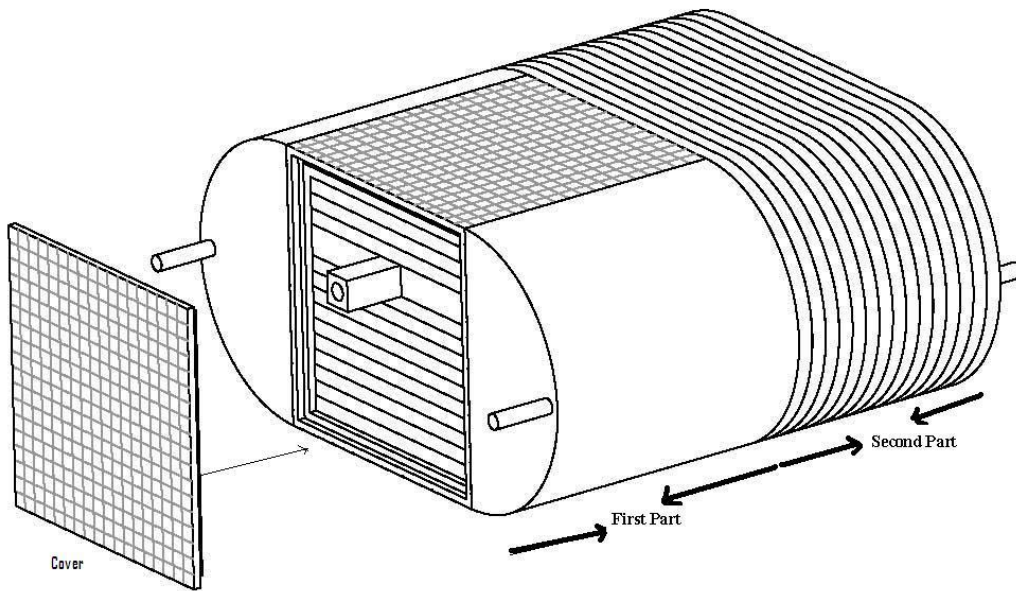


Figure 3.1: Schematic line diagram of ABS plastic IMRT phantom.

Fig. 3.2(a) shows the cubical insert of size $15 \times 15 \times 15 \text{ cm}^3$ which has a cylindrical hole of diameter 8 cm where the gel dosimeter container can be positioned. A large polymer gel sample can be used for the acquisition of dose distributions for entire target volumes. The large gel volume allows a dose distribution measurement of a large target volume and sometimes neighboring critical

structures as well. Fig 3.2(b) shows the line diagram and Fig. 3.2(c) shows the photograph of radiochromic film holder where radiochromic film sample of size $15 \times 15 \text{ cm}^2$ can be sandwiched between the plates to form a stack. This stack of radiochromic film can be used for the two dimensional as well as three dimensional dose distribution analysis. The ABS phantom has provision to hold a TLD tray in which TLDs of diameter 4.5 mm and thickness 0.8 mm can be arranged at a spatial resolution of 7 mm (center to center). Fig. 3.3 shows the final assembly of the fabricated ABS plastic IMRT phantom.



Figure. 3.2(a): Holder for Gel dosimeter container.

The suitability of ABS plastic phantom in IMRT dose verification was tested in comparison with Scanditronix-Wellhofer IMRT RW3 phantom. For this purpose pre-treatment dose verification was carried out for five different cases of carcinoma prostate treated by IMRT. Volumetric CT scan (GE Discovery, WI, USA) of the ABS plastic phantom, with ionization chamber (FC65G;

IBA dosimetry, Uppsala, Sweden) located at 5 cm from its proximal surface, using the slice width of 3 mm was taken for the point dose verification. The volumetric CT scan data of the ABS plastic phantom was transferred to the Brain SCAN v5.2 (BrainLAB AG, Germany) treatment planning system.

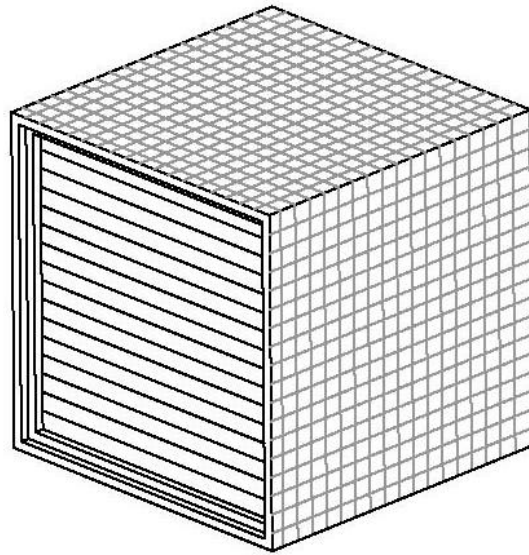


Figure 3.2(b): Schematic line diagram of radiochromic film holder.



Figure 3.2(c): Photograph of radiochromic film holder.

IMRT treatment plans of the patient of carcinoma prostate were planned on the phantom assuming the center of ion chamber as the centre of the tumor. The optimized plan so generated was transferred to the Varis Vision network system (Varian Medical Systems, Palo Alto, CA) and planned doses were delivered to the phantom at the pre-defined position of the chamber with 6 MV photon beam using Varian Clinac 2300 CD (Varian Medical Systems, Palo Alto, CA). The reading of the ionization chamber was converted into absorbed dose to water using methodology described in the IAEA TRS 398 [IAEA TRS-398 2000]. Treatment plan and dose verification were carried out for five different cases of carcinoma prostate. The point of measurement was located in a low dose gradient zone for each of evaluated IMRT treatment plans. The experiment was repeated on a commercial IMRT phantom to compare the dose measurement carried out using the ABS plastic phantom. A number of IMRT treatment plans were transferred to ABS plastic and Scanditronix-Wellhofer RW3 IMRT phantom and dose at equal physical depth were calculated and measured to verify the equivalent of ABS plastic with RW3 as phantom material for the dosimetry purpose.

To demonstrate the use of various detectors in the ABS IMRT phantom, the dose verification measurements were carried out using radiographic film, radiochromic film and TLD along with ionization chamber. Radiographic film (EDR2 film Eastman Kodak Company, Rochester, NYd) was placed in the second part of phantom and was irradiated as per the planned IMRT treatment. Readout of the EDR2 film was carried out using VIDAR Dosimetry Pro Advantage scanner (VIDAR Systems Corporation, Herndon, VA). This way the EDR2 film gave the dose distribution data in the transverse plane. The calibration of EDR2 was carried out in 6 MV x-ray beam. A 15x15 cm² Gafchromic EBT films (Gafchromic EBT; ISP Inc. NJ, USA) was position in the first part of the phantom at a depth of 5 cm and was irradiated as per the planned

IMRT treatment. The irradiated film was read by flatbed scanner (EPSON Expression 10000XL; EPSON, UK). Scanning was done using the EPSON SCAN software with all filters switched off. The images were scanned in transmission mode and saved in RGB uncompressed tagged image file format (TIFF). For EBT films, the absorption peak falls in the red region and therefore the red component of the image was extracted to maximize film readout using ImageJ software (ImageJ 1.41o; National Institute of Health, USA). This way the Gafchromic EBT film gave the dose distribution data in the coronal plane. 2D dosimetric analysis of scanned images was carried out using the IMRT dose verification software (OmniPro-IMRT version 1.5; IBA dosimetry, Uppsala, Sweden). To obtain a calibration curve for EBT film, the film samples of size 4x 4 cm² were positioned in a conventional solid phantom perpendicular to the radiation beam and irradiated with 6 MV X-ray in the known dose range: 50, 100, 200, 300 and 400 cGy. The exposed film samples were scanned in similar manner as mentioned above. A dose response curve was plotted and best fit of these data was used to determine unknown dose values from the knowledge of OD of exposed films using the polynomial expression: $D = a \cdot OD + b \cdot OD^c$

Where a, b and c are free fitting parameters [Ferreira et al 2009].

TLD tray holding LiF: Mg, Ti (MTS-N; TLD, Poland) discs of diameter 4.5 mm and thickness 0.8 mm was position in the first part of the phantom at a depth of 5 cm and was irradiated as per the planned IMRT treatment. The readouts of the TLD discs were taken 24 h after irradiation using a TLD reader (Rexon UL320, USA) with programmable temperature profile. TL readout was taken in integration mode. The standard annealing and analysis process for the TLDs were followed to obtain dose data from the exposed TLDs. The calibration of TLD discs was also carried out in 6 MV X-rays.

3.3 Results and Discussion:

Table 3.2 shows the TPS calculated dose values at a point in Scanditronix-Wellhofer IMRT RW3 phantom and ABS plastic phantom for five different cases of prostate cancer treated by IMRT using 6 MV X-rays. The table also includes ionization chamber measured dose values in these two phantoms at the same points where the dose was calculated by the TPS. A survey of data in this table indicates that TPS calculated and ionization chamber measured dose values at corresponding points in Scanditronix-Wellhofer IMRT RW3 phantom and ABS plastic phantom agree within 2% for all the five cases. If we assume TPS calculated dose as reference dose values then it can easily be concluded from these observations that these two phantoms are quite suitable for pre-treatment dose verification in IMRT.

Table 3.2: TPS calculated and ionization chamber measured dose values in Scanditronix-Wellhofer RW3 and ABS plastic IMRT phantoms.

Case	Calculated and ionization chamber measured dose values and their deviations						
	Scanditronix-Wellhofer RW3 IMRT phantom			ABS plastic IMRT phantom			
	TPS (Gy)	Ionization Chamber (Gy)	% variation	TPS (Gy)	Measured Dose (Gy)	% variation	
1	2.28	2.32	-1.8	2.34	2.30	1.7	
2	2.23	2.24	-0.45	2.22	2.26	1.8	
3	2.1	2.06	1.9	2.11	2.07	1.9	
4	2.23	2.22	0.45	2.19	2.20	-0.5	
5	2.23	2.20	1.3	2.24	2.20	1.8	

Table 3.3 lists the TPS calculated and ionization chamber measured dose values at 5 cm depth in Scanditronix-Wellhofer IMRT RW3 phantom and ABS plastic phantom for five different cases of prostate cancer treated by IMRT using 6 MV X-rays. The TPS calculated dose values in the two phantoms agree with each other within 0.5% for three cases and it shows variation of 2.63% in one case. The ionization chamber measured dose values in these two phantoms agree within 1%. It can be concluded from the data in Table 3.3 that measured as well as calculated doses at a given point in these two phantoms are in agreement with each other. As Scanditronix-Wellhofer IMRT RW3 phantom is a tissue equivalent phantom; the ABS plastic IMRT phantom can also be assumed to be a tissue

Table 3.3: TPS calculated and ionization chamber measured dose values at 5 cm depth in Scanditronix-Wellhofer RW3 and ABS plastic IMRT phantoms.

Case	Calculated and measured dose and their deviations					
	TPS (Gy)			Ionization chamber (Gy)		
	Scanditronix-Wellhofer RW3 Phantom	ABS plastic IMRT phantom	% deviations	Scanditronix-Wellhofer RW3 Phantom	ABS plastic IMRT phantom	% deviations
1	2.28	2.34	-2.63	2.32	2.30	0.86
2	2.23	2.22	0.45	2.24	2.26	-0.89
3	2.1	2.11	-0.48	2.06	2.07	-0.49
4	2.23	2.19	1.79	2.22	2.2	0.90
5	2.23	2.24	-0.45	2.2	2.2	0

equivalent phantom. However, the cost of ABS plastic phantom is about 8-10 times lower than the cost of Scanditronix-Wellhofer IMRT RW3 phantom and similar other commercial phantoms with equivalent features.

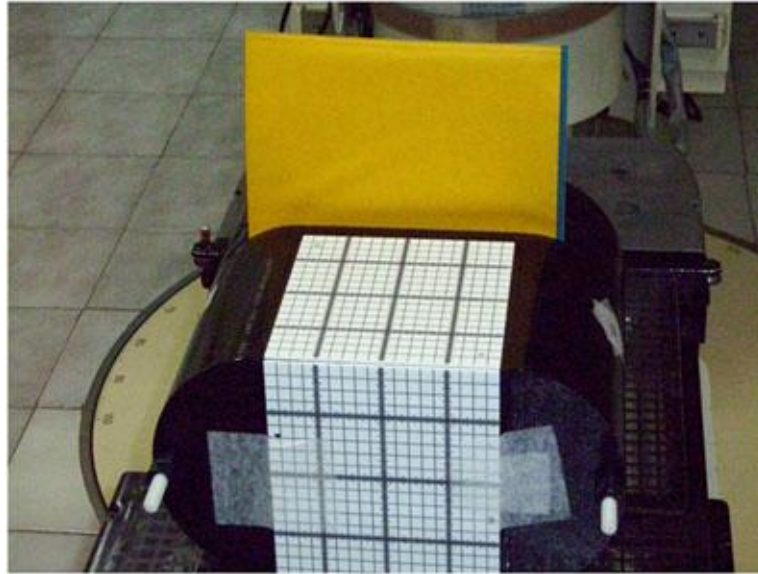


Figure 3.3: Final assembly of the locally fabricated IMRT phantom.

Point doses measured using EBT Gafchromic film in ABS plastic IMRT phantom were found to be within 0.6% in comparisons of TPS calculated dose value. However, the dose measured using TLD discs at the same point were found to be within 2.8%. Fig.3.4 shows (a) Fluence map in coronal plane recorded on Gafchromic EBT film of an IMRT plan in ABS plastic phantom, (b) TPS generated fluence map in coronal plane of an IMRT plan, (c) Comparison of isodose lines recorded on Gafchromic EBT film in ABS plastic phantom and TPS generated isodose line of an IMRT plan in coronal plane, and (d) Gamma analysis of an IMRT plan. Figs. 3.4 and 3.5 indicate close agreement between the information recorded on Gafchromic EBT/ EDR2 films in ABS plastic phantom and TPS generated data for the IMRT plan of a patient.

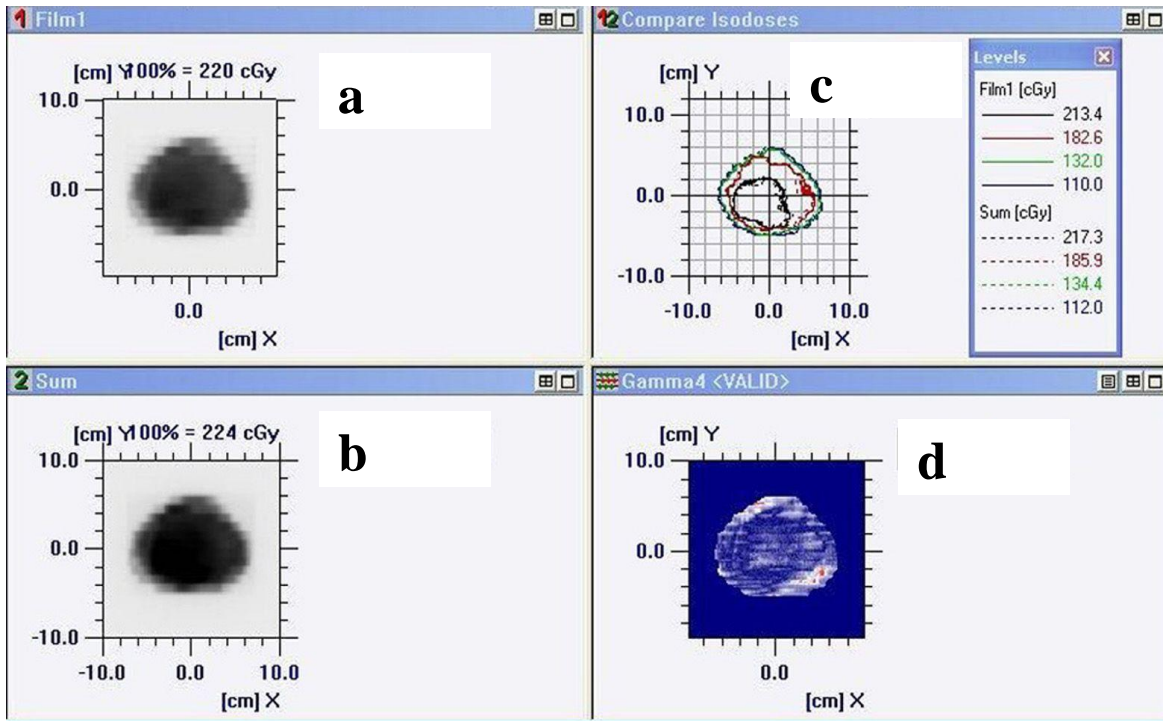


Fig. 3.4: (a) Fluence map in coronal plane recorded on Gafchromic EBT film of an IMRT plan in ABS plastic phantom, (b) TPS generated fluence map in coronal plane of an IMRT plan, (c) Comparison of isodose lines recorded on Gafchromic EBT film in ABS plastic phantom and TPS generated isodose line of an IMRT plan in coronal plane, and (d) Gamma analysis of an IMRT plan.

Fig. 3.5 shows (a) Fluence map in transverse plane recorded on EDR2 film of an IMRT plan in ABS plastic phantom, (b) TPS generated fluence map in transverse plane of an IMRT plan, (c) Comparison of isodose lines recorded on EDR2 film in ABS plastic phantom and TPS generated isodose line of an IMRT plan in transverse plane, and (d) Gamma analysis of an IMRT plan. The correlation coefficient of plans recorded on Gafchromic EBT/ EDR 2 films in ABS plastic phantom were found to be better than 0.990 for the region of interest. The measured dose distribution by EBT/ EDR2 films agreed in the region of interest with the planned dose distribution that passed 3%, 3 mm gamma-index evaluation.

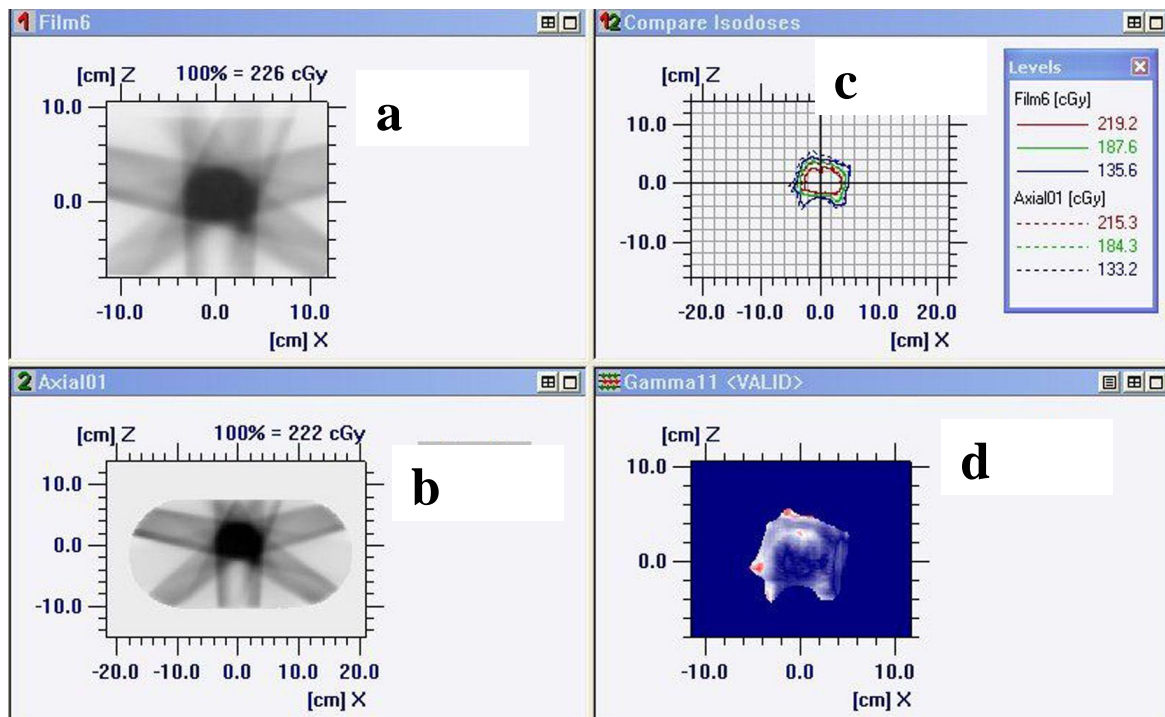


Figure 3.5: (a) Fluence map in transverse plane recorded on EDR2 film of an IMRT plan in ABS plastic phantom, (b) TPS generated fluence map in transverse plane of an IMRT plan, (c) Comparison of isodose lines recorded on EDR2 film in ABS plastic phantom and TPS generated isodose line of an IMRT plan in transverse plane, and (d) Gamma analysis of an IMRT plan.

3.4 Conclusions

A novel IMRT phantom was designed and fabricated using ABS plastic. The studies carried out on this phantom indicate that it is equivalent to plastic/solid water IMRT phantom available commercially. The ABS phantom is a versatile tissue equivalent phantom which can be used for pre-treatment dose verification in IMRT using different types of radiation detectors. The phantom is suitable for dosimetry in 1-D, 2-D and 3-D. Although the present work demonstrate its usefulness in the context of IMRT dose verification only, the phantom material has a wider application as tissue equivalent material for other dosimetry purposes in radiotherapy.

CHAPTER 4

DEVELOPMENT OF PHANTOM AND METHODOLOGY FOR IMRT DOSIMETRIC QUALITY AUDIT FOR THORAX REGION

4.1 Introduction

It is clear from the literature survey, for a precise delivery of IMRT, all steps in the treatment chain need to be accurately managed. Institutional pre-treatment verification is basically a self-evaluation which is prone to miss systematic errors that may be involved in the planning, treatment, and dose analysis procedures. In addition, pre-treatment measurement provides the validation of dose computation accuracy in a phantom, plan parameter transfer from the radiotherapy planning system to the treatment console, and MLC performance for each individual plan. The methods and items that are selected for validating IMRT are rather dependent upon the criteria/decision of each institution. Results of chapter 2 reveal that data of a few hospitals are biased in one direction. The hospitals under this study were having random and biased (skewed towards over or under dose) distribution of the percentage variation in difference between measured and planned doses, while they are using the TPS and beam delivery systems of the same vendor. These results indicate that there are systematic errors in the chain of IMRT treatment process at these centres. Thus dosimetry quality audit prior to commissioning of IMRT may play an important role in avoiding such discrepancies.

A number of national/ international bodies have developed various types and levels of external quality audit programmes for radiotherapy [Derremaux et al 1995, Bridier et al 2000, Ferreira et al 2000 & 2001, Gomola et al 2001, Izewska and Andreo 2000, Marre et al 2000, Swinnen et al 2002, Izewska et al 2002 & 2003 & 2004, Kroutilikova et al 2003, Rassiah et al 2004 and Roue et al 2004]. Many countries in the world, both developing and developed, are providing dosimetry audit

service in conventional radiotherapy. However, a few countries only such as Australia, Finland, UK and US are conducting dosimetry audit in IMRT.

There are three major TLD networks offering postal dose audits, namely (i) the IAEA/WHO (World Health Organization) TLD postal dose audit programme, which operates worldwide; (ii) the ESTRO (European Society for Therapeutic Radiology and Oncology) system, EQUAL, set up for the European Union countries, and (iii) the Radiological Physics Center (RPC) network in North America. Out of these three major audit network, IAEA/WHO TLD audit postal program is limited to Non IMRT type treatment techniques. A complete QAu by personnel from outside the institution is expensive and time consuming. QAu by mailed dosimeters is therefore an alternative to fulfil partially the requirements stipulated under audit programme by national/ international agencies. IAEA in collaboration with World Health Organization (WHO) through the networks of Secondary Standard Dosimetry Laboratories (SSDL) is conducting postal audit on international scale from last three decades (since 1969). Radiation Standards Section of Radiological Physics and Advisory Division, BARC conducts postal audit programme for radiotherapy centres in India and its neighbouring countries (e.g. Nepal, Sri Lanka). The postal audit of RSS is based on IAEA/WHO TLD method and is an audit programme of limited nature. The growth of IMRT centres in India is increasing at rapid rate. To improve the quality of IMRT/VMAT in the country, third party remote quality audit program will play major role. To fulfil this requirement, there is a need to develop phantoms and methods to implement the dosimetry audit program in the country for such complex treatment techniques. In this connection postal dosimetric audit phantom was designed, fabricated and characterised for the said purpose. This chapter describes the newly developed postal QAu phantoms and methodology for IMRT dosimetric quality audit for thorax region.

4.2 Materials and Methods

4.2.1 Design of Phantoms: Anatomy specific IMRT dosimetry audit phantom representing the thorax region was designed, developed and fabricated for postal dosimetry audit in IMRT (Figure 4.1). This phantom has two main sub-assemblies. Part-A is main phantom body and Part-B is a removable part which contains the PTV and OAR structure along with the detector system. The Part-B can be taken out and after placing the detectors, it can be fitted into the Part-A of the phantom to complete the system (Figure 4.2). Figure 4.3 presents photograph showing locations of TLDs and Gafchromic Film for point and planar dose verification. The radiochromic film is placed in sagittal plane so that the impact of maximum MLC leaves involved in IMRT treatment can be monitored. Part-B of phantom contains four pins to prick the radiochromic film to locate the isocentre on it. The phantom is made up of elliptical shape perspex of dimension 30 cm x 17 cm x 15 cm with lung equivalent, bone equivalent, tissue equivalent inserts. The cedar (popularly known as deodar in India) wood, Teflon and ABS plastic was used as lung equivalent, bone equivalent and tissue equivalent materials, respectively. In this phantom, the PTV is a C shaped structure that surrounds a central avoidance structure referred as OAR. The OAR is a cylinder of 2 cm radius. The gap between the OAR and the PTV is 0.5 cm, so the inner arc of the PTV is 2.5 cm in radius. The PTV is 6 cm long and the core is 8 cm long. The phantom has the provision to carry out 1-D and 2-D dosimetry quality audit using the TLD and radiochromic films. The PTV and OAR are made up of black colour ABS so that TLDs can be replaced by Optical stimulated luminescence dosimeter (OSLD). Positional marking on the body surface of the phantom has been provided for its reproducible positioning with the help of laser of treatment delivery machine. The locations of pins to prick the radiochromic film are properly aligned with positional marking on the body surface of the phantom.

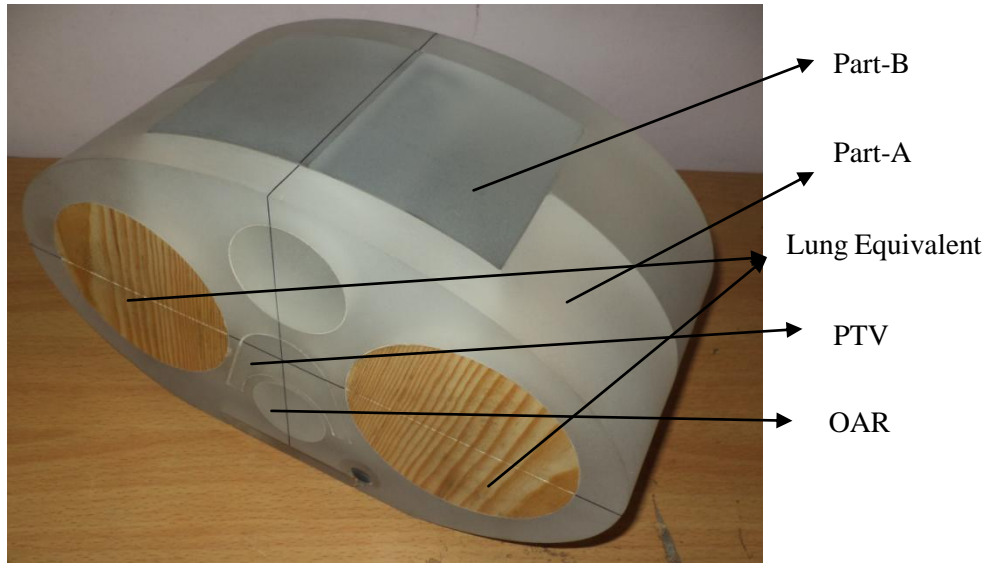


Figure 4.1: Photograph showing IMRT Audit Phantom

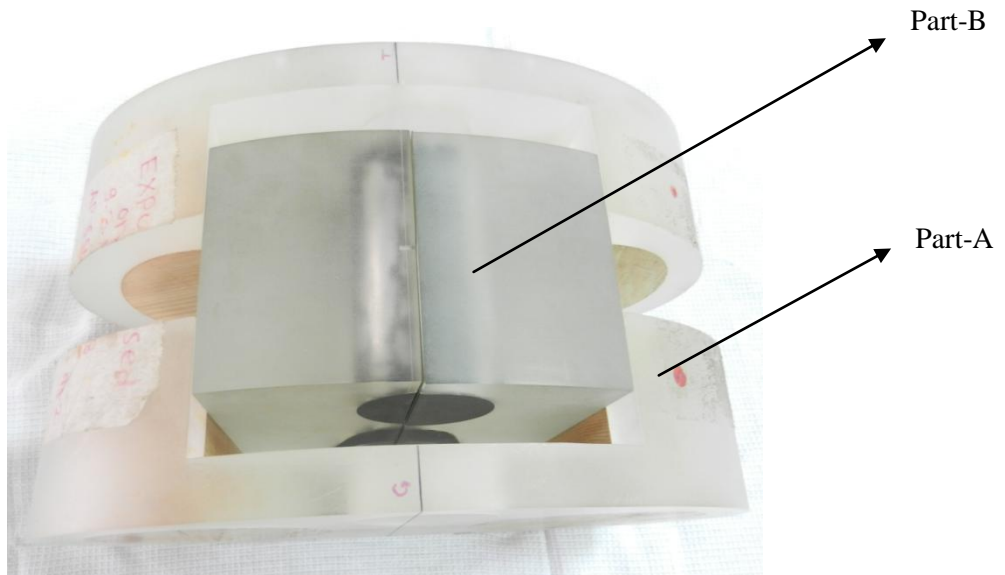


Figure 4.2: Photograph showing removal of Part B containing PTV OAR and Detectors

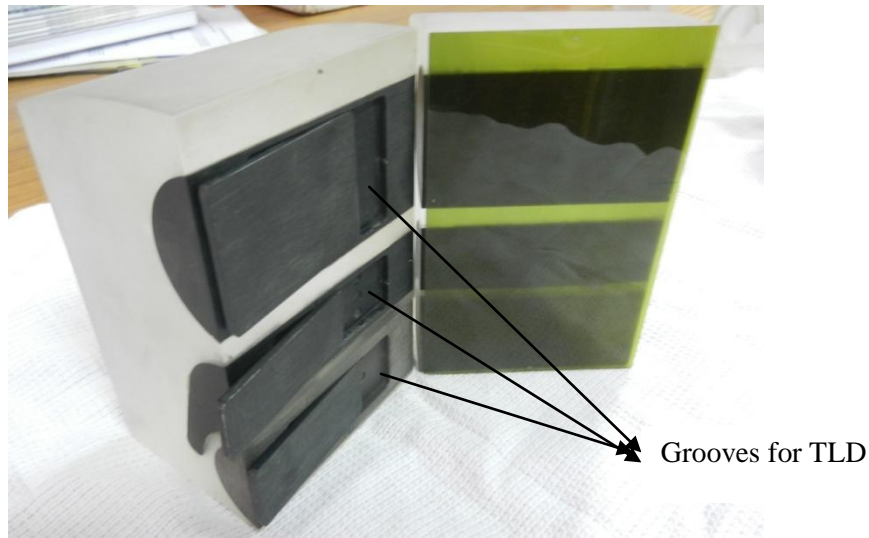


Figure 4.3: Photograph showing locations of TLDs and Gafchromic Film for point and planar dose verification.

4.2.2 Gafchromic film and Epson Expression 10000XL flatbed scanner:

Gafchromic EBT (Ashland ISP Advanced Materials, NJ, USA) is a self-developing radiochromic film (Figure 4.4). It is composed of an active radiochromic layer of thickness 30 μm , which is laminated between two 125 μm matte polyester layers and makes a symmetric structure, different to the asymmetric structure of its predecessor EBT2 (Reinhardt et al 2012).

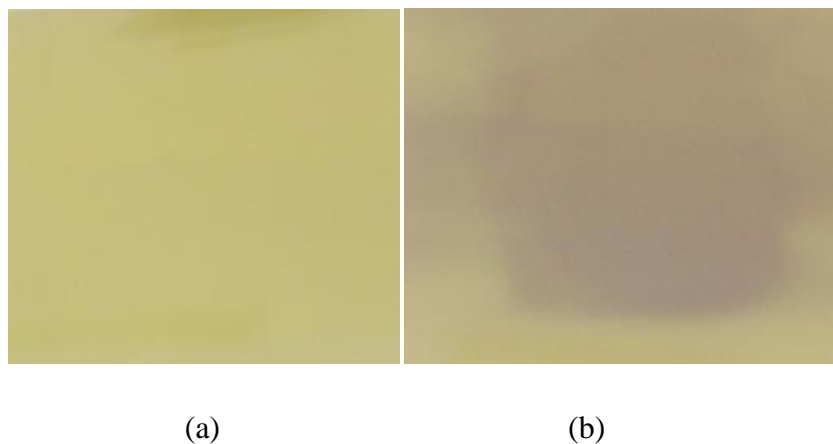


Figure 4.4: Photographs showing EBT3 Film (a) unexposed and (b) exposed for IMRT irradiation.

A model of EBT3 film structure is presented in figure 4.5. The overall physical density of EBT3 film is about 1.33 gm/cc while physical densities of polyester and active monomer are 1.35 gm/cc and 1.20 gm/cc respectively. The total physical thickness and water equivalent thickness of the film are 0.28 mm and 0.37 mm respectively. The matte polyester contains microscopic silica spheres at the surface to eliminate Newton's Rings scanner artefacts in images obtained using a flatbed scanner.

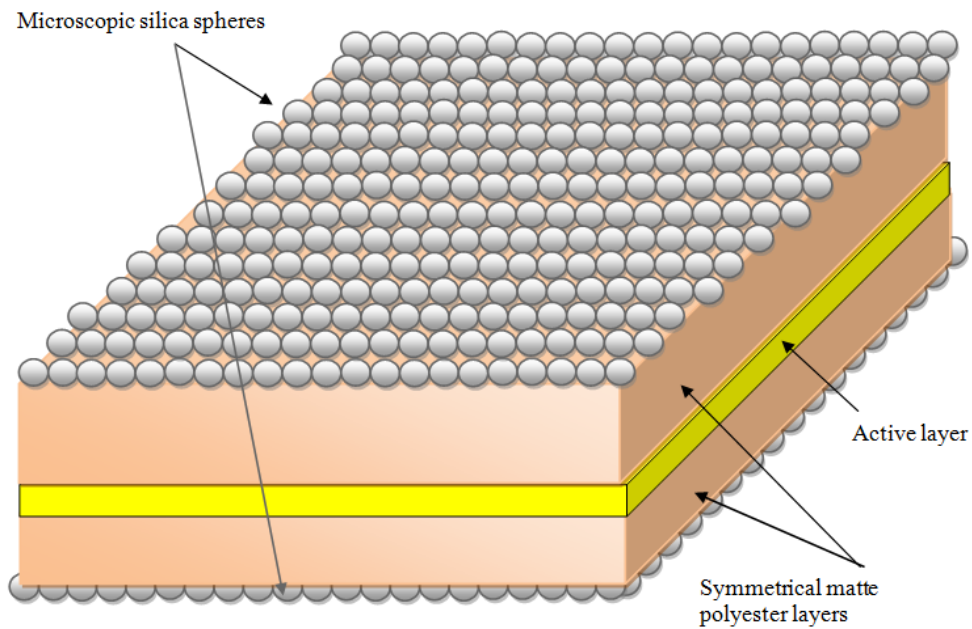


Figure 4.5: Schematic diagram of EBT3 Gafchromic film

The yellow colour of the film arises from the presence of a yellow dye incorporated in the active layer. A marker dye within the active layer is included for the correction of small thickness variations, using multiple colour channels (wavelengths) to correct for the film non-uniformity. The effective atomic number of EBT3 film ($Z_{\text{eff, EBT3}}$) is 6.84 and is close to effective atomic number of water ($Z_{\text{eff, water}} = 7.3$) [Arjomandy et al 2010] while the effective atomic number for

active monomers is 8.27. Gafchromic EBT film incorporates the lithium salt of pentacosanoic acid, 12-diynoate (LiPAD) as active monomer.

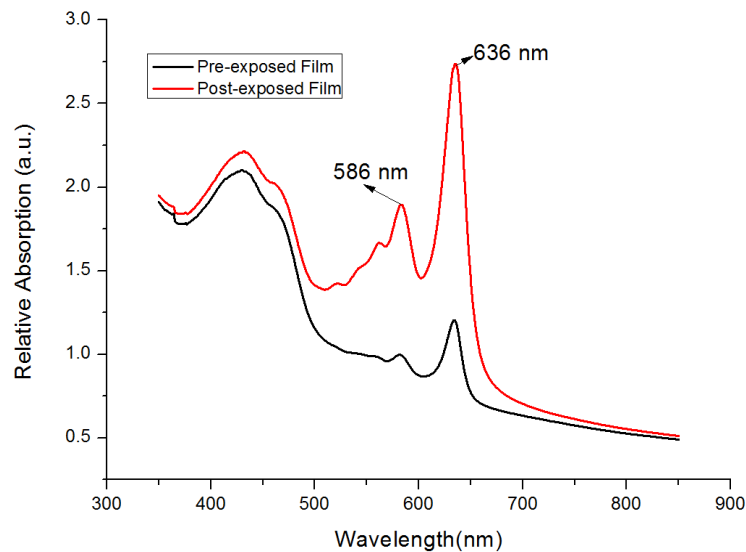


Figure 4.6: Absorption spectra of pre and post exposed EBT3 film.

The absorption spectrum of EBT3 film before and after the irradiation can be seen in the figure 4.6. The major absorption peak can be observed at 636 nm in red region of visible light. Characteristics and applications of Gafchromic EBT3 film for radiotherapy dosimetry have been studied in detail by a number of researchers [Crijns et al 2013, Casanova et al 2013, Sorriaux et al 2013, Lewis et al 2012, Devic et al 2012]. As per the manufacturer's specification, this film has been designed to measure doses up to at least 30 Gy when used with an RGB colour scanner. At doses above 10 Gy the response in the red colour channel approaches saturation, so in the case of single channel dosimetry it is preferable to change to the green colour channel for these measurements. While it may be possible to extend measurement to 50 Gy or higher by using the response in the blue channel, this has not been thoroughly investigated. EBT3 film performance is unaffected with brief exposures (e.g. <1min.) to temperatures up to 70°C, or prolonged exposure (e.g. <1 day) at 50°C.

Epson Expression 10000XL (Figure 4.7) is a colour flatbed scanner with CCD line sensor as light detectors and Xenon gas cold cathode fluorescent lamp as light source. This scanner is equipped with transparency adaptor with transparency size of 309.88 x 419.1 mm². The maximum scan area is 309.88 x 419.1 mm². Optical resolution of this system is 2400 dpi. Maximum interpolated resolution can be obtained up to 12800 dpi. During scanning of the Gafchromic films, all the image adjustment features of scanner were disabled (figure 4.8). As film were used for postal audit program, response of the film at different temperatures which may arise during transport, were studied. Film response in temperature ranges from 40 °C to 60 °C at regular intervals of 5 °C was investigated. For this purpose, pieces of the film were kept at temperatures of 40 to 60 °C for period of one hour and responses of the films were studied by irradiating the film to a dose of 2 Gy.



Figure 4.7: Photograph of flatbed scanner used in this work

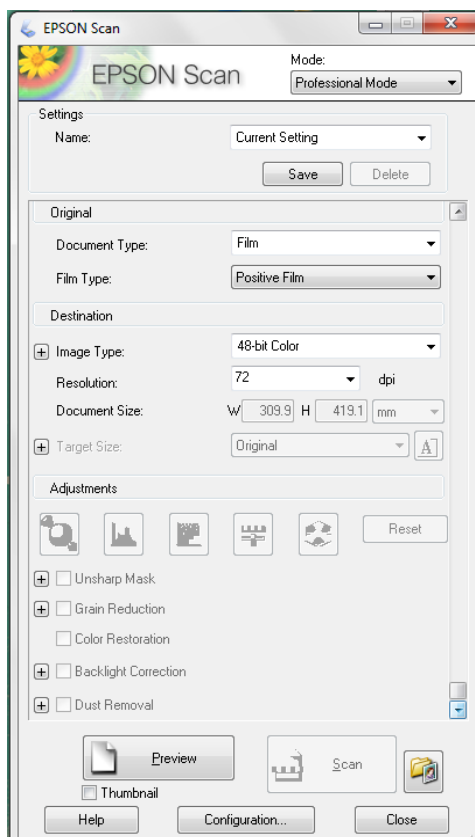


Figure 4.8: Screenshot showing scanner setting used during scanning of Gafchromic film

The calibration of film was carried out in 6 MV x-ray beam by keeping the film at the depth of 5 cm where the absorbed dose to water was predetermined using methodology described in the IAEA TRS 398. For Calibration, EBT3 films were irradiated to 25, 50, 100, 150, 200, 300 and 400 cGy.

4.2.3 TLDs and TLD Reader:

The TL material used is lithium fluoride (LiF: Mg, Ti) disc of size 3.6 mm diameter and 0.15 mm thickness, (type TLD-100). The effective atomic number (Z_{eff}) of TLD-100 is 8.2 and physical density is 2.64 gm/cc. Relative Lithium concentration in TLD-100 for ^6Li and ^7Li are 7.5% and 92.5% respectively. Thermal neutron produces about 1/7 the amount of TL produced by gamma or X-rays due to the ^6Li component. The TL emission spectra of TLD-100 range from 250-600 nm

and maximum emission is found at about 400 nm. The useful range of this dosimeter ranges from a few mR to 10^5 mR. Before each irradiation, the TL discs were annealed at 400°C for 1 hour followed by fast cooling and subsequent annealing at 100°C for 2 hours.

TLD reader (Figure 4.9) used for this work is model UL-230 manufactured by REXON TLD Systems, USA. This reader system can be used for reading of TL dosimeter in various forms such as rod, disc chips and powder. Direct contact heating with linear time/temperature profile is provided as heating system. Possible heating range is from room temperature to 450 °C with resolution of 1 °C and temperature accuracy of ± 4 °C. The user defined temperature profile can be programmed with up to 10-node programmable temperature cycle.



Figure 4.9: Photograph of computerised TLD reader system used in this work

Reader system is also equipped with stable LED reference light for real time PMT drift compensation. The data including actual temperature profile, TL counts, TL glow curve etc for each dosimeter are stored individually. User control nitrogen gas can flow during reading of the dosimeter. The dosimeters read out were carried out in nitrogen environment. All setting

parameters of reader such as temperature profile, EHT voltage etc was kept constant throughout this work. Before choosing the TLD disc for use, their repeatability was determined and only those TLD discs were selected whose repeatability was within 2%. The calibration of TLDs was carried out in 6 MV X-ray beam by keeping the TLDs at the depth of 5 cm where the absorbed dose to water was predetermined using methodology described in the IAEA TRS 398. The TLD discs were irradiated for 20, 50, 100, 150, 200 and 250 cGy. The irradiated TLDs were read out using UL-320 TLD reader. The individual calibration factors for each TLD disc were generated and used.

4.2.4 QA method for IMRT: Volumetric CT scan of the phantom was acquired with slice thickness of 2.5 mm at 120 kVp using helical CT machine (Light Speed VCT, GE medical system).

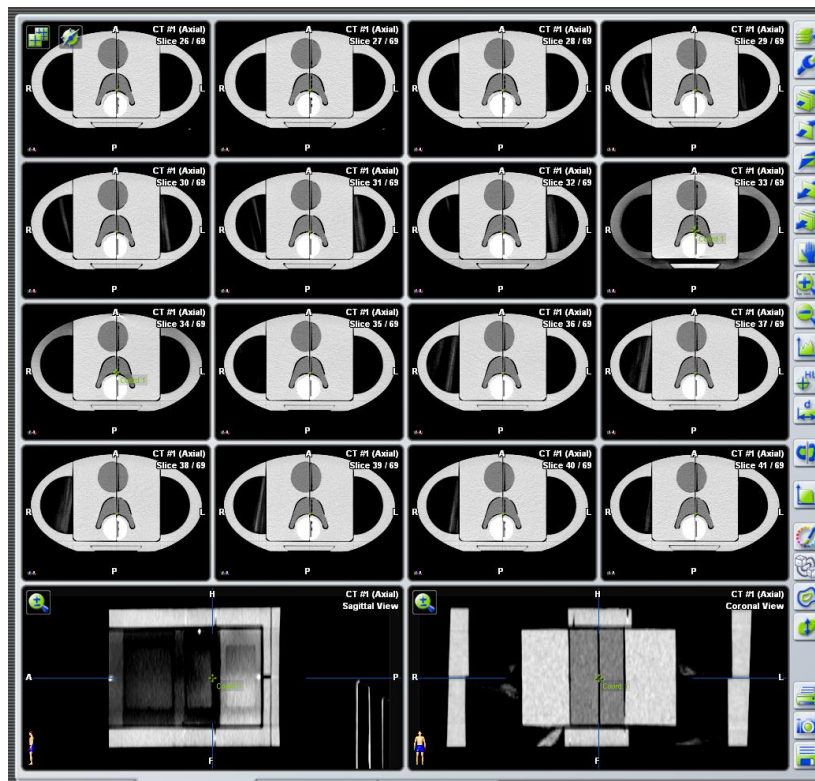


Figure 4.10: Screen shot showing volumetric CT images of phantom

These CT data were electronically transferred to a commercial treatment planning system through hospital network (Figure 4.10). The Body, PTV and OAR of the phantom were contoured in the treatment planning system (Figure 4.11).

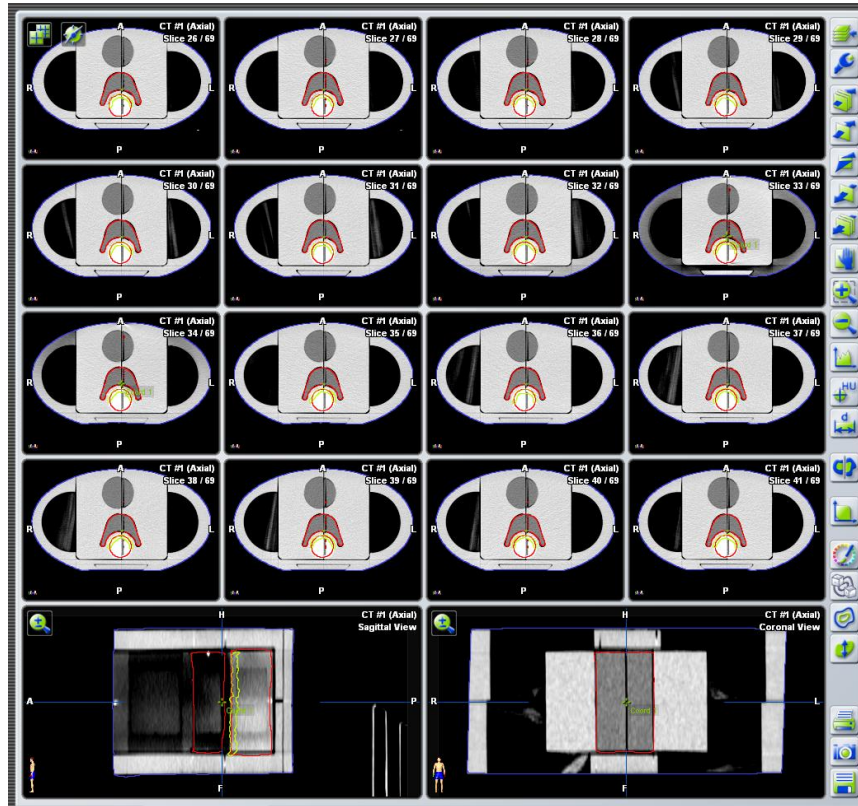


Figure 4.11: Screen shot showing contour for Body, PTV and OAR

The TLD locations were also contoured. The CT data along with contoured structures were supplied to the participating hospitals. The goal for hospitals were set as (1) 95% volume of PTV should receive at least 5000 cGy and 10% of PTV volume should not receive more than 5500 cGy (2) 5% volume of OAR should not receive more than 2500 cGy. The hospitals were asked to generate plan with 6 MV and 9 field beam arrangement at intervals of 40 degree gantry angle. Phantom along with Gafchromic EBT3 film and TLD-100 disc placed in the sagittal plane were supplied to the participating hospitals. A TLD disc and a piece of EBT3 film were also sent to

participating hospital to review the transport condition. These dosimeters reading were compared with background reading of these detectors. When variations were found to be more than 5% with respect to the control detector kept in the lab, the phantom with dosimeter system was resent. The hospitals were supplied a detailed instruction sheet regarding set up of phantom containing detectors for irradiation of treatment plan. The irradiated phantom along with dosimeters was returned to us for further analysis. The dose fluence at EBT film's location was extracted from TPS in DICOM-RT format. Doses at TLD discs locations were also determined from TPS. These data were supplied by hospital to us for analysis. The phantom was irradiated with above mentioned plan with EBT3 film for planar dose verification and TLDs for point dose verification at a number of locations. Figure 4.12 shows the setup of IMRT Audit phantom on treatment delivery system.



Figure 4.12: Photograph showing setup of IMRT audit phantom.

The irradiated films were digitised using Epson Expression 10000XL flatbed scanner and analysed using the OmniPro-IMRT software. The red component of film was extracted for analysis. The isocentre on the film was located with the help of cross-hair and prick mark available on the film. Once the isocentre was located, the film was imported in analysis module. The planar dose

distribution was assessed using gamma criteria of 3%/3 mm. The gamma values are meaningful if resolution (grid) of both data sets is equal and there is no shift between these data sets. However, a high resolution is recommended for good comparison results. Film resolution is more than data obtained from TPS. First film resolution was converted and made equal to the resolution of TPS data and then resolution of these data sets were made equal to 1mm. For gamma evaluation, delta dose and delta distance were set as 3% and 3mm respectively and gamma index were calculated at the point where percentage dose were more or equal to 10%. Gamma values were set as (-1) at the point where percentage dose is less than 10%. The TLD dosimeters were read out using REXON TLD reader. Percentage variation using TLDs were estimated using the following formula

$$\text{Local \% Variation} = [(D_{\text{TPS}} - D_{\text{TLD}}) / (D_{\text{TPS_LD}})] \times 100$$

$$\text{Global \% Variation} = [(D_{\text{TPS}} - D_{\text{TLD}}) / (D_{\text{TPS_PTV}})] \times 100$$

Where, D_{TPS} is calculated dose at TLD location, D_{TLD} is measured dose using TLD disc, $D_{\text{TPS_LD}}$ calculated dose at TLD location, $D_{\text{TPS_PTV}}$ calculated dose to PTV

A trial audit programme at five different radiotherapy centre (located locally) was conducted using TLD discs and EBT3 film using the method described above.

4.3 Results and Discussions

Figures 4.13, 4.14 and 4.15 present dose volume histograms to demonstrate how effectively the hospital is able to achieve the set goal for IMRT dosimetry audit plan for PTV and OAR. Dose volume histogram shown in the figure 4.13 reveals 42.47Gy, 53.56Gy and 57.48 Gy as minimum, mean and maximum dose respectively to the PTV while 95% of PTV is receiving 49.71Gy. Figure 4.14 shows that 10 % of PTV is not receiving dose more than 55.30 Gy.

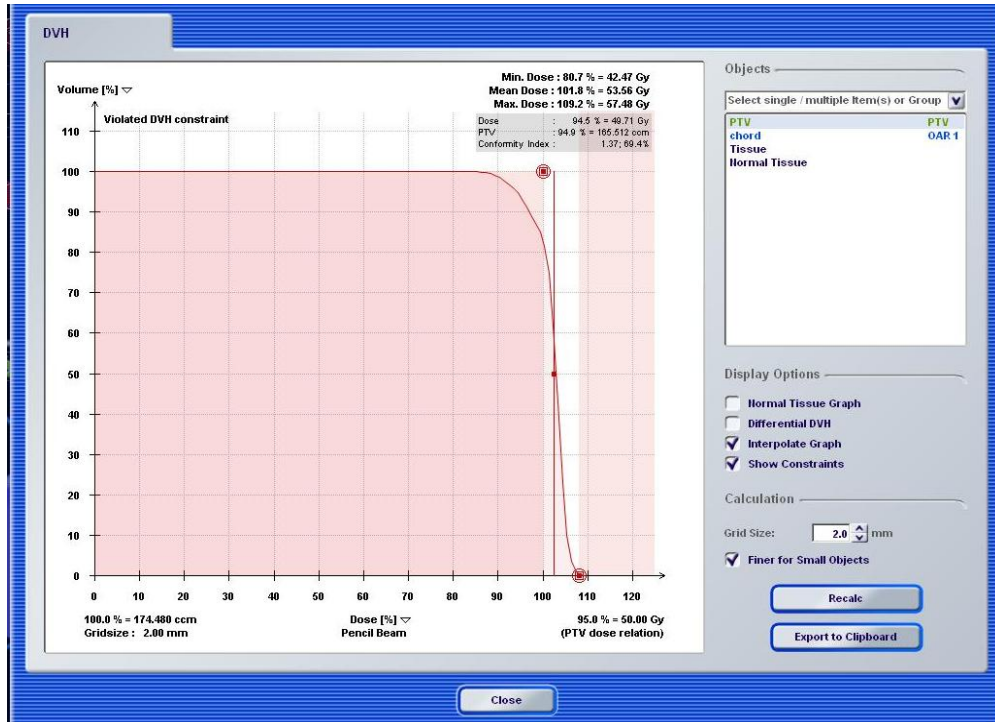


Figure 4.13: Screenshot showing 95% volume of PTV receiving 5000 cGy

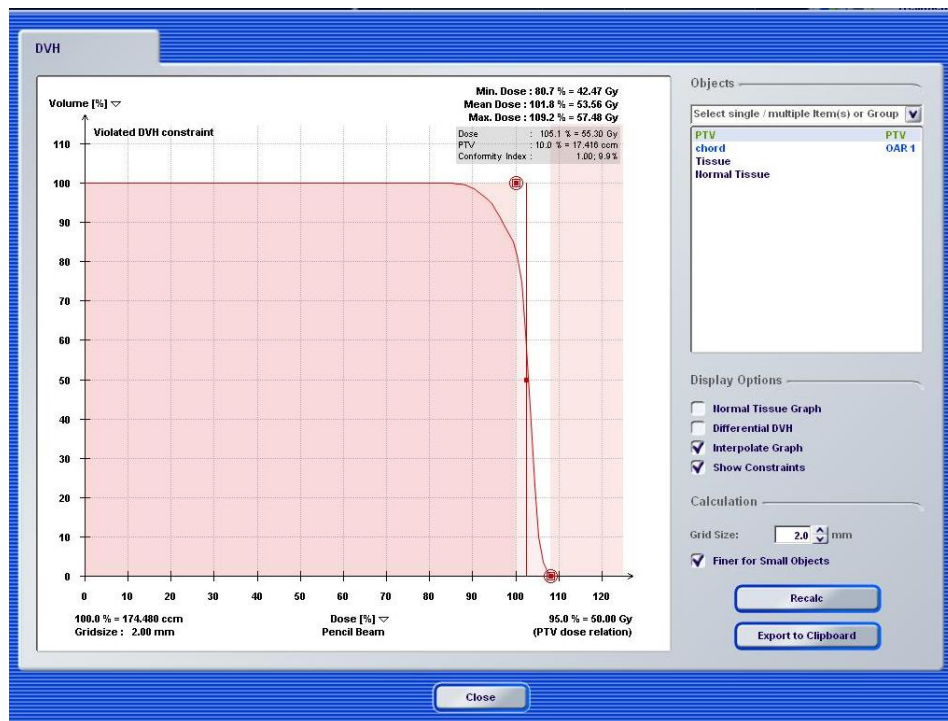


Figure 4.14: Screenshot showing 10% volume of PTV not receiving more 5500 cGy

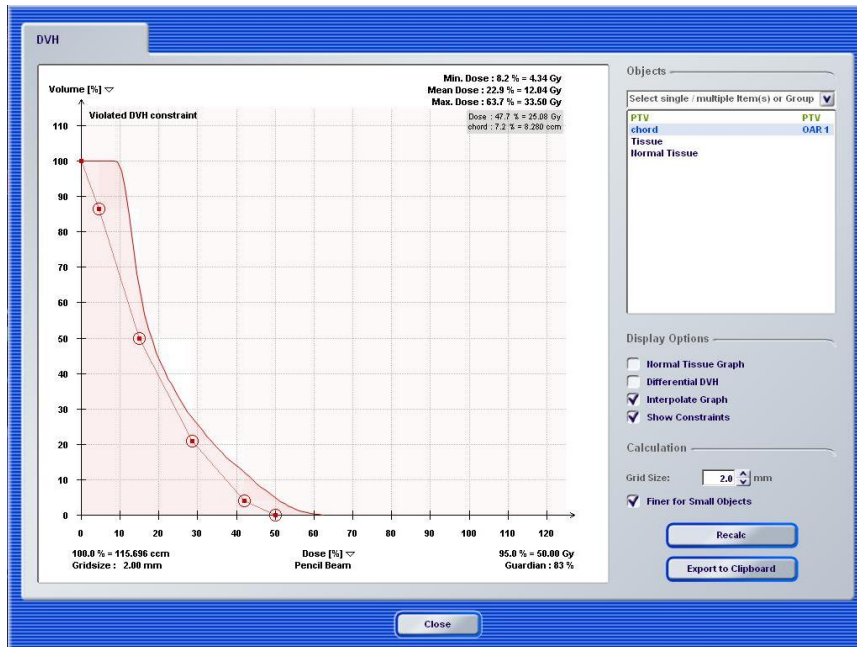


Figure 4.15: Screenshot showing 5% volume of OAR not receiving more 2500 cGy

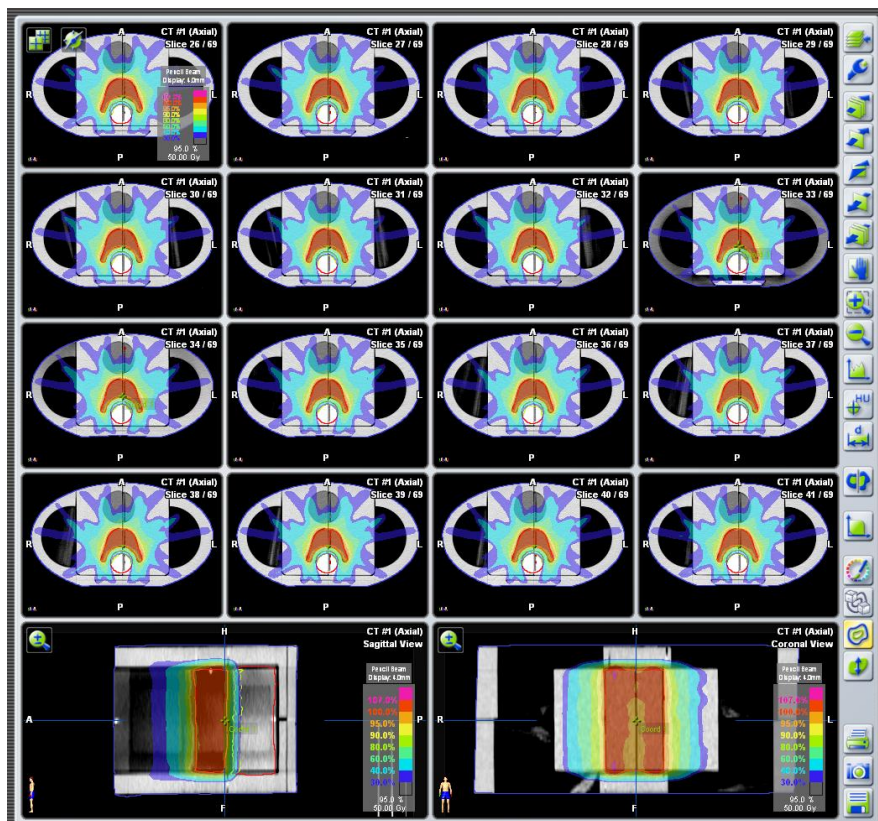


Figure 4.16: Screenshot showing planned dose distribution on different plane of IMRT Audit Phantom

Dose volume histogram shown in the figure 4.15 indicates that 7.2% volume of OAR is getting dose less than 25 Gy in contrast to set criteria that 5% volume of OAR should not receive more than 25 Gy. Figure 4.16 shows the colourwash of dose distribution obtained for given treatment plan requirement at one of the hospitals. Upper portion of the image shows the colorwash of dose distribution for a number of slices in transverse section while lower portion of the image present colorwash of dose distribution for coronal and saggital planes. It can be observed in the figure how efficiently dose to critical structure can be minimised with IMRT.

Table 4.1: Percentage dose variation between measured and planned dose.

Measured (cGy) (A)	Calculated (cGy) (B)	Ratio(B/A)	% Dose Difference	
			Local	Global
46.23	47.56	1.03	-2.80	-0.61
102.69	101.88	0.99	0.80	0.37
104.54	101.72	0.97	2.77	1.30
216.00	216.40	1.00	-0.18	-0.18
220.90	216.52	0.98	2.02	2.02
222.86	217.44	0.98	2.49	2.50
215.13	216.08	1.00	-0.44	-0.44
209.83	216.48	1.03	-3.07	-3.06
220.04	216.56	0.98	1.61	1.60
221.48	217.80	0.98	1.69	1.70
223.38	218.52	0.98	2.22	2.24
221.40	217.68	0.98	1.71	1.71
57.72	56.72	0.98	1.76	0.46
52.55	50.64	0.96	3.77	0.88
29.85	31.08	1.04	-3.96	-0.57
30.09	30.44	1.01	-1.15	-0.16

Table 4.1 shows the results of IMRT dosimetry audit using TLDs at one of the participating hospital. The variations between planned and measured doses for most of the point are less than

3% and maximum up to -3.06 % at some point in case of global comparison however maximum variation is up to -3.96 % for local comparison. Table also shows the ratio of measured and calculated doses which range from 0.98 to 1.04. In this work, global method of comparison is considered as more appropriate and hence used for trial audit.

Figure 4.17 shows the screenshot of measured fluence (A), computed fluence (B), comparison of computed and measured dose distribution (C) and calculated gamma (D). In figure 4.17(C) the computed and measured isodose lines are presented by broken and solid lines respectively. Computed and measured isodose lines are in good correlation with each other. Figure 4.17(D) shows the calculated gamma for set criteria of 3%/3 mm. It can be inferred from the figure that at most of the points, calculated gamma value is less than 1. Figure 4.18 shows the statistics of the calculated gamma. From the figure 4.18 it can be seen that the gamma values for 98.51% of calculated points are less than or equal to 1 while 1.49% of calculated point having gamma value more than 1. The gamma values were calculated at 34940 points. The maximum gamma value in the calculated region was found to be 1.37. The average value of calculated gamma was found to be 0.38 with standard deviation of 0.23.

As described above, trial audit at five different hospitals was conducted at the the hospital located in Mumbai and Table 4.2 shows the consolidated result of the same. It can be inferred from the table that % variation of point dose measured using TLD at different locations ranges from -5.91% to 3.95%, however for most of the points of measurement, percentage deviation were found to be less than 3%. These results are in good agreement with accepted TLD audit result of $\pm 3.5\%$ and $\pm 5\%$ of IAEA and Radiological Physics Centre, respectively.

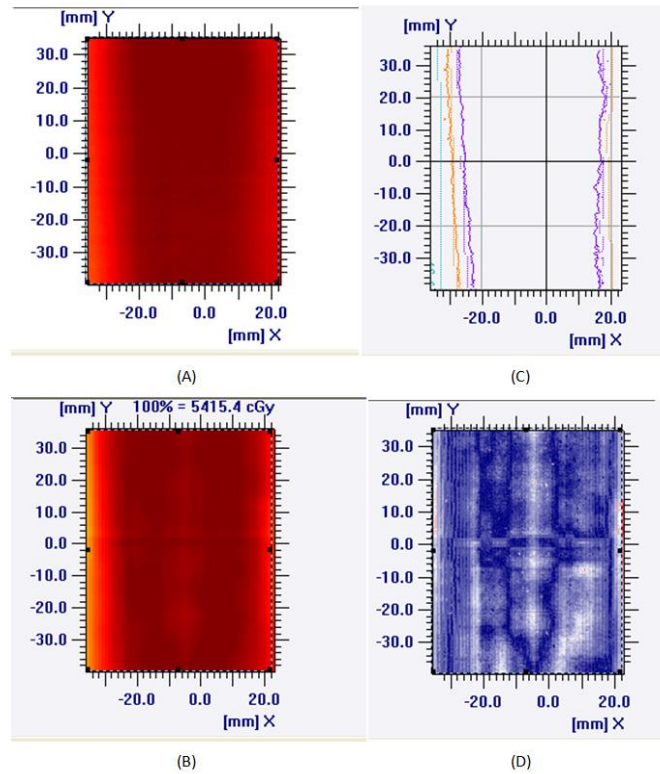


Figure 4.17: Screenshot showing measured fluence (A), computed fluence (B), comparison of computed and measured dose distribution (C) and calculated gamma (D) of IMRT audit plan.

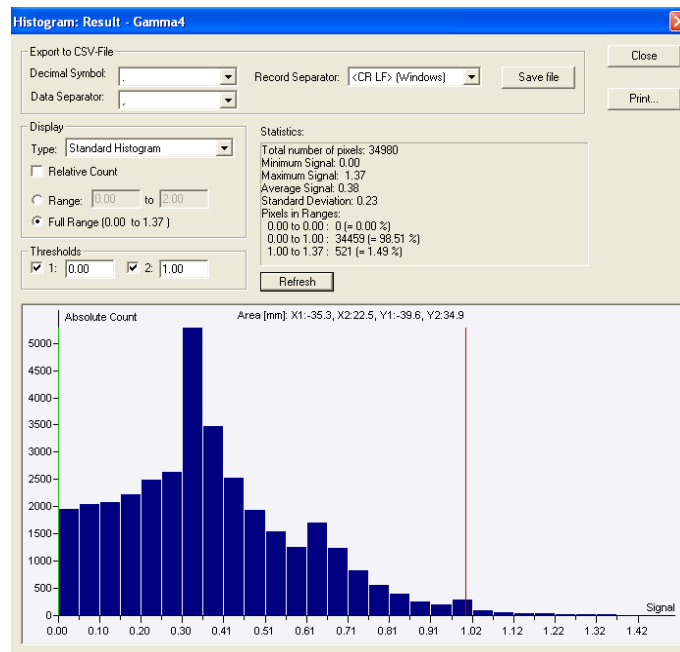


Figure 4.18: Screenshot showing statistics for calculated gamma of IMRT audit plan.

Table 4.2: Consolidated result of trail IMRT dosimetry Audit conducted at different hospitals using TLD and Gafchromic film (H1: Hospital1, H2: Hospital2, H3: Hospital3, H4: Hospital4, H5: Hospital5)

TLD Location	IMRT dosimetry Audit Result									
	H1		H2		H3		H4		H5	
	TLD	Film	TLD	Film	TLD	Film	TLD	Film	TLD	Film
	% Variation	% of Point Pass the set Gamma criteria	% Variation	% of Point Pass the set Gamma criteria	% Variation	% of Point Pass the set Gamma criteria	% Variation	% of Point Pass the set Gamma criteria	% Variation	% of Point Pass the set Gamma criteria
1	1.65		-0.96		0.51		1.02		-0.61	
2	-1.12		1.05		-0.62		-0.62		0.37	
3	0.54		0.85		1.26		1.26		1.30	
4	-3.22		-2.59		2.65		2.65		-0.18	
5	2.07		1.52		2.14		2.14		2.02	
6	3.76		4.62		3.10		3.10		2.50	
7	-1.63	91.30	-2.51	96.23	-1.58	93.45	-1.58	95.60	-0.44	98.51
8	-5.91		-3.64		-2.52		-2.52		-3.06	
9	2.70		2.60		2.65		2.65		1.60	
10	0.54		0.64		0.85		0.85		1.70	
11	3.93		2.96		3.95		3.95		2.24	
12	2.76		2.41		2.40		2.40		1.71	
13	2.23		2.64		1.89		1.89		0.46	
14	1.06		1.04		-1.42		-1.65		0.88	
15	-1.08		1.10		-1.13		-1.13		-0.57	
16	-1.94		-0.90		-1.62		-1.41		-0.16	

The analysis of film result of shows that percentage of point having gamma values less than or equal to 1 at these hospitals were ranges from 91.3% to 98.51%. The result of trial audit is found to be satisfactory. It should be noted here that the entire trial audit was conducted at the hospital having good dosimetry records and situated in the metro city.

4.4 Conclusions

A postal IMRT dosimetry audit phantom was designed and fabricated locally. The results of initial studies conducted using this phantom were found encouraging indicating that the in-house developed dosimetry audit phantom is able to serve the intended purpose. This trial was conducted at the hospitals located in Mumbai. However, country level audit program which include centres from small town will reflect better picture of quality of IMRT treatment program in the country.

CHAPTER 5

DEVELOPMENT OF QUICK, EFFICIENT AND EFFECTIVE PATIENT SPECIFIC IMRT QA USING LOG FILE AND EPID

5.1 Introduction

On the basis of literature survey, QA process for IMRT implementation in clinical practice can be divided in three groups: (1) Commissioning of the IMRT system which includes planning system parameter adjustment, dosimetric tests with different phantoms, adjustment of the delivery system and tests of the data transfer; (2) Regular machine related quality assurance procedures which comprise mechanical precision of static test fields or mechanical and dosimetric precision of dynamic test fields; and (3) Regular patient related quality assurance procedures which involve dosimetric plan verification, dosimetric field by field verification and independent MU checks. First two QA programs are standard in nature and must be followed even without IMRT/ VMAT. The most common IMRT error can be either physical errors e.g. calibration or commissioning of treatment planning and delivery system or catastrophic errors, e.g. wrong field data transfer. In an ideal situation, TPS used for IMRT are designed and commissioned to accurately simulate the beam delivery system; Machine QA programme for MLC calibration and known mechanical problems for each MLC and delivery type and Patient-specific QA focuses on potential clinical errors. Measurement based patient specific IMRT QA is performed only for limited number of times and require considerable time of delivery system as well as of medical physicist. However, catastrophic type of errors can occur at any time during the course of treatment. If the treatment planning system has been commissioned suitably for IMRT and adequate periodic machine QA for IMRT are in place, measurement based patient specific IMRT QA can be replaced with software based IMRT QA. Trajectory log file which is 'free information' and can be harvested for purposes of documenting individual patient treatments. Data in log files does not require any additional time

or dose for the patient. Log file analysis is being used as primary tool for such documentation from several years at hospitals such as Memorial Sloan Kettering Cancer Centre, New York. Litzenberg et al 2002, Ramsey et al 2001 and Dinesh Kumar et al 2006 have utilised directly or indirectly log file data for the purpose of patient specific IMRT QA. People debate about future of patient specific IMRT QA that it would be more accurate and considerably less time consuming to perform such QA with software rather than hardware as measurement-based patient-specific QA for IMRT is both time-consuming and potentially inaccurate, since the measurements are made in phantoms rather than actual patients [Siochi et al 2013]. Log file data, however, is not independent as miscalibration of leaf positions or failures in MLC positioning pots can result in erroneous command from MLC controller as signal for both positioning and monitoring of leaf position is coming from the same erroneous source. Such a system, however, is not completely 'foolproof' as the leaf position data in the Log/Trajectory files is produced by the MLC controller itself. There is no independent verification of these data as the same MLC controller that moves the leaves also monitors leaf positions and writes the Log/Trajectory files. EPID images, on the other hand, can monitor MLC leaf position completely independent of the MLC controller and MLC position pots. Confirmation of MLC leaf positions independently with the EPID can therefore be a useful commissioning tool for IMRT LINACs and can be used for routine verification of each patient's IMRT treatment plan and treatment delivery without extra dose to patient, or physics QA time on the LINAC. Although numerous reports exist on EPID dosimetry for IMRT, we believe that no one has specifically addressed the issue of using EPID for verification of Log file data. This chapter describes the methodology to compare leaf positions as measured from EPID images for IMRT treatment to the data in the Log/Trajectory files and use them as tools for quick, efficient and effective patient specific IMRT QA.

5.2 Materials and Methods

The experiments were performed using a Truebeam LINAC equipped with 120 leaves MLC and flat panel based MV/kV imaging system. Truebeam is copyright names by Varian Medical Systems, Palo Alto, California.

5.2.1 Multileaf Collimator System

The Varian Millennium MLC-120 consists of two banks of 60 leaves: 0.5 cm width for the central 20 cm of the field and 1.0 cm width for the outer 20 cm and can provide a maximum field of $40 \times 40 \text{ cm}^2$. The leaves can over travel across the beam central axis with a maximum distance of 16 cm and can extend beyond another on the same carriage with a maximum distance of 14.5 cm. Speed of carriage and leaves varies from 0 to 1.2 cm/sec and from 0 to 2.5 cm/sec respectively.

5.2.2 Electronic Portal Imaging Device (EPID)

The EPID attached with Varian's Truebeam linear accelerator is aS1000 (Portal Vision, Varian Medical Systems, Palo Alto, CA) amorphous silicon flat panel imaging device. The EPID is mounted on a strong robotic arm. This arm allows it to be positioned at different vertical (80.0 to +0.0 cm), lateral (-18.5 cm to +15.5 cm) and longitudinal (-20.0 cm to +24.0 cm) positions. It can acquire images at the maximum rate of 20 frames per second (fps). Major components of EPID are: Copper build-up plate of thickness 1 mm just below the exterior plastic housing. This plate plays an important role in MV imaging to absorb x-ray photons and emit the recoil electrons. It also helps in improving the efficiency of system by providing partial shielding to other components of EPID from scattered radiation. Below the copper plate, a phosphor screen made up of 0.4 mm thick Gadolinium Oxysulfide ($\text{Gd}_2\text{O}_2\text{S: Tb}$) is provided. This phosphor screen absorbs the incoming electrons from the copper plate and converts them into light photons. These light

photons fall on a sensitive image forming layer which consists of photodiodes arranged in a 1024 x 768 pixel matrix on 1 mm glass substrate. Each pixel consists of a photodiode which integrates the incoming light in charge captures and a thin film transistor (TFT) to act as a three terminal switch for readout. The final major component is the readout circuitry.

5.2.3 Trajectory Log

Truebeam control system generates a trajectory log file which records the actual axis position and delivers MUs at periodic intervals of 20 ms along with their expected values. The system is configured to record 60,000 data sets for a period of 20 minutes at an interval of 20 ms. The trajectory log file stores data in a binary format which needs to be converted into a readable format for intended application. A single binary file generated includes information about expected and actual values of gantry angle, collimator angle, jaws positions, couch position, delivered dose in MU, beam status, control points, carriage position and MLC leaf positions. The file records the linear dimensions in cm, rotational scale in degree and dose in MU. The leaf positions stored in the trajectory log file are the position of leaves at isocentre. After each dynamic MLC (DMLC) field delivery the trajectory log file for that particular field is written to a file on the control system computer automatically in treatment mode and upon activation in research mode operation of the Truebeam LINAC. There is no trajectory log file record when the beam is paused either due to minor fault or user interruption by pressing beam off button. A complete file description may be found elsewhere [True beam Trajectory Log File Specification, 2011].

5.2.4 Experiment

Initial experiments were carried out with Cline6EX (C-Series Machine, Varian Oncology System). The EPID images (without averaging) and corresponding log files were acquired. EPID system

without averaging acquires images in cine mode. As there is no reliable time or dose stamp on the EPID images, which make difficult to synchronise the EPID images with the corresponding log file record. Moreover, in C-series machine, EPID system does not capture the image in beam hold off condition which further complicates the synchronisation of EPID image with log file records. So, the experiments were transferred to Truebeam linear accelerator where EPID system stores time stamp and also captures the image frame in beam hold off condition.

Afterward, all the measurements were performed in research mode option of Truebeam linear accelerator. In the research mode operation of LINAC the patient treatment is not allowed. The treatment plan files need to be converted into XML format to run in the research mode. An in-house program was developed to convert the DVA file (proprietary file format used to run dynamic treatment file by Varian Medical System) into XML file without modification of any beam parameters except the addition of movie MV imaging acquisition sequence. The XML file was loaded on a Varian Truebeam LINAC in research mode with the MV detector panel positioned at the isocenter plane. After beam delivery, the EPID images are exported in XIM format: a proprietary image format used by Varian and were analyzed with the library supplied by Varian using an in-house developed program in Matlab. In addition to the raw data (image intensity at each pixel), the EPID also records the start time, MV dose start, MV dose stop, MV detector longitudinal, MV detector lateral, MV detector vertical, pixel width and pixel height indices along with some other information for each image and stores them in the XIM header. These information were used in data analysis. However, if we import the images in DICOM format, information such as start time, MV dose start, MV dose stop etc are not available in the header file. These information are very important for synchronising the EPID images with trajectory log data.

The trajectory log binary file after each irradiation is stored at the network drive system. An in-house Matlab code was developed to convert the binary file into text file to extract the required information from trajectory log.

5.2.4.1 Calibration and Determining the Centre of EPID detector system

The DVA file for field sizes 1by1, 2by2, 3by3, 4by4, 6by6, 10by10, 14by14 and 20by20 cm² were converted into the XML file and run in the research mode. The dose and dose rate was 100 MU and 300 MU/min respectively. The images and log file were acquired. The images of these fields were used for locating the centre of detector system (pixel position/coordinates). Once the centre was located, A-bank and B-Bank leaf positions from the centre were determined using the number of pixel from centre, 50% of centre pixel intensity and pixel size information from the header file. Higher field sizes due to round edge of leaves were taken care during the calibration process. These images were also used to study the variation in leaves position determined from the EPID images and Trajectory log file. The difference in leaf position (LP) was determined using the following formulae:

$$\text{Difference in LP} = \text{LP from Trajectory Log} - \text{LP from EPID Images}$$

All the differences were given in cm. These data were also used to study the difference in leaf position in stationary field

5.2.4.2 Effect of Leaf Velocity

The DVA files with A-bank leaves moving and B-bank leaves fixed and vice-versa were prepared and later converted into XML format to produce a sweeping field using A-bank/B-bank leaves. Doing so, changing fields were produced by moving A-bank/B-bank leaves. The speed of leaves

was changed by modifying MU for a set dose rate. The EPID images and trajectory log were acquired with 50 MU and 100 MU for a dose rate of 600 MU/min. The EPID images were synchronised with trajectory log record as depicted in figure 5.1. The time start stamp with some modification was used to synchronise the EPID images with trajectory log records. A modified time stamp was introduced for each trajectory log by taking care of time for creation of one EPID image and one trajectory log record. The differences in leaves position for stationary and moving leaves were determined.

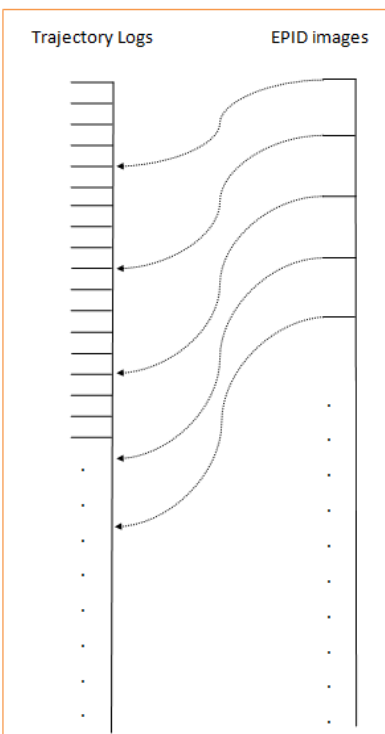


Figure 5.1: Schematic diagram for synchronisation of Trajectory log records and EPID images

5.2.4.3 IMRT cases

Ten IMRT treatment files were randomly selected and their DVA files were converted into XML format. The IMRT plan was generated using dose rate of 300 MU/min and dose per field was taken

automatically from the planned files. The EPID images and trajectory log file data were acquired and processed as mentioned above. Data of each field was analysed separately.

5.2.5 Software Developments

Software tools were developed to extract and analyse the following data:

- (i) MLC leaf positions from EPID images for C-series machine and Truebeam,
- (ii) To extract useful data from MLC log file of C-Series LINAC
- (iii) To extract useful information from the trajectory log binary file of Truebeam LINAC,
- (iv) To compare leaf positions derived from EPID images with log file/trajectory log data and
- (v) To analyze IMRT treatment files using the Matlab programming language.

5.3 Results and Discussion

5.3.1 C-Series Machine

Table 5.1 shows the number of record/frame in log file and acquired EPID images while either A-bank or B-bank leaves were moving with set dose of 50, 100 and 1000 MU at dose rate of 600 MU/min. It can be inferred from the table, for dose of 100 MU and 1000 MU, number of acquired images and log file records are almost constant for both situations while for 50 MU, number of frames/records vary significantly. Figure 5.2 shows the plot of beam hold OFF flag obtained from log file during A-bank and B-bank moving conditions for dose of 50 MU and dose rate of 600 MU/min while no beam hold OFF flag was noticed during delivery of 100 MU and 1000 MU dose. Beam hold off flag 1 indicates the beam is OFF during that particular instance. Less number of records and frames for lower MU is attributed to significant beam hold OFF during which neither

log file record nor EPID images getting recorded. Control computer does this whenever an MLC leaf cannot move fast enough to be in correct position, so beam is halted until leaf 'catches up' and is in correct position. This occurs more frequently for small number of MU because there is less time required for treatment delivery. EPID should be capable of acquiring at least 15 frames/sec, but in real treatment it is usually fewer frames because of timing problems, beam holdoffs, etc.

Table 5.1: Number of record/frame generated in log file/EPID images on C-series machine

MU with dose rate 600MU/min	Number of Record/Frame		Number of Record/Frame	
	A bank moving		B bank moving	
	Log File	EPID	Log File	EPID
50	130	13	163	17
100	195	87	195	88
1000	1892	901	1892	900

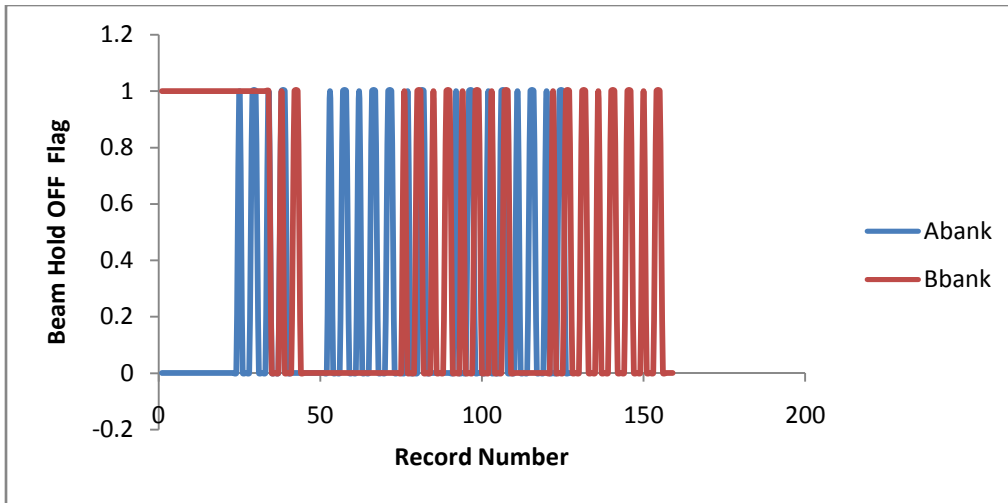


Figure 5.2: Plot of Beam hold OFF flag during A-bank and B-bank moving condition for dose of 50 MU and dose rate of 600 MU/min.

Figures 5.3a and 5.3b shows the plot of leaf position information derived from log file record and EPID images respectively. It can be inferred from the figure that due to improper synchronisation and absence of EPID images during beam hold off condition, correct leaf positions of moving leaves are difficult to derive.

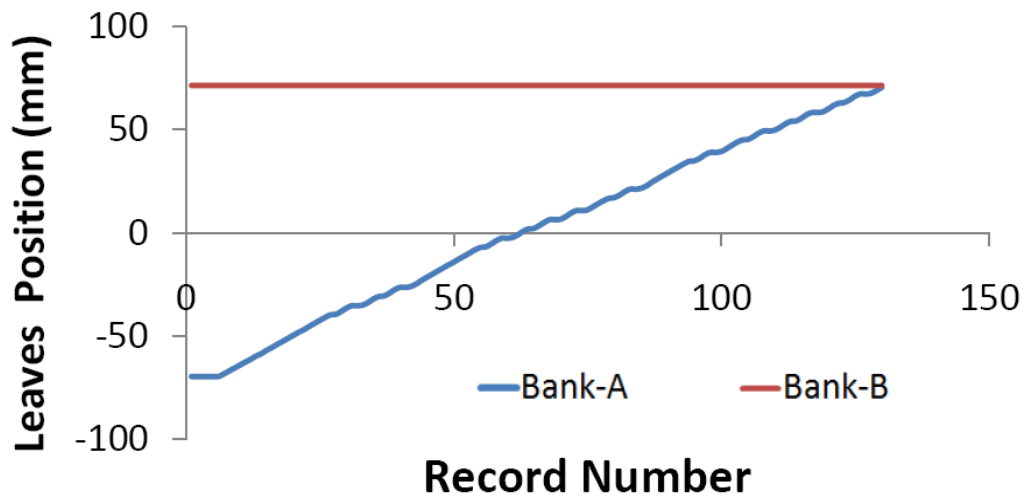


Figure 5.3a: Plot of leaf position information derived from log file record (50 MU and 600 MU/Min)

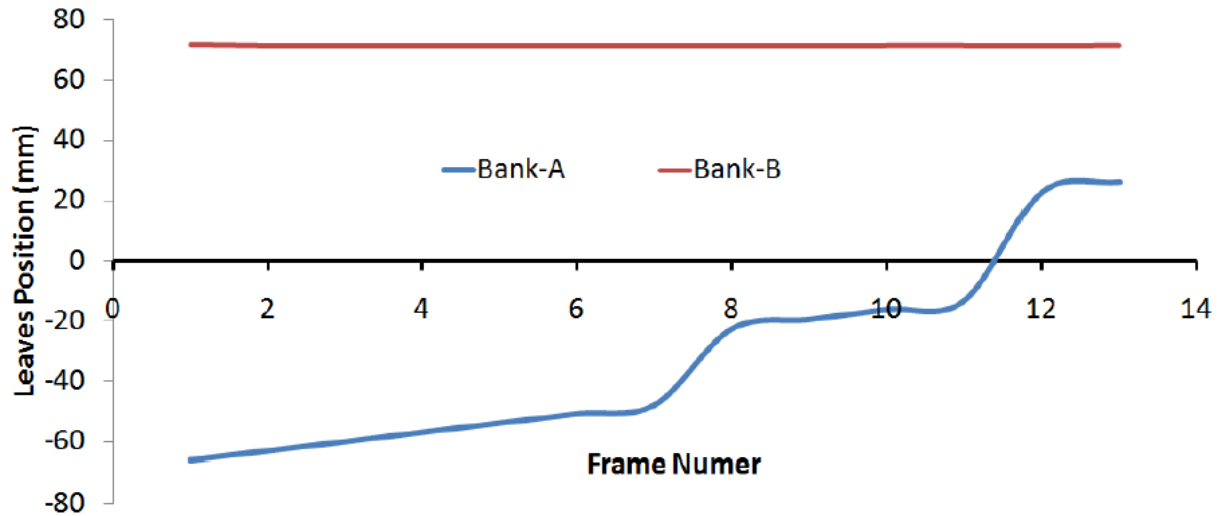


Figure 5.3b: Plot of leaf position information derived from EPID images (50 MU and 600 MU/Min)

Figures 5.4a and 5.4b show the plots of leaf position information derived from log file record and EPID images respectively for dose 1000 MU and dose rate 600 MU/min. There was no beam hold during irradiation of 1000 MU with 600 MU/min. It can be inferred from this figure that moving leaves with no beam hold off can be synchronised.

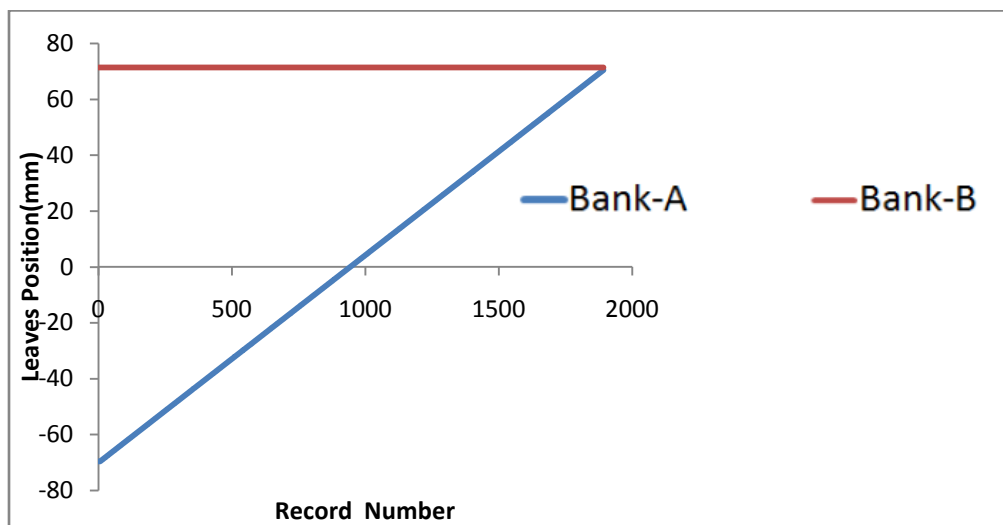


Figure 5.4a: Plot of leaf position information derived from log file record (1000 MU and 600 MU/Min)

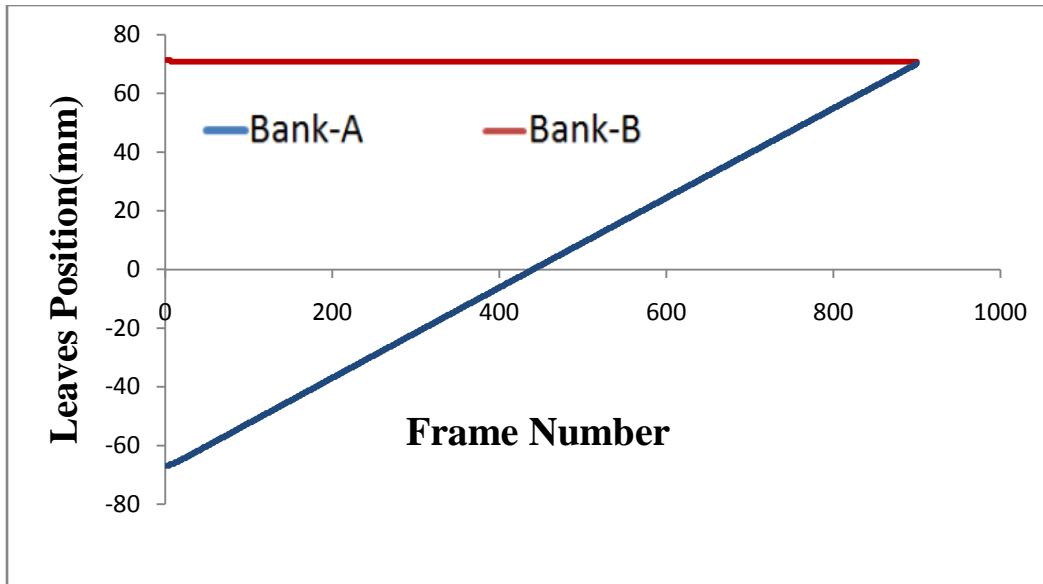


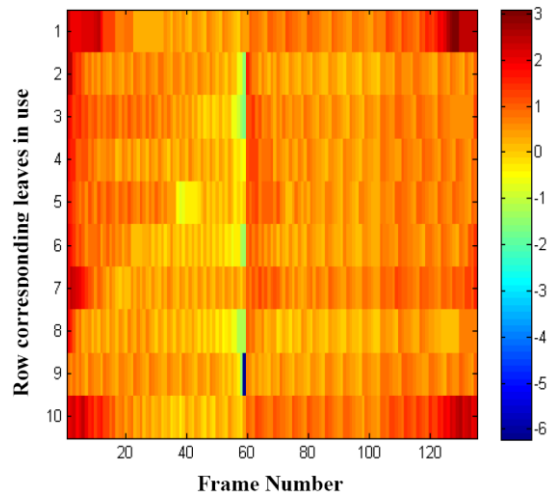
Figure 5.4b: Plot of leaf position information derived from EPID images (1000 MU and 600 MU/Min)

However, in real practice to get situation without beam hold OFF is rare. Figure.5.5 shows the difference in leaf positions determined from log file record and EPID images for A and B bank for a sliding window IMRT treatment field in the form of matrix (Figure 5.5a & c) and histogram (Figure 5.5b & d). Figure 5.5a and 5.5c are plots of difference in leaf positions with time. For sliding window IMRT, at the beginning of each treatment beam, both A bank and B bank of MLC leaves are positioned at extreme left edge of beam (-y position) and almost completely closed. As soon as beam is turned on, first A-bank leaves start to move in extreme right side (+y) direction, followed by B-bank leaves moving towards extreme right side (+y). At the end of treatment the MLC leaves are again almost completely closed, with both A and B bank leaves positioned at the extreme right side (+y) of the field. If during treatment any MLC leaf cannot move fast enough to be in correct position then a beam hold off is automatically initiated. Beam holds are recorded in the log file. It can be observed, at beginning error in leaves of B-bank is less as leaves are either stationary or moving very slow and later (at about frame number 100) error is more as leaves start

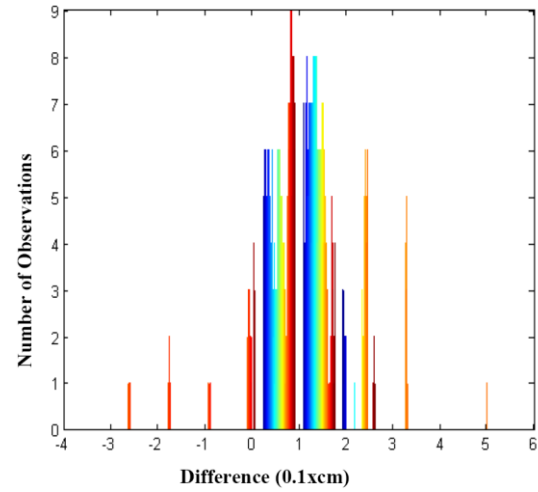
moving fast or in beam hold OFF situation. Similarly, for the A-bank error at earlier stage (at about frame number 60) is more due to reason mentioned above. On the analysis of log file data it was observed that corresponding to these frame numbers, there were few beam hold off flag and so frames of EPID images were missed. However, occurrence of beam hold off was not significant. Figure 5.5b and 5.5d are error histograms of differences in leaf positions determined from log file record and EPID images for A and B bank respectively for an IMRT treatment field. The colour bar in the image indicates the occurrence of differences in mm. It can be observed from the figure 5.5 that most of the time the error in leaf positions are within 2 mm for A-bank and within 3 mm for B-bank except at locations of beam hold off. The frequency of occurrence of error more than 2 or 3 mm is very less. On the basis of this study we can conclude that if beam hold off is not present during the treatment (which is not practical), method can be used for determining difference in leaf positions from log file record and EPID images in C-series machine by synchronising the log file record with EPID images by distributing them in equal intervals. However, due to presence of beam hold and non availability of time and dose stamp on the EPID images, above discussed methods are not suitable to make a patient specific IMRT QA tool for Varian's C-series machine.

5.3.2 Truebeam Machine

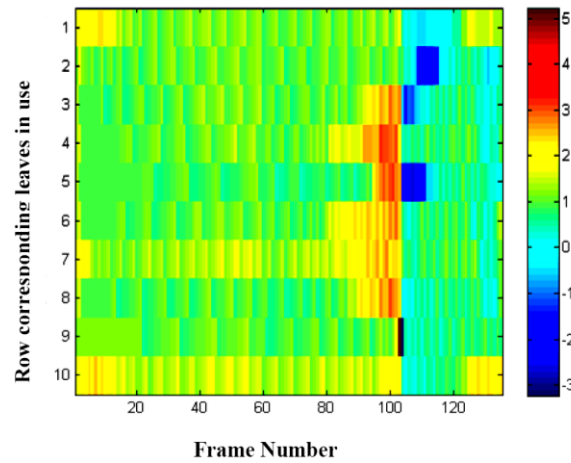
Figure 5.6 shows the error histogram of differences in leaf positions determined from trajectory log record and EPID images for leaves of bank A and B for stationary field of 1by1 cm². Similar experiments were performed for 2by2, 3by3, 4by4, 6by6, 10by10, 14by14 and 20 by20 cm². It was found that the differences for stationary fields are less than 0.5 mm for all the field sizes. For stationary field, leaves position recorded in trajectory log are more reliable as leaves are stationary.



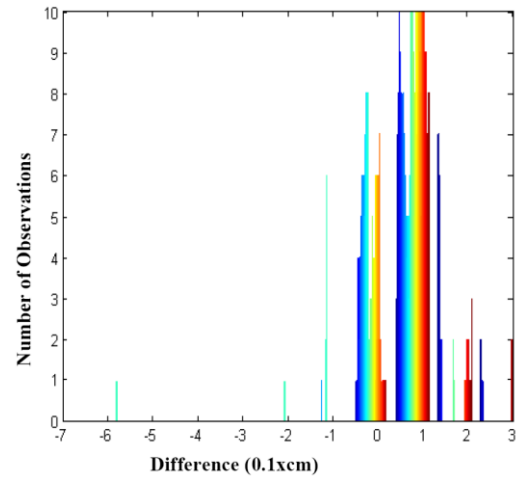
(a) Bank-A



(b) Bank-A

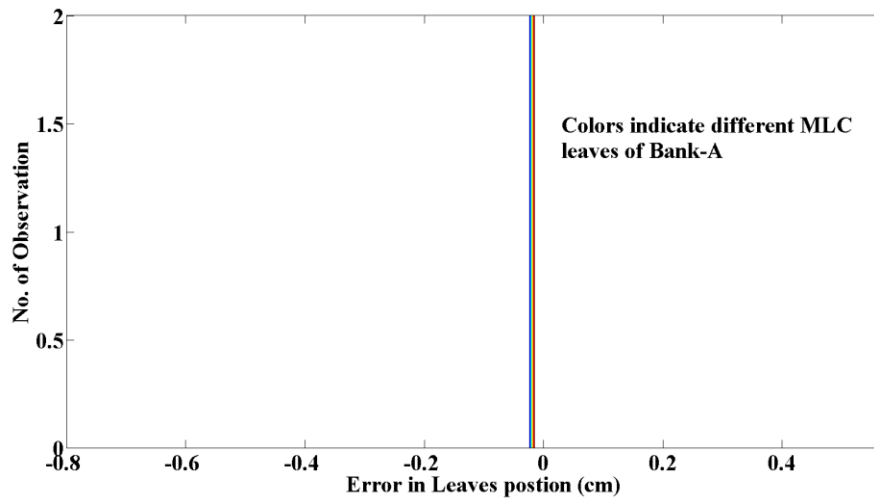


(c) Bank-B

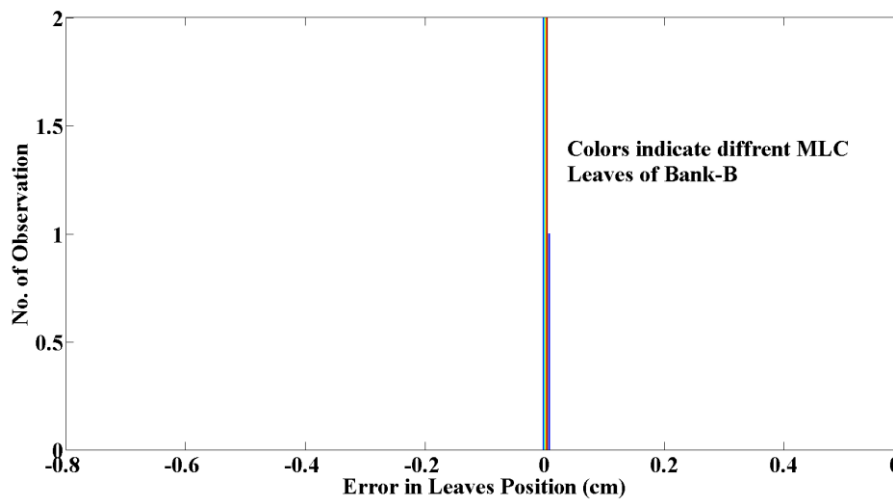


(d) Bank-B

Figure 5.5: Matrix and error histogram showing difference in leaf positions determined from log file record and EPID images for A and B bank for an IMRT treatment field(C-Series Machine).



(a) Bank-A



(b) Bank-A

Figure 5.6: Error histograms of differences in leaf positions determined from trajectory log record and EPID images for A and B bank respectively for stationary field (1by1 cm²)

The field sizes were determined precisely from EPID images for stationary field. This result indicates that the methodology used for detecting error in leaves position is satisfactory and reliable. Figure 5.7 shows error histogram of difference in leaf positions determined from trajectory log records and EPID images for leaves of bank A and B while leaves of A-bank are

moving and leaves of B-bank are stationary. Figure 5.8 shows error histogram of differences in leaf positions determined from trajectory log records and EPID images for leaves of bank A and B while leaves of B-bank are moving and leaves of A-bank are stationary respectively. The dose rate and dose were varied so that different speed in leaves motion can be introduced. It can be observed that magnitudes of errors are more when speed of leaves is higher as observed in C-series machine. The errors in moving leaves are more than the stationary leaves but less than 2 mm. The larger error in moving leaves can be attributed to the synchronisation error of EPID images for less than 20 ms and error in the log file data.

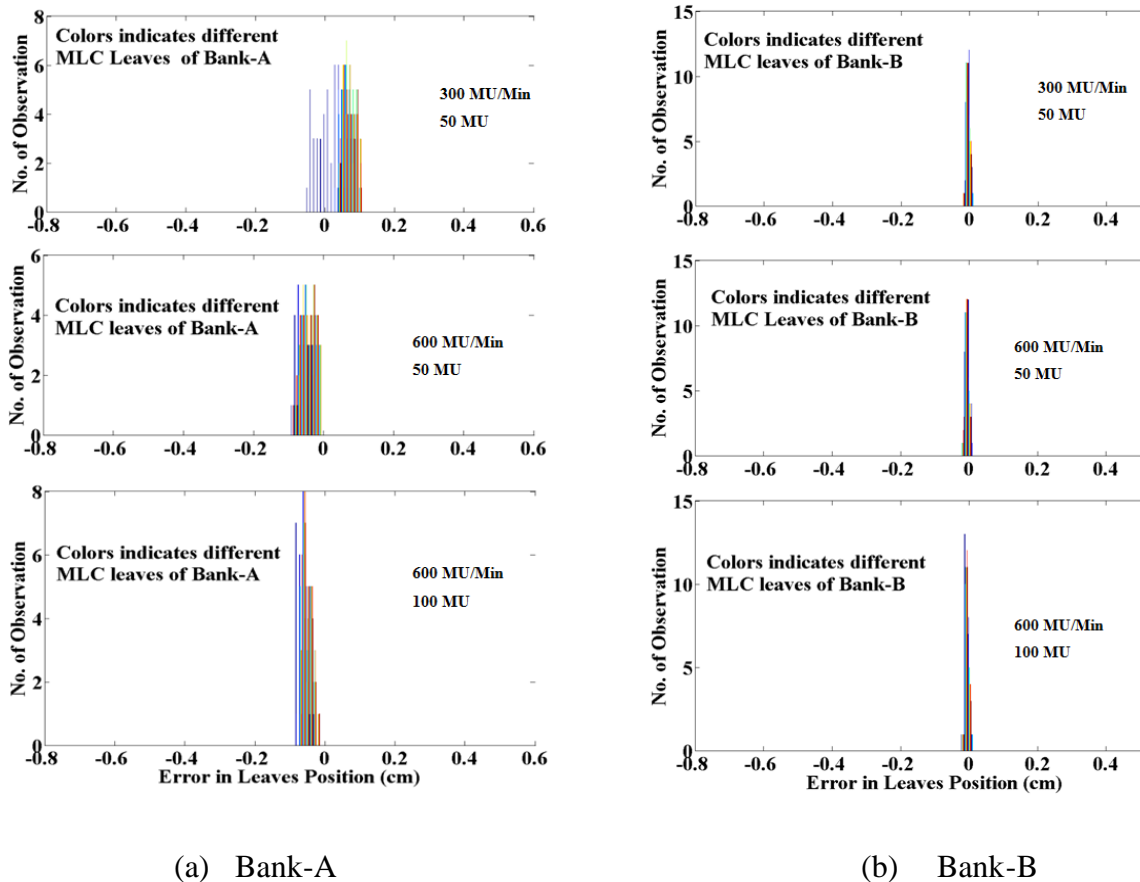


Figure: 5.7 Error histograms of differences in leaf positions determined from trajectory log record and EPID images for A and B bank while leaves of A-bank are moving and leaves of B-bank were stationary.

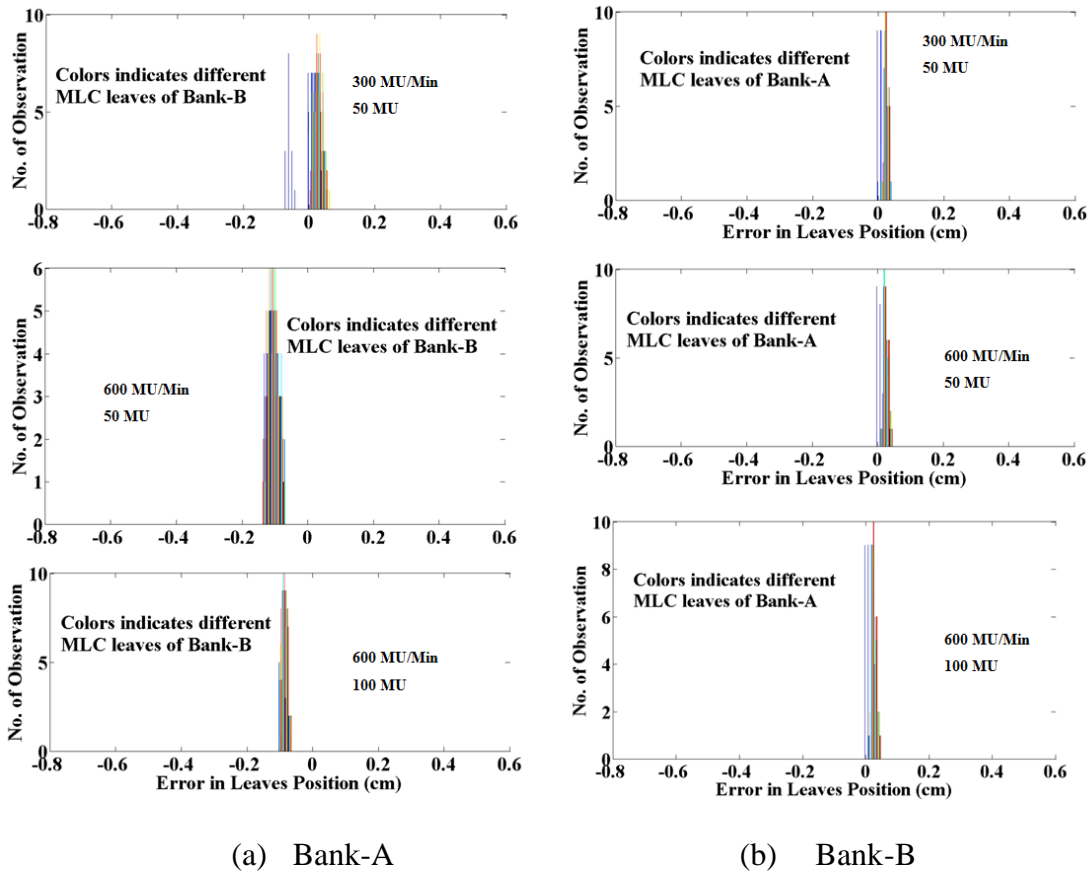
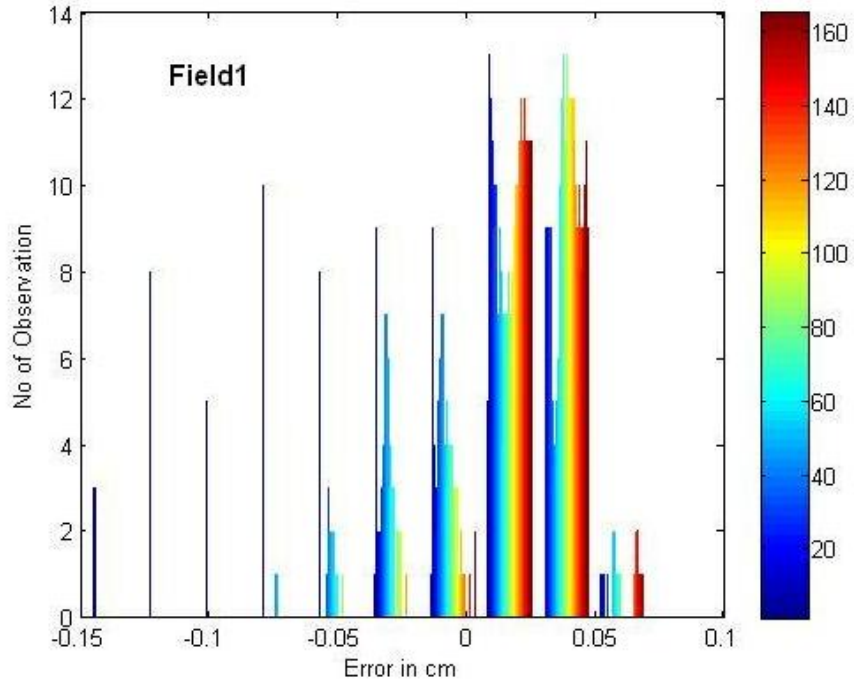
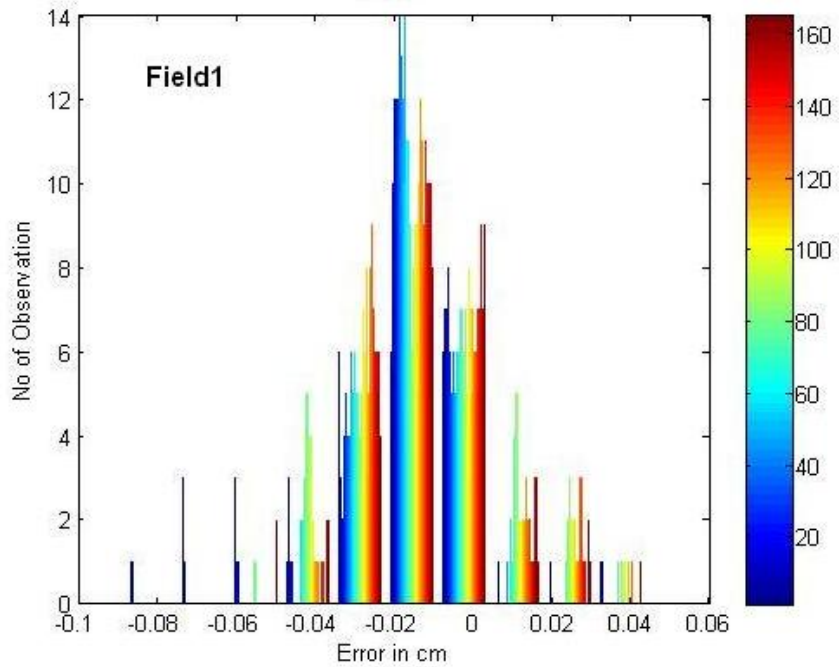


Figure 5.8: Error histograms of differences in leaf positions determined from trajectory log record and EPID images for A and B bank while leaves of B-bank are moving and leaves of A-bank were stationary.

For Truebeam linear accelerator, trajectory log and EPID images can be well synchronised (within error of distance travelled in less than 20 ms) with time stamp available in the header file of XIM images. The EPID images can be used for verification of leaves position during the dynamic treatment. Figure 5.9 shows error histogram of differences in leaf positions determined from trajectory log record and EPID images for A and B bank respectively for a five fields IMRT case. It can be seen from the figure that the errors for all the fields are within 2 mm.



(a) Field1(Bank-A)



(b) Field1(Bank-B)

Figure 5.9: Error histograms of differences in leaf positions determined from trajectory log record and EPID images for A and B bank for one field of a five fields IMRT case (TrueBeam LINAC).

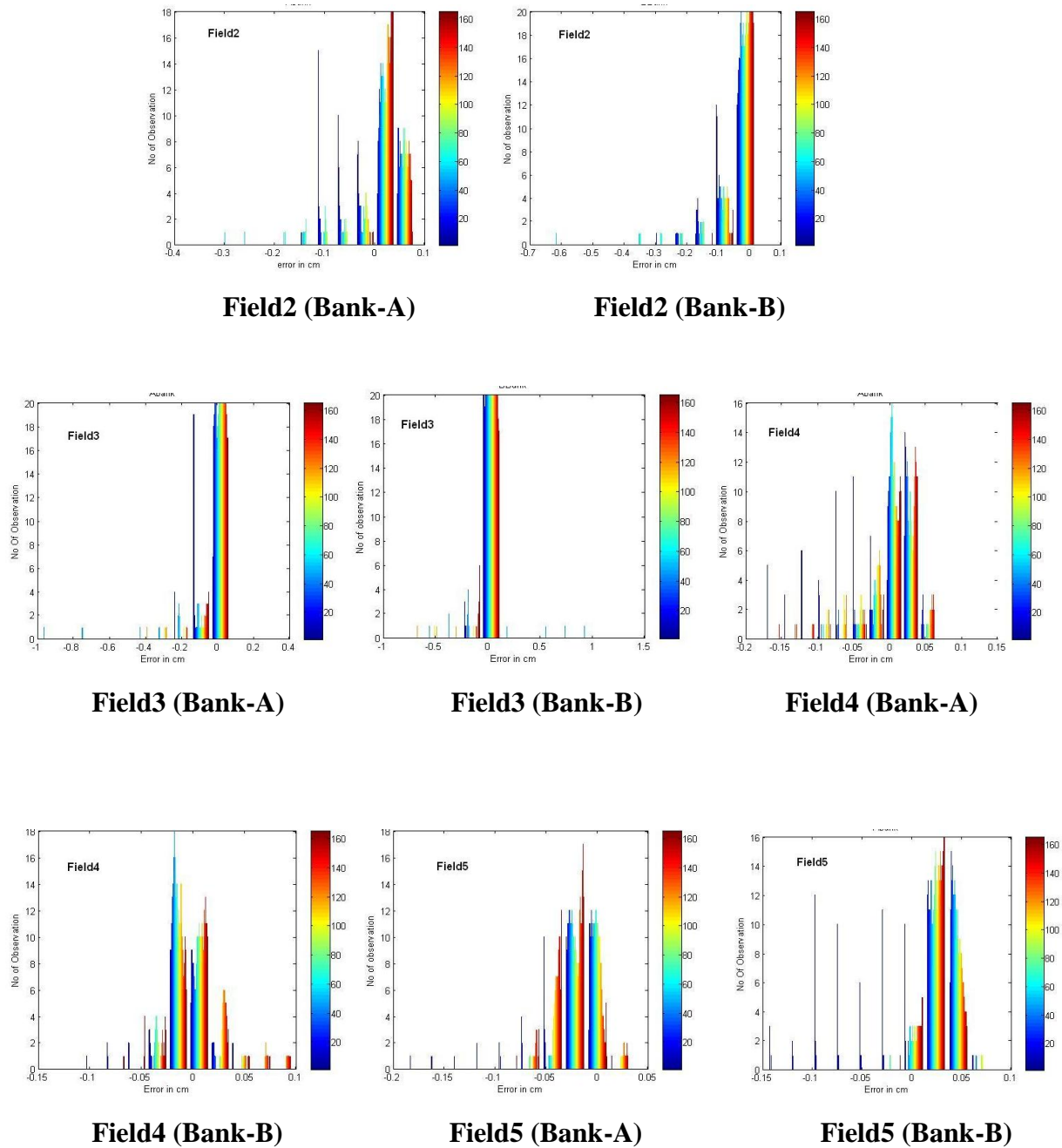


Figure 5.10: Error histograms of differences in leaf positions determined from trajectory log record and EPID images for A and B bank for other fields of an IMRT case.

Similar results were obtained for all the ten IMRT cases. From the figure 5.5 and 5.9, it can be seen that results for Truebeam LINAC are better than C-series LINAC which can be attributed to the

fewer beam holds on Truebeam because Truebeam pre-calculates required dose rate and MLC leaf speeds before treatment begins so that during treatment dose rate and leaf speed are continuously adjusted to ensure that leaves are always in correct position and hence no beam holds are required. Positioning accuracy of MLC leaves is slightly better for Truebeam LINAC than C-series LINAC. EPID images on Truebeam have time stamp in header file so it is easy to match EPID images with correct data line in log file. But for C-series LINAC, time of EPID images can only be inferred or approximated. The methodology can be used for establishing the accuracy of trajectory log data where trajectory log files are used as QA tool for IMRT verification as well as for independent routine IMRT QA by generating single number like gamma index to indicate pass or fail of an IMRT treatment plan. Error of 2 mm in leaves position during dynamic treatment may be considered as acceptable limit. A QA indices, such as if numbers of occurrences for 2 mm error are found more than 5% of total number of occurrences, the dosimetric review of planned is advisable can be introduce.

5.4 Conclusions

The positions of MLC leaves recorded in the log files was imaged through the EPID to investigate the authenticity of data recorded in the log files for stationary, moving and IMRT treatment portals. The results of the study indicated that MLC positions indicated in the log files are comparable to MLC positions recorded by EPID within 2mm. Thus, this study establishes that comparing the log files with EPID images is a quick, efficient and effective patient specific IMRT QA tool. This QA methodology can also be utilized for routine real time QA of IMRT delivery.

CHAPTER 6

THREE DIMENSIONAL GAMMA ANALYSIS IN VOLUMETRIC DOSE VERIFICATION IN INTENSITY MODULATED RADIATION THERAPY

6.1 Introduction

A number of dosimetry systems are being used for QA of these advance techniques. The 2D detector array system [Song et al 2013, Hussein et al 2013, Guillot et al 2013, Stasi et al 2012, Sharma D.S. et al 2010, Yewondwossen 2012, Létourneau et al 2004, Jursinic and Nelms 2003] and film dosimetry system [Hu et al 2013, Casanova et al 2013, Ju at al 2002, 2010, Wilcox et al 2007, Esthappan et al 2002, Bucciolini et al 2004, Childress et al 2005,] are very commonly used for planar dose verification, while ionisation chamber [Martens et al 2000, Leybovich et al 2003, Low et al 2003, Dong et al 2003], diode [Higgins et al 2003], alanine [Budgell et al 2011], MOSFET [Deshpande et al 2013] etc are used for point dose measurements. Apart from 2D and 1D dosimetry system, Gel dosimeter as a 3D dosimetry system [Gustavsson et al 2003, Low et al 1999] has also been used for the dosimetry QA but the use of this dosimetry system is always limited to research level and it is not accepted as a routine dosimetry QA system. Apart from gel dosimetry system, electronic dosimetry systems such as Delta4 (ScandiDos, Sweden), ArcCHECK (SunNuclear, USA), COMPASS (IBA Dosimetry GmbH Germany) are claimed to be three dimensional dosimetry QA system [Sadagopan et al 2009, Boggula et al 2010, Li et al 2012]. The dose distributions of an IMRT plan can be compared by the dose difference of the planned and measured dose distribution. The drawback of the dose-difference method is its high sensitivity to steep dose gradients, where small spatial shifts can lead to high dose differences [Blanpain et al 2009]. The concept of distance to agreement (DTA) was introduced to take these spatial shifts into account. It was proposed to use the dose difference in low gradient regions and

the DTA in steep gradient regions [Van Dyk et al 1993, Harms et al 1998]. The gamma (γ) method combines both dose-difference and DTA criteria by defining a distance in the dose-space domain and an acceptance ellipsoid around each point of the reference dose. For these points, the index is the minimal distance to a point of the evaluated dose [Blanpain et al 2009]. An error is reported if it is greater than 1, i.e., if the closest point is outside the ellipsoid. The γ index is now routinely used in verification of delivered treatment plan with one generated by treatment planning systems. Gamma analysis plays important role in deciding the planned and delivered IMRT treatment fluence along with absolute dose verification at a point in routine dosimetry QA in IMRT.

Per-beam planar 2D γ –tests may be impracticable in understanding the clinical significance of dose discrepancies as some time it can produce false positive results due to presence of hot and/or cold areas that exaggerate smaller errors found within the combined dose distributions and false negative results at certain locations where significant dose error may exhibit in the combined dose distribution [Nelms et al 2011]. In addition, the 2D γ -analysis used in planar verification for combined dose distributions is dependent on the selected plane of verification [Al Sa'd et al 2013]. Error may be present in the plane other than selected for the analysis.

The use of electronics 3D dosimetry systems are picking up as dosimetry device for routine practice as IMRT treatments are planned and finalised with predetermined volumetric dose distribution to planning target volume (PTV) and organ at risk (OAR). However, dose verification using planar detector and point dose measurement is not suffice to verify the volumetric set dose criteria during the planning of IMRT. 3D dosimetry systems allow volumetric comparisons of planned and delivered dose using the dose volume histogram for organ of interest. To be more practical, 3D gamma analysis methods make it possible to analyse planned and delivered dose verification taking into account small setup errors of the dosimeter and phantom and/or detector.

This chapter describes the results of volumetric dose verification using dose at 98%, 95%, 2% volume of interest and 3D gamma analysis methods by incorporating quantitative 3D gamma analysis tools in Computational Environment for Radiotherapy Research (CEER). As per our knowledge, the 3D gamma analysis tools of CEER have not been used by any one to demonstrate its suitability for 3D IMRT QA.

6.2 Materials and Methods

All measurements were conducted using a Varian Rapid Arc (Varian Oncology System, USA) medical linear accelerator with a nominal energy of 6 MV. Five head & neck and five thorax region IMRT cases were planned using Eclipse (Varian Oncology System, USA) treatment planning system. The dose computation was performed using Analytical Anisotropic Algorithm (AAA) at a grid size of $0.25 \times 0.25 \times 0.25 \text{ cm}^3$. The planned IMRT cases were transferred to the treatment delivery system using the record & verifying system (Aria ver 10). All QA measurements were performed in the QA mode of the delivery system. These IMRT QA plans were executed with COMPASS dosimetry system in place and delivered dose fluences were measured without any alteration in the planned treatment parameters.

6.2.1 COMPASS 3D dosimetry system

The COMPASS 3D dosimetry system consists of two major components: dose computational software and a MatriXX/ transmission detector system with a gantry attachable inclinometer. The system used in this work had MatriXX evolution as the detector system. The COMPASS has a separate and dedicated beam model to create virtual linear accelerator using the photon beam data of the LINAC. The collapsed cone convolution/superposition algorithm (CC) is the dose engine implemented in COMPASS. The COMPASS dose computation software was commissioned using the machine data which was used for commissioning of treatment planning system of the hospital.

The system uses a model of the linear accelerator to generate a predicted fluence according to the treatment plan (DICOM RT Plan). The predicted fluence is used to calculate the detector response through a detector model. The computed detector response is compared to the measured response obtained from the executing an IMRT beam. The resulting difference is used to modify the predicted fluence and generate a corrected fluence which is called as the reconstructed fluence. From this reconstructed fluence, the 3D dose is reconstructed using the dose engine implemented in the COMPASS on a phantom / patient CT. Thus COMPASS can calculate the dose to CT data set imported from treatment planning system using the treatment delivery machine data as well as the measured fluence by MatriXX/Transmission detector. The COMPASS can also be used as an independent verification system for the routinely used treatment planning system of the hospital. The COMPASS uses the same CT data set with contoured RT structure which is used in the treatment planning system and therefore it is able to compare the anatomical dose distribution of planned and delivered treatment. It can also compare the planned and actual DVH of each contoured RT structure. A specially designed gantry adaptor having source to detector distance of 100 cm for mounting the MatriXX for Varian LINAC supplied by manufacturer was used during data fluence measurement. An additional build-up of 2.0 cm of water-equivalent phantom slabs above MatriXX was placed while fixing it (MatriXX+slabs) to the gantry using the gantry adaptor. The sampling time for measurements was set to 100 ms. An inclinometer was attached to the MatriXX, which provides the real position of the gantry angle at any given time. Therefore, COMPASS system measures the delivered fluence with original gantry angles. The DICOM files (RT plan, RT dose, RT structures, and CT images) of ten patients from the TPS were imported to storage media and transferred into COMPASS system. The dosimetric comparisons with respect to

the following parameters were done with TPS planned and COMPASS reconstructed dose distribution.

- (i) Dose at 98% volume of PTV and OAR
- (ii) Dose at 95% volume of PTV and OAR
- (iii) Dose at 2% volume of PTV and OAR

6.2.2 CERR

As the 3D gamma calculation tool available in the COMPASS does not calculate % of fails and pass volume for set gamma criteria, the CERR software was modified and used in this work. The CERR is a software platform for developing and sharing research results in radiation therapy treatment planning. It is written in Matlab language. The CERR import and display treatment plans from a wide variety of commercial or academic treatment planning systems. Software allows import and registration of experimental data with the planning data [CERR website]. 3D Gamma calculation tools allow the calculation of gamma for preset acceptance criteria for the volume of interest. The 3D gamma calculation tools were modified for determining the % of fails and passes volume for set gamma criteria. DICOM files (RT plan, RT dose, RT structures, and CT images) of each patient for planned and delivered dose were extracted from the TPS and COMPASS system. These files were imported into the CERR platform, which convert these files compatible to display and analysis in CERR. Using 3D gamma calculation tools, the % of fail and pass volume was determined.

6.2.3 3D Gamma calculation:

The gamma evaluation methods combine distance-to-agreement (DTA) criterion with a dose difference criterion through a composite analysis. In this method, closest Euclidean distance is measured in normalised distance-dose space for each reference point with all evaluated points. The closest Euclidean distance is given by [Low et al 1998]:

$$\gamma(r_m) = \min\{\Gamma(r_m, r_c) \} \forall \{r_c\}$$

Where

$$\Gamma(r_m, r_c) = \sqrt{\frac{r(r_m, r_c)^2}{\Delta d^2} + \frac{\delta(r_m, r_c)^2}{\Delta D^2}}$$

$$r(r_m, r_c) = |r_m - r_c|$$

$$\delta(r_m, r_c) = D_c(r_c) - D_m(r_m)$$

$\Gamma(r_m, r_c)$ is a generalised gamma function computed for each measurement point with all calculated position, r_m is position of measurement point, r_c is spatial location of the calculated distribution relative to the measurement point, Δd is the passing criteria for isodose distance, ΔD is the passing criteria for dose, $D_c(r_c)$ is the dose calculated at r_c and $D_m(r_m)$ is the measured dose at r_m . The 3-D Gamma calculation method is based on the methodology given by Wendling et al (2007). Schematic diagram of 3D gamma calculation in CERR is shown below.

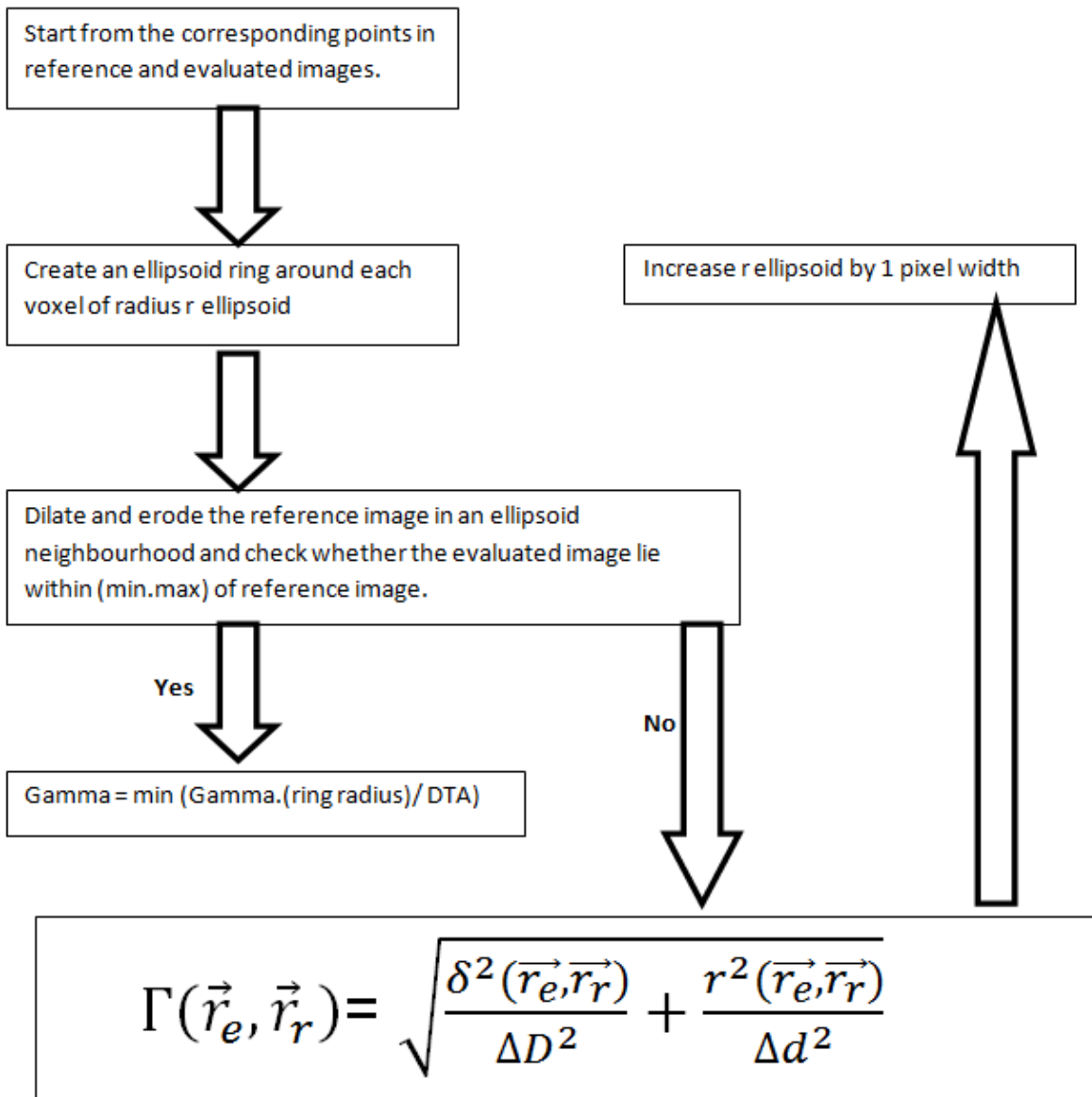
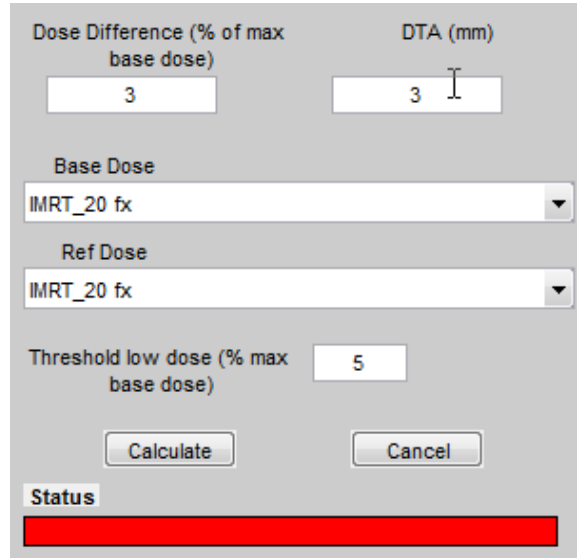


Figure 6.1: Schematic of 3D gamma calculation in CERR

Gamma 3D calculation tools provide user to set the passing criteria for dose difference and DTA. It also provides the threshold dose below which gamma test will not be performed. The 3D gamma was calculated for acceptance criteria of 3% and 3mm. The threshold dose of 5% was chosen below which gamma calculations were not performed. The input parameter used for gamma

calculation is given in figure 6.2. The gamma values at each voxel location in patient data matrices were evaluated. The values of gamma index less or equal to unity were recorded to quantify the volume of interest passing the set criteria (figure 6.3).



The screenshot shows a software interface for 3D gamma calculation. It features several input fields and dropdown menus. The 'Dose Difference (% of max base dose)' field is set to 3. The 'DTA (mm)' field is also set to 3. The 'Base Dose' dropdown menu is set to 'IMRT_20 fx'. The 'Ref Dose' dropdown menu is also set to 'IMRT_20 fx'. The 'Threshold low dose (% max base dose)' field is set to 5. There are 'Calculate' and 'Cancel' buttons at the bottom. A 'Status' bar at the very bottom is highlighted in red.

Figure 6.2: Screenshot showing input field for 3D gamma calculation

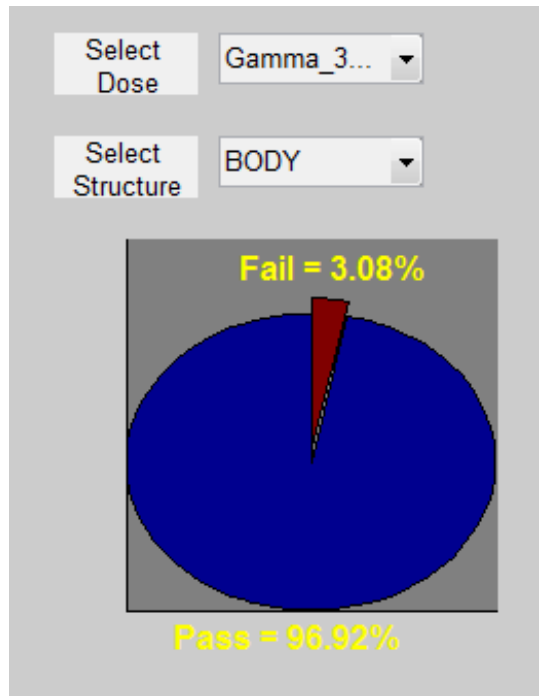


Figure 6.3: Screenshot showing result for 3D gamma calculation

6.3 Results and Discussions

Figure 6.4 shows the visual comparison of dose difference in planned and indirectly measured dose distribution on the patient CT data in transverse plane.

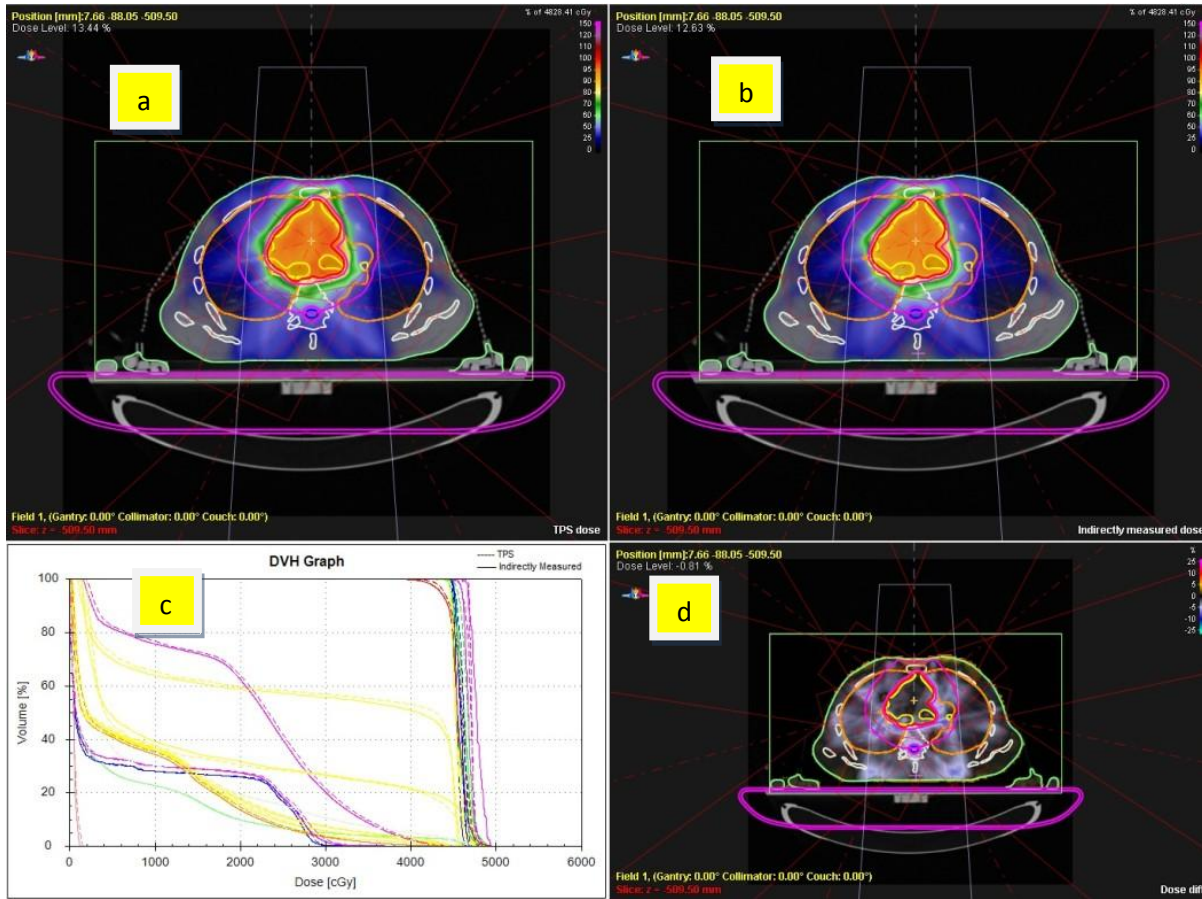


Figure 6.4: Screenshot showing comparison in term of dose difference of planned and indirectly measured dose distribution on patient CT data and dose volume histogram (a) Planned dose distribution (b) Indirectly measured dose distribution (c) Dose Volume histogram comparison for planned and indirectly measured dose distribution (d) Map of dose difference between planned and indirectly measured dose distribution.

Figure 6.4(a) shows the planned dose distribution, figure 6.4(b) shows the indirectly measured dose distribution, figure 6.4(c) shows the dose volume histogram comparison for planned and indirectly measured dose distribution, and figure 6.4(d) shows the map of dose difference between planned and indirectly measured dose distribution. This type of comparisons can be made for whole dose cube by selecting CT slices one by one. Similar comparison can be made in other planes also. Figure 6.5 shows the screen shot showing dosimetric comparison in the three planes. In this way, comparisons can be made for different plane by selecting CT slices one by one. The dose difference at different organ of interest can also be visualised and quantified.

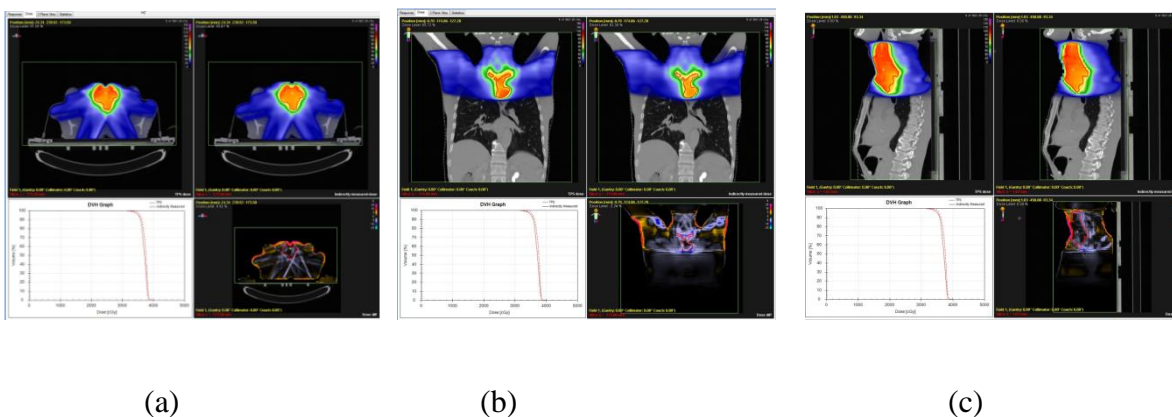


Figure 6.5: Screenshot showing comparison in term of dose difference of planned and indirectly measured dose distribution on patient CT data in (a) Transverse (b) Coronal and (c) Sagittal Plane

The volumetric dose verification method gives great confidence to radiotherapy team about the assurance of accurate dose delivery. Volumetric dose verification data for ten patients treated with IMRT techniques are presented in table 6.1.1.to 6.1.10. The following ICRU 83, the dosimetric parameters for IMRT treatment plan, near-minimum dose (dose at 98% volume), median dose (dose at 50% volume) and near-maximum dose (dose at 2% volume) for planning treatment volume and organ at risk were estimated for planned and indirectly measured dose distribution and their variations were analysed. It can be observed from tables that variation in absolute dose at

98%, 50% and 2% volume of PTV are ranges from -31.92 cGy to 192.53 cGy, -5.97 cGy to 58.07, -48.44 cGy to 54.78 cGy respectively and the relative dose variation is in the range of -0.49 % to 2.87%, -0.09% to 1.22%, -0.89% to 1.28% with respect to near minimum dose to PTV respectively. Maximum variation in absolute dose at 98%, 50% and 2% volume of organ at risk is in the range of -55.19 cGy to 308.11 cGy, -309.86 cGy to 211.58, -128.49 cGy to 373.01 cGy and the relative dose variation is in the range of -0.83 % to 4.65%, -4.66% to 4.99%, -1.94% to 5.63% with respect to near minimum dose to PTV respectively. Figure 6.6 and figure 6.7 are showing bar diagram for dose difference between planned and measured dose distribution in PTV and OAR respectively. It can be noted that the variation of dose for organ at risk is higher than the PTV. Most of the time dosimetric QA in IMRT is focused on the accuracy of dose delivery to PTV, however the verification method should have the equal importance for the organ at risk also as overall efficiency of treatment techniques depend on effectively planned dose which has been delivered throughout the irradiated volume.

Following abbreviations have been used in the table 6.1:

(i) PTV-Planning Target Volume, (ii) SC-Spinal Cord (iii) LP-Left Parotid, (iv) RP-Right Parotid, (v) LX-Larynx (vi) LL-Left side of Lung (vii) RL-Right side of Lung (viii) MB-Mandible (ix) LEO- Left Eye Orbit, (x) REO- Right Eye Orbit, (xi) BS-Brain Stem (xii) ES-Esophagus (xiii) H-Heart (xiv) PB- Proximal Bronch (xv) Pt-patient

Table 6.1: Volumetric dose analysis of TPS calculated and measured dose in IMRT patients.

Table 6.1.1: Volumetric dose analysis of TPS calculated and measured dose for patient1

Dose Volume	Parameters	TPS(cGy)	Indirectly Measured		
			Dose (cGy)	Difference (cGy)	%
PTV	Dose at 98 % volume	3510.95	3459.01	51.94	1.50
PTV	Dose at 50 % volume	3761.63	3725.85	35.77	1.03
PTV	Dose at 2% volume	3844.39	3863.11	-18.71	-0.54
H	Dose at 98 % volume	0.91	0.00	0.91	0.03
H	Dose at 50 % volume	22.91	26.70	-3.79	-0.11
H	Dose at 2% volume	175.35	148.44	26.91	0.78
LL	Dose at 98 % volume	0.00	0.00	0.00	0.00
LL	Dose at 50 % volume	46.40	34.64	11.76	0.34
LL	Dose at 2% volume	2504.22	2436.72	67.49	1.95
RL	Dose at 98 % volume	3.20	0.00	3.20	0.09
RL	Dose at 50 % volume	54.18	38.83	15.34	0.44
RL	Dose at 2% volume	2403.37	2335.86	67.51	1.95

Table 6.1.2: Volumetric dose analysis of TPS calculated and measured dose for patient2

Dose Volume	Parameters	TPS (cGy)	Indirectly Measured		
			Dose (cGy)	Difference (cGy)	%
PTV	Dose at 98 % volume	6,775.70	6,621.79	153.91	2.32
PTV	Dose at 50 % volume	7,246.25	7,188.18	58.07	0.88
PTV	Dose at 2% volume	7,447.42	7,506.61	-59.19	-0.89
RP	Dose at 98 % volume	1,455.14	1,376.90	78.23	1.18
RP	Dose at 50 % volume	4,483.31	4,612.59	-129.28	-1.95
RP	Dose at 2% volume	7,300.10	7,417.44	-117.34	-1.77
LP	Dose at 98 % volume	673.84	627.8	46.04	0.70
LP	Dose at 50 % volume	1,500.85	1,572.14	-71.28	-1.08
LP	Dose at 2% volume	6,012.13	5,832.39	179.74	2.71
LX	Dose at 98 % volume	3,772.79	3,827.98	-55.19	-0.83
LX	Dose at 50 % volume	4,978.04	4,955.22	22.83	0.34
LX	Dose at 2% volume	6,515.71	6,469.16	46.55	0.70
LL	Dose at 98 % volume	82.97	85.93	-2.95	-0.04
LL	Dose at 50 % volume	186.77	166.78	19.99	0.30
LL	Dose at 2% volume	2,656.36	2,490.41	165.95	2.51
MB	Dose at 98 % volume	516.1	480.12	35.98	0.54
MB	Dose at 50 % volume	4,078.25	4,082.73	-4.48	-0.07
MB	Dose at 2% volume	6,687.44	6,639.82	47.62	0.72
SC	Dose at 98 % volume	81.11	134.42	-53.32	-0.81
SC	Dose at 50 % volume	2,891.50	2,804.30	87.2	1.32
SC	Dose at 2% volume	3,895.27	3,794.42	100.85	1.52

Table 6.1.3: Volumetric dose analysis of TPS calculated and measured dose for patient3

Dose Volume	Parameters	TPS (cGy)	Indirectly Measured Dose(cGy)	Difference	
				(cGy)	%
PTV	Dose at 98 % volume	5,887.08	5,773.19	113.89	1.97
PTV	Dose at 50 % volume	6,173.51	6,115.98	57.53	1.00
PTV	Dose at 2% volume	6,340.75	6,352.50	-11.75	-0.20
MB	Dose at 98 % volume	32.47	28.16	4.32	0.07
MB	Dose at 50 % volume	1,863.53	1,739.03	124.5	2.16
MB	Dose at 2% volume	5,838.58	5,655.76	182.82	3.17
LP	Dose at 98 % volume	380.69	423.42	-42.73	-0.74
LP	Dose at 50 % volume	2,460.56	2,411.03	49.53	0.86
LP	Dose at 2% volume	6,172.98	5,838.28	334.69	5.80
SC	Dose at 98 % volume	0	0	0	0
SC	Dose at 50 % volume	3.56	24.81	-21.25	-0.37
SC	Dose at 2% volume	1,467.44	1,388.08	79.37	1.37

Table 6.1. 4: Volumetric dose analysis of TPS calculated and measured dose for patient 4

Dose Volume	Parameters	TPS (cGy)	Indirectly Measured Dose(cGy)	Difference	
				(cGy)	%
PTV	Dose at 98 % volume	6737.29	6630.65	106.64	1.61
PTV	Dose at 50 % volume	7257.16	7243.35	13.81	0.21
PTV	Dose at 2% volume	7464.17	7489.04	-24.87	-0.38
RP	Dose at 98 % volume	853.32	807.73	45.59	0.69
RP	Dose at 50 % volume	3131.88	3441.74	-309.86	-4.67
RP	Dose at 2% volume	6960.4	7088.9	-128.49	-1.94
MB	Dose at 98 % volume	1181.06	1157.56	23.5	0.35
MB	Dose at 50 % volume	6648.58	6680.69	-32.11	-0.48
MB	Dose at 2% volume	7468.99	7447.57	21.43	0.32
LX	Dose at 98 % volume	3362.03	3053.92	308.11	4.65
LX	Dose at 50 % volume	4959.73	4827.03	132.69	2.00
LX	Dose at 2% volume	6152.75	6183.52	-30.77	-0.46
RL	Dose at 98 % volume	84.3	65.77	18.53	0.28
RL	Dose at 50 % volume	186.71	128.34	58.37	0.88
RL	Dose at 2% volume	3095.13	2722.12	373.01	5.63
SC	Dose at 98 % volume	60.8	103.03	-42.22	-0.64
SC	Dose at 50 % volume	2885.02	2835.08	49.94	0.75
SC	Dose at 2% volume	3841.58	3633.7	207.88	3.14

Table 6.1.5: Volumetric dose analysis of TPS calculated and measured dose for patient 5

Dose Volume	Parameters	TPS (cGy)	Indirectly Measured Dose(cGy)	Difference	
				(cGy)	%
PTV	Dose at 98 % volume	6899.12	6706.59	192.53	2.87
PTV	Dose at 50 % volume	7195.9	7170.64	25.26	0.38
PTV	Dose at 2% volume	7364.12	7326.87	37.25	0.56
SC	Dose at 98 % volume	53.52	96.37	-42.85	-0.64
SC	Dose at 50 % volume	2769.53	2666.04	103.49	1.54
SC	Dose at 2% volume	3867.21	3785.71	81.49	1.21
LP	Dose at 98 % volume	822.55	771.56	50.99	0.76
LP	Dose at 50 % volume	2799.09	2838.85	-39.76	-0.59
LP	Dose at 2% volume	5851.19	5746.92	104.28	1.55
RP	Dose at 98 % volume	898.09	854.37	43.73	0.65
RP	Dose at 50 % volume	2767.04	2862.12	-95.08	-1.42
RP	Dose at 2% volume	5846.08	5807.25	38.83	0.579
LX	Dose at 98 % volume	3140.82	3147.71	-6.89	-0.10
LX	Dose at 50 % volume	4375.54	4390.12	-14.58	-0.22
LX	Dose at 2% volume	5749.46	5611.08	138.38	2.06

Table 6.1.6: Volumetric dose analysis of TPS calculated and measured dose for patient 6

Dose Volume	Parameters	TPS (cGy)	Indirectly Measured Dose (cGy)	Difference	
				(cGy)	%
PTV	Dose at 98 % volume	2,370.07	2,322.34	47.72	2.05
PTV	Dose at 50 % volume	2,642.97	2,636.49	6.48	0.28
PTV	Dose at 2% volume	2,751.06	2,752.20	-1.14	-0.05
LL	Dose at 98 % volume	0	0.03	-0.03	0.00
LL	Dose at 50 % volume	34.38	27.82	6.57	0.28
LL	Dose at 2% volume	1,109.55	1,116.94	-7.39	-0.32
RL	Dose at 98 % volume	0	0.49	-0.49	-0.02
RL	Dose at 50 % volume	41.37	32.33	9.04	0.39
RL	Dose at 2% volume	2,534.94	2,561.23	-26.3	-1.13
SC	Dose at 98 % volume	2,398.44	2,346.65	51.79	2.23
SC	Dose at 50 % volume	93.94	80.77	13.17	0.57
SC	Dose at 2% volume	0	0	0	0.00

Table 6.1.7: Volumetric dose analysis of TPS calculated and measured dose for patients7

Dose Volume	Parameters	TPS (cGy)	Indirectly Measured Dose (cGy)	Difference (cGy)	
PTV	Dose at 98 % volume	4,440.08	4,401.01	39.07	0.89
PTV	Dose at 50 % volume	4,791.41	4,776.44	14.97	0.34
PTV	Dose at 2% volume	4,933.92	4,970.32	-36.4	-0.83
RL	Dose at 98 % volume	20.11	31.1	-10.99	-0.25
RL	Dose at 50 % volume	115.49	145.41	-29.92	-0.68
RL	Dose at 2% volume	508.48	534.2	-25.71	-0.58
ES	Dose at 98 % volume	56.88	63.67	-6.79	-0.15
ES	Dose at 50 % volume	199.54	221.85	-22.3	-0.51
ES	Dose at 2% volume	2,928.47	2,760.35	168.12	3.82
SC	Dose at 98 % volume	78.63	103.37	-24.73	-0.56
SC	Dose at 50 % volume	149.64	167.24	-17.6	-0.40
SC	Dose at 2% volume	1,687.64	1,637.80	49.84	1.13

Table 6.1.8: Volumetric dose analysis of TPS calculated and measured dose for patient 8

Dose Volume	Parameters	TPS (cGy)	Indirectly Dose (cGy)	Measured	Difference (cGy)	
PTV	Dose at 98 % volume	6,448.07	6,479.99	-31.92	-0.49	
PTV	Dose at 50 % volume	6,835.16	6,841.13	-5.97	-0.09	
PTV	Dose at 2% volume	7,007.99	7,056.42	-48.44	-0.75	
SC	Dose at 98 % volume	148.04	63.87	84.17	1.30	
SC	Dose at 50 % volume	3,116.40	3,080.16	36.24	0.56	
SC	Dose at 2% volume	3,914.96	3,896.24	18.72	0.29	
RP	Dose at 98 % volume	1,702.75	1,683.87	18.87	0.29	
RP	Dose at 50 % volume	5,760.35	5,732.73	27.62	0.43	
RP	Dose at 2% volume	6,914.79	6,866.53	48.26	0.74	
LP	Dose at 98 % volume	371.12	370.81	0.31	0.00	
LP	Dose at 50 % volume	1,255.50	1,262.41	-6.9	-0.11	
LP	Dose at 2% volume	5,884.28	5,796.66	87.62	1.35	
MB	Dose at 98 % volume	858.15	862.44	-4.28	-0.07	
MB	Dose at 50 % volume	5,065.80	5,133.76	-67.96	-1.05	
MB	Dose at 2% volume	6,869.53	6,892.65	-23.12	-0.36	
BS	Dose at 98 % volume	286.11	261.06	25.06	0.39	
BS	Dose at 50 % volume	1,935.84	1,883.52	52.32	0.81	
BS	Dose at 2% volume	3,967.70	3,942.38	25.33	0.39	

Table 6.1.9: Volumetric dose analysis of TPS calculated and measured dose for patient 9

Dose Volume	Parameters	TPS	Indirectly Measured	Difference	
		(cGy)	Dose (cGy)	(cGy)	%
PTV	Dose at 98 % volume	4,375.48	4,272.31	103.17	2.41
PTV	Dose at 50 % volume	4,586.33	4,545.15	41.19	0.96
PTV	Dose at 2% volume	4,735.35	4,680.57	54.78	1.28
H	Dose at 98 % volume	21.66	29.13	-7.47	-0.17
H	Dose at 50 % volume	172.24	158.59	13.65	0.32
H	Dose at 2% volume	4,588.86	4,542.24	46.62	1.09
RL	Dose at 98 % volume	29.51	19.12	10.39	0.24
RL	Dose at 50 % volume	530.85	502.05	28.8	0.67
RL	Dose at 2% volume	2,458.71	2,470.99	-12.29	-0.29
SC	Dose at 98 % volume	0	0	0	0.00
SC	Dose at 50 % volume	76.2	69.11	7.09	0.17
SC	Dose at 2% volume	2,856.44	2,742.21	114.23	2.67

Table 6.1.10: Volumetric dose analysis of TPS calculated and measured dose for patient 10

Dose Volume	Parameters	TPS	Indirectly Measured	Difference	
		(cGy)	Dose (cGy)	(cGy)	%
PTV	Dose at 98 % volume	4,317.30	4,238.43	78.87	1.86
PTV	Dose at 50 % volume	4,602.15	4,550.40	51.75	1.22
PTV	Dose at 2% volume	4,753.28	4,777.53	-24.25	-0.57
SC	Dose at 98 % volume	0	0	0	0.00
SC	Dose at 50 % volume	64.2	62.85	1.35	0.03
SC	Dose at 2% volume	2,888.47	2,846.00	42.48	1.00
RL	Dose at 98 % volume	35.49	24.34	11.15	0.26
RL	Dose at 50 % volume	221.77	166.09	55.68	1.31
RL	Dose at 2% volume	4,280.32	4,236.56	43.76	1.03
PB	Dose at 98 % volume	137.4	107.74	29.66	0.70
PB	Dose at 50 % volume	4,290.06	4,078.48	211.58	4.99
PB	Dose at 2% volume	4,588.57	4,556.86	31.72	0.75
LX	Dose at 98 % volume	198.18	147.29	50.89	1.20
LX	Dose at 50 % volume	411.6	457.32	-45.72	-1.08
LX	Dose at 2% volume	4,668.29	4,715.75	-47.46	-1.12

These information play very crucial role in finalising the treatment plan especially where tolerance dose in serial organ is the issue of concern. Figure 6.8 present distribution of calculated gamma value in sagittal, transverse and coronal planes.

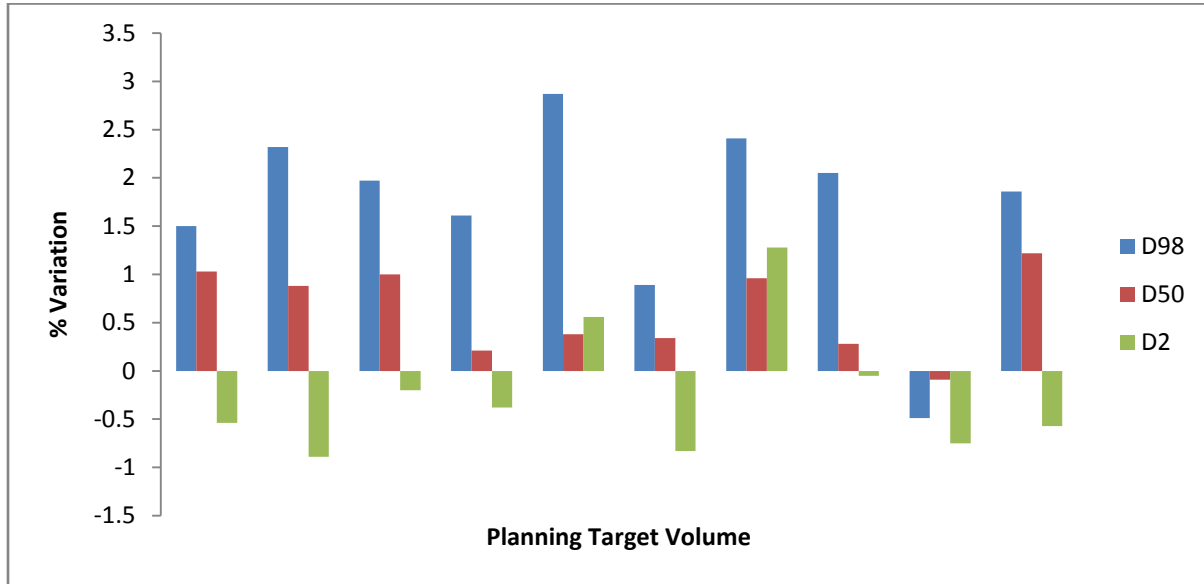


Figure 6.6: Dose difference of planned and indirectly measured dose distribution on patient CT data for 98 %, 50 %, 2 % volume of PTV in ten IMRT cases

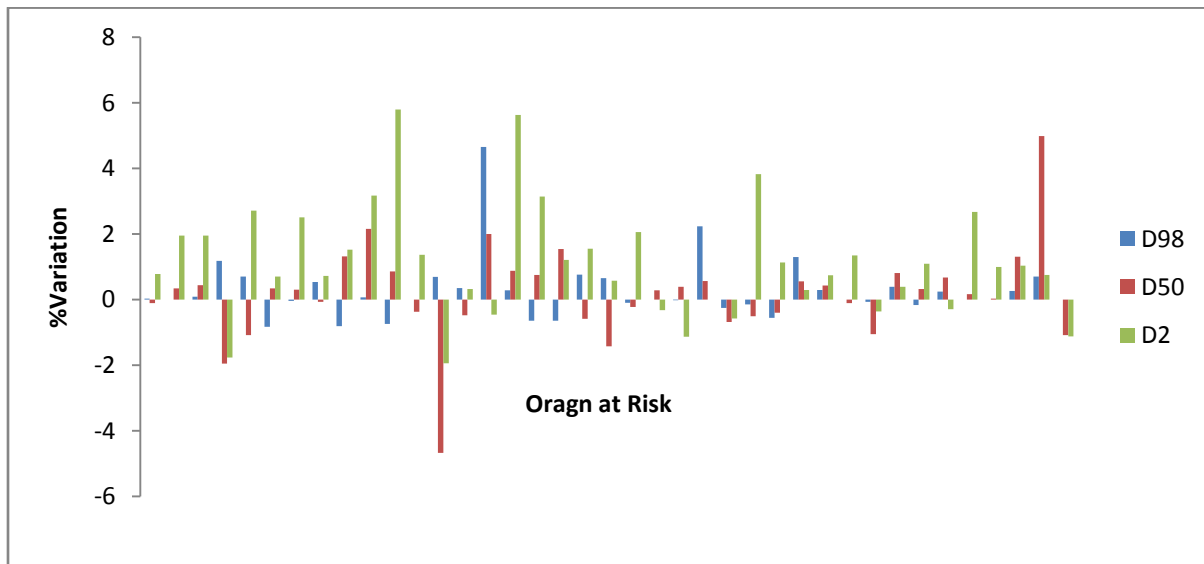


Figure 6.7: Dose difference of planned and indirectly measured dose distributions on patients CT data for 98 %, 50 %, 2 % volume of different organ at risk in ten IMRT cases

Dosimetry QA in IMRT using gamma analysis method is considered as superior in contrast to dose difference or DTA methods as it is a composite method of evaluation and also takes into account small setup errors of the dosimeter phantom and/or detector. Percentage of passing voxel for which 3D gamma values are unity or less than unity for body contour having dose more than 5% for set acceptance criteria of 3% and 3 mm are shown in the figure 6.9.

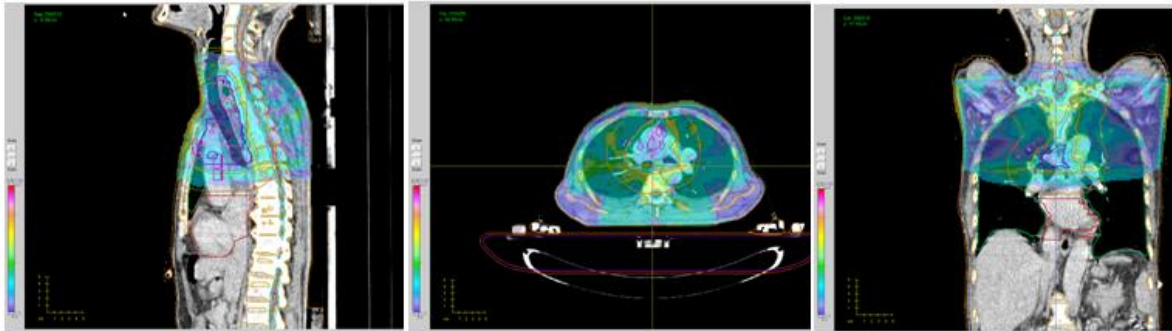


Figure 6.8: Screenshot showing 3D gamma distribution in different plans of patient CT. Colour shows the value of calculated gamma.

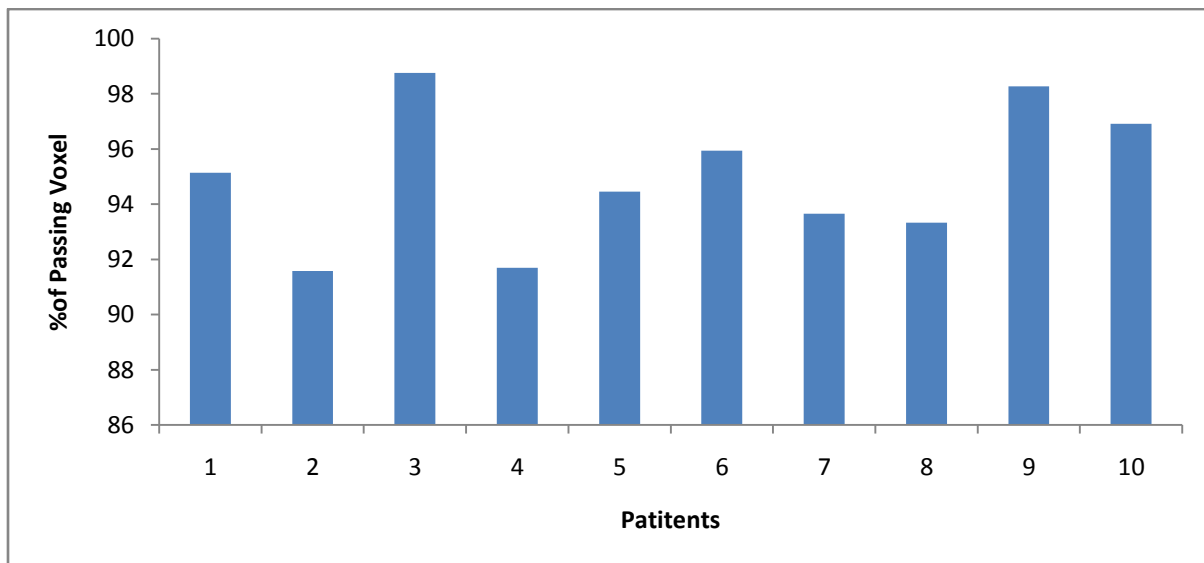


Figure 6.9: Bar diagram showing % of passing voxel in contoured body structure of patient CT data having dose more than 5% with 3% and 3mm set criteria of gamma evaluation

It can be observed from the figure that percentage of passing voxel is more than 90%. The average value of percentage of passing voxel is about 95%. The body contours have maximum volume and can be considered as representative of overall accuracy of treatment delivery. Figure 6.10 present percentage of passing voxel for PTV for different IMRT treatments. It can be inferred from this figure that percentage of passing voxel is more than 94%.

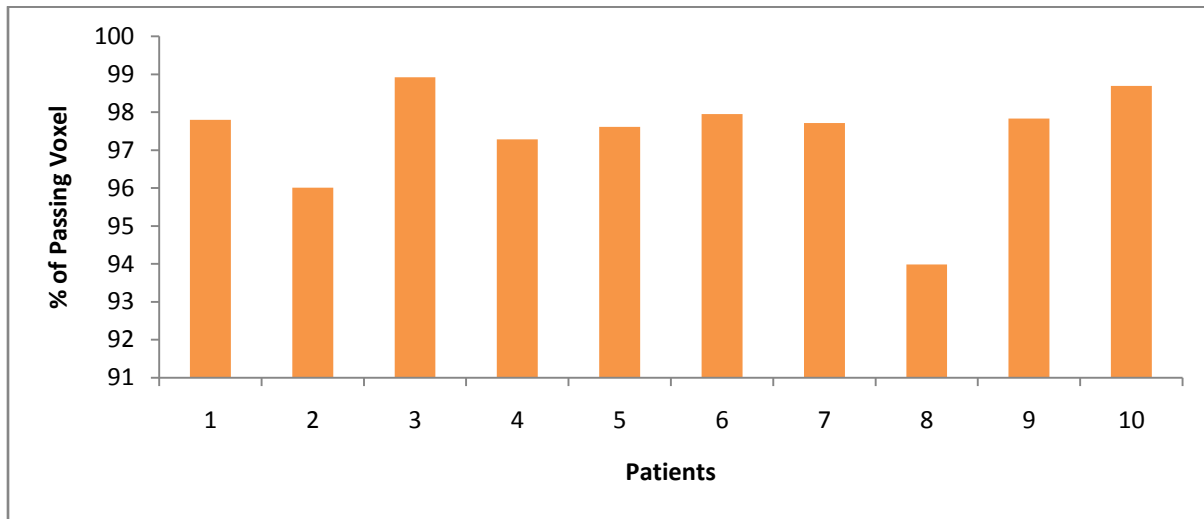


Figure 6.10: Bar diagram showing % of passing voxel in PTV with 3% and 3mm set criteria of gamma evaluation

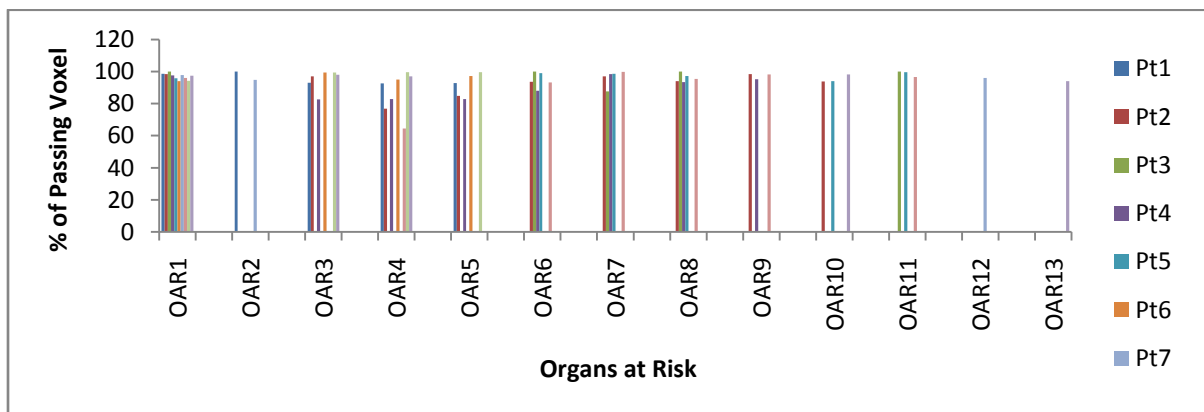


Figure 6.11: Bar diagram showing % of passing voxel in contoured OAR having dose more than 5% with 3% and 3mm set criteria of gamma evaluation

The average value of percentage of passing voxel is more than 97%. Percentage of passing voxel for which gamma values for different OARs having dose more than 5% for ten IMRT cases are shown in the figure 6.11. It can be observed from the figure that percentage of passing voxel ranges from 64.59 to 100%. The average value of percentage of passing voxel is about 95%. Percentage of voxel passing the gamma value varies a lot in case of OAR. It is very important to know how much percentage of a volume is failed to meet set criteria in finalising an effective treatment. These information cannot be obtained where dose verification is carried out using planar or point dosimetry methods.

Analysis tools available in COMPASS system provide information about average 3D gamma for region of interest [Al Sa'd et al 2013]. Since the valid gamma index ranges from zero, the average value of 3D gamma does not provide information about the % of volume/ voxel fails to set tolerance. Further, significant % of volume/voxel may fail the set tolerance in spite of average gamma value less than 1. Therefore, to quantify the error in planned and delivered dose using 3D gamma index method, determination of % of volume / voxel for gamma index less than 1 is more significant.

6.4 Conclusions

A systematic study was carried out to evaluate 3D gamma as part of patient specific QA of ten IMRT cases. The 3D gamma values were determined incorporating 3D gamma calculation tool in CERR using the 3D dose matrix derived from COMPAAS 3D dosimetry QA system. This study demonstrates the usefulness of 3D dosimetry QA in IMRT where medical physicist and radiation oncologist can evaluate the dose was delivered in the same manner as it was planned.

CHAPTER 7

DEVELOPMENT OF A DYNAMIC PHANTOM FOR QA IN 4D RADIOTHERAPY

7.1 Introduction

The images used for delineating GTV, CTV, PTV and OAR are considered as fundamental stone of radiotherapy treatment process. Proper delineation of these volumes demands an accurate imaging system. Accuracy of imaging system becomes more important when tumor is located very near to a critical structure. It may be noted that inaccuracy in imaging system may lead to failure of radiotherapy treatment. In a conventional CT imaging system, respiratory induced internal motion can introduce significant artifacts/errors in images; consequently treatment designed on such data may lead to suboptimal end result. A simple approach to account for the respiratory motion in 3D CT based treatment techniques is to increase the margins relative to the actual tumour size. This way the clinical target receives the prescribed dose but results in an increase in dose to the normal tissue which is undesirable. Another advanced method to correct for respiratory motion is through four-dimensional radiation therapy (4D RT); respiratory gated radiotherapy where 4D CT system is used as imaging device. In this technique, treatment beam is turned ON only when the tumor reaches a specified location otherwise beam will remain OFF. This approach allows design of smaller field opening and minimum healthy tissue irradiation.

4D CT system accommodates the respiratory motion of the patient during scanning and produces accurate images of tumor at different phases of breathing cycle. The accuracy of these 4D CT images increases the accuracies of tumor/OAR delineation. 4D CT images also provide the tumor trajectory information over the period of breathing cycle. 4D CT scans are acquired synchronously with a respiratory signal and provide multiple 3D CT image data sets, sorted by respiratory phase. These CT data are used for treatment planning. There are a number of sources of error in 4D CT

imaging systems such as patient motion during image acquisition while reconstruction assumes that the patient is motionless during acquisition of a single set of CT images. In reality, the gantry of the CT scanner rotates at a finite speed. Along with the chance of error at imaging process, possibility of error at delivery level cannot be completely ignored.

To make the efficient use of this technique, a dynamic phantom is required for QA of imaging, planning and delivery of 4D radiotherapy system [Jiang et al 2008]. The phantom should be able to quantify the volumetric and positional aliasing of CT in the presence of 3D target motion, evaluate the target localization accuracy of onboard imaging system, test the accuracy and consistency of tumour tracking and respiratory gating device and dosimetry accuracy of dose delivery. To meet the above QA requirement, a dynamic phantom for 4D radiotherapy system was developed. This chapter describes the design feature and performance of indigenously developed dynamic phantom for QA in 4D radiotherapy.

7.2 Materials and Methods

7.2.1 Dynamic Phantom System

The dynamic phantom system consists of a tissue equivalent body; lung equivalent cylinder, surrogate, motion control system and software. The phantom body represent average human thorax in shape (elliptical), proportion and composition. The physical dimensions of the phantom are 30 cm (width) x 30 cm (length) x 20 cm (height). The lung equivalent lobe of the phantom incorporates moveable lung equivalent cylinder containing a target with provision to hold different types of detectors. The moveable lung equivalent cylindrical inserts have 45 cm length and 10 cm diameter. The moveable insert incorporate PTV away from centre (i.e. off axis) in such way that three dimensional motion in PTV such as inferior to superior, lateral and anterior-posterior can be

provided through linear translation and rotation of the lung equivalent rod. There are three replaceable PTVs, first contains PTV only, second contains PTV with copper marker and the third PTV has provision to incorporate TLD. Copper marker present in the PTV can be visualised in the images and which can be used to track the motion of the PTV. This phantom is equipped with three synchronised motors. First motor provides linear translation motion, second motor provides rotational motion to the movable lung equivalent cylinder and so provide complex three dimensional displacements to the PTV. The third motor is used for providing motion to the platform of infrared reflector i.e. surrogate. Figure 7.1 shows the photograph of indigenously developed dynamic phantom with its control system. Figure 7.2 shows photographs of different inserts to be used with the dynamic phantom. This phantom is expected to provide dose verification option in 1-D, 2-D and 3-D along with respiratory motion. The current inserts can be easily replaced with other inserts as per requirement of QA and dosimetry.

7.2.2 Motion Control System

A dedicated motion control system with graphical user interface (GUI) was developed. Figure 7.3 shows the photographs of control system developed for this phantom. The control system is used to synchronise three motors to produce a patient specific respiratory motion pattern as well as user defined standard motion pattern. Motion control unit is connected with laptop through Ethernet wire. Dynamic phantom is equipped with three independent sensors which are used to calibrate the drive systems to assure the repeatable motion pattern. First step in operation of the phantom is to set zero for all the three axes. The control system stores this zero position with the help of three independent sensors and which is remain in the memory until it is reset to zero at some other location by the user. Whenever the system is made ON next time, all the motion drive systems can be send to zero position by clicking on homing button provided in GUI. Once

homing is done, the system is ready to play a given respiratory motion pattern. The system can load the respiratory pattern from Real Time Position Management (RPM) system file of patient acquired during imaging and user defined pattern which include Sin, Cos, Triangular, Sin6, Cos4 and constant motion pattern. User defined pattern can be selected from a drop down menu. These patterns can be imposed on the three drive systems. Individualised, amplitude and phase shift can be set for the drive system. An input field has been provided for frequency of the motion pattern. The motion patterns are displayed in real time as time vs amplitude for all the drive systems. The three drive systems can be synchronised and also can be played independently. The RPM file for a standard motion pattern can be generated by placing the infrared reflector on the surrogate platform and recording the motion pattern played for surrogate platform using infrared camera installed in the imaging room. The GUI system can provide the x, y, z coordinate of the target with time so that trajectory of the target during motion can be predicted. Figure 7.4 represents a 3D graph showing the trajectory of target during motion. These data can be used to calculate the location of target and also used to compare the location of target from the 4D imaging system.

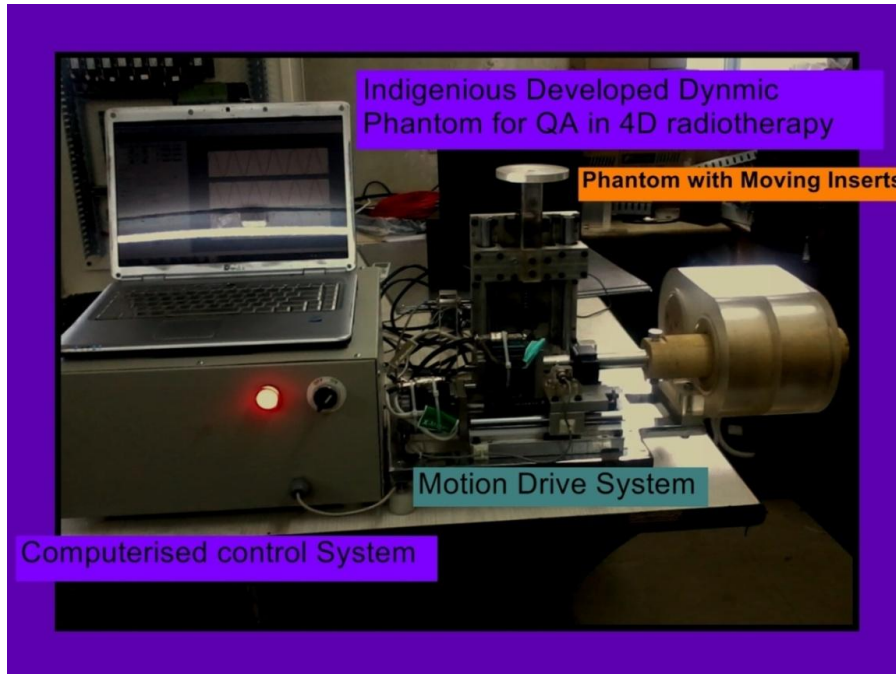


Figure 7.1: Photograph of indigenously developed dynamic phantom with control system



Figure 7.2: Photograph of some of the inserts available with the dynamic phantom.

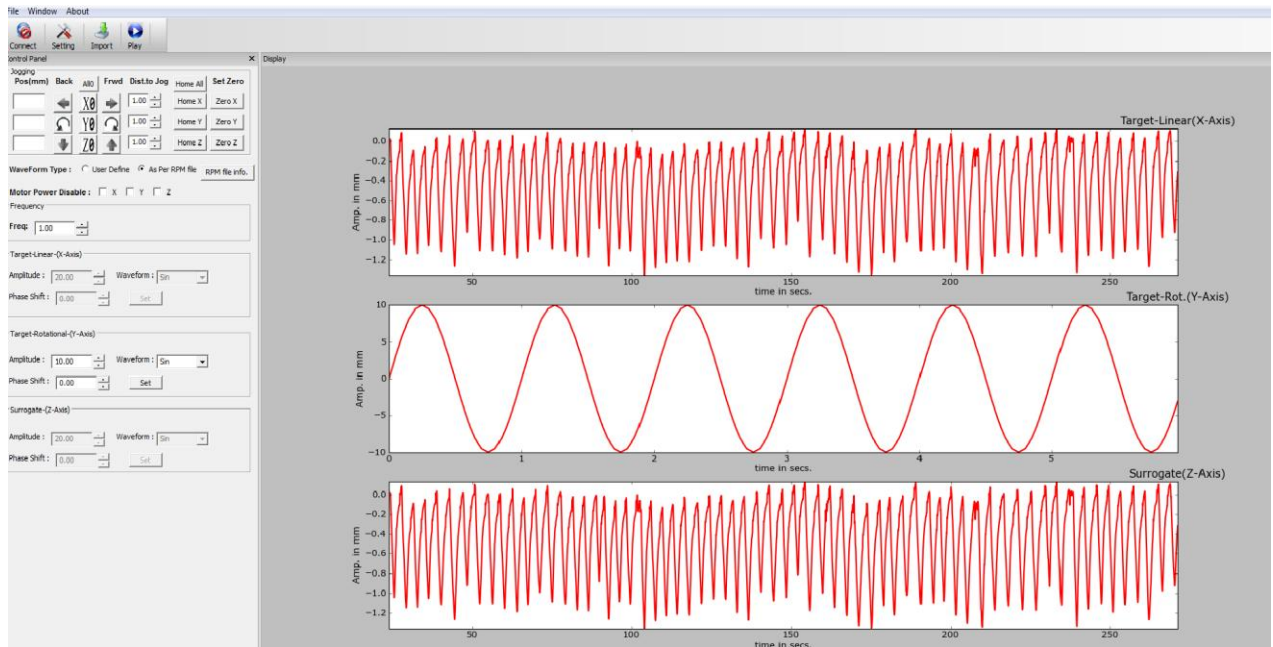


Figure 7.3: Screenshot of control system of dynamic phantom.

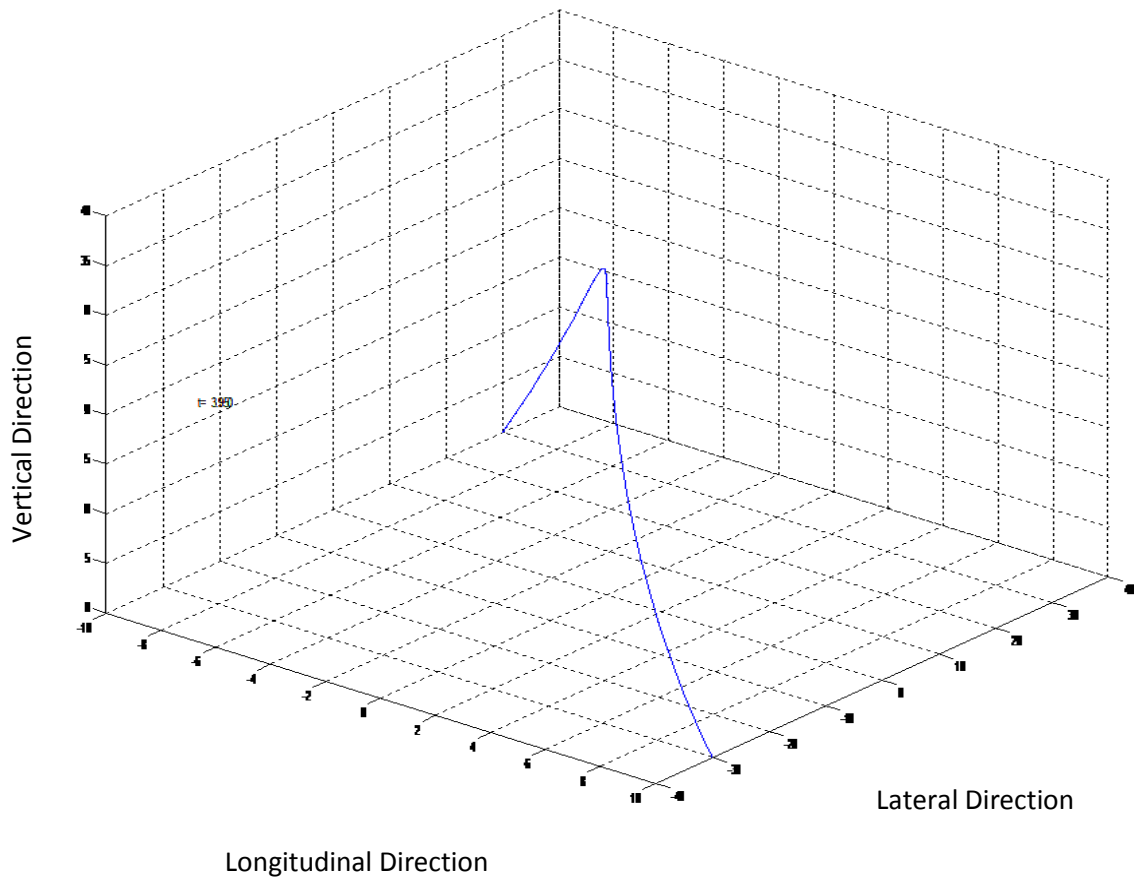


Figure 7.4: 3D graph showing the trajectory of target during motion.

7.2.3 Experimental Method

A sinusoidal motion pattern having 0.25 sec frequency, 10 mm linear amplitude with 90 degree phase difference and 90 degree rotational amplitude with 270 degree phase difference was played during the data acquisition is shown in figure 7.5.

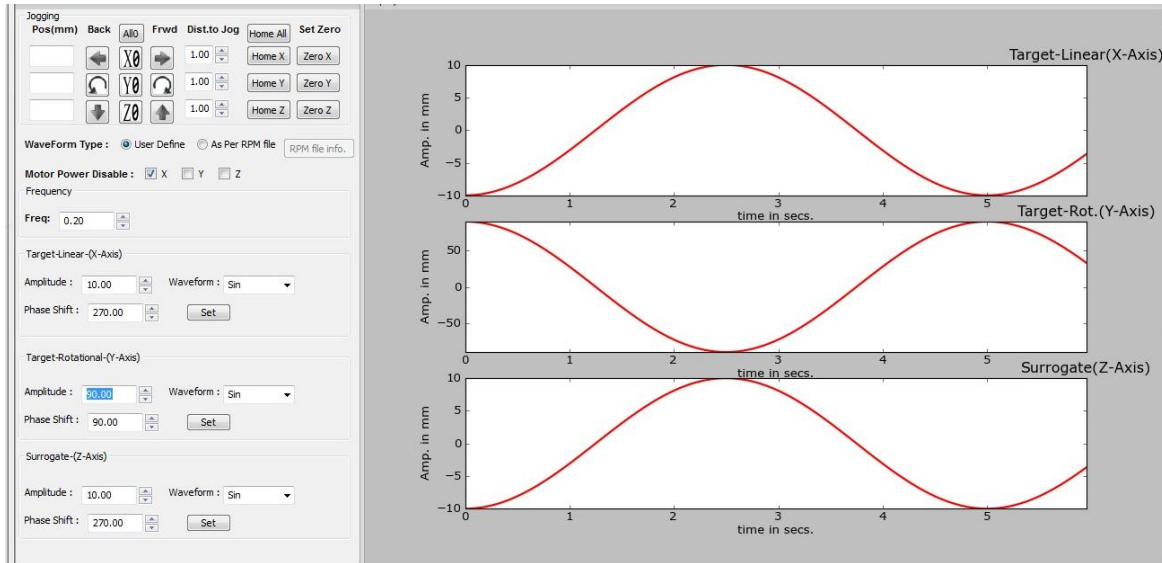


Figure 7.5: Screen shot showing the motion pattern played during the 4D CT data acquisition.

Varian RPM Respiratory Gating System (Varian Medical Systems, Palo Alto, CA) was used to acquire sinusoidal motion pattern (simulating patient breathing pattern). The RPM was used to monitor and track the motion of the PTV incorporated into the phantom. This was performed by tracking the vertical displacement of infrared reflective markers rigidly mounted on a plastic block on the surrogate platform by means of an infrared video camera which is attached with the CT table (figure 7.6). Infrared reflective markers were illuminated by infrared light. The camera is connected to a computer, that runs RPM software to track the marker motion in real-time. The motion of the infrared reflector marker is displayed by a graphical interface on the RPM

workstation (figure 7.7). The motion pattern is sampled at a rate of 30 Hz. The system captures the position of the markers as a function of time during motion. Based on amplitude analysis, a specific motion phase is calculated for each position of the motion cycle. Motion phases are reported in percent values, 0% corresponding to end-inhalation (crest) and 50% to end-exhalation (trough). The software detects end-inhale and end-exhale positions and assigns relative phases in between by linear interpolation. The CT tube ON/OFF state can also be recorded with the motion pattern for retrospective selection of CT images. At each sample, the RPM system records the amplitude and phase along with flag which is used for retrospective 4D-CT, and reflects the time during which the CT x-ray tube is on.

CT data were acquired using GE light Speed RT 16 Scanner (GE Medical Systems, Milwaukee, WI) having 80 cm gantry aperture (bore).

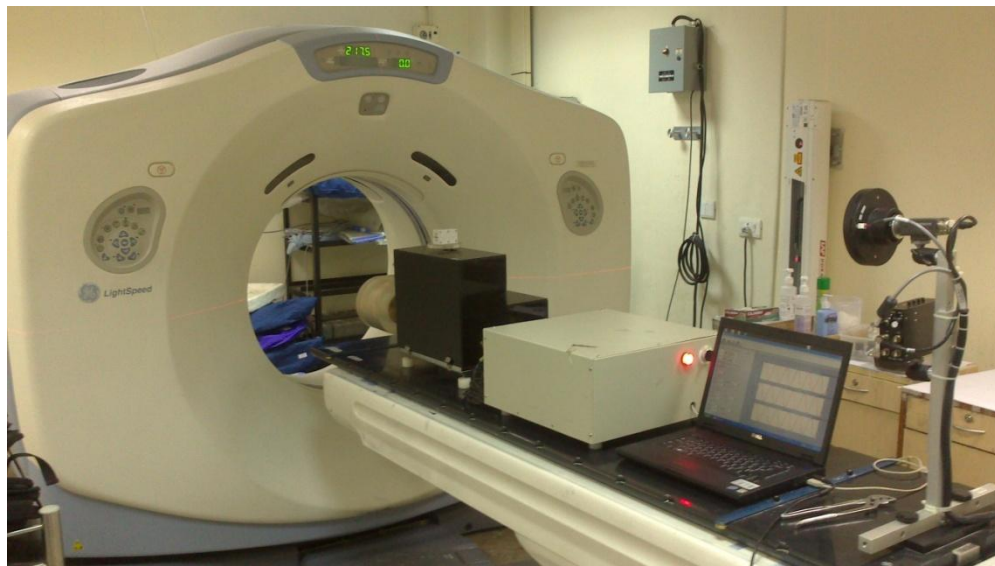


Figure 7.6: Photograph showing experimental set up during 4D imaging of Dynamic Phantom.

The tube current is variable between 10 to 800 mA, and the tube voltage settings are 80, 100, 120, and 140 kVp. Figure 7.6 shows the experimental setup at 4D CT system. The scanner also has 10 to 50 cm transaxial field of view (FOV) and enables one to acquire images with slice thickness ranging between 0.63 and 10.0 mm. The scanner gantry can rotate full 360 degree at variable time of 0.5, 0.6, 0.7, 0.8, 0.9, 1, 2, and 3 sec per rotation.

CT data were acquired in cine mode with 435 mA and 120 kV where the x-ray tube was set ON at consecutive couch positions, and turned OFF when the couch translated from one position to the next position. During the acquisition of our data, an axial field of view of 10 mm at each bed position, cine duration of one respiratory period of the phantom plus 1 s, and a gantry rotation of 1 s were used. The cine interval between images was 0.5 s and the total reconstruction angle was 360°. GE Advantage4D software was used to retrospectively sort images into temporally coherent volumetric image data sets. The software reads the reconstructed images as well as the corresponding RPM respiratory data file. DICOM image headers contain time stamps reporting the moment of data acquisition. Advantage4D software compares these time stamps with recorded time stamps in the RPM file. Based on the precise temporal correlation, a specific amplitude and phase as recorded by the RPM system is associated with each axial image. For building the volumetric data set for different phase, tolerance value for phase was taken as 6%. All the images were transferred to treatment planning system (Eclipse, Varian Medical System) through hospital network system. Location of copper marker placed inside the target at different time were calculated from the motion pattern and compared with the location determined from the constructed 4D images. The volumes of target in different phases were also determined. A 4D radiotherapy plan was generated using 6MV x-ray beam by choosing two arbitrary phases. The plan was generated such that 95% of volume was covered by 95% of isodose line. Then the dose at

the target location was determined. The plan was transferred to delivery system and executed along with RPM system on the medical linear accelerator (Trilogy, Varian Medical System). Dynamic phantom was irradiated with TLDs placed at the target location. Other parameters of the phantom were kept same as it was during imaging and planning procedures.

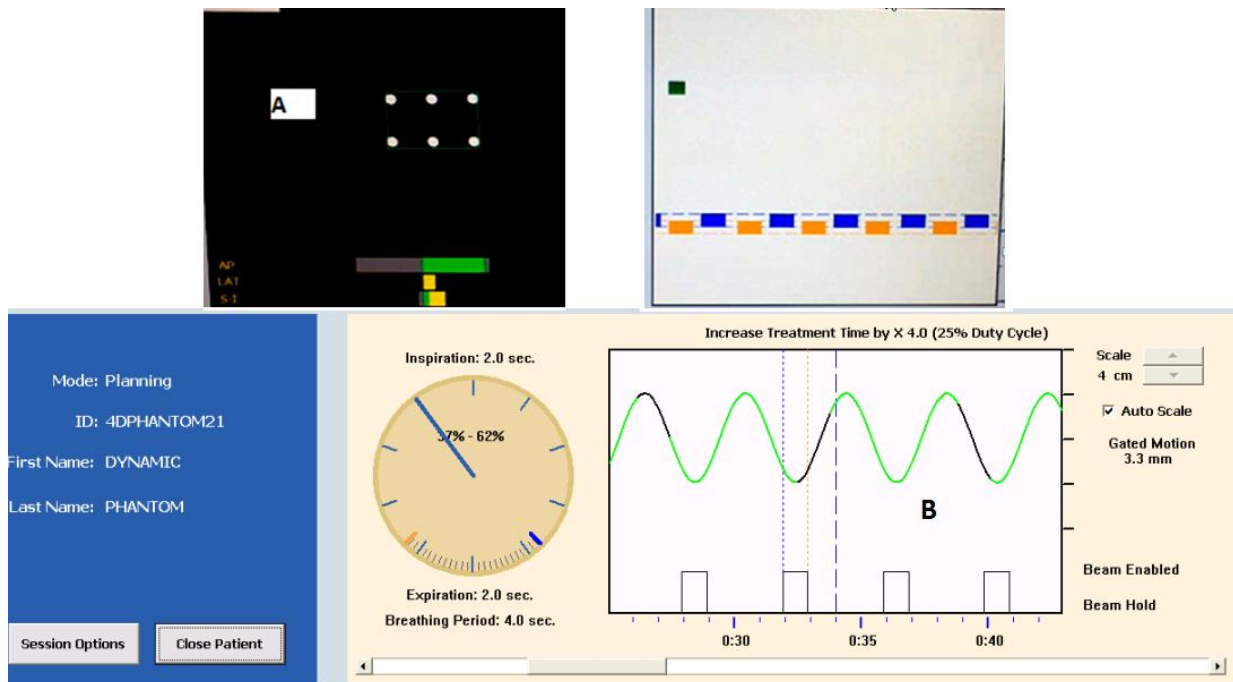


Figure 7.7: Screenshot showing Graphical User Interface of Real Time Position Management system



Figure 7.8: Screenshot showing sorted images of the phantom at 30% phase and associated motion pattern.

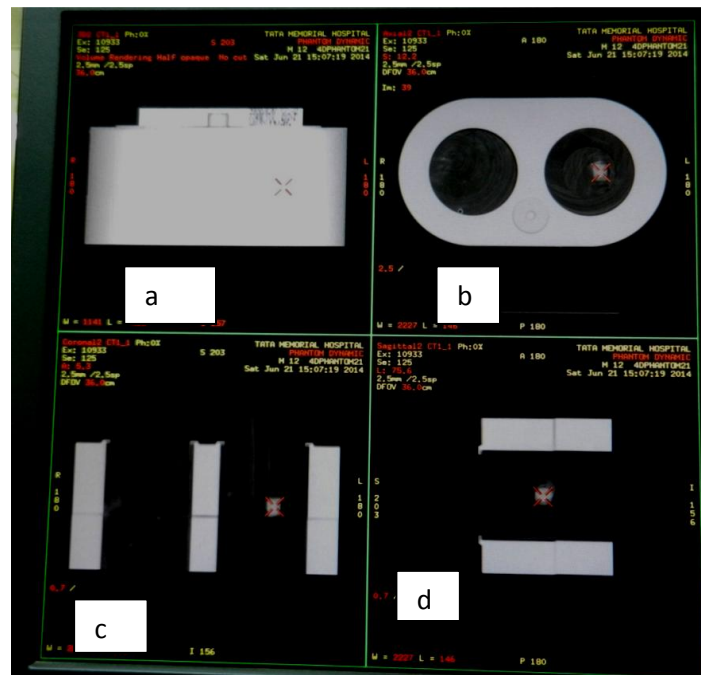


Figure 7.9: Screenshot showing reconstructed image of the phantom: (a) Three dimensional view (b) Transversal Section (c) Coronal Section (d) Sagittal Section. Target placed in lung equivalent lobe is visible in the three sections.



Figure 7.10: Screenshot captured during motion of target and showing displacement of copper marker placed inside the target in different section.

7.3 Results and Discussions

Figure 7.7 shows the respiratory pattern recorded by RPM system for set respiratory motion pattern. Image zone marked with letter A is showing tracking of reflector marker placed on surrogate platform while zone marked with B represent the motion pattern recorded by the RPM system. The green colour on motion pattern indicates x-ray beam is ON while black colour indicated x-ray beam is OFF. From the screenshot we can see the recorded period by RPM is 4 sec which is same as the set value at the control system of dynamic phantom. We can also see the sinusoidal pattern recorded by the RPM system which is similar to the set pattern at the control system of dynamic phantom. It shows the RPM system attached with the 4D CT system is working properly.

Figure 7.8 is screenshot showing sorted images of the phantom at 30% phase. Bottom portion of the screenshot shows the motion pattern used for sorting of the images. Copper wire kept inside the PTV is visible in some slices and invisible in others as the marker is moving along with PTV. Set time (breathing) period of motion pattern was 4 sec and software calculated breathing period which is also called as respiratory cycle was found to be 3.97 sec. So, set time period and 4D CT estimated time period is in good agreement to each other. Figure 7.9 shows screenshot of the reconstructed images of the phantom (a) 3D view, (b) transversal view, (c) coronal view, and (d) sagittal view. The imaging software can display the displacement of tumor in different section for full respiratory cycle after activating movie option and trajectory of region of interest can be visualised in different planes. Figure 7.10 is the screenshot captured during motion of target and it shows displacement of copper marker placed inside the PTV in different section. Movement of copper wire in coronal section can be seen clearly. The displacement was qualitatively visualised by superimposing the grid. Table 7.1 shows the calculated and imaging system determined positions of copper marker located in the PTV. From the table it can be observed that the deviation in displacement ranges from 0.1 to 0.5 mm. Error in positional accuracy during motion derived from the 4D CT system is found to be clinically insignificant.

Table 7.1: Comparison of positional accuracy of copper marker during motion

Displacement	Calculated value (mm)	Estimated value from CT Images (mm)
Longitudinal	20	19.9
Lateral	20	20.5
Vertical	10	10.2

Table 7.2: Volume of aluminium cube determined from reconstructed software for different phase of image acquisition

Phase	Actual Volume (cc)	Measured Volume (cc)
0%	5.33 cc	5.49
10%		5.43
20%		5.26
30%		5.59
40%		5.48
50%		5.44
60%		5.25
70%		5.50
80%		5.55
90%		5.45

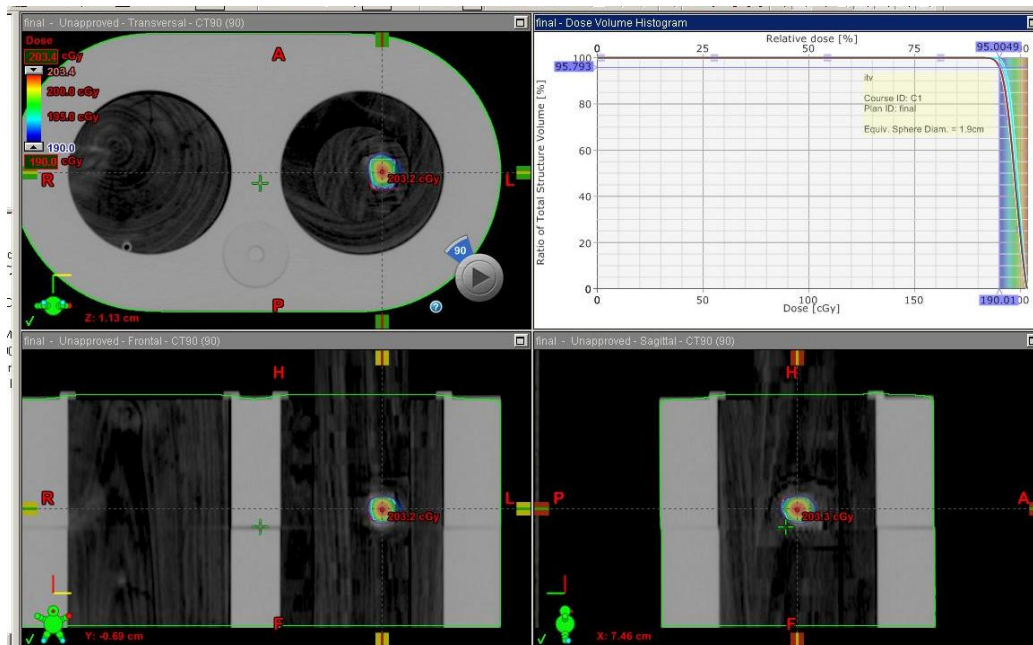


Figure 7.11: Screenshot showing dose distribution in different plane along with resulted dose volume histogram for gated radiotherapy planned on Dynamic Phantom.

The volume of target calculated using its physical dimensions was found to be 5.33 cc. Table 7.2 shows the estimated volume of target in different phases. The variation in volume ranges from 5.25 cc to 5.59 cc. Percentage variation of measured volume in different phases range from -1.5% to 4.87 %. The observed variations are in good agreement with the results reported by Shen et al 2003. This result shows that the 4D system reconstructed the images with proper phase sorting correctly. The above mentioned QA result and methodology gives enough confidence that the 4D imaging system is working as per standard and can be implemented in clinical practice safely. Figure 7.11 shows screenshot showing the placement of beam and calculated dose distribution in different planes along with dose volume histogram. The minimum and maximum doses derived from the treatment planning system at detector location were 181.3 cGy and 203.4 cGy respectively while mean dose was 196.8 cGy. The measured dose was found to be 203.7 cGy. The variation in planned and delivered dose was about 3.5%.

7.4 Conclusions

A dynamic phantom for QA in 4D radiotherapy was designed, fabricated and demonstrated for its functionality. The values and pattern of the studied QA parameters were found as expected. Thus this study indicates that the in-house developed dynamic phantom system is suitable for conducting QA in 4D radiotherapy. This dynamic phantom has unique feature to determine the location of the marker which shows the position of target at a particular time. A thorough study for QA in 4D radiotherapy using this phantom for different vendor's 4D radiotherapy system may be considered as future work.

CHAPTER 8

SUMMARY AND CONCLUSIONS

8.1 Summary and Conclusions

The study was initiated with a national survey on IMRT QA using a well structured questionnaire. The survey reveals that majority of Indian hospitals have adequate machine specific IMRT QA programme but highly inadequate QA programme for the treatment planning system. The survey also revealed that pre-treatment dose verification is carried out at almost all the centres but measurement techniques and plan acceptance criteria are institution specific. Thus, a variety of IMRT QA program in totality is being followed at the Indian hospitals. There is a need to evolve a national protocol for IMRT QA so that treatment outcomes of all the IMRT centres of country can be compared.

As per result of this survey, almost all IMRT practicing hospitals have the program of pre-treatment dose verification using ionization chambers of sensitive volumes ranges from 0.01 to 0.65 cc and pre-treatment dosimetric verification were performed by combining dose from all the gantry angles to a single gantry angle using a slab phantom. However, patients are treated from different gantry angles. An issue often discussed about ability of the dose calculation algorithms of treatment planning system to properly take into account in-homogeneities, especially in low-density regions. Additionally, it is well known that dose calculation errors can be enhanced due to very small fields which are typical for the IMRT technique.

A multi phantom dosimetry study using slab, homogeneous and inhomogeneous phantoms was conducted to investigate the accuracy of pre-treatment dose verification in IMRT at Indian hospitals. This study revealed that the type of the phantom does not play significant role in overall results of dosimetry QA based on point dose measurement. Variations in planned and measured dose were within the tolerance limit. However, data of a few hospitals are biased and showing variations in one direction.

It was also observed that a variety of equipments and methods for planning, delivery and quality assurance (QA) are being used at the hospitals. Considering wide variability in delivery, planning, QA and pre-treatment dose verification methods, dose verification data acquired by the hospitals as part of their institutional pre-treatment dose verification program in IMRT were collected from 10 different hospitals in the country. The statistical analysis of these data was conducted to assess the quality of the IMRT practice at these institutions. This study revealed that IMRT centers are having random and biased (skewed towards over or under dose) distribution of the percentage variation in difference between measured and planned doses, while they are using the TPS and beam delivery systems of the same vendor. The analysis of the results of the IMRT pre-treatment dose verification also revealed that there are systematic errors in the chain of IMRT treatment process at a few centers included in this study. The dosimetry quality audit prior to commissioning of IMRT may play an important role in avoiding such discrepancies.

As mentioned above, type of phantoms used for pre-treatment dose verification process does not play major role for point dose measurement, however considering the complexity involved in IMRT process, point dose measurement based verification is not sufficient. A number of IMRT phantom with facility for holding different types of detectors are available commercially for this purpose. Majority of these phantoms are made up of solid / plastic water material. Though these

phantoms are suitable for pre-treatment dose verification in IMRT but they are very costly and some of these have limited measurement options. Therefore, there is a need to design and fabricate IMRT phantom which is made up of tissue equivalent material with options to verify the dose at a point and obtain dose distribution in 2D and 3D. In addition, the phantom should be made available at a reasonable cost. In the light of these requirements, a versatile IMRT phantom was designed and fabricated from using low cost tissue equivalent material Acrylonitrile Butadiene Styrene (ABS) plastic. This ABS plastic phantom was used for the pre-treatment dose verification measurement in IMRT using ionization chamber, TLDs, radiochromic and radiographic films to demonstrate its suitability. Measurements were also carried out using commercially available Scanditronix-Wellhofer IMRT RW3 phantom to compare the results obtained using ABS IMRT phantom. The studies carried out on this phantom indicate that it is equivalent to commercially available plastic/solid water IMRT phantom. The ABS phantom is a versatile tissue equivalent phantom which can be used for pre-treatment dose verification in IMRT using different types of radiation detectors. The phantom is suitable for dosimetry in 1D, 2D and 3D. Though the suitability of material is demonstrated for IMRT dose verification, it can be used as a tissue equivalent phantom material for dosimetry purposes in other radiotherapy techniques.

Chapter 2 highlighted the need of the dosimetry quality audit program prior to commissioning of IMRT. Considering importance of dosimetry quality audit program an anatomy specific IMRT dosimetry audit phantom representing the thorax region was designed and fabricated for postal dosimetry audit in IMRT. Methodology for postal IMRT audit using TLD for point dose and radiochromic film for planar dose verification was established. Trial audit at five different hospitals was conducted. Percentage variation of point dose measured using TLD at different locations were ranges from -5.91% to 3.95%, however for most of the point of measurements,

percentage deviation were found to be less than 3%. Planar dose verification was carried out using gamma with 3% and 3mm acceptance criteria. Percentage of point having gamma values less than or equal to 1 at these hospitals were ranges from 91.3% to 98.51%. The results of initial studies conducted using this phantom were found encouraging indicating that the in-house developed dosimetry audit phantom and methods are suitable to serve the intended purpose. This trial was conducted at hospital located near Mumbai. However, country level audit program which includes radiotherapy centres from a spectrum of cities (small town and metros) will reflect the true picture of IMRT treatment program in the country.

It is debated in the literature that future patient specific IMRT QA should be more accurate and considerably less time consuming in execution such as QA with software rather than hardware. Because measurement-based patient-specific IMRT QA is both time-consuming and potentially inaccurate as measurements are made in phantoms rather than actual patients. In this connection, patient specific IMRT QA tool using EPID and MLC log files were studied. The software tools were also developed to extract and analyse the following data:

- (i) MLC leaf positions from EPID images for C-series and true beam LINACs,
- (ii) To extract useful data from MLC log file of C-Series LINAC
- (iii) To extract useful information from the trajectory log binary file of Truebeam LINAC,
- (iv) To compare leaf positions derived from EPID images with log file/trajectory log data and
- (v) To analyze IMRT treatment files using the matlab programming language.

Methodology to compare leaf positions measured from EPID images and position recorded in the Log/Trajectory files for IMRT treatment were established and this method was used as tools for quick, efficient and effective patient specific IMRT QA.

IMRT treatments are planned and finalized with predetermined volumetric dose distribution to planning target volume (PTV) and organ at risk (OAR). However, dose verification using point and planar detectors is not sufficient to verify the volumetric set dose criteria during the planning of IMRT. The 3D dosimetry systems allow volumetric comparisons of planned and delivered dose using the dose volume histogram (DVH) for organ of interest. Practically, 3D gamma analysis method makes it possible to analyze planned and delivered dose by taking into account the small setup errors of the dosimetry phantom and detector. The 3D dose verification analysis for IMRT treatment was carried out by two different evaluation techniques, namely (i) by evaluating dose at 98% of volume (D_{98}), dose at 50% of volume (D_{50}) and dose at 2% of volume (D_2) from the DVH, and (ii) by 3D gamma analysis method using COMPASS 3D dosimetry system and computational environment for radiotherapy research (CERR) software platform by incorporating quantitative 3D gamma analysis tools. The dosimetric comparisons with respect to dose at 98%, 50% and 2% volume of PTV and OAR were done with TPS planned and COMPASS reconstructed dose distribution. The 3D gamma evaluations for the indirectly measured and planned dose distributions were calculated by modifying the CERR. Using 3D gamma calculation tools, the percentage fail and pass volume of interest for set acceptance criteria of 3% and 3 mm were determined. Percentage of passing voxel (for which gamma values are one or less than one) for body contour, PTV and organ at risk for set acceptance criteria of 3% and 3 mm were determined. Percentage of passing voxel is more than 90% for body contour. The average value of percentage of passing voxel is about 95%. The body contours have maximum volume and can be considered as representative of overall accuracy of treatment delivery. Percentage of passing voxel is more than 94% for PTV. The average value of percentage of passing voxel is more than 97%. The percentage of passing voxel ranges from 64.59 to 100% for OAR. The average value of percentage

of passing voxel is about 95%. Percentage of voxel passing the gamma value varies a lot in case of OAR. It is very important to know what percentage of a volume is outside the set criteria in finalising an effective treatment plan. This method may be considered as an appropriate method for 3D dose verification in advanced radiotherapy process.

Four-dimensional radiation therapy is defined as the explicit inclusion of the temporal changes of anatomy during the imaging, planning and delivery of radiotherapy. In respiratory gated radiotherapy, the treatment beam is turned on only when the tumor reaches a specified location. This approach allows design of smaller field opening and minimizing extent of healthy tissue irradiation. Respiratory induced motion of tumors and normal tissues can cause significant artifacts in images acquired by helical CT scanning system and ultimately hamper overall treatment quality. The 4DCT system accommodates the respiratory motion of the patient during scanning and produces accurate images of tumor at different phases of breathing cycle. The accuracy of these 4DCT images increases the accuracy of tumor delineation. The 4DCT images also provide the tumor trajectory information over a period of breathing cycle. The 4DCT scans were acquired synchronously with a respiratory signal which provided multiple 3DCT image data sets, sorted by respiratory phase. These CT data were used for treatment planning. There are a number of sources of errors in 4DCT imaging such as patient motion during image acquisition while reconstruction assumes that the patient is motionless during acquisition of a single set of CT images. In reality, the gantry of the CT scanner rotates at a finite speed. To make the efficient use of this technique, a dynamic phantom is required for QA of imaging, planning and delivery of 4D radiotherapy system. The phantom should be able to quantify the volumetric and positional aliasing of CT in the presence of 3D target motion, evaluate the target localization accuracy of onboard imaging system, test the accuracy and consistency of tumour tracking and respiratory

gating device, and dosimetry accuracy of the dose delivery. To meet the above QA requirements, a versatile dynamic phantom for 4D radiotherapy system was developed. A sinusoidal motion pattern was played during the 4DCT data acquisition. The volume of target and position of copper marker kept inside target were verified. A 4D radiotherapy plan by choosing two arbitrary phases were generated using 8 fields 6MV x-ray beams from a number of gantry angles. The plan was generated in such a manner that 95% of volume was covered by 95% of isodose line. The dose at the target location was determined. The recorded breathing period was 4 sec which was the same as set value on the dynamic phantom. Set time (breathing) period of motion pattern was 4 sec and software calculated breathing period (also called as respiratory cycle) was found to be 3.97 sec. So, set time period and measured time period is in good agreement. Calculated volume of target was found to be 5.33 cc. While estimated volume of target in different phases ranges from 5.25 cc to 5.59 cc. Percentage variation of measured volume in different phase ranges from -1.5% to 4.87 %. The observed variations are in good agreement with results reported in literature. Deviations in calculated and estimated position of copper marker were ranges from 0.1 to 0.5 mm. The minimum and maximum doses derived from the treatment planning system at detector location were 181.3 cGy and 203.4 cGy respectively while mean dose was 196.8 cGy. The measured dose was found to be 203.7 cGy. The variation in planned and delivered dose was about 3.5%.

A dynamic phantom for QA in 4D radiotherapy was designed, fabricated and its suitability in 4DRT was demonstrated. In the study, it was found that this phantom is suitable of doing QA in 4D radiotherapy. All the studied parameters are found as expected. Further, this dynamic phantom has a unique feature which can estimate the location of marker which shows the position of the target at a particular time. A thorough study for QA in 4D radiotherapy using this phantom for different vendors of 4D radiotherapy system may be considered as future work.

In summary the works presented cover full range of dosimetry QA procedure highlighting the need of a national QA protocol for IMRT, the need of IMRT dosimetry audit in the country, development of low cost IMRT phantom, development of dosimetry audit phantom and methodology, development of software based dosimetry QA, 3D dosimetry QA methods and development of dynamic phantom for QA in radiotherapy.

8.2 Future work

Though a significant peace of studies were carried out for QA and dosimetry in advanced radiotherapy, it is important to state the future requirements in this area. Accordingly, following studies can be initiated as continuation of the works presented in this thesis:

- Establishment of dosimetry audit program for IMRT and other advanced radiotherapy techniques in the country,
- Index based dose verification method using procedures demonstrated in chapter 5 and its extension for VAMT.
- Comparative study of developed dynamic phantom with commercially available phantoms.

Bibliography

- [1] Dikshit R., Gupta C. P., Hettige C. R., Gajalakshmi V., Aleksandrowicz L., Badwe R., Kumar R., Roy S., Suraweera W., Bray F., Mallath M., Singh P. K., Sinha D. N., Shet A. S, Gelband H., and Jha P. Cancer mortality in India: a nationally representative survey. *Lancet*, 379:1807-1816, 2012.
- [2] Brahme A. Optimization of stationary and moving beam radiation therapy techniques. *Radiother Oncol.*, 12:129-140, 1988.
- [3] Web S. Optimization of conformal dose distributions by simulated annealing. *Phys Med Biol.*, 34:1349-1370., 1989.
- [4] Convery D.J. and Rosenbloom M.E. The generation of intensity-modulated fields for conformal radiotherapy by dynamic collimation. *Phys Med Biol.*, 37:1359-1374., 1992.
- [5] Holmes T and Mackie TR. A filtered back projection dose calculation method for inverse treatment planning. *Med Phys.*, 21:303-313, 1994.
- [6] Mageras G. S. and Mohan R. Application of fast simulated annealing to optimization of conformal radiation treatment. *Med Phys.*, 20:639-647, 1994.
- [7] Bogdanich W. THE RADIATION BOOM: Radiation Offers New Cures, and Ways to Do Harm. *The New York Times*, January 23, 2010.
- [8] W Bogdanich. THE RADIATION BOOM: As Technology Surges, Radiation Safeguards Lag. *The New York Times*, January 26, 2010.
- [9] Thwaites D. J., Mijnheer B. J., and Mills J. A. Quality assurance of external beam radiotherapy. *Radiation oncology physics: a handbook for teachers and students*. International Atomic Energy Agency, Vienna,, 2005.

- [10] Low D A, Moran J M, Dempsey J F, Dong L, and Oldham M. Dosimetry tools and techniques for IMRT. *Med Phys.*, 38(3):1313-38, March 2011.
- [11] Molineu A, Followill DS, Balter PA, Hanson WF, Gillin MT, Huq MS, Eisbruch A, and Ibbott GS. Design and implementation of an anthropomorphic quality assurance phantom for intensity-modulated radiation therapy for the radiation therapy oncology group. *Int. J. Radiat. Oncol., Biol., Phys.*, 63:577- 583, 2005.
- [12] BenchmarkTMIMRT QA phantom. <http://civco.com/oncology/physics/phantom/benchmark/>. Last accessed on 10/10/2008.
- [13] Computerized imaging reference systems, inc. norfolk, va, usa. <http://www.cirsinc.com/products/modality/m6/radiation-therapy/>. Last accessed on 31/07/2014.
- [14] IBA Dosimetry Germany. http://www.iba-dosimetry.com/sites/default/files/brochure/I_mRT_Phantom_01.pdf, The phantom solution for IMRT. Last accessed on 31/07/2014.
- [15] Standard Imaging; Middleton, WI USA. IMRT Dose Verification Phantom. <http://www.standardimaging.com/phantoms/imrt-dose-verification-phantom/>. Last accessed on 31/07/2014.
- [16] Ezzell G A, Galvin J M, Low D, Palta J R, Rosen I, Sharpe M B, Xia P, Xiao Y, Xing L, and Yu CX. Guidance document on delivery, treatment planning, and clinical implementation of IMRT: Report of the IMRT subcommittee of the AAPM Radiation Therapy Committee. *Med. Phys.*, 30(8):2089-115, 2003.
- [17] Steciw S, Warkentin B, Rathee S, and Fallone B G. Guidance document on delivery, treatment planning, and clinical implementation of IMRT: Report of the IMRT

- subcommittee of the AAPM Radiation Therapy Committee. *Med. Phys.*, 32:600 - 612, 2005.
- [18] Gustavsson H, Karlsson A, Back SAJ, Olsson L E, Haraldsson P, Engstrm P, and Nystrm H. MAGIC-type polymer gel for three-dimensional dosimetry: intensity-modulated radiation therapy verification. *Med. Phys.*, 30:1264-71, 2003.
- [19] Xu Y. Wu CS. Three-dimensional dose verification for intensity modulated radiation therapy using optical CT based polymer gel dosimetry. *Med. Phys.*, 33:1412-1429, 2006.
- [20] Standard Imaging; Middleton, WI USA. Respiratory Gating Platform. <http://www.standardimaging.com/phantoms/respiratory-gating-platform/>. Last accessed on 31/07/2014.
- [21] Computerized Imaging Reference Systems, Inc. Norfolk VA USA. Dynamic Thorax Phantom. <http://www.cirsinc.com/products/modality/18/dynamic-thorax-phantom/>. Last accessed on 31/07/2014.
- [22] Modus Medical Devices Inc. Canada. Respiratory Motion Phantom. <http://modusmed.com/qa-phantoms/respiratory-motion>. Last accessed on 31/07/2014.
- [23] Baskar R, Lee K A, Yeo R, and Yeoh K W. Cancer and Radiation Therapy: Current Advances and Future Directions. *Int J Med Sci*, 9(3):193-199, 2012.
- [24] Transition from 2-D Radiotherapy to 3-D Conformal and Intensity Modulated Radio Therapy. IAEA-TECDOC-1588. International Atomic Energy Agency, Vienna, Austria, 2008.
- [25] Boyer A. L., Desobry G. E., and Wells N. H. Potential and limitations of invariant kernel conformal therapy. *Med.Phys.*, 18:703-12, 1991.

- [26] Kuban D. A. and Dong L. High-dose intensity modulated radiation therapy for prostate cancer. *Curr Urol Rep.*, 5:197-202, 2004.
- [27] Kallman P, Lind B, and Ekloff A et. al. Shaping of arbitrary dose distribution by dynamic Multileaf collimation. *Phys Med Biol.*, 33:1291-1300, 1988.
- [28] International Commission on Radiation Units and Measurements. Prescribing, Recording and Reporting Photon Beam Therapy. ICRU Report No. 50. International Commission on Radiation Units and Measurements, Bethesda, MD, 1993.
- [29] Prescribing, Recording and Reporting Photon Beam Therapy (Supplement to ICRU Report 50). ICRU Report No. 60. International Commission on Radiation Units and Measurements, Bethesda, MD., 1999.
- [30] Prescribing, Recording and Reporting Photon Beam Intensity-Modulated Radiation Therapy (IMRT). ICRU Report No. 83. International Commission on Radiation Units and Measurements, Bethesda, MD., 2010.
- [31] Prescribing, Recording and Reporting Photon Beam Therapy. ICRU Report No. 71. International Commission on Radiation Units and Measurements, Oxford University Press, Oxford, 2004.
- [32] Prescribing, Recording and Reporting Electron Beam Therapy. ICRU Report No. 78. International Commission on Radiation Units and Measurements, Oxford University Press, Oxford, 2007.
- [33] Quality assurance in radiotherapy. WHO Report. World Health Organisation, Geneva, Switzerland, 1988.
- [34] Accidental Overexposure of Radiotherapy Patients in Bialystok. International Atomic Energy Agency, Vienna Austria, 2004.

- [35] New York State Department of Health. LINAC/IMRT Significant Misadministration -Software Error Suspected (Notice No.BERP 2005-1). http://www.health.ny.gov/environmental/radiological/radon/radioactive_material_licensing/docs/berp2005_1.pdf, 2005.
- [36] Scottish ministers for the ionising radiation (medical exposures) regulations. Unintended overexposure of patient Lisa Norris during radiotherapy treatment at the Beatson Oncology Centre, Glasgow in January 2006. <http://www.scotland.gov.uk/Publications/2006/10/27084909/0>, 2006.
- [37] The French Nuclear Safety Authority. Report concerning the radiotherapy incident at the university hospital centre (CHU) in Toulouse- Rangueil Hospital. http://www.french-nuclear-safety.fr/Media/Files/Toulouse_ASN_report1.pdf, 2007. Last accessed on 24/07/2014.
- [38] Ash D. and Bates T. Report on the clinical effects of inadvertent radiation under dosage in 1045 patients. *Clin Oncol*, 6(4):214-226, 1994.
- [39] Dutreix A., Derremaux S., Chavaudra J., and van der Schueren E. Quality control of radiotherapy centres in Europe: beam calibration. *Radiother. Oncol.*, 32:256-264, 1994.
- [40] Sawyer D, Aziz KJ, Backinger CL, Beers ET, Lowery A, and Sykes SM et. al. Do it by Design: an Introduction to Human Factors in Medical Devices. US Department of Health and Human Services, Public Health Service, Food and Drug Administration, Center for Devices and Radiological Health, 1996.
- [41] Xing L. and Li J. G. Computer verification of fluence map for intensity modulated radiation therapy. *Med Phys.*, 27(9):2084-92, September 2000.

- [42] Izewska J and Andreo P. The IAEA/WHO TLD postal programme for radiotherapy hospitals. *Radiother Oncol*, 54:65-72, 2000.
- [43] Zhen W Thompson RB Enke CA. Saw C B, Ayyangar KM. Quality assurance procedures for the Peacock system. *Med Dosim.*, 26(1):83-90., Spring 2001.
- [44] Watanabe Y. Point dose calculations using an analytical pencil beam kernel for IMRT plan checking. *Phys Med Biol.*, 46(4):1031-8, April 2001.
- [45] De Brabandere M., Van Esch A., Kutcher G. J., and Huyskens D. Quality assurance in intensity modulated radiotherapy by identifying standards and patterns in treatment preparation: a feasibility study on prostate treatments. *Radiother Oncol.*, 62(3):283-91, March 2002.
- [46] Litzenberg D. W., Moran J. M., and Fraass B. A. Verification of dynamic and segmental IMRT delivery by dynamic log file analysis? *J. Appl. Clin. Med. Phys.*, 3:63-72, 2002.
- [47] Low D. A., Dempsey J. F., Markman J., Mutic S., Klein E. E., Sohn J. W., and Purdy J.A. Toward automated quality assurance for intensity- modulated radiation therapy. *Int J Radiat Oncol Biol Phys.*, 53(2):443-52., June 2002.
- [48] Ju Sang Gyu, Ahn Yong Chan, Huh Seung Jae, and Yeo Inhwan Jason. Film dosimetry for intensity modulated radiation therapy: Dosimetric evaluation. *Med. Phys.*, 29:351, 2002.
- [49] Childress N L, Dong L, and Rosen I I. Rapid radiographic film calibration for IMRT verification using automated MLC fields. *Med Phys.*, 29(10):2384-90, October 2002.
- [50] Chuang CF, Verhey LJ, and Xia P. Investigation of the use of MOSFET for clinical IMRT dosimetric verification. *Med Phys.*, 29(6):1109-15, Jun 2002.
- [51] Izewska J., Bera P, and Vatnitsky S. IAEA/WHO TLD postal dose audit service and high precision measurements for radiotherapy level dosimetry. *Radiation Protection Dosimetry.*

- [52] Yang Y and Xing L. Using the volumetric effect of a finite-sized detector for routine quality assurance of multileaf collimator leaf positioning. *Med Phys.*, 30(3):433-41, March 2003.
- [53] Li J G., Dempsey J F., Ding L, Liu C, and Palta J R. Validation of dynamic MLC controller log files using a two-dimensional diode array,. *Med. Phys.*, 30:799-805, 2003.
- [54] Leybovich L. B., Sethi A., and Dogan N. Comparison of ionization chambers of various volumes for IMRT absolute dose verification. *Med. Phys.*, 30(2):119-23, 2003.
- [55] Low D A and Dempsey J F. Evaluation of the gamma dose distribution comparison method. *Med. Phys.*, 30:2455-2464, 2003.
- [56] Jones A O Kleiman M T. Patient setup and verification for intensity-modulated radiation therapy (IMRT). *Med Dosim.*, 28(3):175-83., fall 2003.
- [57] Jursinic P A and B E Nelms. A 2-D diode array and analysis software for verification of intensity modulated radiation therapy delivery. *Med. Phys.*, 30:870-879, 2003.
- [58] Higgins P D, Alaei P, Gerbi B J, Dusenbery K E. In vivo diode dosimetry for routine quality assurance in IMRT. *Med. Phys.*, 30:3118-23, 2003.
- [59] Izewska J., Andreo P, Vatnitsky S, and Shortt K R. The IAEA/WHO TLD postal dose quality audits for radiotherapy: a perspective of dosimetry practices at hospitals in developing countries. *Radiother Oncol*, 69:91-97, 2003.
- [60] L'etourneau D, Gulam M, Yan D, Oldham M, and Wong JW. Evaluation of a 2D diode array for IMRT quality assurance. *Radiother Oncol.*, 70(2):199-206, 2004.

- [61] Yeo I.J., Ardakani A. B., Cho Y., Heydarian M., Zhang T., and Islam M. EDR2 film dosimetry for IMRT verification using low-energy photon filters. *Med. Phys.*, 31:1960 -63, 2004.
- [62] Yang Y, Xing L. Quantitative measurement of MLC leaf displacements using an electronic portal image device. *Phys Med Biol.*, 49(8):521-33, April 2004.
- [63] Bouchard H., Seuntjens J. Ionization chamber-based reference dosimetry of intensity modulated radiation beams. *Med Phys.*, 31(9):2454 - 65, September 2004.
- [64] Chang J., Obcemea C. H., Sillanpaa J., Mechalakos J., Burman C. Use of EPID for leaf position accuracy QA of dynamic multi-leaf collimator (DMLC) treatment. *Med Phys.*, 31(7):2091-6, July 2004.
- [65] Izewska J., Vatnitsky S, and Shortt K R. IAEA/WHO postal dose audits for radiotherapy hospitals in Eastern and South-Eastern Europe. *Cancer Radiother.*, 8(suppl 1):S36-S43, 2004.
- [66] Moran J. M., Radawski J., Fraass B. A. A dose gradient analysis tool for IMRT QA. *J. Appl. Clin. Med. Phys.*, 6:62-73, 2005.
- [67] Winkler P, Zurl B, Guss H, Kindl P, and Stueckschweiger G. Performance analysis of a film dosimetric quality assurance procedure for IMRT with regard to the employment of quantitative evaluation methods. *Phys. Med. Biol.*, 50:643, 2005.
- [68] Woo M. K., Nico A. Impact of multileaf collimator leaf positioning accuracy on intensity modulation radiation therapy quality assurance ion chamber measurements. *Med Phys.*, 32(5):1440-5, May 2005.

- [69] Wiezorek T, Banz N, Schwedas M, Scheithauer M, Salz H, Georg D, Wendt TG. Dosimetric quality assurance for intensity-modulated radiotherapy feasibility study for a filmless approach. *Strahlenther Onkol.*, 181(7):468-74, July 2005.
- [70] DineshKumar M., Thirumavalavan N., Venugopal Krishna D., and Babaiah M. QA of intensity-modulated beams using dynamic MLC log files. *J Med Phys.*, 31:36 - 41, 2006.
- [71] Vieira SC, Bolt RA, Dirkx ML, Visser AG, and Heijmen BJ. Fast, daily linac verification for segmented IMRT using electronic portal imaging. *Radiother Oncol.*, 80(1):86-92, July 2006.
- [72] van Zijtveld M, Dirkx ML, de Boer HC, and Heijmen BJ. Dosimetric pre-treatment Verification of IMRT using an EPID: clinical experience. *Radiother Oncol.*, 81(2):168-75, November 2006.
- [73] Soares CG. New developments in radiochromic film dosimetry. *Radiat Prot Dosimetry.*, 120(1-4):100-6, 2006.
- [74] Dobler B, Lorenz F, Wertz H, Polednik M, Wolff D, Steil V, Lohr F, and Wenz F. Intensity-modulated radiation therapy (IMRT) with different combinations of treatment-planning systems and linacs: issues and how to detect them. *Strahlenther Onkol.*, 182(8):481 -8, August 2006.
- [75] Zeidan OA, Stephenson SA, Meeks SL, Wagner TH, Willoughby TR, Kupelian PA, and Langen KM. Characterization and use of EBT radiochromic film for IMRT dose verification. *Med Phys.*, 33(11):4064-72, November 2006.
- [76] Yoon M, Lee D H, Shin D, Lee S B, Park S Y, and Cho K H. Accuracy of inhomogeneity correction algorithm in intensity-modulated radiotherapy of head-and-neck tumors. *Med Dosim.*, 32(1):44-51, Spring 2007.

- [77] Nelms BE and Simon JA. A survey on planar IMRT QA analysis. *J Appl Clin Med Phys.*, 8(3):2448, July 2007.
- [78] De Martin E, Fiorino C, Broggi S, Longobardi B, Pierelli A, Perna L, Cattaneo GM, and Calandrino R. Agreement criteria between expected and measured field fluences in IMRT of head and neck cancer: the importance and use of the gamma histograms statistical analysis. *Radiother Oncol.*, 85(3):399-406, December 2007.
- [79] Poppe B., Djouguela A., Blechschmidt A., Willborn K., Röhmann A., and Harder D. Spatial resolution of 2D ionization chamber arrays for IMRT dose verification: single detector size and sampling step width. *Phys Med Biol.*, 52(10):2921-35, May 2007.
- [80] Palta JR, Liu C, and Li JG. Quality assurance of intensity-modulated radiation therapy. *Int J Radiat Oncol Biol Phys.*, 71(1 Suppl.):S108-12, 2008.
- [81] Basran P S and Woo M K. An analysis of tolerance levels in IMRT quality assurance procedures. *Med Phys.*, 35(6):2300 -7., June 2008.
- [82] Pawlicki T, Yoo S, Court LE, McMillan SK, Rice RK, Russell JD, Pacyniak JM, Woo MK, Basran PS, Shoales J, and Boyer AL. Moving from IMRT QA measurements toward independent computer calculations using control charts. *Radiother Oncol.*, 89 (3):330-7, December 2008.
- [83] Amin MN, Norrlinger B, Heaton R, and Islam M. Image guided IMRT dosimetry using anatomy specific MOSFET configurations. *J Appl Clin Med Phys.*, 23(9):3, Jun 2008.
- [84] Howell R M, Smith I P, and Jarrio CS. Establishing action levels for EPID-based QA for IMRT. *J Appl Clin Med Phys.*, 9(3):2721., June 2008.

- [85] Oldham M, Sakhalkar H, Guo P, and Adamovics J. An investigation of the accuracy of an IMRT dose distribution using two- and three-dimensional dosimetry techniques. *Med. Phys.*, 35:2072 -2080, 2008.
- [86] Han Y, Shin EH, Lim C. Kang SK, Park SH, Lah JE, Suh TS, Yoon M, Lee SB, Cho SH, Ibbott GS, Ju SG, and Ahn YC.. Dosimetry in an IMRT phantom designed for a remote monitoring program. *Med Phys.*, 35:2519-27, 2008.
- [87] Koh WY, Ren W, Mukherjee RK, and Chung HT. Internal audit of a comprehensive IMRT program for prostate cancer: a model for centers in developing countries. *Int J Radiat Oncol Biol Phys.*, 74(5):1447-54, August 2009.
- [88] Collomb-Patton V, Boher P, Leroux T, Fontbonne JM, Vela A, and Batalla A. The DOSIMAP, a high spatial resolution tissue equivalent 2D dosimeter for LINAC QA and IMRT verification. *Med Phys.*, 36(2):317-28, February 2009.
- [89] Sadagopan R, Bencomo JA, Martin RL, Nilsson G, Matzen T, and Balter PA. Characterization and clinical evaluation of a novel IMRT quality assurance system. *J Appl Clin Med Phys.*, 10(2):2928, May 2009.
- [90] Fraser D, Parker W, and Seuntjens J. Characterization of cylindrical ionization chambers for patient specific IMRT QA. *J Appl Clin Med Phys.*, 10(4):2923, September 2009.
- [91] Ferreira BC, Lopes MC, and Capela M. Evaluation of an Epson flat bed scanner to read Gafchromic EBT films for radiation dosimetry. *Phys Med Biol.*, 54(4):1073-85, February 2009.
- [92] Anjum MN, Parker W, Ruo R, and Afzal M. Evaluation criteria for film based intensity modulated radiation therapy quality assurance. *Phys Med.*, 26(1):38-43, January 2010.

- [93] Saminathan S, Manickam R, Chandraraj V, and Supe S S. Dosimetric study of 2D ion chamber array matrix for the modern radiotherapy treatment verification. *J Appl Clin Med Phys.*, 11(2):3076, April 2010.
- [94] Anjum M N, Parker W, Ruo R, Aldahlawi I, and Afzal M. IMRT quality assurance using a second treatment planning system. *Med Dosim.*, 35(4):274-9, Winter 2010.
- [95] Bailey D W, Kumaraswamy L, and Podgorsak M B. A fully electronic intensity modulated radiation therapy quality assurance (IMRT QA) process implemented in a network comprised of independent treatment planning, record and verify, and delivery systems. *Radiol Oncol.*, 44(2):124-30, Jun 2010.
- [96] Kruse J. J. On the insensitivity of single field planar dosimetry to IMRT inaccuracies. *Med Phys.*, 37(6):2516-24, June 2010.
- [97] Nelms BE, Zhen H, and Tome WA. Per-beam, planar IMRT QA passing rates do not predict clinically relevant patient dose errors. *Med Phys.*, 38(2):1037-44, February 2011.
- [98] Korevaar EW, Wauben DJ, van der Hulst PC, Langendijk JA, and Van't Veld AA. Clinical introduction of a linac head-mounted 2D detector array based quality assurance system in head and neck IMRT. *Radiother Oncol.*, 100(3):446-52, September 2011.
- [99] Olch A. J. Evaluation of the accuracy of 3DVH software estimates of dose to virtual ion chamber and film in composite IMRT QA. *Med Phys.*, 39(1):81-6, January 2012.
- [100] Wu C., Hosier K. E., Beck K. E., Radevic M. B., Lehmann J, Zhang H. H., Kroner A., Dutton S. C., Rosenthal S. A., Bareng J. K., Logsdon M. D., and Asche D. R. On using 3D -analysis for IMRT and VMAT pretreatment plan QA. *Med Phys.*, 39(6):3051-9, June 2012.

- [101] Sun B, Rangaraj D, Boddu S, Goddu M, Yang D, Palaniswaamy G, Yaddanapudi S, Wooten O, and Mutic S. Evaluation of the efficiency and effectiveness of independent dose calculation followed by machine log file analysis against conventional measurement based IMRT QA. *J Appl Clin Med Phys.*, 13(5):3837, September 2012.
- [102] Stasi M, Bresciani S, Miranti A, Maggio A, Sapino V, and Gabriele P. Pretreatment patient-specific IMRT quality assurance: a correlation study between gamma index and patient clinical dose volume histogram. *Med Phys.*, 39(12):7626 -34, December 2012.
- [103] Chung K, Yoon M, Son J, Yong Park S, Lee K, Shin D, Kyung Lim Y, and Byeong Lee S. Radiochromic film based transit dosimetry for verification of dose delivery with intensity modulated radiotherapy. *Med Phys.*, 40(2):021725., February 2013.
- [104] Carlone M, Cruje C, Rangel A, McCabe R, Nielsen M, and Macpherson M. ROC analysis in patient specific quality assurance. *Med Phys.*, 40(4):042103, April 2013.
- [105] Siochi R. A., Molineu A., and Orton C. G. Patient-specific QA for IMRT should be performed using software rather than hardware methods: Point/Counterpoint. *Med.Phys.*, 40:070601-3, 2013.
- [106] Qin S, Zhang M, Kim S, Chen T, Kim LH, Haffty BG, and Yue NJ. A systematic Approach to statistical analysis in dosimetry and patient-specific IMRT plan verification measurements. *Radiat Oncol.*, 8(1):225, September 2013.
- [107] Hussein M, Rowshanfarzad P, Ebert MA, Nisbet A, and Clark CH. A comparison of the gamma index analysis in various commercial IMRT/VMAT QA systems. *Radiother Oncol.*, 109(3):370-6., December 2013.
- [108] Caivano R, Califano G, Fiorentino A, Cozzolino M, Oliviero C, Pedicini P, Clemente S, Chiumento C, and Fusco V. Clinically relevant quality assurance for intensity modulated

- radiotherapy plans: gamma maps and DVH-based evaluation. *Cancer Invest.*, 32(3):85-91, March 2014.
- [109] Bakhtiari M, Parniani A, Lerma F, Reynolds S, Jordan J, Sedaghat A, Sarfaraz M, and Rodgers J. Evaluation of a software system for estimating planned dose error in patients, based on planar IMRT QA measurements. *Radiol Oncol.*, 48(1):87-93, January 2014.
- [110] Pulliam K., Kerns J, Howell R, Followill D, O'Daniel J, and Kry S. A survey of IMRT QA practices for more than 800 Institutions. *Med Phys*, 41:432, 2014.
- [111] Intensity Modulated Radiation Therapy Collaborative Working Group. Intensity modulated radiotherapy: current status and issues of interest. *Int. J. Radiat. Oncol., Biol., Phys.*, 51:880-914, 2001.
- [112] Saarilahtia K., Mauri K, Juhani C, Tuomo H, Timo A, Heikki J, and Mikko T. Intensity modulated radiotherapy for head and neck cancer: evidence of preserved gland function. *Int. J. Radiat. Oncol., Biol., Phys.*, 74:251-258, 2005.
- [113] Galvin JM, Ezzell G, Eisbruch A, Yu C, Butler B, Xiao Y, Rosen I, Roseman J, Sharpe M, Xing L, Xia P, Lomax T, Low DA, and Palta J. Implementing IMRT in clinical practice: a joint 113 document of the American Society for Therapeutic Radiology and Oncology and the American Association of Physicists in Medicine. *Int. J. Radiat. Oncol. Biol. Phys.*, 58:1616-1634, 2004.
- [114] Bortfeld T., Schmidt-Ullrich R., De Neve W., and Wazer D. E. *Image-Guided IMRT*. Springer- Verlag Berlin Heidelberg New York, 2006.
- [115] Palta J. R., Kim S., Li J. G., and Liu C. Tolerance limits and action levels for planning and delivery of IMRT. In: *Intensity-Modulated Radiation Therapy: The State Of The Art*.

American Association of Physicists in Medicine Medical Physics Monograph No. 29.
Medical Physics Publishing, Madison, WI, USA, 2003.

- [116] Ibbott G. S, Molineu A., and Followill D. S. Independent evaluations of IMRT through the use of an anthropomorphic phantom. *Technol Cancer Res Treat*, 5:481 - 487, 2006.
- [117] Stock M., Kroupa B, , and Georg D. Interpretation and evaluation of the gamma index and the gamma index angle for the verification of IMRT hybrid plans. *Phys. Med. Biol.*,50:399-411, 2005.
- [118] McDermott L N., Wendling M, Sonke J J, van Herk M, and BJ. Mijnheer. Replacing pretreatment verification with in vivo EPID dosimetry for prostate IMRT. *Int. J. Radiat. Oncol. Biol. Phys.*, 67:1568-1577, 2007.
- [119] Sanchez-Doblado F., Hartmann G. H., Pena J., Capote R., Paiusco M., Rhein B., Leal A., and Lagares J. I. Uncertainty estimation in IMRT absolute dosimetry verification. *Int. J. Radiat. Oncol. Biol. Phys.*, 68:301-310, 2007.
- [120] Gillis S., De Wagter C, Bohsung J, Perrin B, Williams P, and Mijnheer BJ. An intercentre quality assurance network for IMRT verification: results of the ESTRO QUASIMODO project. *Radiother Oncol.*, 76(3):340-353, 2005.
- [121] Van Esch A., Bohsung J, Sorvari P, Tenhunen M, Paiusco M, Iori M, Engstrom P, Nystrom H, and Huyskens DP. Acceptance tests and quality control (QC) procedures for the clinical implementation of intensity modulated radiotherapy (IMRT) using inverse planning and the sliding window technique: Experience from five radiotherapy departments. *Radiother Oncol*, 65:53-70, 2002.

- [122] Arnfield M. R., Wu Q., Tong S., and Mohan R. Dosimetric validation for multileaf collimator-based intensity-modulated radiotherapy: A review. *Med. Dosim.*, 26:179-188, 2001.
- [123] Doblado F., Capote R., Rosello J. V., Leal A., Lagares J. I., Arrans R., and Hartmann G. H.. Micro ionization chamber dosimetry in IMRT verification: Clinical implications of dosimetric errors in the PTV. *Radiother. Oncol.*, 75:342 - 8, 2005.
- [124] Ju S. G., Ahn Y. C., Huh S. J., , and Yeo I. J. Film dosimetry for intensity modulated radiation therapy: Dosimetric evaluation. *Med Phys.*, 29:351-355, 2002.
- [125] Both S, Alecu IM, Stan AR, Alecu M, Ciura A, Hansen JM, and Alecu R. A study to establish reasonable action limits for patient-specific quality assurance in intensity modulated radiation therapy. *J Appl Clin Med Phys.*, 8(2):1-8, March 2007.
- [126] Godart J, Korevaar E W, Visser R, Wauben D J, and Van't Veld A A. Reconstruction of high-resolution 3D dose from matrix measurements: error detection capability of the COMPASS correction kernel method. *Phys Med Biol.*, 56(15):5029- 43, August 2011.
- [127] Zhen H, Nelms BE, and Tome WA. Moving from gamma passing rates to patient DVH based QA metrics in pretreatment dose QA. *Med Phys.*, 38(10):5477-89, October 2011.
- [128] Visser R, Wauben DJ, de Groot M, Godart J, Langendijk JA, van't Veld AA, and Korevaar EW. Efficient and reliable 3D dose quality assurance for IMRT by combining independent dose calculations with measurements. *Med Phys.*, 40(2):021710, February 2013.
- [129] Winkler P, Hefner A, Georg D. Dose-response characteristics of an amorphous silicon EPID. *Med Phys.*, 32(10):3095-105, October 2005.
- [130] Mijnheer BJ, De Wagter C, Gillis S, and Olszewska A. QUASIMODO: an ESTRO project for performing quality assurance of treatment planning systems and IMRT, 2004.

- [131] Budgell G, Berresford J, Trainer M, Bradshaw E, Sharpe P, and Williams P.. A national dosimetric audit of IMRT. *Radiother Oncol*, 99:246-52, 2011.
- [132] Deshpande S., Kumar R., Ghadi Y., Neharu R.M., and Kannan V. Dosimetry Investigation of MOSFET for clinical IMRT dose verification. *Technol Cancer Res Treat.*, 12:193-198, 2013.
- [133] Determination of Absorbed Dose in a Patient Irradiated by Beams of X or Gamma Rays in Radiotherapy Procedures. ICRU Report No.24. International Commission on Radiation Units and Measurements, Bethesda, MD., 1976.
- [134] Kutcher GJ, Coia L, Gillin M, William F. H, Steven L, Morton R J., Palta J., Purdy J A., Lawrence E. R, Goran K. S, Mona W, and Linda W. Comprehensive QA for radiation oncology: report of AAPM Radiation Therapy Committee Task Group 40. *Med Phys.*,21(4):581-618, 1994.
- [135] Design and implementation of a radiotherapy programme: Clinical, medical physics, radiation protection and safety aspects. IAEA-TECDOC-1040. International Atomic Energy Agency, Vienna, Austria, 1998.
- [136] Dixon P. and O'Sullivan B. Radiotherapy quality assurance: time for everyone to take it seriously. *Eur. J. Cancer*, 39:423-429, 2003.
- [137] Ibbott G. S., Followill D. S., Molineu H. A., Lowenstein J. R., Alvarez P. E., and Roll J. E. Challenges in credentialing institutions and participants in advanced technology multi-institutional clinical trials. *Int. J. Radiat. Oncol., Biol., Phys.*, 71:S71-S75, 2008.
- [138] Ezzell G A, Burmeister JW, Dogan N, LoSasso T J, Mechalakos J G, Mihailidis D, Molineu A, Palta JR, Ramsey C R, Salter B J, Shi J, Xia P, Yue NJ, and Xiao Y. IMRT Commissioning: Multiple institution planning and dosimetry comparisons, a report from

- AAPM Task Group 119. *Med Phys*, 36:5359-5373, 2009.
- [139] Ramsey C., Spencer K., Alhakeem R., and Oliver A. Verification of dynamic and segmental IMRT delivery by dynamic log file leaf position error during conformal arc and intensity modulated arc treatments. *Med. Phys.*, 28:67 -72, 2001.
- [140] Absorbed dose determination in external beam radiotherapy: An international code of practice for dosimetry based on standards of absorbed dose to water: International Atomic Energy Agency (IAEA) technical series report 398. International Atomic Energy Agency, Vienna Austria, 2000.
- [141] Chung J B, Kim J S, Ha S W, and Ye S J. Statistical analysis of IMRT dosimetry quality assurance measurements for local delivery guideline. *Med Phys*, 6:27, 2011.
- [142] Commissioning and Quality Assurance of Computerized Planning System for Radiation Treatment of Cancer. TRS430. International Atomic Energy Agency, Vienna Austria, 2004.
- [143] Benedick F., Karen D., Margie H., Gerald Ku., George S., Robin S., and Jake V. D. American Association of Physicists in Medicine Radiation Therapy Committee Task Group 53: Quality assurance for clinical radiotherapy treatment planning. *Med. Phys.*, 25:1773-1829, 1998.
- [144] Eric E. Klein, Joseph Hanley, John Bayouth, Fang-Fang Yin, William Simon, Sean Dresser, Christopher Serago, Francisco Aguirre, Lijun Ma, Bijan Arjomandy, Chihray Liu, Carlos Sandin, and Todd Holmes. Task Group 142 report: Quality Assurance of medical accelerators. *Med. Phys.*, 36:4197-4212, 2009.

- [145] Clark C H, Hansen V N, Chantler H, Edwards C, James H V, Webster G, Miles E A, Guerrero Urbano M T, Bhide S A, Bidmead A M, and Nutting C M. Dosimetry audit for a multi-centre IMRT head and neck trial. *Radiother Oncol*, 93:102-108, 2009a.
- [146] Clark C H, Miles E A, Urbano M T, Bhide S A, Bidmead A M, Harrington K J, and Nutting C M. Pre-trial quality assurance processes for an intensity-modulated radiation therapy (IMRT) trial: PARSPORT, a UK multicentre Phase III trial comparing conventional radiotherapy and parotid-sparing IMRT for locally advanced head and neck cancer. *Br J Radiol*, 82:585-594, 2009b.
- [147] Schiefer H, Fogliata A, Nicolini G, Cozzi L, Seelentag WW, Born E, Hasenbalg F, Roth J, Schnekenburger B, Mñch-Berndl K, Vallet V, Pachoud M, Reiner B, Dipasquale G, Krusche B, and Fix MK. The Swiss IMRT dosimetry intercomparison using a thorax phantom. *Med Phys*, 37:4424-4431, 2010.
- [148] Kumar R, Sharma S D, Amols H I, Mayya Y S, and Kushwaha H S. A survey on the quality assurance procedures used in intensity modulated radiation therapy (IMRT) at Indian Hospitals. *J Cancer Sci Ther*, 2.6:166-70, 2010.
- [149] Jang S.Y., Liu H.H., and Mohan R. Underestimation of low-dose radiation in treatment planning of intensity-modulated radiotherapy. *Int J Radiat Oncol Biol Phys*, 71:1537-1546, 2008.
- [150] Das I.J., Ding G.X., and Ahnesj A. Small fields: Nonequilibrium radiation dosimetry. *Med Phys*, 35:206-215, 2008.
- [151] Papatheodorou S., Rosenwald JC, Zefkili S, Murillo MC, Drouard J, and Gaboriaud G. Dose calculation and verification of intensity modulation generated by dynamic multileaf collimators. *Med Phys*, 27:960-971, 2000.

- [152] Xing L., Curran B, Hill R, Holmes T, Ma L, Forster KM, and Boyer AL. Dosimetric Verification of a commercial inverse treatment planning system. *Phys Med Biol*, 44:463-478, 1999.
- [153] Capote R., S'anchez-Doblado F, Leal A, Lagares JJ, Arrns R, and Hartmann GH. An EGSnrc Monte Carlo study of the microionization chamber for reference dosimetry of narrow irregular IMRT beamlets. *Med Phys*, 31:2416-2422, 2004.
- [154] Deng J, Pawlicki T, Chen Y, Li J, Jiang SB, and Ma CM. The MLC tongue-and-groove effect on IMRT dose distributions. *Phys Med Biol*, 46:1039-1060, 2001.
- [155] Li JS, Lin T, Chen L, Price RA Jr, and Ma CM. Uncertainties in IMRT dosimetry. *Med Phys*, 37:2491-2500, 2010.
- [156] Kruse J J. Optimized point dose measurement for monitor unit verification in intensity modulated radiation therapy using 6 MV photons by three different methodologies with different detector-phantom combinations: A comparative study. *J Med Phys*, 35:144-50, 2010.
- [157] Sarkar B, Ghosh B, Sriramprasad, Mahendramohan S, Basu A, Goswami J, et al. Optimized point dose measurement for monitor unit verification in intensity modulated radiation therapy using 6 MV photons by three different methodologies with different detector-phantom combinations: A comparative study. *J Med Phys* (2010) 35:144-50.
- [158] Tissue Substitutes in radiation Dosimetry and Measurements. ICRU Report No.44. International Commission on Radiation Units and Measurements, Bethesda, MD., 1989.
- [159] Derreumaux S., Chavaudra J, Bridier A, Rossetti V, and Dutreix A. A European quality assurance network for radiotherapy: dose measurement procedure. *Phys. Med. Biol.*, 40: 1191-1209, 1995.

- [160] Bridier A., Nyström H., Ferreira I., Gomola I., and Huyskens D. A comparative description of three multipurpose phantoms (MPP) for external audits of photon beams in radiotherapy: the water MPP, the urine MPP and the EC MPP. *Radiother Oncol*, 55: 285-293, 2000.
- [161] Ferreira I H., Dutreix A, Bridier A, Chavaudra J, and Svensson H. The ESTROQUALity assurance network (EQUAL). *Radiother Oncol*, 55:273-284, 2000.
- [162] Gomola I., Dam J V, Isern-Verdum J, Verstraete J, Reymen R, Dutreix A, Davis B, and Huyskens D. External audits of electron beams using mailed TLD dosimetry: preliminary results. *Radiother Oncol*, 58:163-168, 2001.
- [163] Marre D., Ferreira I.H., and Bridier A. Energy correction factors of lif powder TLDs irradiated in high energy electron beams and applied to mailed dosimetry for quality assurance networks. *Phys Med Biol*, 45:3657-3674, 2000.
- [164] Swinnen A., Verstraete J, and Huyskens D P. Feasibility study of entrance in vivo dose measurements with mailed thermoluminescence detectors. *Radiother. Oncol.*, 73:89-96, 2004.
- [165] Kroutilkova D., Novotny J, and Judas L. Thermoluminescent dosimeters (TLD) quality assurance network in the Czech Republic. *Radiother Oncol*, 66:235-244, 2002.
- [166] Rassiah P., Ng KH, DeWerd LA, and Kunugi K. A thermoluminescent dosimetry postal dose inter-comparison of radiation therapy centres in Malaysia. *Australas Phys Eng Sci Med*, 27:25-29, 2004.
- [167] A Rou, Venselaar J. L. M., Ferreira I. H., Bridier A., and Van Dam J. Development of a TLD mailed system for remote dosimetry audit for ¹⁹²Ir HDR and PDR sources. *Radiother. Oncol.*, 83:86-93, 2007.

- [168] Reinhardt S., Hillbrand M, Wilkens JJ, and Assmann W. Comparison of Gafchromic EBT2 and EBT3 films for clinical photon and proton beams. *Med Phys.*, 39:5257-5262, 2012.
- [169] Arjomandy B., Tailor R, Anand A, Sahoo N., Gillin M., Prado K, and Vicic M. Energy dependence and dose response of Gafchromic EBT2 film over a wide range of photon, electron and proton beam energies. *Med Phys.*, 37(5):1942-1947, 2010.
- [170] Crijs W., Maes F., van der Heide U. A., and van der Heuvel F. Calibrating page sized Gafchromic EBT3 films. *Med Phys.*, 40:012102-13, 2013.
- [171] Sorriaux J, Kacperek A, Rossomme S, Lee JA, Bertrand D, Vynckier S, and Sterpin E. Evaluation of Gafchromic REBT3 films characteristics in therapy photon, electron and proton beams. *Med Phys*, 29(6):599-606, 2013.
- [172] Lewis D., Micke A., Yu X., and Chan M.F. An efficient protocol for radiochromic film dosimetry combining calibration and measurement in a single scan. *Med Phys.*, 39:6339-6350, 2012.
- [173] Devic S., Tomic N., Aldelaijan S., Deblois F., Seuntjens J., and Chan M.F. Lewis D. Linearization of dose-response curve of the radiochromic film dosimetry system. *Med Phys*, 39:4850-4857, 2012.
- [174] True beam Trajectory Log File Specification, 2011, USA Varian Medical System.
- [175] Song J Y., Kim Y H, Jeong J U, Yoon MS, Ahn SJ, Chung WK, and Nam TK. Dosimetric evaluation of MapCHECK 2 and 3DVH in the IMRT delivery quality assurance process. *Med Dosim.*, 39(2):134-138, 2014.
- [176] Guillot M, Gingras L, Archambault L, Beddar S, and Beaulieu L. Performance assessment of a 2D array of plastic scintillation detectors for IMRT quality assurance. *Phys Med Biol.*, 58(13):4439-4454, 2013.

- [178] Sharma D. S., Mhatre V., Heigrujam M., Talapatra K., and Mallik S. Portal dosimetry for pretreatment verification of IMRT plan: A comparison with 2D ion chamber array. *J. Appl. Clin. Med. Phys.*, 11:3268-3274, 2010.
- [179] Yewondwossen M. Characterization and use of a 2D-array of ion chambers for brachytherapy dosimetric quality assurance. *Med. Dosim.*, 37(3):250-256, 2012.
- [180] Jursinic P. A. and Nelms B. E. 2-D diode array and analysis software for verification of intensity modulated radiation therapy delivery. *Med. Phys.*, 30:870-879, 2003.
- [181] Hu Y, Wang Y, Fogarty G, and Liu G. Developing a novel method to analyse Gafchromic EBT2 films in intensity modulated radiation therapy quality assurance. *Australas Phys Eng Sci Med.*, 36(4):487-494, 2013.
- [182] Ju S G., Han Y, Kum O, Cheong K H, Shin E H, Shin J S, Kim J S, and Ahn Y C. Comparison of film dosimetry techniques used for quality assurance of intensity modulated radiation therapy. *Med Phys.*, 37(6):2925-2935, 2010.
- [183] Wilcox E., Daskalov G., and Nedialkova L. Comparison of the Epson Expression 1680 flat bed and the Vidar VXR-16 Dosimetry PRO film scanners for use in IMRT dosimetry using Gafchromic and radiographic film. *Med Phys.*, 34:41-48, 2007.
- [184] Esthappan J., Mutic S., Harms W. B., Dempsey J. F., and Low D. A. Dosimetry of therapeutic photon beams using an extended dose range film. *Med Phys.*, 29:2438-2445, 2002.
- [185] Bucciolini M., Buonamici F. B., , and Casati M. Verification of IMRT fields by film dosimetry. *Med Phys.*, 31:161-168, 2004.
- [186] Childress N. L., Salehpour M., Dong L., Bloch C., White R. A., and Rosen I. I. Dosimetric accuracy of Kodak EDR2 film for IMRT verifications. *Med Phys.*, 32:539-548, 2005.

- [187] Martens C, De Wagter C, and De Neve W. The value of the Pin Point ion chamber for characterization of small field segments used in intensity-modulated radiotherapy. *Phys. Med. Biol.*, 45:2519-2530, 2000.
- [188] Low D. A., Parikh P., Dempsey J. F., Wahab S., and Huq S. Ionization chamber volume averaging effects in dynamic intensity modulated radiation therapy beams. *Med. Phys.*, 30:1706-1711, 2003.
- [189] Dong L., Antolak J., Salehpour M., Forster K., O'Neill L., Kendall R., and Rosen I. Patient-specific point dose measurement for IMRT monitor unit verification. *Int. J. Radiat. Oncol., Biol., Phys.*, 56:867-877, 2003.
- [190] Low D A, Dempsey JF, Venkatesan R, Mutic S, Markman J, Mark Haacke E, and Purdy J A. Evaluation of polymer gels and MRI as a 3-D dosimeter for intensity modulated radiation therapy. *Med Phys.*, 26(8):1542-51, 1999.
- [191] Boggula R, Lorenz F, Mueller L, Birkner M, Wertz H, Stieler F, Steil V, Lohr F, and Wenz F. Experimental validation of a commercial 3D dose verification system for intensity-modulated arc therapies. *Phys. Med. Biol*, 55(19):5619-5633, 2010.
- [192] Li F, Li J, Xing J, Zhang Y, Fan T, Xu M, Shang D, Liu T, and Song J. Analysis of the advantage of individual PTVs defined on axial 3D CT and 4D CT images for liver cancer. *J Appl Clin Med Phys.*, 13(6):62-70, 2012.
- [193] Blanpain B. and Mercier D. The delta envelope: a technique for dose distribution comparison. *Med. Phys.*, 36:797-808., 2009.
- [194] Van Dyk J., Barnett R. B., Cygler J. E., and Shragge P. C. Commissioning and quality assurance of treatment planning computers. *Int. J. Radiat. Oncol., Biol., Phys.*, 26: 261-273., 1993.

- [195] Harms W. B., Low D. A., Wong J. W., and Purdy J. A. A software tool for the quantitative evaluation of 3D dose calculation algorithms. *Int. J. Radiat. Oncol., Biol., Phys.*, 25:1830-1836, 1998.
- [196] Al Sa'd M., Graham J, Liney G P, and Moore C J. Quantitative comparison of 3D and 2.5D gamma analysis: introducing gamma angle histograms. *Phys. Med. Biol.*, 58:2597-2608, 2013.
- [197] Computational Environment for Radiotherapy Research (CERR). <http://www.cerr.info/about.php>. Last accessed on Sep 30, 2013.
- [198] Low D. A., Harms W. B., Mutic S., and Purdy J. A. A technique for the quantitative evaluation of dose distributions. *Med. Phys.*, 25:656-661, 1998.
- [199] Wendling M., Zijp L J., McDermott L N., Smit E J., Sonke J.J., Mijnheer B. J., and van Herk M. A software tool for the quantitative evaluation of 3D dose calculation algorithms. *Med Phys.*, 34:1647-1654, 2007.